EVALUATION OF PASSIVE ANTHROPODYNAMIC MANIKINS INTENDED FOR LABORATORY SEAT TESTING UNDER VEHICULAR EXCITATIONS

Suresh Kumar Patra

A thesis

in

the Department

of

Mechanical Engineering

Presented in Partial Fulfillment of the Requirements
for the Degree of Master of Applied Science
at Concordia University
Montréal, Québec, Canada

September 2006

Your file Votre référence
ISBN: 978-0-494-20761-1
Our file Notre référence
ISBN: 978-0-494-20761-1

ABSTRACT

Evaluation of Passive Anthropodynamic Manikins intended for Laboratory seat testing under Vehicular Excitations

Suresh Kumar Patra

The vibration attenuation performance of suspension seats employed in heavy vehicles are influenced by energy dissipation property of the seated body. Owing to complexities associated with biodynamic response behavior of the human body, the performance assessments of suspension seats are invariably accomplished through laboratory or field experimentation. Such laboratory experiments involve certain safety and ethical concerns, while field measurements yield difficulties in interpretation of the results due to lack of controlled conditions. In this dissertation, two prototype anthropodynamic manikins, designed to replace human subjects in assessments of seat, are evaluated through laboratory experiments and analyses of the biodynamic responses.

The apparent mass (APMS) responses of manikins are characterized under different levels of vibration excitations and three body masses (55 kg, 75 kg and 98 kg). The measured responses are compared with the standardized values to assess the APMS prediction abilities of the manikins. The results suggest the need for deriving more reliable APMS responses of seated humans of particular masses. The applicability of the manikins for seating dynamics is then assessed for a range of seats and vibration spectra of different vehicles. The seat effective acceleration transmissibility (S.E.A.T) of five different seats are measured using human subjects, equivalent inert mass and the prototype manikins. The results suggest that equivalent inert mass could provide

reasonably good prediction of seat performance, when excitations dominate in the low frequency range. Under high frequency excitations, the inert mass yields poor estimate of the seat-human system performance, while the manikins provide better estimations.

The need for tuning of the manikins was identified to improve their biodynamic response prediction abilities. An analytical model of one of the manikin was thus formulated and analyzed to perform the necessary design refinements. System identification technique was applied to derive uncertain parameters of the model so as to satisfy the measured APMS responses for three body masses. Additional parameter identification was performed to realize desirable parameters that would satisfy the standardized biodynamic response. The results suggested that only minor refinements of the prototype would be needed to enhance the biodynamic response prediction ability of the manikin, which may translate into improved applicability of the manikin for assessment of suspension seats.

ACKNOWLEDGEMENTS

I am sincerely grateful to my supervisors Dr. Subhash Rakheja and Dr. Paul-Émile Boileau, for their constant guidance and dedication throughout the thesis work. Their valuable advice and contributions have helped to make the final appearance of this thesis.

I would like to acknowledge the technical support provided by Mr. Jerome Boutin in the experimental set up. I thank all the friends and colleagues who participated in my experiments as test subjects. I wish to acknowledge the contribution of Mr. Pierre Marcotte and Mr. Hugues Nelisse for helping me in learning the software PULSE and also in data analysis.

Financial support provided by the Institut de recherché en santé et en sécurité du travail du Quebec (IRSST) is gratefully acknowledged. Finally I would like to extend my appreciation to my family and friends for their unyielding love, companionship, and understanding.

TABLE OF CONTENTS

CHAPTER 4

DEVELOPMENT AND DESIGN REFINEMENTS OF A MANIKIN MODEL

CHAPTER 5

CONCLUSION AND RECOMMENDATION FOR FUTURE WORK

LIST OF FIGURES

LIST OF TABLES

LIST OF ABBREVIATIONS AND SYMBOLS

ABBREVIATIONS

APMS	Apparent Mass
CPB	Constant Proportional Band analyzer
DPMI	Driving-point mechanical impedance
DRI	Dynamic Response Index
DIN	Deutches Institut for Normung
DOF	Degree-of-freedom
HL	Hands in lap
HP	High pass
ISO	International Standard Organization
LP	Low pass
NB	No back support
PSD	Power Spectral Density
rms	Root-mean square
SEAT	Seat Effective Amplitude Transmissibility
$(S.E.A.T)_M$	SEAT value of seat-manikin system
$(S.E.A.T)_H$	SEAT value of seat-human system
$(S.E.A.T)_R$	SEAT value of seat-inert mass system
STHT	Seat-to-Head Transmissibility
WBVVS	Whole-Body Vehicular Vibration Simulator
WBV	Whole-Body Vibration

SYMBOLS

ω	angular frequency (rad/sec)
j	complex phasor $(=\sqrt{-1})$
$F(j\,\omega)$	complex Force
$a(j\,\omega)$	complex acceleration due to excitation
$M(j\,\omega)$	complex apparent mass
$S_{Fa}(j\,\omega)$	cross spectral density of the force response $F(j\,\omega)$ at driving point and $a(j\,\omega)$
$S_a(j\,\omega)$	auto spectral density of acceleration $a(j\,\omega)$ due to excitation
a_{rms}	overall root-mean square acceleration (*rms*) acceleration (m/s^2)
$\ddot{x}(t)$	instantaneous *rms* acceleration
$M_0(j\,\omega)$	apparent mass of the rigid seat
$M_c(j\,\omega)$	apparent mass of the coupled manikin-seat system
$H_A(\omega)$	acceleration transmissibility
$\ddot{x}_2$	*rms* seat acceleration (m/s^2)
$\ddot{x}_1$	*rms* base acceleration (m/s^2)
$S_{\ddot{x}_2\ddot{x}_1}$	cross spectral density of the seat acceleration and base acceleration
$S_{\ddot{x}_1}$	auto spectral density of the base acceleration
f	excitation frequency (Hz)
f_c	cut-off frequency (Hz)
$G^*p(f)$	target PSD of the vertical vibration at the seat base
f_l	lower frequency limit
f_u	upper frequency limit

a_{1w}	overall frequency-weighted *rms* acceleration
a_{2w}	overall frequency-weighted *rms* acceleration at the seat-load interface
$\%D_{M-H}$	percent deviation of the SEAT values of a seat-manikin combination with respect to seat-human combination
$\%D_{M-R}$	percent deviation of the SEAT values of a seat-manikin combination with respect to seat-inert mass combination
$\%D_{R-H}$	percent deviation of the SEAT values of a seat-inert mass combination with respect to seat-human combination
$\gamma^2_{\ddot{x}_2\ddot{x}_1}$	coherence
θ	angular displacement
M1 (m_1), M2 (m_2), M3 (m_3)	Mass (kg)
x_1	displacement of mass m_1 from static equilibrium
x_0	displacement of fixed mass m_0
h_i	damper mounting height (m)
l	link length (m)
v_i	relative velocity (m/s)
F_i	damper force
C1 (c_1)	damping co-efficient due to principal mass (m_1)
C2 (c_2), C3 (c_3)	damping co-efficient due to damper and friction due to guiding rod for masses m_2 and m_3
K1 (k_1) K2 (k_2) K3 (k_3)	spring rates due to spring supported by masses m_1, m_2 and m_3
c_{eq}	equivalent damping co-efficient due to principal damper
F	resultant force at the lower mass (m_0)
U	objective function
W_k	weighting function in vertical direction

λ	weighting factor
χ	vector of model parameters
N	number of discrete frequencies

CHAPTER 1

INTRODUCTION AND SCOPE OF RESEARCH

1.1 Introduction

The drivers of heavy road as well as off road vehicles are exposed to whole body vibration and shocks arising from the tire-terrain interactions. Such vibrations are of large magnitudes and occur in the relatively low frequency range (lower than 20 Hz). Prolonged exposure to such low frequency, high magnitude vibration has been associated with sensation of discomfort and an array of musculoskeletal disorders, problems such as low back pain, spinal deformities [1]. Epidemiological studies have also shown that there exists a strong association between back disorders among the exposed population to whole body vibration and years of exposure [2-4]. The health and safety risks posed by the exposure to vibration and shock in off-road vehicles has led to a considerable effort in characterization of the vibration exposure of various vehicles, and developments in assessment methods and mechanisms for attenuation of vibration transmitted to the occupant [1, 5-8]. Heavy road and off-road vehicles invariably employ suspension seats for attenuating vibration along the vertical axis, and to provide a controlled and comfortable posture for drivers.

The assessment of vibration comfort characteristics of suspension seats is a highly complex task due to excessive variations in the body sizes and weights, individual preferences, driving conditions, inter- and intra-subject variations, and most of all the energy absorption by the body. The vibration performance is thus mostly assessed through subjective and objective measurements [1, 9]. Since the subjective methods yield

inconsistent results due to excessive variations in the individuals preferences, the objective methods are considered more desirable to assess vibration attenuation performance of suspension seats. The objective methods involve either field or laboratory measurements [1, 5, 9]. The field measurements, however, tend to be costly and yield considerable variabilities in the data, which pose difficulties in interpretations. Alternately, laboratory evaluations performed under carefully controlled conditions can provide effective assessments of vibration isolation performance in a highly efficient manner. The laboratory assessments of seats performed using rigid loads as well as human subjects have established that the dynamic response of seats is greatly influenced by the human body dynamics [7, 10]. Consequently, the use of human subjects, which poses many ethical concerns related to the safety risks associated with the shock and vibration exposure of human subjects, and require extremely safe or man-rated vibration simulators. The variations in subjects weight and built further yields considerable variations in the measured data. Upon recognizing such complexities, many studies have proposed human body models, which may be used in conjunction with analytical models of the seats to derive the vibration transmission characteristic of the coupled human-seat system. The vast majority of the models however have been developed on the basis on the biodynamic responses acquired under excitations and sitting postures that hardly represent vehicular driving conditions [1].

The other attractive alternative to replace the human subjects in the routine laboratory seat testing is the use of anthropodynamic manikin having representative vertical impedance as that of the human subjects. The ethical concerns associated with laboratory shock and vibration exposure of human subjects and repetitive experiments

could be circumvented through the use of anthropodynamic manikins. A number of active and passive anthropodynamic manikins have thus been developed in the recent years [11-20]. The validity of these anthropodynamic manikins has been demonstrated for a limited number of seats and vibration excitations [11-20]. Moreover, the vast majority have been evaluated only for the 50^{th} percentile mass group.

This dissertation research concerns with systematic assessments of two anthropodynamic manikins developed by INRS (France) and BaUA (Germany), for their applications in evaluating a wide range of suspension seats. The experiments were designed to evaluate: (i) the ability of the manikins to predict the biodynamic responses of human subjects with standing body masses of 55, 75 and 98 kg under different vibration magnitudes; and (ii) the effectiveness in assessing the vibration isolation performance of different suspension seats subject to vibration excitations due to a number of vehicles. A mathematical model of one of the prototypes is formulated and validated to propose design refinements for enhancing its predictions abilities.

1.2 Review of Relevant Literature

The assessments of anthropodynamic manikins for their applicability in seating dynamics appropriate considerations of the seat design factors, vibration evaluation of seats, human responses to vibration, vehicular vibration, experimental methods, etc. The reported relevant studies are thus reviewed and briefly discussed in the following sections to formulate the scope of this dissertation research.

1.2.1 Human Response to Vibration

The biodynamic response behaviors of the human body subject to whole-body vibration of different types and magnitudes have been widely investigated [21-26]. The

responses presented in terms of driving-point mechanical impedance (DPMI), apparent mass (APMS) and absorbed power, have been studied to identify resonant frequencies, frequency weighting, and the role of seat design factors, sitting postures and nature of excitations [1, 10, 29, 30]. Direct measures of the biodynamic responses of the body have been characterized by transfer functions, relating either the force and motion at the driving-point (e.g. DPMI, APMS or absorbed power) or the vibration transmitted to different body segments to the input vibration [31].

The biodynamic response behavior of the human body subjected to whole-body vibration can be defined using two principal biodynamic response functions: (i) "to the body" force-motion relationship at the human seat interface as a function of the vibration frequency, expressed as DPMI or AMPS; and (ii) "through the body" response function, generally termed as seat-to-head vibration transmissibility (STHT) for the seated occupant [1, 28]. The to-the-body functions relate the vibration force developed at the driving-point and a measure of vibration (velocity or acceleration), whereas through the body biodynamic responses describes the transmission of vibration to various segments of the body and thus could be used to measure the resonant frequencies of various body segments [31]. Relatively fewer studies have investigated the STHT responses of seated subjects exposed to WBV. Paddan [32] has compared the STHT magnitude reported in different studies, which show extreme variabilities among different datasets.

The biodynamic responses measured in different laboratories have shown considerable differences in the magnitude as well as the phase data, which have been attributed to an array of factors related to anthropometry, seat design and nature of vibration. These include: the subject mass, height and build [1, 21, 29]; seat geometry and

height [1, 30]; sitting posture [29, 30, 32]; and magnitudes and spectral components of vibrations. The variabilities in the reported DPMI and APMS data, however, are significantly smaller than those observed in the STHT datasets. The data reported by different investigators have thus been synthesized to derive the ranges of DPMI and APMS magnitude and phase responses under conditions considered to be representative of vehicle driving [34, 35]. These ranges adapted in the ISO 5982 [35] are considered to be valid for subjects seated on a rigid platform, with feet supported and vibrated, and maintaining an erect seated posture without backrest support while exposed to vertical vibration of 1-3 m/s^2 overall *rms* acceleration in the 0.5-20 Hz frequency range. The ranges of biodynamic responses in terms of DPMI magnitude and phase have also been defined in German standard, DIN 45676 [36], which are considered applicable for both sitting and standing human subjects exposed to WBV.

1.2.2 Review of Biodynamic Models of Human Body

The evaluation of the vibration transmission properties of the coupled seat-human system can be evaluated using two methods (i) laboratory or field measurements of the coupled seat-human system; and (ii) development and analysis of the coupled seat-human body models. The first method can yield reliable assessment of the vibration transmission properties when representative subjects sample and test conditions are employed. Such experiments with human subjects, however, involve certain ethical concerns. Alternatively, a number of biodynamic models have been developed to study the vibration transmission properties of the coupled seat-human systems. They range from simple single-DOF to complex non-linear multi-DOF models. Majority of the models proposed in the literature are lumped-parameter models, where the parameters have been

identified from either measured mechanical impedance or vibration transmissibility response characteristics of the human subjects under selected type and magnitudes of vibration. However, the methodology for derivation of model parameters based upon curve fitting of the measured DPMI or STHT magnitude or and phase pose two major problems; (i) the model can be considered valid only in the vicinity of the test conditions; and (ii) more than one set of parameters could yield reasonably good agreement with the target, while the model parameter may not relate to any specific body segment. Furthermore, a number of models have been derived based on ejection seat data and represent the human response to high-intensity vibration and shock [23]. It may thus be questionable whether these models could be applied in conjunction with vibration environment experienced by vehicular drivers.

The Dynamic Response Index (DRI) model proposed by Coermann [23] is the widely used single-DOF model that relates to human response to relatively severe of vibration or shocks. The model consisted of mass of the upper torso and head supported on the spring stiffness of the spine. Values of damping in the spine and associated tissues were based on the mechanical impedance measurements. An improved DRI model was proposed by Payne [37] to account for the differences between single events or shocks and continuous vibration. This model consisted of four parallel and uncoupled single-DOF models and is realized upon combining the DRI model, also known as "spinal" or "shock response" model with three additional single-DOF models, referred to as the "visceral", body vibration", and "low frequency". Fairley and Griffin [21] proposed a single-DOF model which is based on the measured mean apparent mass responses of 60 subjects, including male, female and children, sitting erect without back support. The feet

of subjects seated on a rigid platform were vibrated under 1.0 m/s^2 (*rms* acceleration) random vibration. The single-DOF model consisted of two masses, the upper body and the lower body masses coupled through visco-elastic properties of the spinal structure. A third mass, representing the mass of the legs was included in the model only when the feet were supported on a stationary footrest. This model, however, did not consider seat-to-head transmissibility data and the effects of back support of the posture.

Suggs [38] proposed a two-DOF biodynamic model of the human body to characterize the response over a frequency range comprising the first two resonant frequencies of the body. The model comprises of two lumped masses: one of the mass represents pelvis and the abdomen, while the other represents the head and chest, and both the masses are suspended from a common rigid frame representing the spinal column. The model was derived from the measured mechanical impedance characteristics of 11 male subjects, showing primary and secondary resonances of the seated subjects near 4.5 Hz and 8 Hz respectively [22]. Allen [39] developed a two-DOF biodynamic model of the human body comprising a "primary system" to characterize the upper body response and a "secondary system" representing the head.

A number of multi-DOF models, of the seated human subjects have also been proposed by many researches. Mertens [40, 41] developed a comprehensive biodynamic model involving the comparison of both the impedance and vibration transmissibility magnitude and phase characteristics with experimental results. The model comprised of five lumped masses representing the legs, buttocks, abdominal system, chest system and head. The study was intended for ejection seat applications.

The international standard ISO Committee Draft CD 5982 [42] proposed a four-DOF biodynamic model to characterize both the standardized driving-point mechanical impedance and the seat-to-head transmissibility of the human body exposed to vibration. The model represents both seating and standing human subjects, while model parameters differed depending on the posture. The masses of the model did not correspond with any specific body segment of the human body.

Boileau [10] proposed a four-DOF linear human driver model, based upon the magnitude and phase of the measured mechanical impedance and seat-to-head vibration transmissibility. The model comprised of four masses, representing the four body segments: the head and neck, the chest and upper torso, the lower torso, and the thighs and pelvis in contact with the seat. The mass due to lower legs on the feet was not included in the model, assuming its negligible contributions to the biodynamic response of the seated body, which has been established from the other reported studies [21].

Wu [43] proposed a three-DOF lumped-parameter model with four masses, coupled by linear elastic and damping elements. The masses were introduced with an objective to describe the biodynamic behavior related to two resonant peaks observed in the apparent mass and the seat-to-head transmissibility magnitude responses near frequencies of 5 Hz and 10 Hz, respectively. The masses of the model did not correspond to any physiological structures within the body, while the total model mass was constrained to be close to the body mass supported by the seat.

A comparative study [44] of different biodynamic models of the seated human body exposed to WBV was performed to evaluate their relative merits and limitations. In this study, 11 biodynamic models representing the seated human body were selected from

the published literature. Out of the 11 models considered only three of these models were defined to satisfy simultaneously both the DPMI and the STHT responses, namely the multi-DOF models proposed by Mertens [40], ISO CD 5982 [42], and Boileau et al. [10]. The other models considered in the study were the single-DOF models proposed by Coermann [23], Fairley and Griffin [21] and the Dynamic Response Index (DRI) model [21]; two-DOF models of Suggs [22] and Allen [39]; and multiple DOF models defined by Payne [37], Amirouche and Ider [45] and a non-linear model defined by Patil and Palanichamy [46].

The validity of the above models in predicting the biodynamic responses in terms of either DPMI/APMS or STHT or both have been demonstrated for a particular body mass and sitting posture. The biodynamic responses of seated subjects are significantly influenced by the seat geometry, sitting posture and the body mass. The above reported models are limited to a particular body mass and a sitting posture with no back support. Rakheja et al. [47] grouped the measured APMS data for four different subject masses (< 60 kg; 60.5-70 kg; 70.5-80 kg; and > 80 kg) to demonstrate the body mass effects on the APMS responses. The study proposed model parameters to characterize the body-mass dependent APMS response characteristics. Wang et al [29] performed measurements of APMS responses of subjects seated with no back support, a vertical back and an inclined back support. The study also considered the effects of hands position, seat height and body mass on the measured APMS responses. Rakheja et al [47] further proposed a model comprising the upper and middle-sections of the body supported against an inclined backrest through visco-elastic elements. The model was derived on the basis of

the APMS responses measured under relatively lower magnitudes of vibration in the 0.5-40 Hz range.

1.2.3 Review of Suspension Seats

The ride vibration environment of off-road vehicles comprises of comprehensive magnitudes of low frequency vibration along all the three translational and rotational axes. The transfer of such vibration to the operator occurs through the feet, seat back and seat cushion. It has been reported that the vertical component of such vibration is usually higher. Off-road vehicles, due to their interaction with uneven terrains and also high centre of mass location yield high levels of longitudinal and lateral vibrations, which could be comparable to those of the vertical vibration [1]. Rakheja [48] proposed a multi-axis seat vibration isolator in the early 80's. However the commercial suspension seats employed in heavy-road and off-road vehicles are designed to attenuate vibration in the vertical mode alone, since the attenuation of vibration along other axes requires complex suspension mechanism, which would involve excessive cost and alterations.

The vibration isolation performance of a conventional cushion seat is inferior to that of the vertical mode suspension seats, which are designed to achieve low natural frequency in the order of 1.5 Hz or lower. This frequency is well below the frequency of dominant off-road vehicle vibration which predominates in the 2-3.25 Hz frequency range for majority of wheeled vehicles [1, 5]. The low natural frequency or low stiffness is realized upon integrating additional restoring elements below a relatively hard seat cushion, which is intended to support the weight of the driver. The commercially available seat-suspensions exhibit natural frequencies in the 1-2 Hz range and are

equipped with a weight adjustment mechanism in order to provide either a mid-ride or a selected ride height for the drivers in the 50-100 kg weight range.

A seat suspension system invariably comprises either an air spring or a mechanical spring interposed between the seat structure and the base, and a double acting hydraulic damper to absorb vibration energy. The suspension seats travel is mostly limited to 100 to 160 mm in order to limit the relative travel of seated driver and to ensure stable sitting posture for performing the desired tasks. The maximum travel in some suspension seats, such as those designed for forklift trucks is limited to only 40 to 50 mm. While a low natural frequency design is desirable to attain improved vibration isolation, it causes excessive static and dynamic motions of the driver with respect to the controls. The excessive relative motions of the low natural frequency suspension are thus limited by either rubber or metal motion-limiting end stops.

A few studies have investigated the dynamic performance characteristics of various passive suspension seats through laboratory or field measurements, and development and analysis of linear and non-linear analytical models [10, 48-51]. A limited number of active and semi-active suspension seat concepts have also been explored to enhance the steady-state vibration isolation performance [48, 52, 53]. An active suspension seat employs active elements that have the capability of providing or dissipating energy using additional power source and control devices. Active suspensions could provide high load bearing capacity and low dynamic stiffness. The relative displacement, therefore, is no longer directly related to the natural frequency of the suspension [9]. The applications of such suspensions to heavy-road and off-road vehicles

have been limited due to their excessive cost and complexities, and unproven reliability in the harsh vehicular environment.

Studies have further established that the dynamics of the seated human body contributes considerably to the overall performance of seats [7, 10, 48, 54, 55]. The evaluations of suspension seats thus necessitate the considerations of the coupled seat-human subject dynamics. The international standard, ISO-7096 [56], provides guidelines for laboratory evaluations of suspension seats that must be performed with human subjects of specific body masses, namely 55 and 98 kg. A recent study [55], however, suggests that the contributions due to human body dynamics are significant only for seats with higher natural frequency, such as those employed in forklift trucks and automobiles. A few studies have developed coupled human-seat models by integrating the human body biodynamic model to the two-DOF suspension model to study the contributions of the human driver [10, 54, 57].

Alternatively, a few studies have proposed the use of human body simulators or manikins to assess the vibration comfort of seats without involving human subjects. Many passive and active anthropodynamic manikins have been developed to assess the performance of the suspension seats for the laboratory seat testing [11-20]. Primary results attained with the anthropodynamic manikins suggest that the manikins can mimic the contributions due to human response to vibration.

1.2.4 Assessment of Human Exposure to Whole Body Vibration (WBV)

Subjective evaluations have been widely used to obtain data on the relative ride ranking of different vehicles or component designs but these do not provide any quantitative design information to the designer. Subjective evaluations are considered to

be complex and expensive when a large number of prototype seats are involved, whereas these can be effective in obtaining the ride perception when relatively small number of prototype seats is involved [1].

A number of vibration tolerance criteria have been established on the basis of subjective responses, relative ride quality ranking of a group of vehicles, tolerance related to machine productivity, vibration interference with normal control tasks, health aspects due to vocational exposures competitive significance, and cost/benefit ratio of potential ride-improvement [1, 48]. Although reasonable similarities in the proposed comfort criteria have been shown with respect to input frequency, the subjective response data have been inconsistent and insufficient to derive a generally acceptable comfort criterion with respect to intensity of vibration due to semantic problems, age and moods of subjects at the time of experiments, etc.

Alternative methods based on direct measures of physical quantities such as velocity, acceleration, jerk, and absorbed power have also been proposed as ride evaluation criteria [57, 58]. Objective measures of mean square jerk and acceleration have shown good correlation with subjective human responses [59]. In general, a considerable similarity exists among the ride evaluation criteria, regardless of the types of subjective or objective measures. Although a generally acceptable criterion for objective assessment of human perception of whole-body vibration exposure does not yet exist, a number of guidelines have been proposed and standardized.

On the basis of the subjective assessments Janeway proposed a vertical vibration comfort criterion for automotive passengers [57], which has been recommended by the Society of Automobile Engineers (Ride Vibration Manual J6a[58])for many years . The

criterion is limited to vertical vibration only and suggests that the human body is more sensitive to vertical vibration in the 1-20 Hz range.

Presently, the most commonly acceptable standard for evaluating human exposure to whole-body vibration is the ISO 2631-1 [60]. The standard defines the frequency-weighting functions to account for variations in human sensitivity to vibration frequency, for vibration along three translational and three rotational axes. Its earlier version also proposed the WBV exposure limits in view of human perception, preservation of working efficiency or human fatigue and preservation of health, in terms of magnitude of vibration in the 1-80 Hz frequency range and exposure duration [61].

The absorbed power, a measure of the rate of vibration energy absorbed by the human body attributed to its visco-elastic properties, has also been proposed for assessing the vibration exposure. The vibration energy absorbed by a seated occupant is strongly related to the magnitude of vibration. The absorbed power criterion, proposed by Pradko and Lee [62], has been widely used to characterize vibration environment of military vehicles [63]. The vibration energy absorbed by the human body is also considered as a significant measure for assessing the injury risk [64]. A few studies have thus characterized the biodynamic responses of the seated occupants exposed to WBV in terms of absorbed power [65-67].

It is to be noted that the vast majority of the criteria have been established on the basis of different subjective and objective measures observed under exposure to sinusoidal vibration, which may not fully describe the human response to random vehicle vibration. Furthermore, the occupant sitting posture and conditions are not sufficiently

described in these studies, to assess the suitability of the proposed limits for automotive environments.

1.2.5 Analysis of Vibration Attenuation Performance of Seats

The vibration comfort performances of static and dynamic seats have been related to their natural frequencies, resonant response, vibration attenuation performance and static and dynamic relative deflections [57, 68-70]. Verterasian [6] used a 'ride number' determined by the resonance frequency of the seat, the resonant acceleration transmissibility and the transmissibility at 10Hz. The study concluded that the proposed 'ride number' provides a better correlation with the subjective judgments of ride in different seats than that attained with the measurement of vibration using the method defined in ISO 2631 [71]. The analysis of vibration comfort performance of seats, however, should incorporate the dynamic properties of seats and components, vehicle spectrum and the occupant response.

The dynamic performance or isolation efficiency of static and dynamic seats are frequently evaluated in terms of S.E.A.T (Seat Effective Amplitude Transmissibility), defined as the ratio of frequency-weighted acceleration due to vibration transmitted to seat-buttock interface to the frequency-weighted acceleration at the seat base (input) [1]. This measure utilizes W_k-weighting defined in the ISO-2631-1 [71] or W_b-weighting defined in the British Standard BS [73]. The method yields a simple index to describe the vibration isolation performance but does not provide information related to resonant frequency and amplification. A SEAT value of 100 % indicates that there is no overall improvement or degradation in vibration discomfort produced by the seat, although the seat may amplify low frequency vibration and attenuates high frequency vibration. A

SEAT value of 100 % thus indicates that sitting on the floor (or on a rigid seat) would produce similar vibration discomfort. A SEAT value of greater than 100 % indicates that the vibration discomfort has been increased by the seat. A SEAT value of less than 100 % indicates vibration isolation provided by the seat. The SEAT measure has been used in many studies to determine the relative comfort performance of seat, and the influence of variations in seat design parameters, vehicle operating parameters and road conditions [14].

Performance characteristics of static and dynamic seats are mostly evaluated through field or laboratory tests. Field tests, however, are more expensive and difficult to interpret due to lack of controlled test conditions. The seats are thus mostly evaluated in laboratory under controlled test conditions. The international standard ISO 7096 [56] outlines the laboratory evaluation method for operator seat-vibration for earthmoving vehicles. This Standard specifies a laboratory-based method for measuring and evaluating the effectiveness and acceptance level of the seat in reducing the vertical whole-body vibration transmitted to the operators of earthmoving machines at frequencies between 1 and 20 Hz. The standard also specifies the input spectral class, which is based on representative measured data from vehicles in typical working conditions. The laboratory test is more severe than the typical vibration environment as the input spectral class is a representative envelope for the vehicles within the class. The standard uses two different criteria for the evaluation of seats one being SEAT factor and the other is the maximum transmission ratio or the damping test in accordance with ISO 10326-1 [72].

The standard specifies the use of two subjects, one with body mass of 55 (-3 to 0) kg and another of 98 (0 to +3) kg. Each person shall adopt a natural position on the seat

and maintain this posture throughout the test. The evaluation of the operators seat according to ISO-7096 has been critically commented by Hinz [74]. The study recommended changing the selection of subjects according to the 5^{th} and 95^{th} percentile masses of the population of vehicle drivers instead of the fixed masses. The study also recommended the inclusion of several subjects near the 50^{th} percentile in order to assess the variability of the SEAT factor. The study also proposed for considering other anthropodynamic parameters for the selection of subjects, such as body height and body mass supported by the seat.

1.2.6 Anthropodynamic manikins

Current laboratory-based assessment methods for seats involve repetitive tests with representative sample of human subjects. Laboratory exposure of human subjects to vibration requires careful consideration of safety, and ethical, medical and legal issues, which necessitate expensive 'human-rated' vibration simulators. Moreover, this method also suffers from several disadvantages, such as large inter- and intra-subject variability, poor repeatability of the test results, and poor objectivity, as the choice of a small group of test persons cannot be regarded as being representative. Moreover, the test results can be influenced by even slight variations in the test conditions.

Owing to the ethical concerns and poor repeatability of the measurements with human subjects, considerable efforts have been mounted in developing human body surrogates in the form of mechanical systems for assessment of coupled seat-occupant systems dynamics. Matthews [11] developed a single-DOF mechanical manikin, comprising a mass suspended by four elastic bands from a rigid frame. The damping was adjusted such that the vibration transmissibility of a suspension seat loaded with the

manikin was in agreement with that of the seat loaded with a person. Matthews [11] and Tomlinson [13] compared the results attained with a single subject and showed an agreement between the acceleration transmissibility magnitudes of seat-human and seat-manikin systems in the 0 to 3 Hz.

Suggs [12] developed two-DOF human body simulator on the basis of the measured DPMI responses of the human body. The manikin comprised of two masses supported by coil compression springs and viscous dampers on a common rigid frame. The vibration transmissibility of seats measured with the manikin agreed reasonably well with that of the seat loaded with human subjects under high magnitudes of vibration. Mansfield and Griffin [14] developed a single-DOF anthropodynamic manikin to measure the dynamic characteristics of a seat in a car traveling over six different roads. The vibration performance of the seat was also measured using twelve human subjects. The results showed no significant differences between the SEAT values measured using the manikin and the subjects. The variability in the SEAT values was also less for manikin when compared with that for the human subjects.

The mechanical manikins in general consist of rigid platform that interfaces with the elastic cushions. The manikins thus yield poor contact with seats designed with contoured cushions. Gu [15] developed a manikin that employed an elastic lower torso to attain better coupling between the manikin and the seat cushion. The manikin was designed to provide weight distribution comparable to that of a male 50^{th} percentile human subject. The vibration isolation data for a sear loaded with the manikin were compared with those attained with the seat loaded with three human subjects of different

masses. The comparisons revealed good agreements in resonant transmissibility under medium levels of random excitations.

Huston [16] designed and constructed a single-DOF human analog, incorporating a spring-mass-damper system. The sprung mass was attached a horizontal steel plate through linear bearings together with a spring and a damper. The manikin permitted the use of different springs and damping fluids of varying viscosity to vary the properties of the manikin. The upper and lower masses could also be varied. Experiments were performed with a 93 kg human subject, a rigid mass of 93 kg and the manikin weighing 93 kg. The results showed that the natural frequency of the seat with human subject was reproducible by the manikin, whereas the rigid mass showed a slight decrease in the resonant frequency. The rigid mass also overestimated the seat transmissibility in the lower 1/3 octave frequency bands whereas a good correlation was found with manikin.

The mechanical manikins generally exhibit nonlinear properties due to friction inherent in the guiding and damping mechanisms. Lewis [17] explored alternative damping and springing devices so as to overcome the non-linear phenomena, like friction, which had performance limitations for the previously developed anthropodynamic manikins. The study suggested the use of viscous damping in the manikins to realize the apparent mass modulus close to that of an ideal system up to 25 Hz with minimal sensitivity to excitation magnitudes.

Toward [18] developed a prototype single-DOF anthropodynamic manikin. Comprising a 46 kg moving mass constrained to move vertically along two steel precision shafts. These shafts were attached to two aluminum plates at the top and the base to make up for the 7.4 kg static mass. Four compression springs were fitted between

the moving mass and the base plates together with a low friction viscous damper, which in a previous study [17] had shown to give linear response over a range of input magnitudes. The validity of the prototype manikin was assessed through measurements performed on three different seats including an automotive static seat and two suspension seats. The data acquired for the seats loaded with the manikin, an equivalent rigid mass and human subjects were compared. Apart from the SEAT values, the inter-and intra-subject variability of the data were also quantified. The results showed that the manikin yields results similar to those obtained with human subjects, but with a greater repeatability. Although the rigid mass also gave reproducible measurements of the seat transmissibility and SEAT values, the transmissibility values were not consistent with those obtained using human subjects.

The passive manikins [11-18] constructed as single-DOF systems neglect the higher frequency body modes. Moreover, the passive manikins often suffer from unwanted nonlinearities, due to friction or nonlinear damping thus preventing the use of the dummy at low excitation levels. The vast majority of the manikins could not account for the variations in the body mass. A few studies have thus explored active anthropodynamic manikins to eliminate the nonlinear effects [20, 21]. Cullmann, Wölfel [20] designed an active vibration manikin to characterize the seated human response. The study performed experiments with a car seat exposed to broad band excitations of three different magnitudes, while the manikin was configured for the 5^{th}, 50^{th} and 90^{th} percentile body masses. Measurements were also performed with 20 male and 20 female subjects. The comparisons of the results attained with the manikin and human subjects revealed that the manikin could predict the human responses reasonably well.

Lewis [21] developed an actively controlled prototype manikin for measuring the vibration transmissibility of seats in vehicles. The manikin provided means of varying stiffness and damping forces as a function of excitation frequency to mimic a multi-DOF dynamical system and thus the APMS responses of human subjects of different body mass. The experiments performed with four different seats loaded with manikin and seven human subjects revealed that vibration transmission measurements with the manikin were more repeatable than with either the group of seven subjects or with repeated measurements using same subject. The SEAT values obtained under different excitations revealed good agreements between the values attained with the manikin and human subjects.

1.3 Scope and Objectives of the Dissertation Research

The overall objective of this investigation is to contribute towards development and standardization of anthropodynamic manikins, and a methodology for laboratory assessments of seats and vehicle vibration. This is sought via systematic experimental and analytical analysis of two prototype passive anthropodynamic manikins developed by INRS in France and BauA in Germany. The specific objectives of the study include the following:

(i) Characterize and the apparent mass response of the manikins under different excitations, and evaluate their APMS prediction abilities for various body masses.

(ii) Evaluate the vibration isolation performances of the seat-occupant, seat-manikins and seat-inert mass systems using different suspension seats and representative excitations of different vehicles.

(iii) Conduct a thorough analysis of the measured data to assess the suitability of manikins for applications to different seats, vehicular excitations, and body mass.

(iv) Develop a linear analytical model of one of the prototype manikin; evaluate its APMS response and demonstrate its validity.

(v) Perform parametric sensitivity analysis and identify design parameters of the manikin to realize the idealized APMS responses for the 5^{th}, 50^{th}, and 95^{th} percentile male populations.

(vi) Establish reliable references values as a function of excitation magnitude for effective design of anthropodynamic manikin.

1.4 Organization of the Dissertation

The present dissertation is organized into five chapters, illustrating the systematic development of the preceding objectives. Chapter 1 presents the review of the reported relevant studies for building the essential knowledge of suspension seats, prevalent test methodologies, and the anthropodynamic manikins, which formed the basis for the scope of the dissertation.

Chapter 2 presents the experiment design involving the synthesis of selected vibration excitations, instrumentation, data acquisition and analysis for characterizing the apparent mass responses of the manikins. The results are discussed to highlight the influence of vibration magnitude and manikin mass on the dynamic response of the manikins. The results are further compared to the standardized response of the seated human subjects exposed to WBV to assess the APMS prediction abilities of the manikins.

Chapter 3 presents the experimental design involving synthesis of selected vehicular spectra, instrumentation, data acquisition and analysis of performance characteristics of the candidate seats loaded with human subjects, inert mass and manikins. The measured data are analyzed to derive the isolation effectiveness of different seats-load combinations and excitations. The results are discussed to highlight the comparisons of responses of the seat-manikin, seat-mass and seat-human systems

under broad-band as well as vehicular excitations. The relative performance characteristics of candidate seats are further evaluated through the analysis of the deviation in the SEAT values attained with manikins, inert mass and human subjects.

In chapter 4 a mathematical model of one of the manikin is formulated and validated using the measured data. Parametric sensitivity analyses are performed to identify design refinements that could enhance the APMS prediction abilities of the manikin. Reliable reference values as a function of excitation magnitudes are established.

The major highlights and contributions of the study together with the conclusions and recommendations for future work are presented in Chapter 5.

CHAPTER 2

APPARENT MASS CHARACTERIZATION OF ANTHROPODYNAMIC MANINKINS

2.1 Introduction

The vibration attenuation effectiveness of a suspension is known to be affected by its dynamic interactions with the seated human body, apart from the nature of vehicle vibration [1, 5, 7, 55, 57]. The vibration transmission performance of a seat is thus assessed upon consideration of the coupled seat-occupant system dynamics [7, 9, 43, 57]. Owing to the complexities associated with dynamic characterization of the human occupant, the performance characteristics of suspension seats are mostly assessed through either laboratory or field trials. The field methods could yield data with relatively large variability's and thus pose difficulties in the interpretation of results. The laboratory-based methods on the other hand, may involve repetitive trails with a number of human occupants, and raises certain ethical concerns about subject safety associated with vibration exposure. Moreover, the dynamic interactions of the human occupant with a suspension seat would depend upon many intrinsic and extrinsic factors, such as occupant anthropometry, nature of vibration, seat geometry and postural support conditions. The strong influences of these factors have been widely reported in many studies on biodynamic responses of seated occupant to vibration [21, 27, 29, 33]. The laboratory or field based methods may thus require a large sample of human occupants and wide-range of test conditions. The measured data frequently yield large intra subject variability due to variations in individual's anthropometry and postural tendencies. The International Standard (ISO-7096) outlines a laboratory based test method for suspension seats for construction machinery. The method requires vibration attenuation assessment of seats

with subjects weighing 55 kg (-3 to 0) and 98 kg (0 to +5), while exposed to representative vibration spectrum of a particular class of vehicle.

Alternatively, considerable efforts have been made to develop mechanical-analogues model of the seated body on the basis of the laboratory-measured biodynamic responses, such as driving-point impedance or apparent mass or seat-to-head vibration transmissibility [21-24, 27]. Such models, when integrated to the analytical model of the seat suspension permit design of the suspension seat and analysis of the coupled seat occupant system [9, 10, 43, 57]. The result of the coupled models, however, are known to differ from the measured seat-occupant responses in many type of seats [9], while a reasonably good correlations between the model and measured results have been demonstrated for a few low frequency suspension seats [57]. The considerable response errors of the seat-occupant model may be attributed to large inter-subject variability of the biodynamic responses of the occupant, and lack of consideration of the coupling between elastic seat surface and soft buttock and back tissues of the seated body.

Alternatively, several anthropodynamic manikins have been developed to replace the seated human occupant for assessment of coupled seat occupant system [11-20]. A few prototype manikins have been recently developed in Europe, which characterize the biodynamic characteristics of seated occupants of three different body masses in the vicinity of 5^{th}, 50^{th} and 95^{th} percentile male population. This chapter briefly describes the design of two prototypes anthropodynamic manikins are measured in laboratory and compared with those recommended in DIN-45676 and ISO-5982 standards. The suitability of manikins for the vibration performance assessments of suspension seats are discussed on the basis of their biodynamic response prediction abilities.

2.2 Description of the Prototype Manikins

Two different prototype anthropodynamic manikins developed by Institut Nationale de Recherché en Securite (INRS) in France and Federal Institute for Occupational Safety and Health (FIOSH, German acronym BAuA) in Germany were loaned to Institut de recherché Robert-Sauve en Sante et en securite du travail (IRSST) for their potential applications in evaluating suspension seats. The prototype provided by INRS is referred to as manikin 'F', while that provided from FIOSH is referred as manikin 'G'. Both the manikins were designed with different combinations of mass, spring and damper elements to mimic the biodynamic response of the seated occupants. Moreover the manikins also offered sufficient flexibility to achieve static seated mass and biodynamic response of subjects with three different standing masses; 55, 75 and 98 kg.

2.2.1 Description of Manikin G

The manikin G, pictorially shown in Figure 2.1 (a), comprises of a seat base, a base frame and a load platform supported on a set of springs and a damper. The seat base is made of wood that can be placed on elastic seat cushions. A base frame is fixed to the base plate and load platform is attached to the base frame through an arm pivoted to the base frame. The load-platform arm is further supported on a damper and a set of springs. The load platform is designed to hold different masses to realize total manikin mass equivalent to the body mass supported by the seat. For this purpose, six different steel plates of masses of 3, 4, 5, 15, 15 and 15 kg are provided. Different combinations of these masses are used to realize equivalent masses due to body masses of 55, 75 and 98 kg. Two additional masses (2.5 kg each) are also attached to the base frame to realize mass equivalent to the 98 kg body mass.

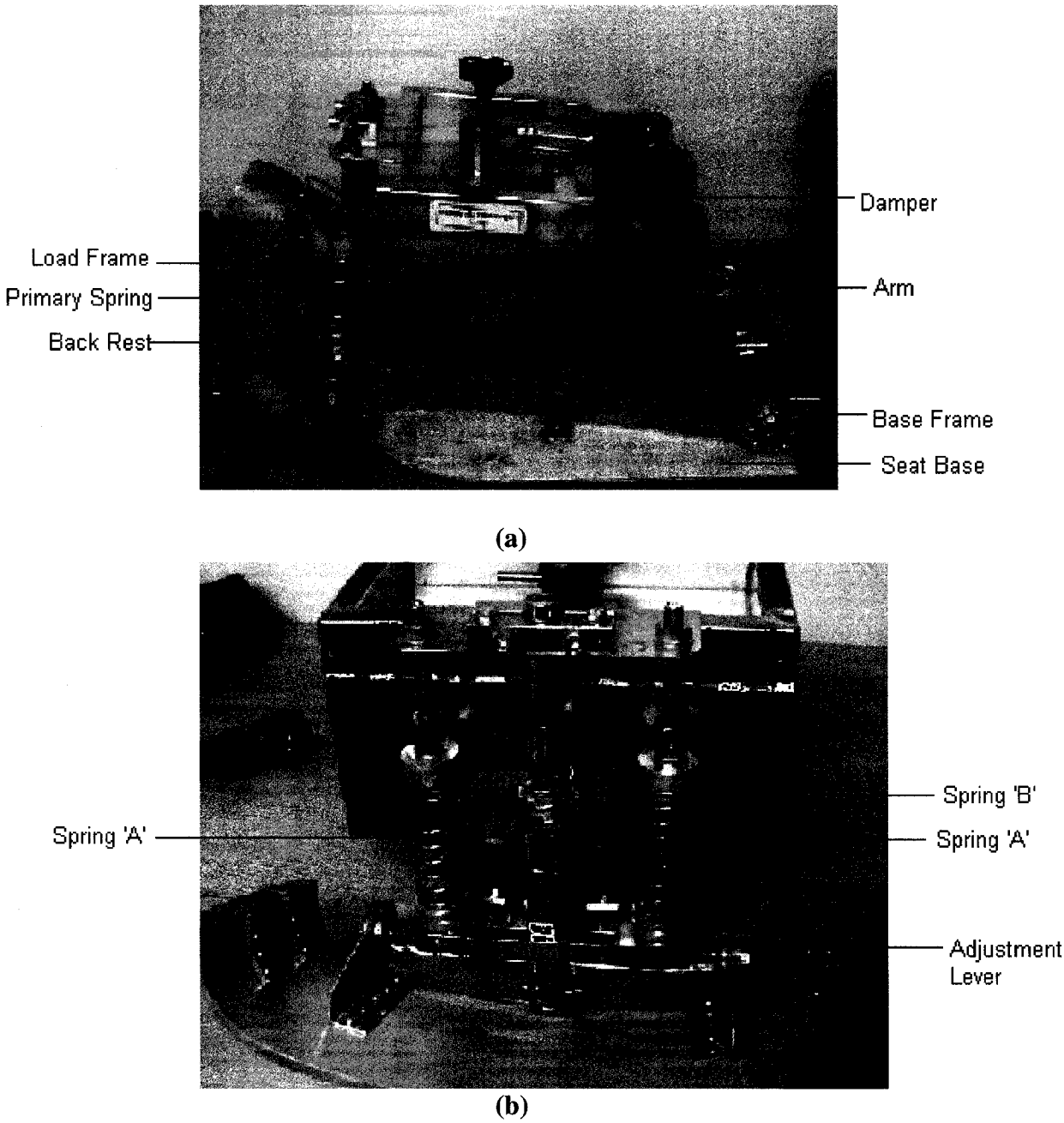

Figure 2.1: Pictorial view of manikin G: (a) side-view; (b) rear-view

The base frame of the manikin G, when placed on seat is adjusted to ensure its orientation along the horizontal axis. An adjustment mechanism is also provided to realize horizontal position of the base frame, when the manikin is used on seats with considerable inclination of cushion. The manikin also comprises of a curved wooden back support, which could rest against the seat backrest. A total of three coil springs, constrained along the vertical axis are provided, as illustrated in Figure 2.1 (b) of the manikin G. Two springs located at the extremities (spring A) are used when the manikin is configured to represent body masses of 55 and 75 kg. The middle spring (spring B) is also used for 98 kg body mass configuration. Selected plate masses are inserted in the load platform using the centering bolt as shown in Figure 2.1 (a), to realize desirable configuration for different masses. Table 2.1 summarizes the masses and springs to be used for the 55, 75 and 98 kg body mass configurations. The masses are fastened to the load platform using the centering bolt as shown in Figure 2.1 (a). The total manikin is also presented in the table, upon consideration of the masses due to the base plate, base frame and the load platform of 19 kg. This manikin mass represents the body mass to be supported by the seat cushion. Studies have shown that mass resting on the seat is 73 % to 75 % of the total mass of the body [21, 27]. The total mass of the manikin G, however, tends to be higher than the reported percent body mass supported by the seat. The total manikin mass for the 55 kg body mass configuration is higher than the total body mass, and would be expected to yield considerably higher magnitude of the biodynamic response. The configuration corresponding to higher body mass of 98 kg, however, yields somewhat reasonable manikin mass that equals 79.6 % of the body mass.

Table 2.1: Selection of masses and springs for manikin G

Body mass configuration (kg)	55	75	98
Masses	15+15+4+3	15+15+5+4+3	15+15+15+5+4 Two additional masses at the base plate (2.5 kg each)
Springs	A,A	A,A	A,B,A
Manikin Mass (kg)	56	61	78
Percent body mass (%)	101.82	81.33	79.60

2.2.2 Description of Manikin F

The manikin 'F', pictorially shown in Figure 2.2 (a), comprises of a wooden seat base, an aluminum base frame attached to the wooden seat base, springs, masses and two hydraulic dampers. An aluminum back support is also provided to position the manikin against the backrest of the seats. The manikin is placed on the seat, the base frame and the principal mass M1 are oriented along the horizontal axis by using the adjustable articulation provided with the base frame. The base frame supports three different masses namely, M1, M2 and M3, as shown in Figure 2.2 (a). The mass M1 serves as the principal mass and is supported on the base frame through three pairs of springs, denoted as K1, K12, and K13. A particular pair of springs is used for a selected body mass configuration. The base value of mass M1 corresponds with the 55 kg body mass configuration. Two plate masses of 9.5 and 20.5 kg can also be appended to the bass mass M1 to realize 75 and 98 kg body mass configuration respectively. For the 55 kg configuration, the principal mass M1 is supported on the spring pair, labeled as 'K1'. For the 75 kg configuration, two pairs of springs (K1 and K12) are used to support the

principal mass M1 with an additional mass of 9.5 kg. All the three pairs of springs (K1, K12, and K13) are used for 98 kg configuration involving the base mass M1 and both plates of 9.5 and 20.5 kg.

Apart from the adjustable principal mass, the manikin comprises of two fixed but independent masses M2 and M3, as shown in figure 2.2 (a). The mass M2 (5 kg) is guided by two vertical columns, and is supported on two coil springs (K2) and a viscous damper, as shown in the rear pictorial view in Figure 2.2 (c). The mass M3 (2 kg) slides on a vertical shaft and is supported on a single coil spring (K3). Four cylindrical masses, total of 4 kg, are also attached to the wooden seat base which adds to the base mass. While these masses are retained at the seat base for 55 and 75 kg body mass configurations, the 98 kg configuration requires that these masses be added to the principal mass M1.

The manikin F has two dampers, one of the hydraulic dampers is inserted between the mass M2 and the seat base and the other hydraulic damper which is also the principal damper 'C1' is supported between the principal mass M1 and the base frame. This damper, as shown in Figure 2.2 (a), is oriented in the horizontal axis. An L-shaped linkage with a pivot fastens the horizontal damper to the mass M1. The position of the principal damper is varied for different body mass configurations. These positions are marked with color codes on the fixed damper support. The white, green and red colored settings correspond to 55, 75 and 98 kg body mass configurations respectively.

Table 2.2 lists the total manikin mass corresponding to the three body mass configurations, the springs and the masses M1, M2, M3. The table also presents the manikin mass as the percent of the standing body mass. The results suggest the manikin

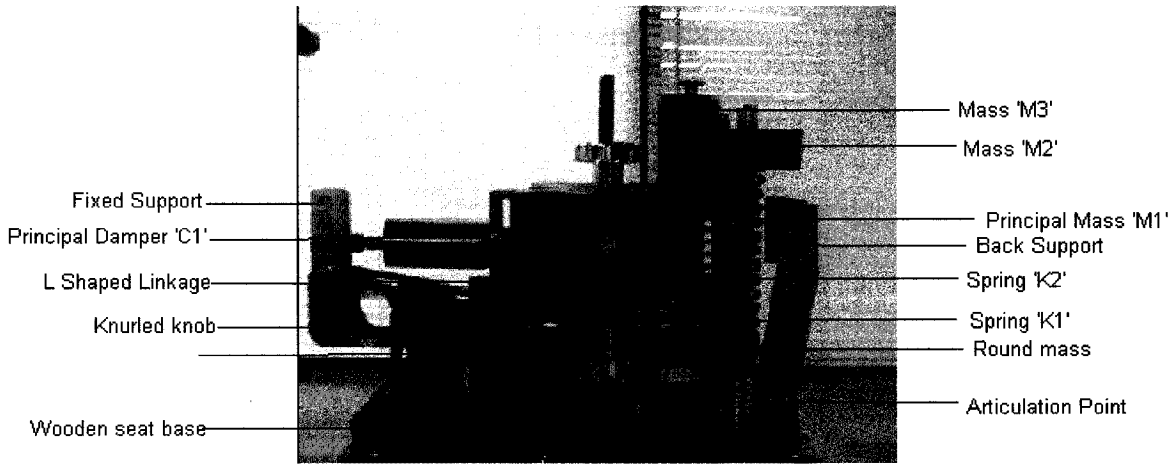

(a)

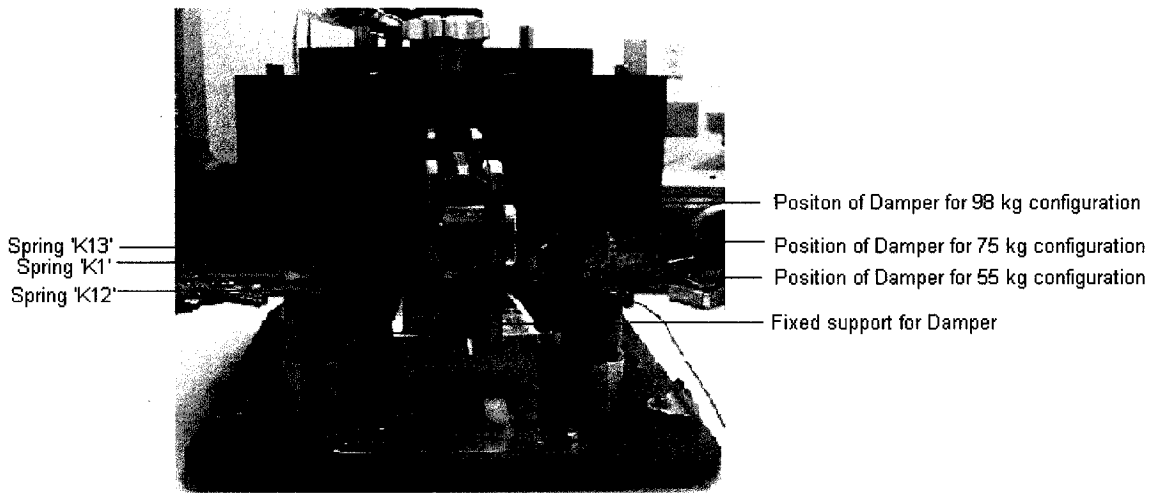

(b)

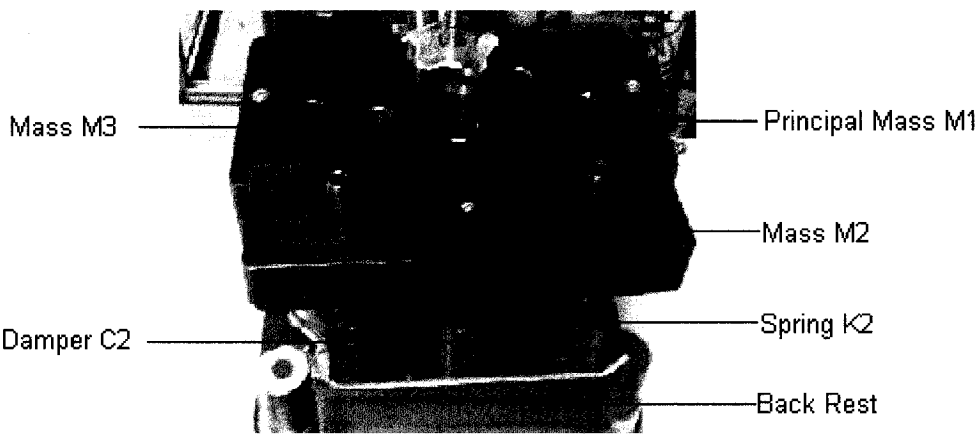

(c)

Figure 2.2: Pictorial views of manikin F: (a) side-view; (b) front view; (c) rear view

mass represents 81.8, 72.6 and 76.5 percent of the body mass corresponding to 55, 75 and 98 kg configurations, respectively. These are close to the reported range of body mass supported by a seat.

Table 2.2: Selection of masses and springs for manikin F

Body mass configuration (kg)	55	75	98
Springs	K1, K2, K3	K1, K12, K2, K3	K1,K12, K13, K2, K3
Manikin Mass (kg)	45	54.5	75
Percent body mass (%)	81.81	72.6	76.5

2.3 Characterization of the biodynamic response of the manikins

The anthropodynamic manikins were initially assessed in view of ability to predict the biodynamic response of seated occupant, exposed to vertical vibration. The biodynamic responses of both the manikins are characterized in terms of apparent mass relation the force response to an acceleration excitation at the manikin-seat interface such that

$$M(j\omega) = \frac{S_{Fa}(j\omega)}{S_a(j\omega)} \tag{2.1}$$

where, $M(j\omega)$ is the complex apparent mass, $S_a(j\omega)$ is the auto spectral density of acceleration $a(j\omega)$ due to excitation, $S_{Fa}(j\omega)$ is the cross spectral density of the force response $F(j\omega)$ at the driving-point and $a(j\omega)$, ω is the circular frequency of excitation and $j = \sqrt{-1}$.

The apparent mass (AM) characteristics of the manikins configured for three body masses were measured in the laboratory using the methodology described in the reported studies [21, 27, 33]. The measured apparent mass magnitude and phase responses of the manikins for each body mass are compared with the responses recommended in DIN 45676 [36] and ISO 5982 [35] to assess their apparent mass prediction performance.

2.3.1 Experimental Methods

The apparent mass characteristics of both manikins were investigated using the Whole Body Vehicular Simulator (WBVVS) available at the IRSST laboratory. The simulator is pictorially shown in Figure 2.3. The simulator comprises a vibration platform supported on two servo-hydraulic actuators, which are oriented to generate motions along the vertical axis alone. A two channel servo-control is used to generate different types of deterministic and random vibrations for assessing the dynamic responses of the manikins and seats.

The apparent mass response characteristics of a manikin alone were measured by placing it on a rigid seat. For this purpose, a rigid seat, available in the IRSST laboratory, was installed on the vibration platform of the WBVVS. The test rigid seat provided a seat height of 424 mm and comprised a flat (406 mm wide and 410 mm deep) seat pan. The seat did not have a backrest. The rigid seat was mounted on a force platform, which was fixed to the WBVVS using four strain gauge type load cells. The signal from the load cells were summed together to measure the vertical force response of the manikin and the seat structure. A single-axis accelerometer (B&K 4381) was installed on the seat pan to measure acceleration due to vertical excitation. Another single axis accelerometer (B&K 4381) was also placed on the load platform of manikin G to measure the vibration

transmitted to the masses. A total of three accelerometers were used to measure acceleration responses of the three moving masses of manikin F.

The apparent mass characteristics of both manikins were measured under broad-band white noise random excitations in the 0.4 – 20 Hz range.

Figure 2.3: Pictorial View of the Whole Body Vertical Vibration Simulator with rigid seat

The measurements were performed under two different magnitudes of random vibration, defined in terms of the overall rms acceleration, given by:

$$a_{rms} = \sqrt{\frac{1}{T}\int_0^T \ddot{x}^2(t)dt} \tag{2.2}$$

where, a_{rms} is the overall rms acceleration and $\ddot{x}(t)$ is the instantaneous rms acceleration measured at the seat pan and T is duration of measurement.

The excitation signals were synthesized to realize overall rms accelerations of 0.5 and 1 m/s^2 for characterizing the apparent mass response of manikin G. the apparent mass response of manikin F was measured using higher excitations, 1 and 2 m/s^2, due to relatively higher friction of the damper seals. Figure 2.4 illustrates power spectral density (PSD) acceleration due to different excitations in the 0.4-20 Hz frequency range. The figure shows nearly flat acceleration PSD due to excitation in the frequency range of interest.

The apparent mass characteristics of both manikins were measured for all three body mass configurations under selected excitations. Table 2.3 shows the test matrix for characterizing the apparent mass response of both the manikins. The total force due to the manikin and the rigid seat and the excitation acceleration were used to derive the apparent mass magnitude and phase responses of the coupled seat and manikin, using EQ (2.1). The apparent mass of the seat structure alone was also measured in the similar manner under same excitations, which was subsequently applied to perform inertial correction to derive the apparent mass responses of the manikin alone [43]. The measured force and acceleration signals were acquired in the multi-channel Pulse system and analyzed using 50 Hz and frequency resolution of 0.0625.The coherence between the two

signals was also monitored during the experiments, which was observed to be nearly a unity value.

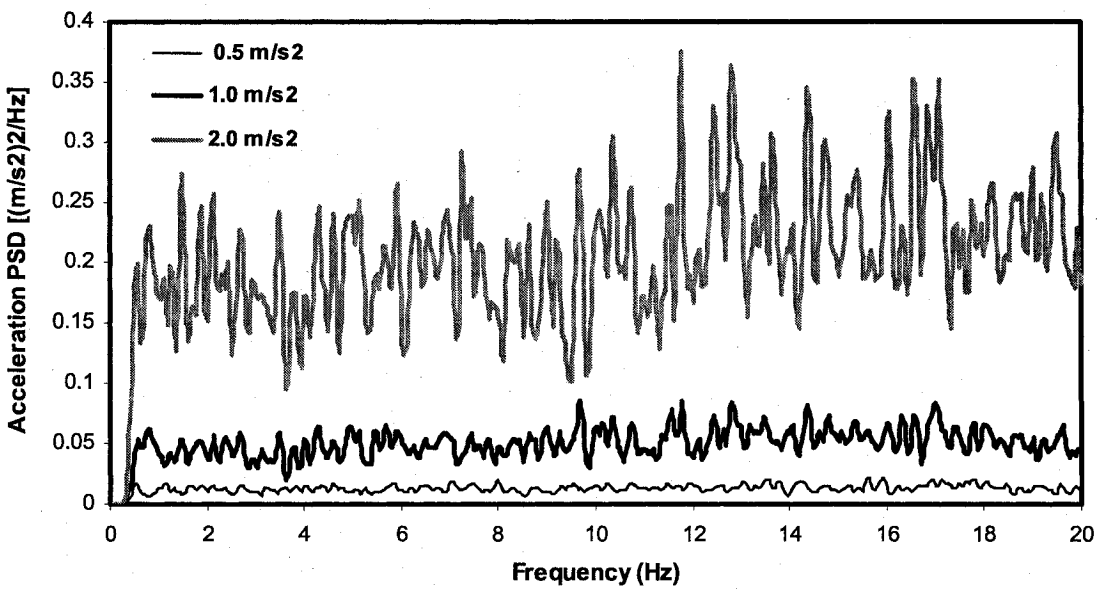

Figure 2.4: PSD of acceleration due to synthesized white noise random excitations

Table 2.3: Test matrix for characterizing the apparent mass response of the manikins

Excitations, a_{rms} (m/s^2)	Manikin G			Manikin F		
	55 kg	75 kg	98 kg	55 kg	75 kg	98 kg
0.5	×	×	×	-	-	-
1	×	×	×	×	×	×
2	-	-	-	×	×	×

2.3.2 Apparent Mass of the seat and supporting structure

The measurements were initially performed to characterize the apparent mass response of the rigid seat (M_0). A strap was used to restrain the manikin's base plate to the seat pan. The WBVVS was operated to generate broad-band random vibration of desired a_{rms}, and the force and acceleration signals were acquired in the 6-channel signal acquisition and analysis system (PULSE). The measured signals were analyzed to determine the apparent mass magnitude (M_0) and phase response of the seat structure alone in the 50 Hz bandwidth with frequency resolution of 0.0625. The measurements revealed identical apparent mass response, irrespective of the excitation magnitude. Figure 2.5 illustrates the apparent mass magnitude and phase response of the seat structure, which shows constant magnitude and negligible phase in the 0.4-20 Hz frequency range. The measured apparent mass magnitude is in the order of 36.5 kg, identical to the static mass of the seat and its supporting structure. This apparent mass response was used to perform the inertial correction of the apparent mass response of the manikin and the seat structure.

2.3.3 Measurement of Apparent Mass of Manikins

The selected manikin was placed on the rigid test seat and appropriately adjusted to the desired body mass configuration. A strap was used around the base plate and the seat pan to ensure consistent adherence of the manikin with the rigid seat pan. The WBVVS was operated to generate a selected excitation, and the force and acceleration signals were acquired in the 6-channel PULSE system. The measured data were analyzed to compute the apparent mass due to coupled manikin and the seat structure using the formulation described in EQ (2.1).

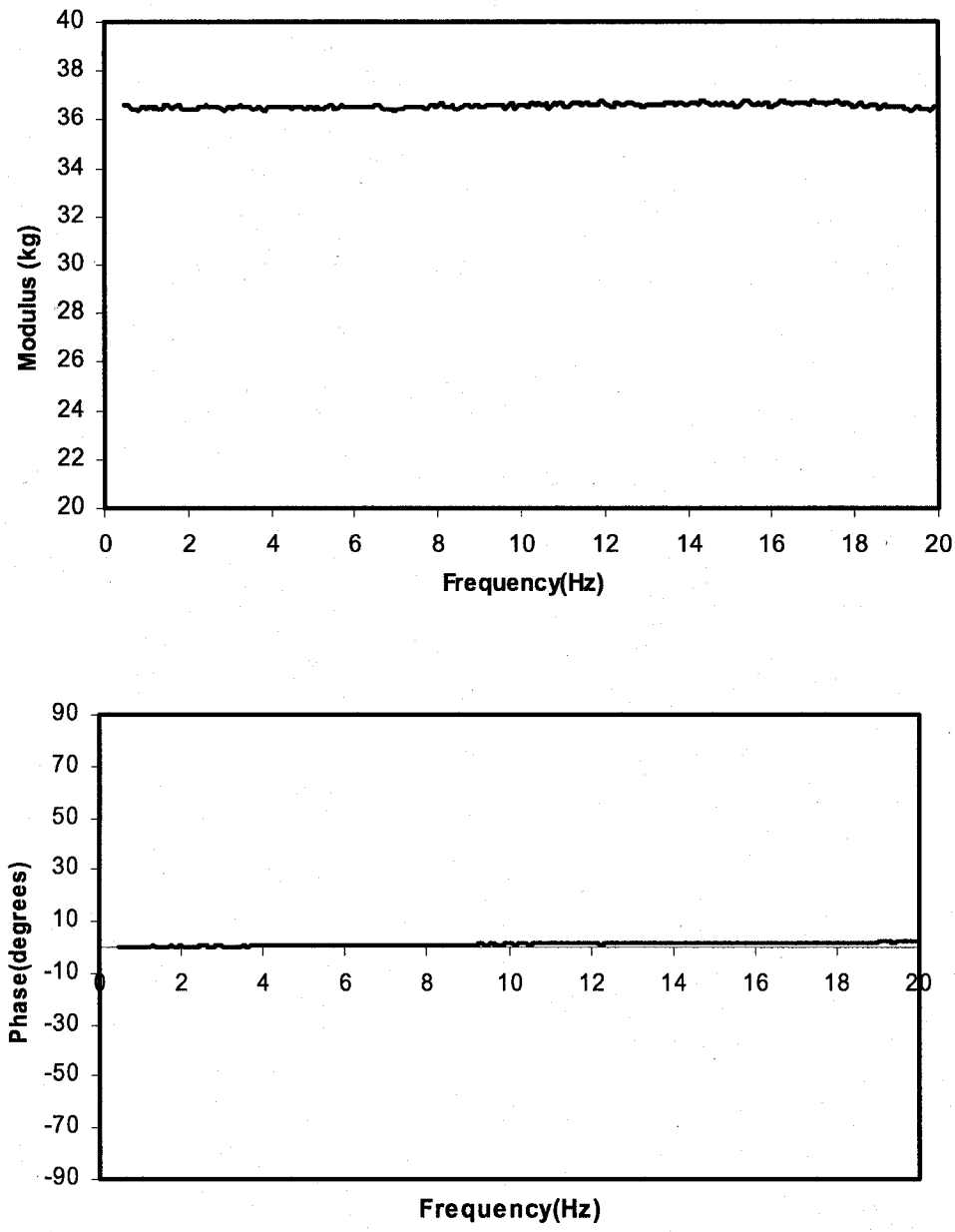

Figure 2.5: Apparent Mass response of the rigid seat under white noise random excitation of: (a_{rms} = 1 m/s^2)

The apparent mass response of the manikin alone was then derived upon applying the apparent mass of the seat structure alone, such that

$$M(j\omega) = M_c(j\omega) - M_0(j\omega) \tag{2.3}$$

where $M_c(j\omega)$ is the apparent mass of the coupled manikin-seat system and $M(j\omega)$ is that of the manikin alone.

A Pulse language (PL) program was used to perform the above correction automatically, which permitted direct acquisition of the corrected apparent mass response. The coherence of the measured force and acceleration signals in the entire frequency range was also monitored, which generally showed near unity value of the coherence. The acceleration responses measured at different masses were also analyzed to determine the vibration transmitted to each mass. The measured data were smoothened using the moving average technique.

Apart from many other factors, the apparent mass responses of the seated human occupant exposed to vertical vibration are known to be most significantly influenced by variation in the body mass [1, 21, 33]. The apparent mass responses are thus frequently normalized with respect to the seated body mass in an attempt to reduce the body mass induced variability of the measured data [1, 10, 21, 43, 76]. The measured data for both the manikins corresponding to each body mass configuration are also normalized with respect to the respective static mass supported by the seat. The normalized apparent mass responses are evaluated to study the effects of excitation magnitude. The apparent mass responses of both manikins are compared with those reported for the human subjects to evaluate their apparent mass prediction abilities.

2.4 Apparent Mass response of the anthropodynamic manikins

The force and acceleration data acquired at the driving-point at the seat-manikin interface are analyzed to determine the apparent mass responses of both manikins corresponding to each mass configuration, using EQs (2.1) and (2.3). Figure 2.6 illustrates the apparent mass response of manikin G configured for 55, 75 and 98 kg body mass configuration and subject to 0.5 and 1 m/s^2 white noise random excitations. The apparent mass magnitude near the low frequency of 0.4 Hz corresponds to the static masses of the manikin, irrespective of the excitation magnitude. The apparent mass magnitude increases with the excitation frequency until it approaches its peak value near the primary resonant frequency. The results show primary resonant responses around 4 Hz, 3.7 Hz and 4.2 Hz, respectively for the 55, 75 and 98 kg body mass configurations.

The magnitude responses decreases rapidly at frequencies above the fundamental resonance and reveal secondary resonant peak in 7.6 Hz to 8.5 Hz range for all the three body masses. The frequency corresponding to the secondary peak, however, is influenced by the body mass and the excitation magnitude. The manikin G with the higher body mass configuration (98 kg) yields secondary peak at slightly lower frequency of 7.6 Hz, when subjected to 0.5 m/s^2 excitation. Both the 55 and 75 kg configurations under the same excitation yield identical secondary peak frequency of 8.5 Hz. The secondary resonant frequency and the corresponding magnitude of the 98 kg configuration tend to decrease slightly, when the excitation magnitude is increased to 1 m/s^2, suggesting non linear damping property of the manikin. The magnitude response increases with excitation frequency at frequencies above 15 Hz, irrespective of the body mass

configuration and the excitation magnitude. This suggests presence of a resonance above 20 Hz.

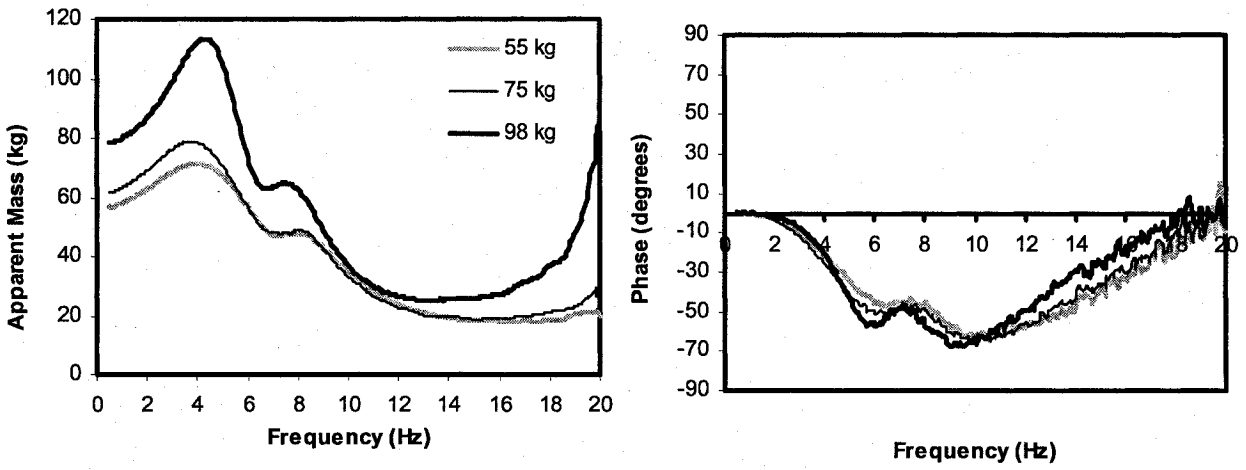

(a)

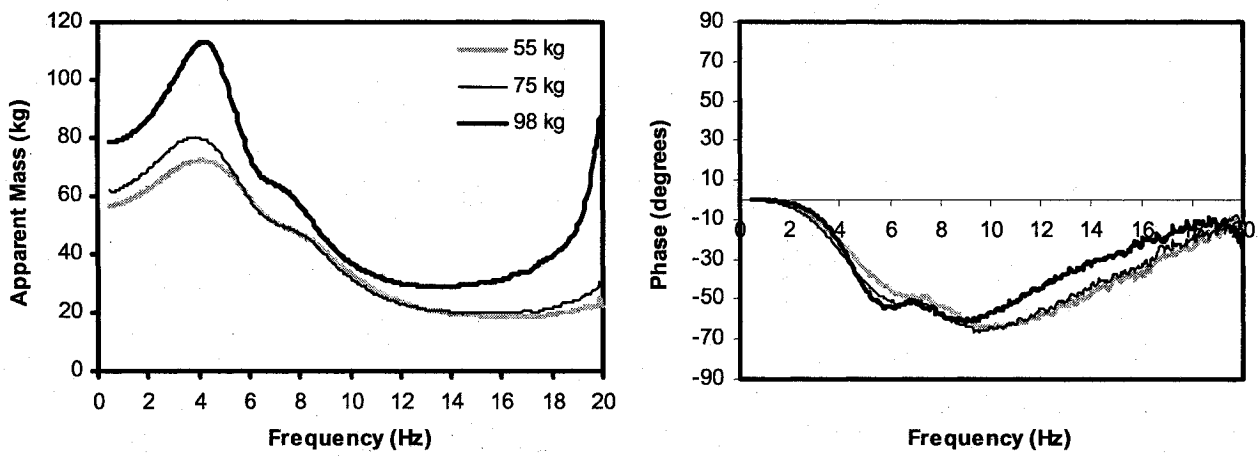

(b)

Figure 2.6: Apparent mass response of manikin F under white noise random excitations of: (a) a_{rms} = 0.5 m/s^2 (b) a_{rms} = 1 m/s^2

The apparent mass magnitude responses of the manikin G with 55 and 75 kg configurations are quite comparable, except at frequencies below 5 Hz, where the 75 kg configuration yields slightly higher magnitude. The 98 kg configuration, however, yields significantly higher magnitude in the entire frequency range. The peak magnitude of the 98 kg configuration is approximately 1.4 and 1.6 times those of the 55 and 75 kg configurations, respectively, for both magnitudes of excitation. The apparent mass phase response of the manikin decreases gradually with frequency and approaches near 70 degrees near 10 Hz, and gradually diminishes to zero with increasing frequency above 10 Hz. The phase response reveals only slight variations with the body mass and the excitation magnitude.

Figure 2.7 illustrates the apparent mass magnitude and phase responses of manikin F for the three body mass configurations and two excitation magnitudes. Unlike the apparent mass response of manikin G, the results show strong effect of excitation magnitude on both the magnitude and phase responses. The magnitude as well as phase responses to lower magnitude excitation (1 m/s^2) resemble those of a single-degree-of freedom (system), irrespective of the body mass configuration. The peak magnitude for the 98 kg configuration occurs near the resonant frequency of 5 Hz, while those for the 55 and 75 kg configuration occur near 5.75 Hz. The peak apparent mass magnitudes for all the body mass configurations are considerably smaller than those of the manikin G. The responses suggest considerably higher damping of manikin F configured for the 55 and 75 kg body masses. A further examination of the hydraulic damper revealed substantial seal friction, which was subsequently quantified in the order of 75 N. The

manikin F thus revealed frequent lock up of the damper, and thus lowers peak magnitude, particularly for the 55 and 75 kg configurations.

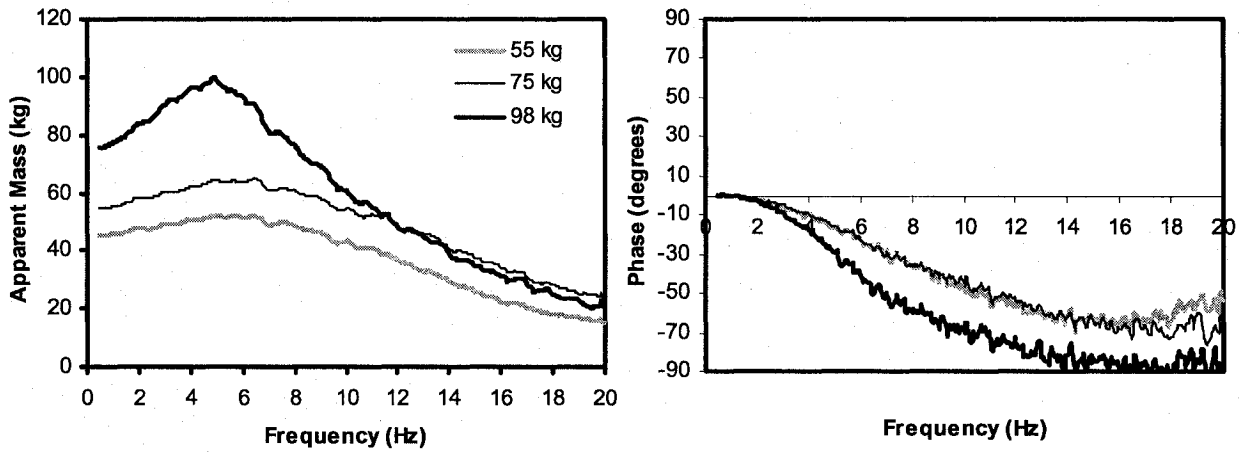

(a)

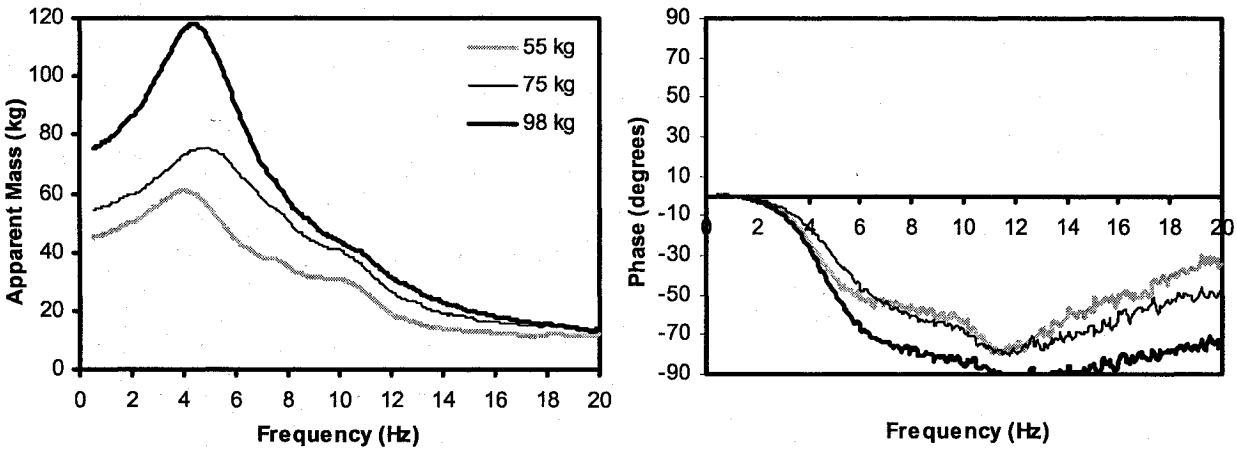

(b)

Figure 2.7: Apparent mass response of manikin F under white noise random excitations of: (a) a_{rms} = 1m/s^2 (b) a_{rms} = 2 m/s^2

The peak magnitudes increase considerably when the excitation is increased to 2 m/s^2 rms acceleration for all three configurations, as evident in figure 2.7(b). The response trends and the peak magnitudes are comparable with those of manikin G. The primary magnitude peaks occur in the vicinity of 4, 4.8 and 4.5 Hz respectively, for the 55, 75 and 98 kg configurations. The magnitude responses also reveal secondary peaks near 10 Hz, as observed for manikin G. The phase response trends under this excitation are also comparable with those observed for manikin G, while lower mass configurations yield lower phase response.

2.5 Factors affecting the apparent mass response of the manikins

The apparent mass responses of the seated human subjects are known to be influenced by many intrinsic and extrinsic factors in a highly complex manner. These include posture, muscle tension, vibration magnitude, back support condition, body mass and hands position [1, 21]. The influence of excitation magnitude and body mass on the apparent mass responses of the manikins is examined to assess their prediction abilities.

2.5.1 Influence of vibration magnitude

The reported studies have suggesting softening effect of the body with increasing vibration magnitude [21, 75]. The primary resonant frequency, considered as frequency corresponding to peak apparent mass magnitude, thus tends to decrease with increasing excitation magnitude. Moreover, the apparent mass magnitude response is strongly affected by the body mass [21, 33], which is also evident from figures 2.6 and 2.7. The measured magnitude responses are thus normalized with respect to the static mass of the respective manikin to study the effect of excitation magnitude alone. For the manikin G, the normalizing factors were taken as 56, 61, and 78 kg, which are the static masses for

the manikin G, for 55, 75, and 98 kg body mass configurations, respectively, as summarized in Table 2.1. It should be noted that the static mass for the 55 kg configuration exceeds the body mass supported by the seat, which is generally in the order of 73-75% [21]. For the manikin F the respective normalizing factors were taken as 45, 54.5, and 75 kg.

Figure 2.8 illustrates the normalized magnitude response of manikin G for the three body mass configurations. The results suggest very little effect of excitation magnitude on the magnitude response of manikin G for all the three mass groups. The effect of vibration magnitude on the normalized apparent mass magnitude is nearly negligible for 55 and 75 kg configurations; only a slight increase in the peak magnitude is observed when the excitation level is increased from 0.5 m/s^2 to 1 m/s^2. The normalized apparent mass response magnitude responses of the 98 kg configuration show negligible effect of the excitation magnitude.

Figure 2.9 illustrates the normalized magnitude response of manikin F for the three body mass configurations. The results suggest a strong influence of excitation magnitude on the magnitude response of manikin F for all the three mass groups. The normalized apparent mass responses for the 55, 75 and 98 kg configurations show a considerable decrease in the resonant frequency as the excitation magnitude is increased. The peak magnitudes, however, increase considerably when the excitation level is increased from 1 m/s^2 to 2 m/s^2. The magnitude responses to 2 m/s^2 level of excitation show sharp resonant peaks, when compared to those under 1 m/s^2 excitation. The frequent lock-up of the principal mass M1, was also observed during the experiments,

under lower excitation of 1 m/s^2, which resulted in relatively higher frequency corresponds to the peak magnitude and lower peak response.

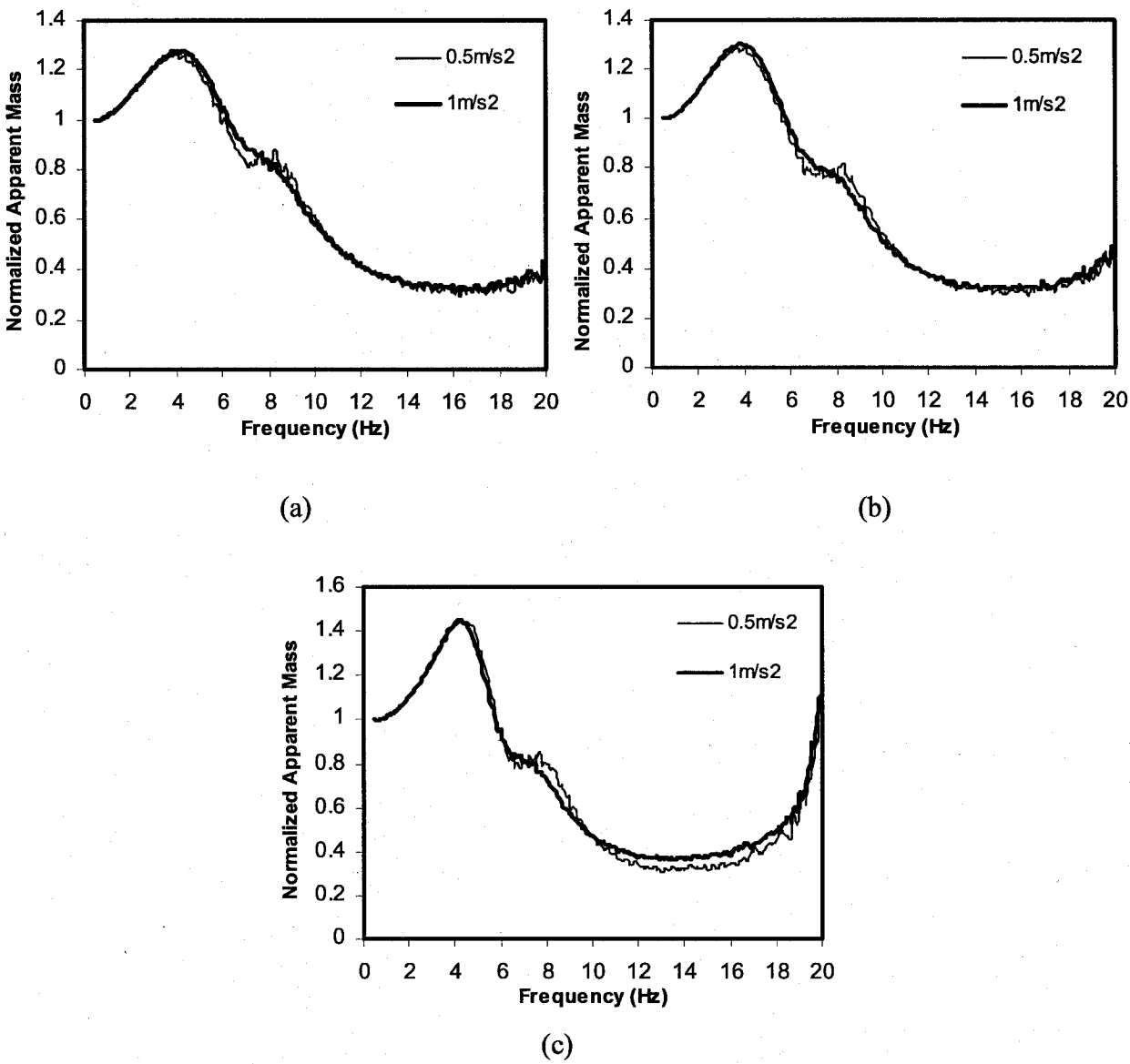

Figure 2.8: Influence of vibration magnitude on the apparent mass magnitude response of manikin G: (a) 55 kg configuration; (b) 75 kg configuration; (c) 98 kg configuration

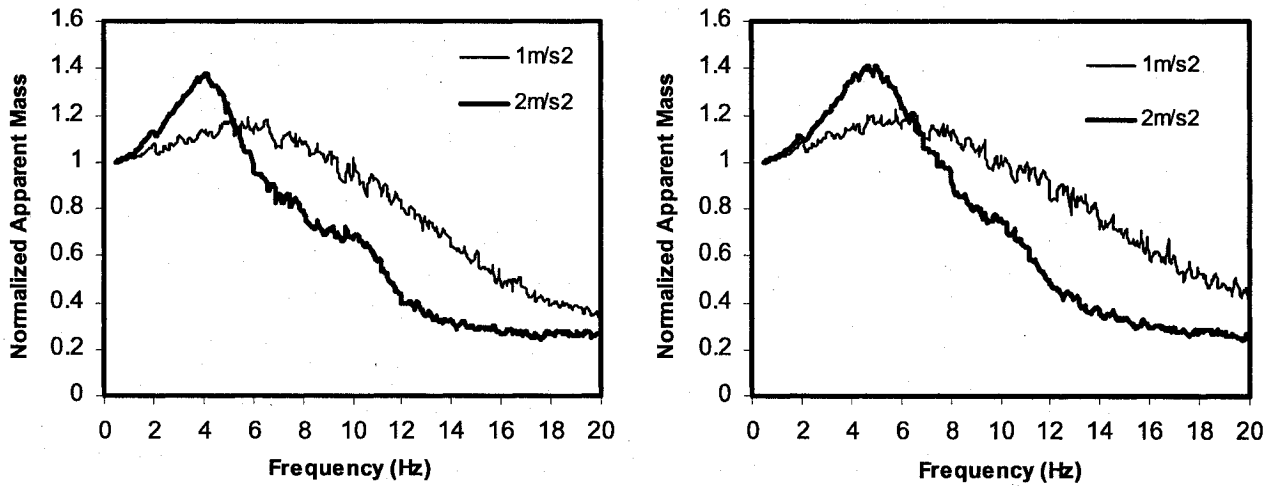

(a)

(b)

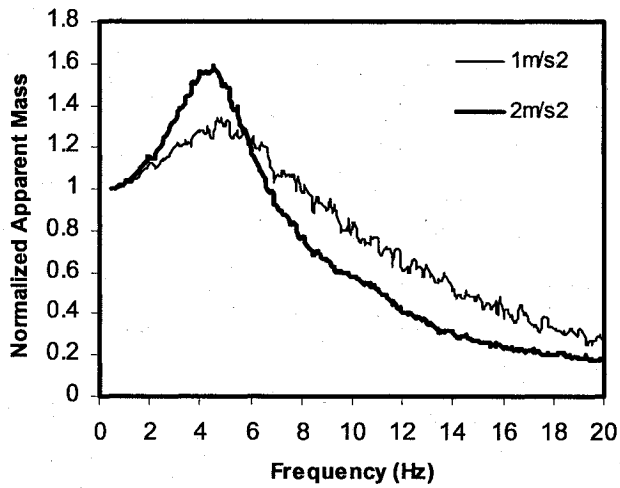

(c)

Figure 2.9: Influence of vibration magnitude on the apparent mass magnitude response of manikin F: (a) 55 kg configuration; (b) 75 kg configuration; (c) 98 kg configuration.

2.5.2 Influence of body mass

Many reported studies have shown a strong influence of body weight on the apparent mass response of seated body exposed to vertical vibration [21, 33]. The peak apparent mass magnitude response generally increases with increasing body mass, while the resonant frequency tends to decrease [1, 21, 74]. Figure 2.10 illustrates comparisons of normalized apparent mass responses of manikin G corresponding to three body mass configurations. The results suggest a strong influence of the body weight on the apparent mass response, irrespective of the excitation magnitude. For the 55 kg configuration, the apparent mass resonant frequency is observed near 4 Hz, which decreases slightly for the 75 kg configuration. The resonant frequency observed for the 98 kg configuration, however, tends to be slightly higher. The measured data thus do not show a clear tendency with regard to the effect of body mass on the primary resonant frequency. The lack of such trend has also been reported for the data acquired for seated human subjects exposed to vertical vibration.

The peak magnitude tends to increase lightly when the manikin mass is increased from the 55 to 75 kg configuration, irrespective of the excitation magnitude. The increase in the peak magnitude, however, is quite significant for the 98 kg configuration. This is mostly attributed to the significantly higher difference in the static masses due to 98 and 55 kg configurations. It should be noted that the total manikin mass for the 75 kg configuration is only 5 kg higher than that for the 55 kg configuration.

Figure 2.11 illustrates comparison of normalized apparent mass magnitude responses of the manikin F corresponding to three body mass configurations and two excitations (a_{rms} = 1 m/s^2 and 2 m/s^2). The responses under two excitations appear to be

distinctly different, which is mostly attributed to the high damper seat friction as discussed in the previous subsection.

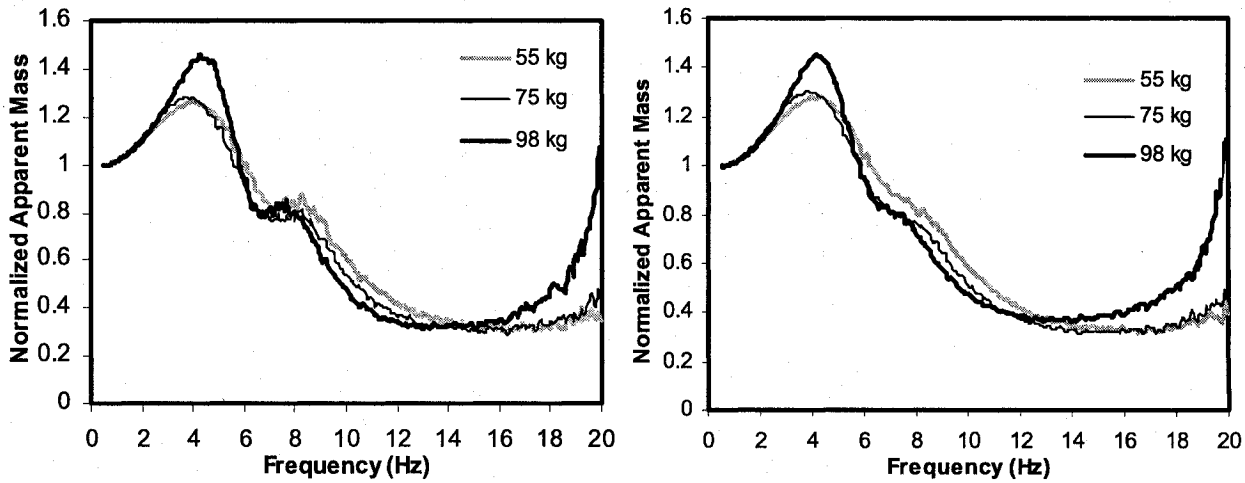

Figure 2.10: Influence of body mass on the apparent mass magnitude response of manikin G: (a) a_{rms} = 0.5 m/s^2 (b) a_{rms} = 1 m/s^2

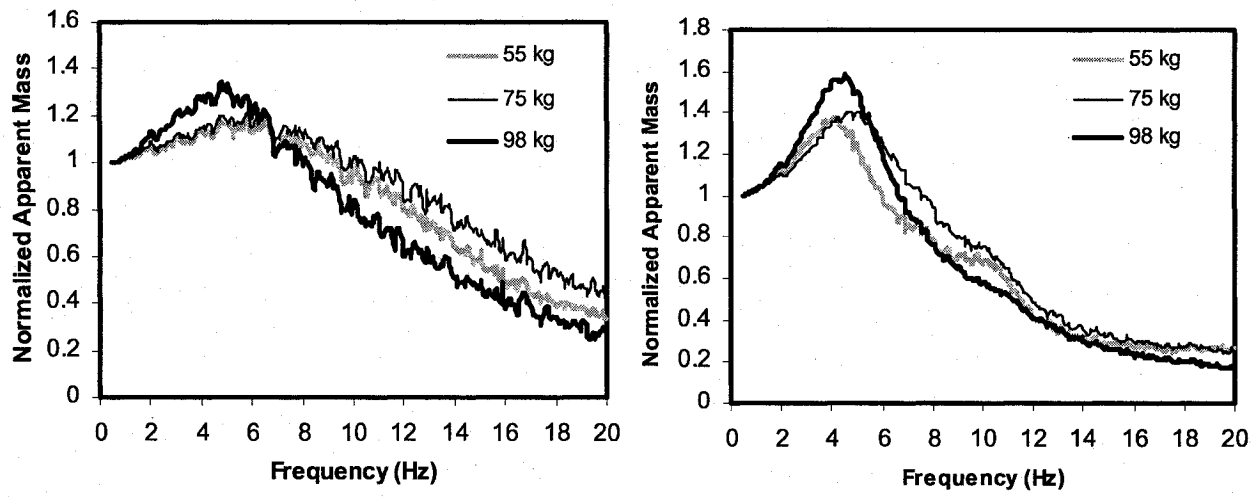

Figure 2.11: Influence of body mass on the apparent mass magnitude response of manikin F: (a) a_{rms} = 1 m/s^2 (b) a_{rms} = 2 m/s^2

The responses under higher excitation level alone are thus discussed to study the effect of body mass. As observed from the magnitude responses of manikin G, the results do not show a definite trend with regard to the body mass effect on the primary resonant frequency. The manikin F with 55 kg configuration exhibits lowest primary resonant frequency, while the highest frequency is observed for the 75 kg configurations. The higher resonant frequency for the 75 kg configuration could be attributed to the contribution of higher overall stiffness due to spring pairs K1 and K12. The peak magnitude response increases with increasing manikin mass.

2.6 Assessment of dynamic characteristics of the anthropodynamic manikins

As stated earlier, anthropodynamic manikins for assessment of dynamic characteristics of seats are developed to simulate both static and dynamic behaviors of seated occupants. The static properties must ensure that the manikin mass corresponding to a particular configuration is comparable to the seat-supported occupant mass within the same body mass group. The dynamic similarity between the manikin and the seated human body is realized by ensuring that the dynamic properties of the seat-manikin system are comparable to those of seat-occupant system. Owing to wide variations in the body mass, nature of whole-body vibration and suspension seat design features, the effectiveness of the manikin under a dynamic conditions must be evaluated over a range of body mass, seat design and vibration environment. The static characteristics of the manikins are assessed by comparing their static masses corresponding to different mass configurations with the seated body masses within the same group, as described in section 2.2.

Considering that the manikins are designed on the basis of measured apparent mass responses of seated human occupants exposed to whole-body vertical vibration, the dynamic performance of a manikin in the first stage can be evaluated in terms of its ability to predict the apparent mass response. The overall effectiveness of the manikins, however, must be assessed from its ability to predict the dynamic behavior of the seat-occupant system. Apart from the static and dynamic properties, the adherence of the manikins with a rigid seat, when vibrated, is ensured by strapping the base of the manikins with that of the rigid seat.

The dynamic performances of the manikins are initially assessed by their ability to replicate the seated body apparent mass responses. For this purpose, the measured apparent mass responses of manikins configured to three different body masses are compared with the standardized responses of seated occupants of similar mean body masses. The two prototype manikins, however, were designed on the basis of two different standardized responses. The manikin F derives its design from the ranges of idealized values of apparent mass response of seated occupants under vertical vibration reported in ISO-5982 [35]. The design of manikin G, on the other hand, is based upon the standardized values reported in DIN-45676 [36]. The ranges of apparent mass responses documented in two standards exhibit certain similarities and large differences. The ISO-5982 [35] defines the range of idealized values for human subjects seated on a rigid platform with feet supported and vibrated, while maintaining an erect seated posture without backrest support. The ranges of driving-point mechanical impedance and apparent mass are reported in the 0.5 to 20 Hz frequency range and are considered applicable for the seated human body, subjected to sinusoidal or broadband random

vibration of unweighted rms amplitude lower than or equal to 5 m/s^2. The data ranges in the document were derived from the synthesis of data reported in different studies where the standing body mass of the subjects varied from 49 to 93 kg, with mean body mass of 75 kg. The mean values of data set involved in the synthesis are thus considered to represent the biodynamic responses of the seated occupants with mean mass of 75 kg, while exposed to vertical vibration in the 0.5 to 20 Hz range. The document also provides a three degree of freedom mechanical equivalent model of the seated occupants, which was derived on the basis of the mean response (mean body mass of 75 kg). The mechanical equivalent model is manipulated by varying the masses alone to derive the apparent mass and driving-point mechanical impedance responses of seated occupants with mean body masses of 55 and 98 kg.

DIN-45676 [36] defines the range of biodynamic responses (impedance magnitude and phase) that are applicable for both sitting and standing human subjects on a hard plate and exposed to whole-body vibration. The ranges for seated occupants are defined for sitting on a rigid platform without a back support as in the case of ISO-5982 [35], with body mass in the 49 to 103 kg range, while subject to 0.5 m/s^2 or greater rms acceleration excitations. The mean values of the reported ranges are taken from ISO-5982 [35] that is considered to represent the biodynamic response of seated 50^{th} percentile population, when exposed to vertical vibration. The mechanical impedance magnitude and phase are defined over 1 to 20 Hz frequency range.

The DIN 45676 uses the mean response of ISO -5982 for establishing the impedance of 75 kg. The response values for subjects weighing near 55 kg are derived from data acquired for 18 subjects with body mass within 49 kg to 60 kg under harmonic

excitation having dominant frequency in the range of 1 Hz to 6 Hz with weighted rms amplitude of 1.49 m/s^2 or less. The response values for 98 kg subjects are obtained from data acquired for 14 subjects of body mass within 81 kg to 106 kg under harmonic excitation having dominant frequency within 1 Hz to 6 Hz with weighted rms amplitude of 1.49 m/s^2 or less.

Figure 2.12 illustrates comparisons of idealized ranges reported in ISO 5982 and the mean apparent mass responses reported in DIN-45676 for three different body masses. It should be noted that the DIN standard specifies the response for higher body mass of 98 kg opposed to 90 kg used in ISO-5982. The data reported for 75 kg body mass in the two documents are identical, while those for other body masses differ considerably in both the magnitude and phase. The magnitude responses for 55 and 98 kg body masses, reported in the DIN standard are considerably higher than the limits specified in ISO-5982, particularly at frequencies below 8 Hz. The low frequency magnitude for the 55 kg body mass, considered to represent the body mass supported by the seat, is in the order of 51.3 kg in the DIN standard. This being in the order of 93 % of total body mass is significantly higher than the widely reported value in the order of 73 %.The low frequency magnitude data reported in ISO-5982 for the same body mass confirms with the proportion of 73 %.

Both the magnitude responses exhibit peaks near 4 Hz. The magnitude responses in the two documents show reasonably good agreement at frequencies above 8 Hz, for both 55 kg and 98 kg body mass, while the phase responses differ most notably at frequencies above 8 Hz. The responses reported in the DIN standard suggest decreasing

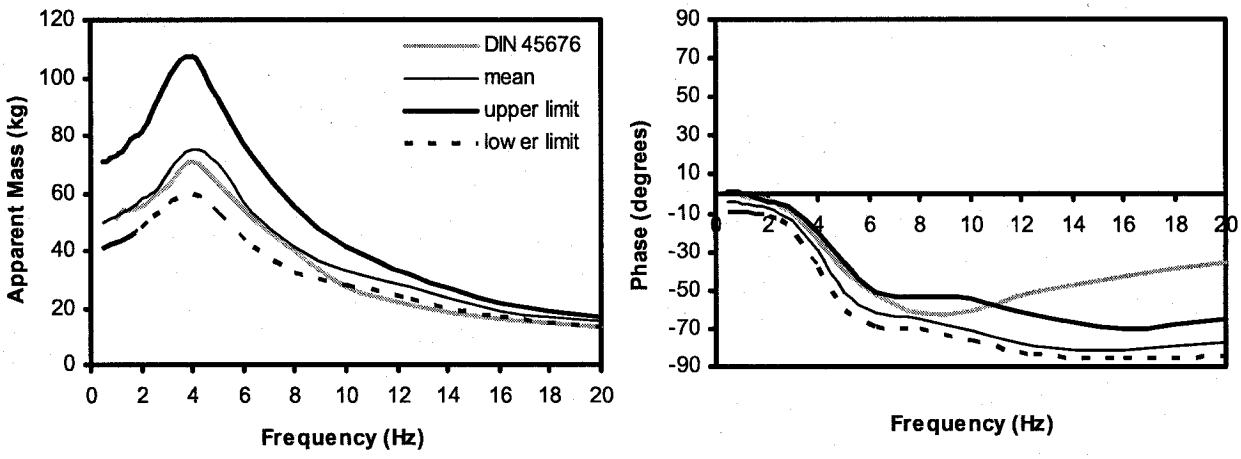

(a)

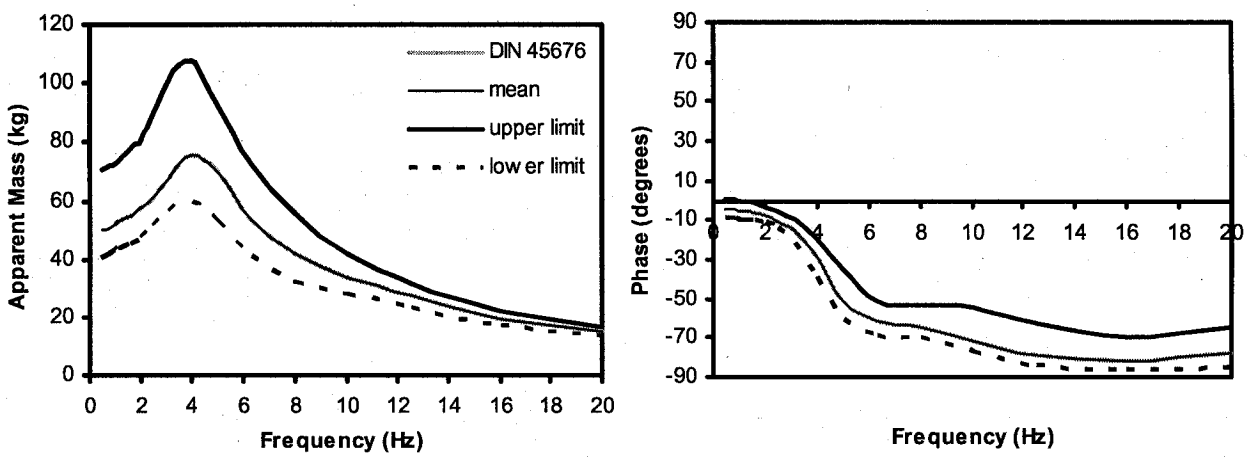

(b)

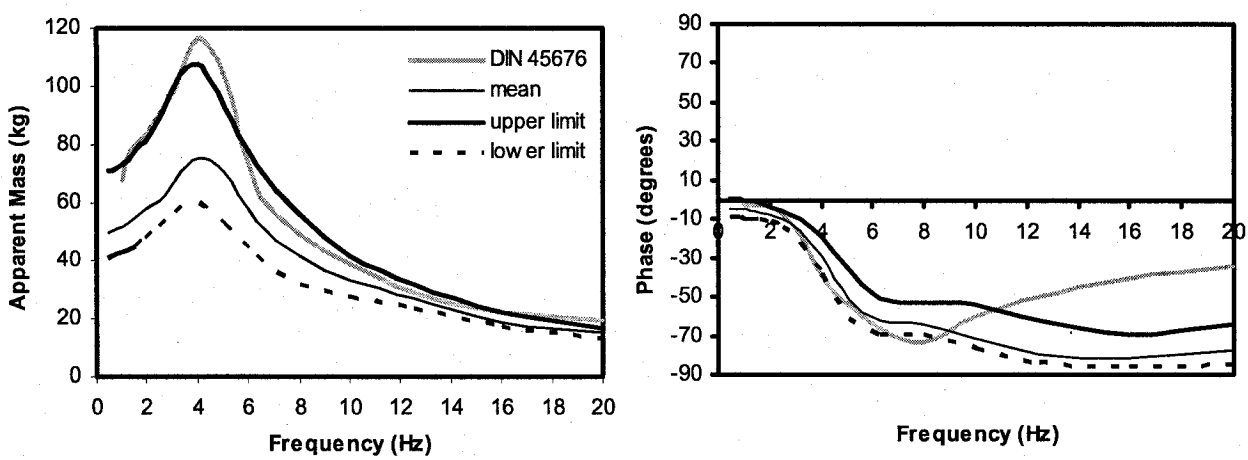

(c)

Figure 2.12: Comparison of Standard Apparent Mass Response; (a) 55 kg (b) 75 kg (c) 98 kg

phase at lower frequency until it approaches near -70 degrees around 8Hz for all three masses. Those trends are nearly identical to that observed in ISO-5982 data. At frequencies above8 Hz, the phase response in the ISO-5982 data asymptotically approach -90 degrees for all three body masses, while those in the DIN document for the 55 and 98 kg masses increase and asymptotically approach towards 0 degrees.

For the 90 kg body mass, the resonant frequency observed from the data reported in ISO 5982 is in the order of 3.6 Hz which is considerably lower than 4 Hz observed from DIN-45676 data for 98 kg body mass. The lower peak magnitude of the ISO 5982 data at resonant frequency could be partially attributed to the fact that the ISO data provides the response for 90 kg body mass opposed to 98 kg used in the DIN document. This would cause relatively higher body mass supported by the seat for the DIN consideration, which is not evident from the low frequency apparent mass response reported for 98 kg body mass.

The results also suggest that both the apparent mass magnitude as well as phase reported in DIN-45676 may be considered inappropriate to serve as the basis for design of antropodynamic manikins. Although the data reported in ISO-5982 appear reasonable, further verification of the model responses are needed, particularly for the lower and higher masses in order to achieve reliable apparent mass responses for designing an anthropodynamic manikin.

2.6.1 Apparent mass response assessment of manikin G

Considering that the manikin G is designed on the basis of the apparent mass responses reported in DIN-45676 [36], the apparent mass prediction performances of this manikin are assessed in relation to the DIN data for three body masses. For this purpose,

the manikin G supported on rigid seat plate was exposed to white noise random excitations of rms acceleration of 1 m/s^2. From Table 2.1, it can be seen that the static weight of manikin G used to represent the 55 kg human subject is 56 kg, which yields an overestimation of the percent body mass supported by the seat, and thus higher magnitude response at low frequencies and in the vicinity of the resonant frequency. The static weight of manikin G used to represent the 75 kg human subject is also slightly higher than those reported in a number of studies [21], while the static mass for 98 kg is comparable. Figure 2.13 illustrates the comparisons of the measured apparent mass responses of manikin G for the three body mass configurations under 1 m/s^2 rms acceleration excitation with those reported in DIN-45676. The results suggest that the apparent mass magnitude and phase responses for 55 kg configuration of the manikin are in reasonably good agreement with the standardized data up to 14 Hz. The resonant frequency and the peak magnitude, observed from the measured data, are also similar to those observed from the standardized data.

Both the apparent mass magnitude and phase responses of the manikin configured for 75 kg body mass tend to deviate considerably from the corresponding standardized data, as shown in Figure 2.13 (b). The measured low frequency magnitude is considerably larger, while the primary resonant frequency is comparable with that observed from standardized data. The measured magnitude response also exhibits a secondary peak near 8 Hz, which is not evident from the standardized data. A number of reported studies have also demonstrated the presence of a secondary resonance near 8 Hz [21]. The measured apparent mass phase response for the 75 kg configuration could be considered in good agreement with that of standardized response only up to 10 Hz. The

apparent mass magnitude response of the 98 kg configuration agrees reasonably well with the standardized data up to frequencies of 15 Hz, while a secondary peak is also evident near 8 Hz. The measured phase response of this configuration, however, deviates considerably from the standardized response at frequencies above 5 Hz.

The measured apparent mass responses of manikin G for the three body mass configuration are also compared with those reported in ISO-5982 [35]. Figure 2.14 illustrates comparisons of the measured with the standardized responses. The results show most significant deviations between the measured apparent mass response and the standardized data for all the three mass configurations, with the exception of magnitude response for the 75 kg configuration. While the measured primary peak frequencies for the 55 and 75 kg configuration agree close to those observed from the target data, the measured resonance frequencies as well as the peak magnitude for 98 kg configuration are considered higher. The measured magnitude response of the 55 kg configuration is also significantly higher in the 0.5-10 Hz range due to higher static mass of the manikins. The measured phase responses for all three configurations differs significantly from the target data, particularly at frequencies above 10 Hz, 6 Hz and 4 Hz for the 55, 75 and 98 kg configurations respectively.

From the above assessment, it is concluded that the static masses of manikin G are greater than the target static masses for the 55 and 75 kg body mass configurations. The measured responses, however, show better agreements with the data reported in DIN-45676, while the phase responses differ.

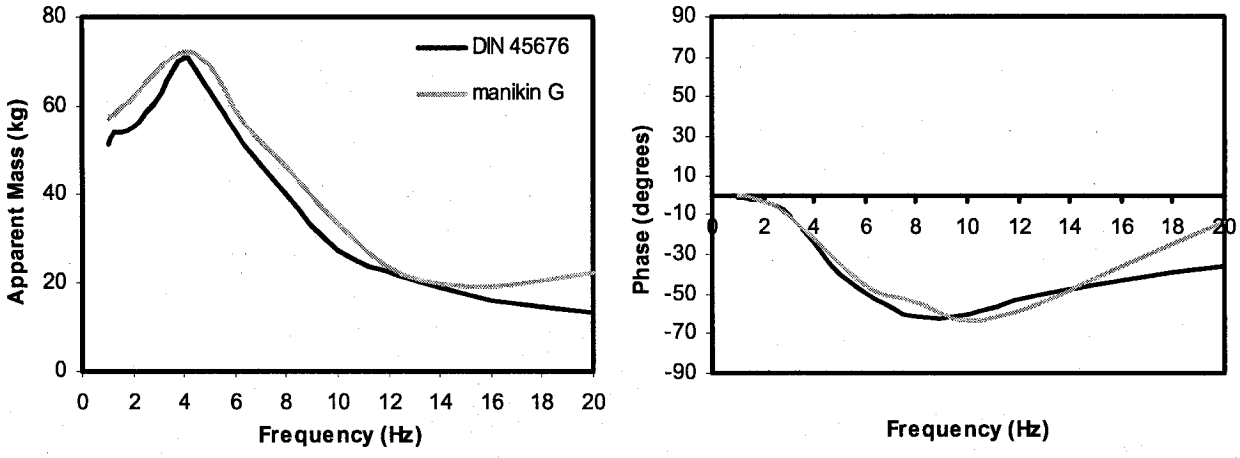

(a)

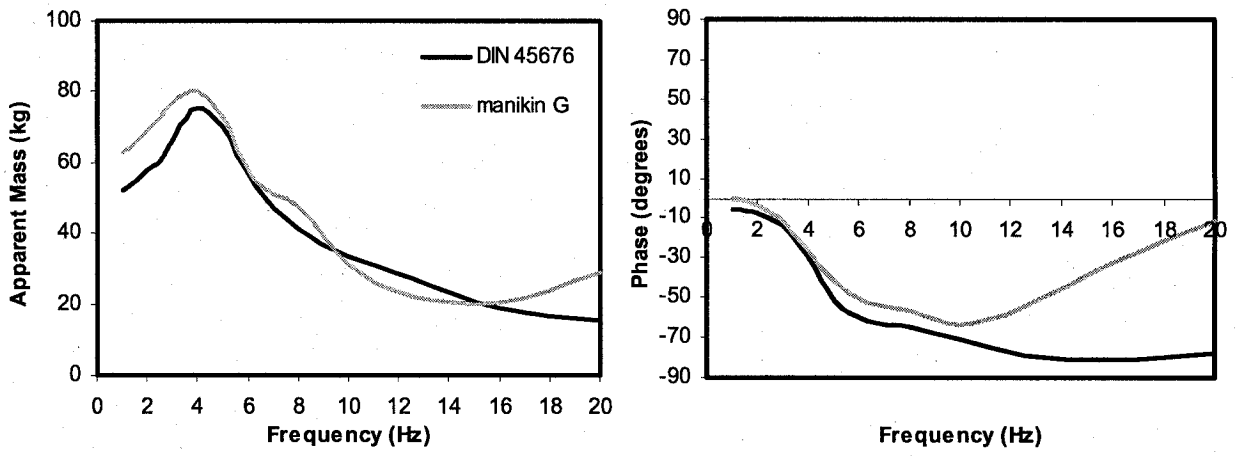

(b)

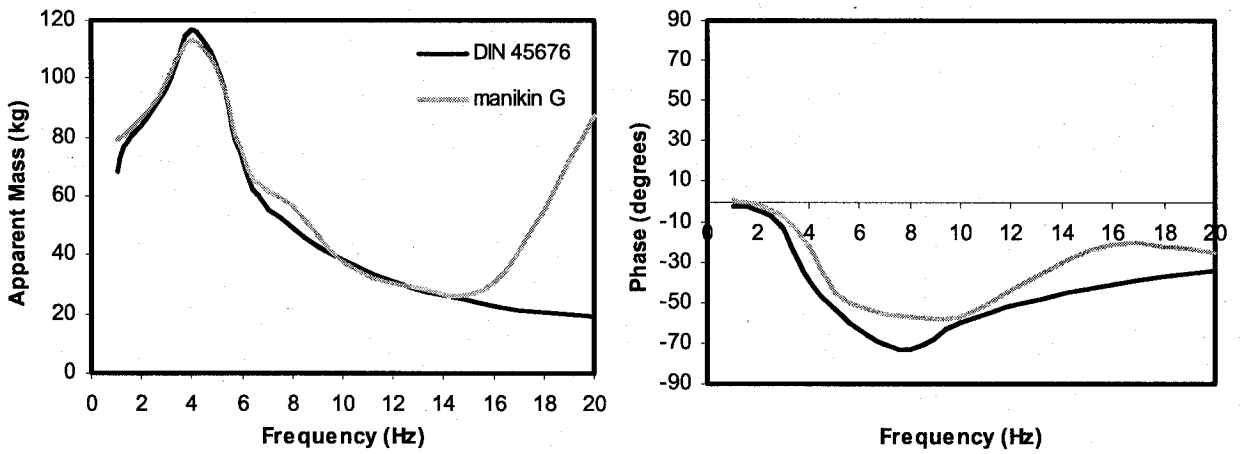

(c)

Figure 2.13: Comparisons of measured apparent mass responses of manikin G with the standardized data in DIN 45676 under white noise random excitation of 1 m/s^2 rms acceleration: (a) 55 kg; (b) 75 kg; and (c) 98 kg

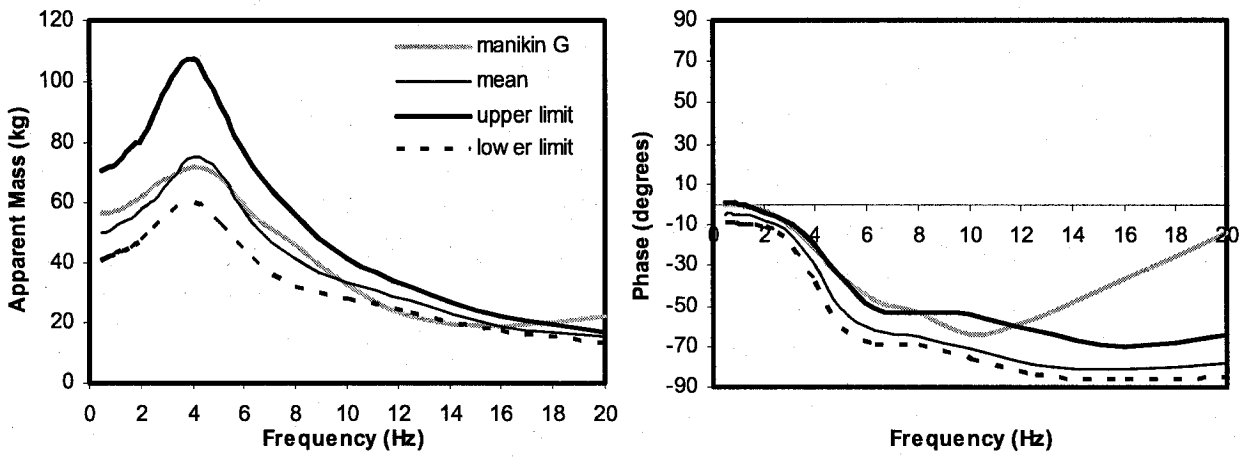

(a)

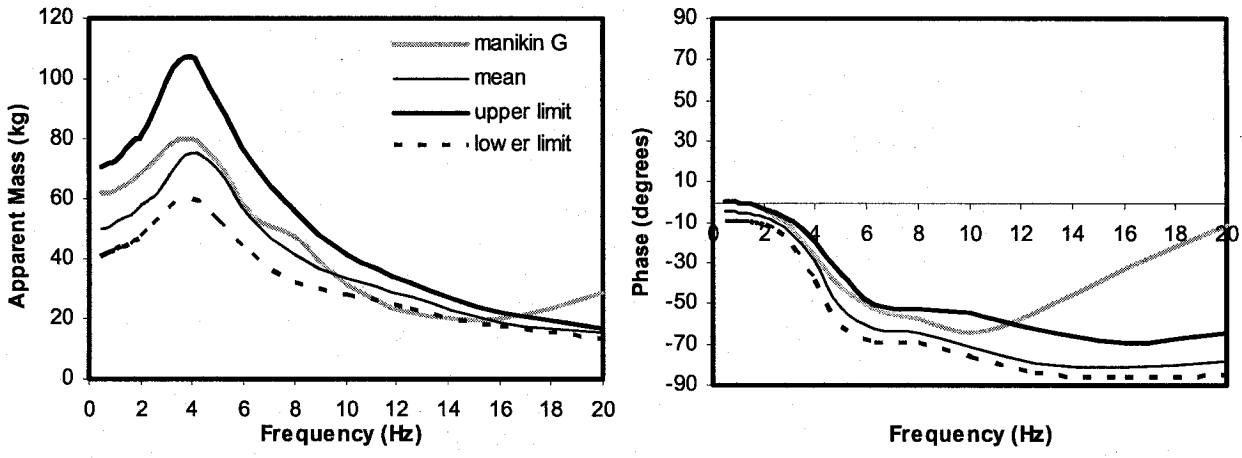

(b)

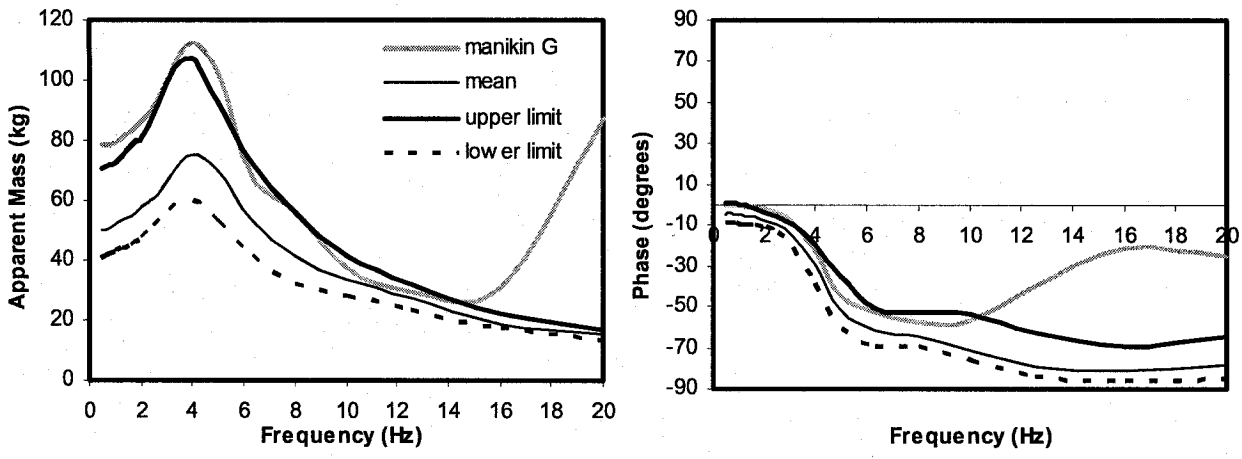

(c)

Figure 2.14: Comparisons of measured apparent mass responses of manikin G with the standardized data in ISO 5982 under white noise random excitation of 1 m/s^2 rms acceleration: (a) 55 kg; (b) 75 kg; and (c) 98 kg/90 kg

2.6.2 Apparent mass response assessment of manikin F

The ability of manikin F in predicting the apparent mass responses of seated occupants exposed to vertical vibration are assessed in relation to idealized ranges reported in ISO-5982 and DIN-45676 documents. It should be noted that unlike manikin G, the manikin F was designed on the basis of idealized ranges reported in ISO-5982 [35]. The measured response could thus be expected to exhibit better agreement with the standardized values in ISO-5982. Owing to the lack of generally acceptable standardized data, the apparent mass prediction performance of manikin F are also assessed using both standards. The apparent mass responses of manikin F were measured under relatively higher levels of excitation due to high damper seal friction, as discussed earlier in section 2. The static mass of manikin F is close to that of the percent human subject body mass supported by the seat, as illustrated in Table 2.2, for all the three mass groups.

Figure 2.15 illustrates comparison of the apparent mass responses of manikin F measured under 2 m/s^2 rms acceleration excitation with the data reported in DIN-45676. The results generally show trends that are comparable with those in the standardized data, while notable differences could be observed in both the magnitude and phase. The measured magnitude response for the mean body mass of 75 kg shows reasonably good agreement with the standardized data, while the frequency corresponding to the peak (5 Hz) is larger than that observed from the target data (4 Hz). The corresponding phase response, however agrees with the target values only up to 12 Hz.

The measured magnitude response for the 98 kg configuration is in good agreement with the standardized data, while large phase error is observed at frequencies above 8 Hz. For the 55 kg configuration, the measured phase response agrees reasonably

well with the target response. The corresponding magnitude response however is lower at frequencies below 8 Hz, which is mostly due to higher static mass implied in the DIN data for this mass configuration.

Far more deviations in the magnitude response could be observed when the measured data are compared with the idealized ranges reported in ISO-5982, as shown in Figure 2.16. The measured phase responses, however, agree reasonable well with the standardized phase responses for all three masses, particularly at frequencies below 12 Hz. The measured magnitude responses are comparable in magnitudes and the primary resonant frequencies for 55 and 75 kg mass configurations, particularly at frequencies below 12 Hz whereas they exhibit considerable deviation for 98 kg mass configuration. The results suggest that for the 55 kg configuration, the resonance frequency of manikin F is same as that of the standardized lower limit, but for the 75 and 98 kg configuration the resonance frequencies are higher. The peak measured magnitude for the 55 and 75 kg configurations are comparable to those of the standardized responses, whereas it is considerably high for the 98 kg configuration. The measured low frequency magnitudes are thus comparable with those reported in ISO-5982, although slight deviations are evident for the 55 and 98 kg configurations. The results presented in Figures 2.15 and 2.16 suggest that measured apparent mass magnitudes of manikin F agree more with the standardized values reported in DIN-45676 for 75 and 98 kg configurations. The phase responses, however, conform somewhat better with those reported in ISO-5982. Moreover, the manikin F would yield poor prediction of apparent mass under lower excitation levels due to its high damper seat friction.

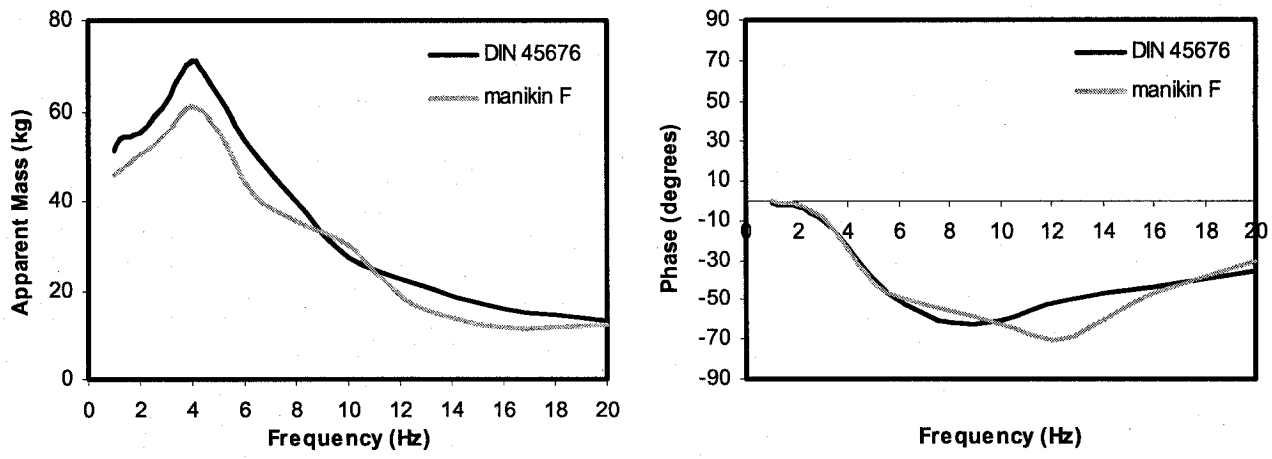

(a)

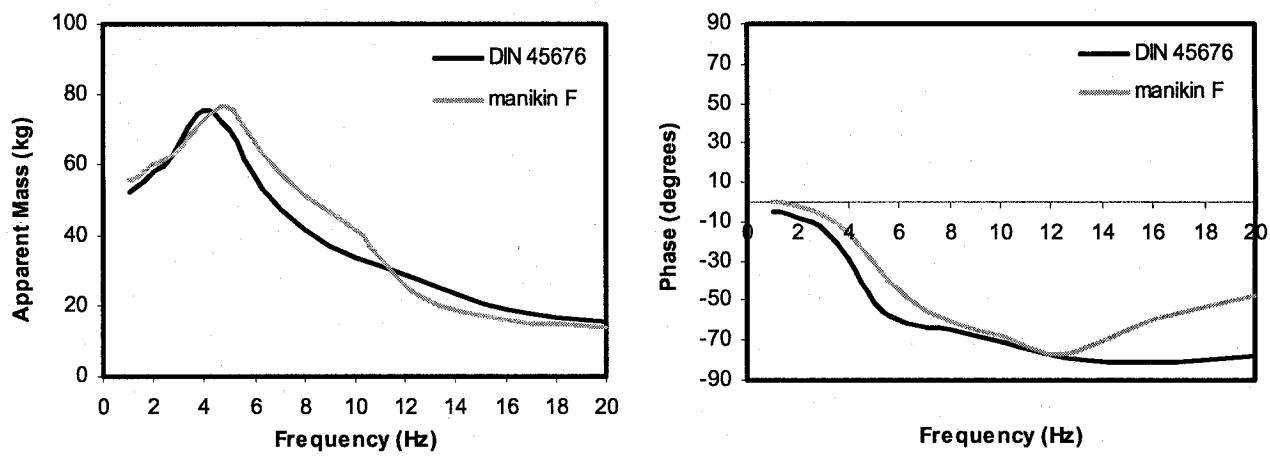

(b)

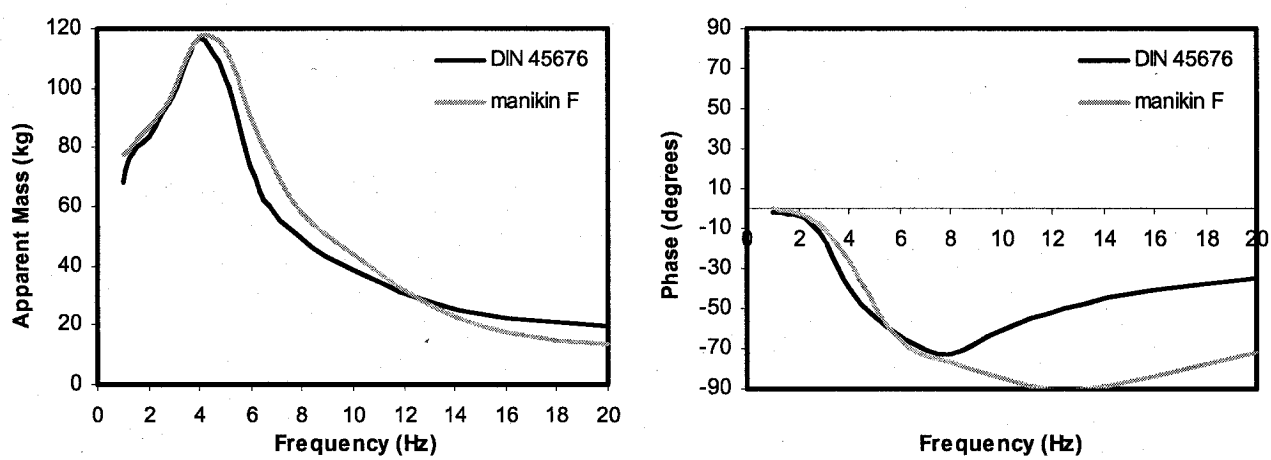

(c)

Figure 2.15: Comparisons of measured apparent mass responses of manikin F with the standardized data in DIN 45676 under white noise random excitation of 2 m/s^2 rms acceleration: (a) 55 kg; (b) 75 kg; and (c) 98 kg

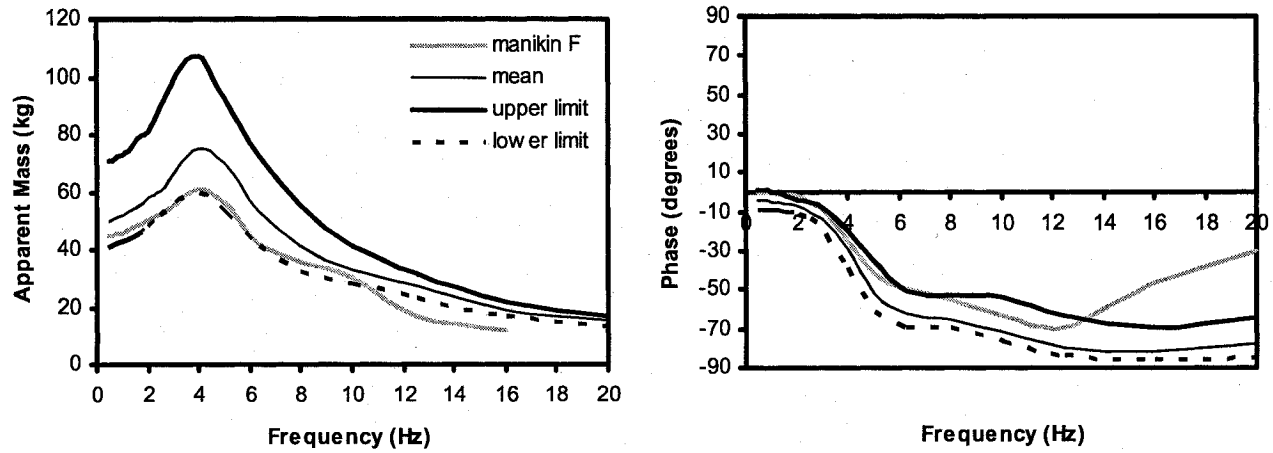

(a)

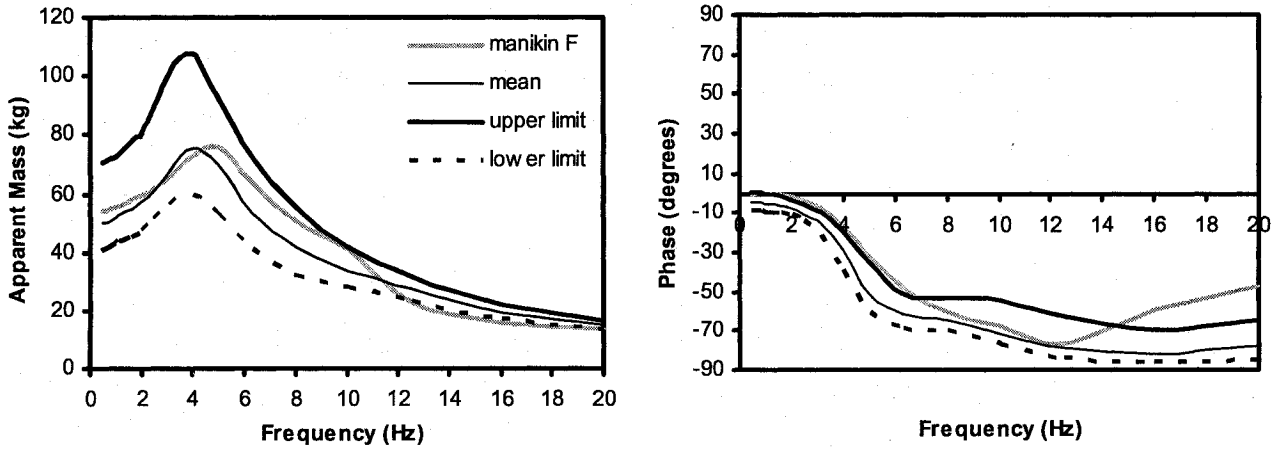

(b)

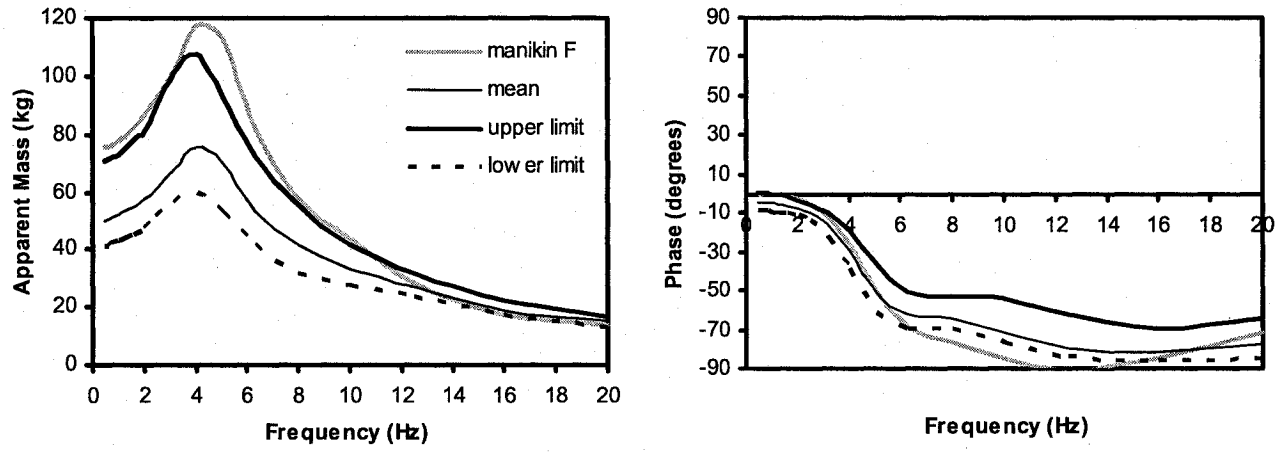

(c)

Figure 2.16: Comparisons of measured apparent mass responses of manikin F with the standardized data in ISO 5982 under white noise random excitation of 2 m/s^2 rms acceleration: (a) 55 kg; (b) 75 kg; and (c) 98 kg/90 kg

2.7 SUMMARY

The design specifications of two anthropodynamic manikins considered for the study are described and their static properties are discussed for three different body mass values representing 5^{th}, 50^{th}, 95^{th} percentile male population. Measurement and data analysis methods required to characterize the biodynamic responses of the manikins under vertical whole body vibration are presented and experiments are performed to characterize the apparent mass responses for different mass configurations. The data are studied to quantify the influence of the magnitude of vibration and body mass on the responses. The apparent mass magnitude and phase responses are compared with the standardized values reported in ISO-5982 and DIN-45676 to assess the biodynamic response prediction abilities of the manikins.

CHAPTER 3

ASSESSMENT OF MANIKINS IN SEATING APPLICATIONS

3.1 Introduction

Suspension seats are widely employed in various vehicles in the industrial, agricultural, forestry, construction and transportation sectors to isolate the drivers from terrain-induced whole-body vertical vibration and shock. For effective attenuation of vibration, it has been established that the resonant frequency of the human-suspension seat system should be well below the dominant frequency of the vehicle vibration, while the suspension damping ratio should be sufficiently low to achieve greatest attenuation of vibration in the important ride frequency range.

A suspension seat comprises of an energy restoring element, either pneumatic or mechanical, an energy dissipating element, motion limiting bump stops and linkages to ensure nearly vertical motion. The performance characteristics of dynamic or suspension seats are mostly evaluated through field or laboratory measurements performed using passive as well as human loads [1, 5, 9, 10, 43]. The current International Standard ISO 7096[56] describes the laboratory test methods applicable to off-road machinery, agricultural tractors and general purpose seats. The standard recommends two different laboratory tests for evaluating the dynamic performance of suspension seats. The first test assesses the resonant response and damping properties of the suspension seat loaded with a specified inert mass. The vibration attenuation performance of the suspension seat is measured in the second test under representative excitations defined for different classes of vehicles, while the seat is loaded with human subjects of specific body masses. The

input motions used for this test are defined as standardized narrow-band random spectra characterizing the vibration environment of the target vehicle.

The above evaluations must be performed using two different human subjects with body masses of 55 kg and 98 kg with tolerances of -3 to 0 and 0 to +5 kg, respectively. The use of the human subjects in such laboratory-based assessments requires careful considerations of safety, ethical, medical and legal issues. The vibration simulator thus must include additional safety features and be safe for human exposure to vibration. Moreover, the use of human subjects could lead to poor repeatability of the test data, even when a single test subject is used [1, 19]. The measured performance is considered to possess poor objectivity as the usage of a small group of test persons cannot be regarded as being representative of the larger driver population [1, 5, 19]. In an attempt to attain more repeatable data and eliminate the associated ethical concerns, considerable efforts are being made to develop anthropodynamic manikins that can replace the human subject for suspension seats assessments.

Few studies have proposed the use of analytical models of the seat and seated human subject to assess the overall vibration isolation and comfort performance [9, 10, 54, 57]. A number of studies have proposed nonlinear analytical models of static as well as suspension seats. These models have been extensively validated when coupled with a inert mass [39, 77-79]. Owing to the important contribution of the human occupant in dissipating the transmitted vibration, a number of studies have also evolved in biodynamic models of the seated occupant to realize coupled human-seat models [10, 43, 57, 79]. While the standardized test method requires the assessments of suspension seats with human occupants, a recent study has concluded that the contributions of human

occupant could be relatively small for low natural frequency suspension seats [55]. The same study showed most important contribution of the occupant dynamics for higher natural frequency seats, such as those employed in automobiles and fork-lift trucks. Other studies suggest that seat with inert mass could be comparable with that of the seat-person system under excitations up to 2 Hz [1, 5, 23]. This is based upon the findings that driving-point mechanical impedance of the human occupant resembles that of the inert mass up to 2 Hz [23].

Owing to the lack of a reliable and proven analytical model of a seat-person system and to the ethical concerns associated with the current assessment methodology, the application of an effective anthropodynamic manikin is extremely desirable. A number of passive and active manikins have thus evolved during the past few years, which are mostly developed on the basis of the measured biodynamic responses of the vibration-exposed seated human subjects [11-20]. A few studies have also established the validity of the developed manikins in replacing the human body when assessing the vibration isolation performance of seats for particular class of vehicles [13-18]. The effectiveness of such manikins, however, has not been evaluated for general applications in wide ranges of seats and for different vehicular vibration spectra.

In this chapter, the performance potentials of the two candidate anthropodynamic passive manikins, described in the previous chapter are assessed for wider seating applications. The vibration transmissibility and seat effective acceleration transmissibility (S.E.A.T) of five different seats are measured using human subjects, equivalent inert mass and the manikins. The data are analyzed to conclude upon the relative effectiveness of the manikins. The equivalent inert mass is taken as the static weight of the manikins

supported on the seat, as opposed to the total body mass considered in a previous study [16, 18].

3.2 Description of test seats

The majority of the heavy road and off-road vehicles, with a few exceptions, exhibit most severe vibration along the vertical axis. The spectral components of the vertical vibration generally predominate in the 0.5 to 5 Hz for off-road wheeled vehicles. The seats employed in modern off-road heavy vehicles range from simple fixed seats to air suspension seats with automatic weight compensation for the driver weight. Suspension seats are designed with low natural frequency, while the dynamic travel is limited by relatively stiff elastic bump stops.

A seat suspension system is designed to minimize the transmission of low frequency vibration to the driver, particularly in the 4-8 Hz frequency range, where the human body is known to be most fatigue sensitive [1]. The suspension seat comprises either a mechanical or air spring with a hydraulic damper between the seat structure and the base. It also consists of rubber or metal end stops to prevent excessive relative motions of the low frequency suspension. These are also equipped with weight adjustment mechanism so as to provide either a mid-ride or selected ride height to the driver in the weight range of 50 to 130 kg. Most of the commercially available suspension seats, with a few exceptions, exhibit natural frequency in the range of 1 to 2 Hz. The vibration attenuation properties of a suspension seat rely not only on its component characteristics but also on the nature of the target vehicle vibration. A suspension seat thus needs to be tuned on the basis of the magnitudes and spectral components of the vehicle. Apart from these, the human occupant may also contribute to

the overall suspension seat performance [1, 5, 7, 10, 55 57, 77]. In this study five different seats are selected to examine the applicability of the manikins for assessing the vibration isolation performance of a wide range of seats. The selected seats include the mechanical as well as pneumatic suspension and could be applied to classes of off-road, road and industrial vehicles. The essential features of the selected seats are briefly summarized below:

a) **Seat A**: This seat employs an air suspension and a cross linkage mechanism with an inclined hydraulic damper. The air spring consisted of an air bag. A control valve was provided for realizing desirable ride height for the operator. The seat also provided adjustabilities to vary the backrest inclination and arm rests. The suspension provided total travel of 162 mm between the elastic end stops. This seat suspension design is recommended for applications in highway trucks.

b) **Seat B**: This suspension seat comprises a behind-the-seat suspension. The sprung seat pan is mounted on a vertical rail through a coil spring and a hydraulic damper. The rail permits the pan motion along the axis of the rail. The vertical travel of the pan is limited by rubber mounts, and the compensation for the operator weight is accomplished manually by varying the preload on the springs. The seat also offers fore-aft adjustment and adjustable arm rests. The suspension provided the total travel of 68 mm. This seat is generally recommended for applications in off-road vehicles, such as agricultural tractors and forestry vehicles.

c). **Seat C**: This suspension seat employed an air spring with cross linkage mechanism and an inclined damper, as in case of seat A. The pneumatic suspension comprised an air bag, and a compressor, operating at 12 volts, is integrated to achieve desired sitting

height through charging and discharging of the air bag. The seat consists of an automatic height leveling mechanism, and adjustable backrest and armrests. The seat also comprises a fore-aft adjustment and yields total suspension travel of 160 mm. This suspension seat could be applied to earth moving vehicles and highway trucks.

d). **Seat D**: This seat comprises a behind the seat suspension as in the case of seat B. The seat employed a mechanical spring with a hydraulic damper. The spring and damper are mounted at the back of the seat along a horizontal axis. The axis of the spring and damper, however, varies with the preload, which is adjusted through a spring preload mechanism. The seat is also supported on a cross linkage mechanism with manual weight adjustment. Fore-aft adjustments for the seat cushion and the seat are also provided. The total travel of the seat is 49 mm, while the seat is recommended for applications in industrial trucks, such as forklift trucks.

e). **Seat E**: This seat employs a mechanical suspension with a cross linkage mechanism and an inclined hydraulic damper. A coil spring is installed horizontally with the cross linkage mechanism and the weight adjustment could be performed manually. The suspension seat provided total free travel of 50 mm, and is recommended for application in industrial vehicles, such as forklift trucks.

Table 3.1 further summarizes the specifications of the selected candidate seats in terms of their travel, construction and type of suspension. The table also lists the natural frequencies, and excitations, which are discussed in the following section.

3.3 Test Methodology

The applicability of the candidate anthropodynamic manikins were evaluated for the selected ranges of suspension seats and different vibration excitations. Three different

types of vibration excitations were considered for the study.

Table (3.1) Specifications of selected suspension seats

Seat	Suspension	Application	Estimated Natural Frequency (Hz)	Spectral Class	Height Adjustment	Load Range (kg)	Travel (mm)
A	Pneumatic	Highway Trucks	1.38	Class II	Pneumatic	†	162
B	Mechanical	Agricultural Tractor	1.56	AG2	Manual	50-130	68
C	Pneumatic	Construction Machinery	1.5	EM4	Automatic	†	160
D	Mechanical	Forklift Truck	2	IT1	Manual	50-130	49
E	Mechanical	Forklift Truck	3.5	FL Spectra	Manual	50-130	50

'†' not specified

These included a swept harmonic excitation in the 0.5-10 Hz frequency range for identifying the resonant frequency of each seat, a broad –band white-noise random excitation for characterizing the frequency response characteristics, and the random vibration spectrum of the particular vehicle intended for each candidate seat for assessing the effectiveness of the manikins. Each test seat was installed on the platform of the whole-body vehicular vibration simulator (WBVVS). The suspension travel of each seat was measured and the mid-ride position was marked with the exception of seat C, which provided automatic ride height adjustment. Each seat was subjected to a 15 minutes run-in test under a harmonic excitation in the vicinity of the anticipated natural frequency, prior to the defined experiments. For this purpose, the seat was loaded with 75 kg inert mass, made up of lead shots contained in small bags, and the suspension was adjusted to mid-ride position. The seat was subjected to sinusoidal vibration in the vicinity of the

suspension natural frequency, while the excitation amplitude was adjusted to cause suspension motion exceeding 75 % of the total travel.

The test suspension seat was instrumented to measure both the excitation and response accelerations were measured using a single-axis piezoelectric accelerometer (B&K 4381) installed at the seat base. The response acceleration at the seat was measured using a tri-axial seat pad accelerometer (B&K 4322). The seat pad accelerometer has been recommended for measurement of acceleration response at the seat-human or seat-load interface [5, 14]. The preliminarily trials with the manikins revealed that the seat-pad accelerometer could not be used to rigid base plates of the manikins. A single-axis piezoelectric accelerometer (B&K 4381) was thus installed at the base plate of the selected manikin to measure the seat response acceleration.

3.3.1 Identification of Resonant Frequency of Suspension Seats

The experiments were initially performed to estimate the resonant frequencies of the candidate suspension seats using method similar to that outlined in ISO 7096 [74]. The selected test seat was loaded with a 75 kg inert mass consisting of lead shot bags and adjusted to its mid-ride position. The WBVVS was then operated under sinusoidal excitations in the 0.5 to 10 Hz frequency range swept at the rate of 1 octave/minute. The selected excitation provided constant displacement amplitude of 12.7 mm up to 2 Hz, and constant acceleration amplitude of 2 m/s^2 at frequencies above 2 Hz. The lead bags were secured in a plastic bag which was restrained to limit the relative motion of the mass with respect to the seat.

The experiments were performed under upward sweep (0.5 to 10 Hz) and downward sweep (10 to 0.5 Hz). The measured acceleration signals were acquired using

multi-channel signal analyzer (B&K Pulse). The acceleration data were analyzed to determine the acceleration transmissibility of the selected seat from:

$$H_A(\omega) = \frac{S_{\ddot{x}_2\ddot{x}_1}}{S_{\ddot{x}_1}} \tag{3.1}$$

where $H_A(\omega)$ is the acceleration transmissibility, $S_{\ddot{x}_2\ddot{x}_1}$ is the cross-spectral density (CSD) of the measured response ($\ddot{x}_2$) and excitation ($\ddot{x}_1$) accelerations, and $S_{\ddot{x}_1}$ is the auto spectral density of the acceleration excitation.

The analyses were performed using a bandwidth of 50 Hz and frequency resolution of 0.0625 Hz. Figure 3.1 illustrates the measured acceleration transmissibility response of candidate seats. The resonant frequency of each seat was identified as the frequency corresponding to peak acceleration transmissibility. It should be noted that the nonlinear suspension seats could exhibit considerably different resonant frequencies when subject to different loads and excitations. The identified frequencies are thus considered to provide an estimate of the suspension natural frequency corresponding to selected excitation and load. The results suggest that the respective resonances of the candidate seats A, B, C, D and E occur near 1.38 Hz, 1.56 Hz, 1.5 Hz, 2 Hz, and 3.5 Hz, which are summarized in Table 3.1. It should be noted that suspension seats D and E exhibit relatively higher resonant frequencies due to their relatively small travel. Moreover, the frequency response characteristics reveal considerably higher friction due to associated with behind-the-seat suspension designs (seats B and D), which causes lock-up behavior at low frequencies.

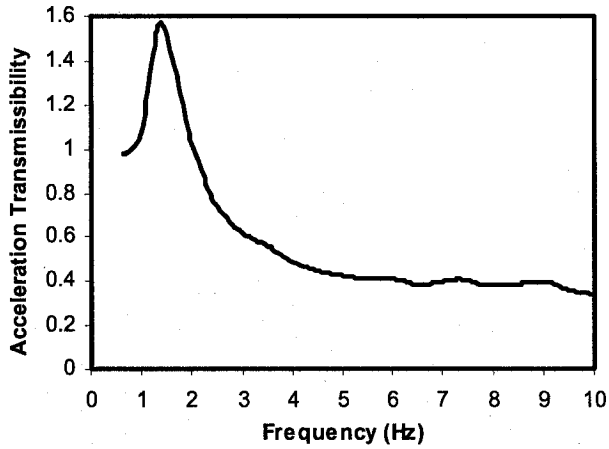

(a)

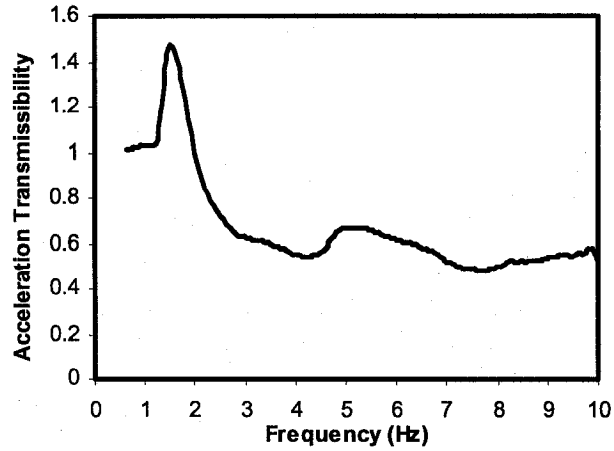

(b)

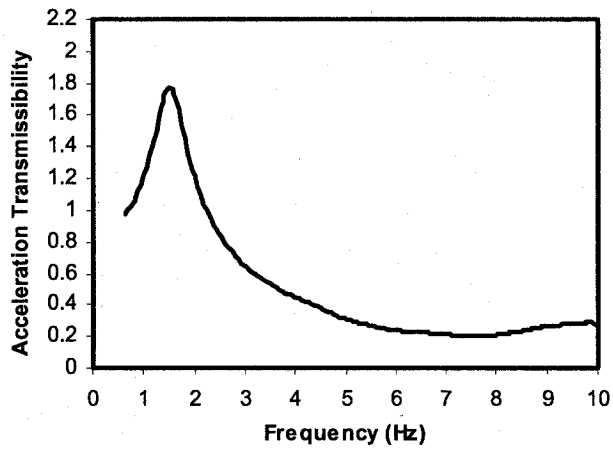

(c)

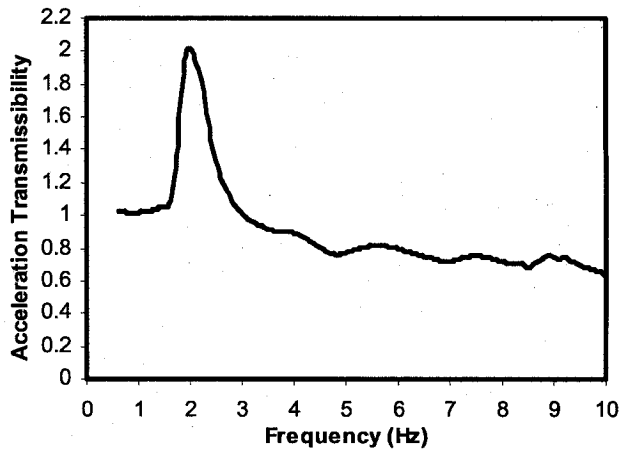

(d)

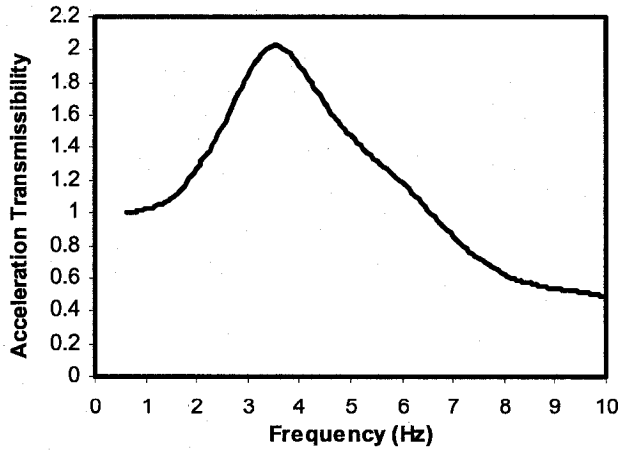

(e)

Figure 3.1: Measured acceleration transmissibility responses of candidate seats loaded with 75 kg inert mass and subjected to swept harmonic excitation in the 0.5 to 10 Hz frequency range: (a) Seat A; (b) Seat B; (c) Seat C; (d) Seat D; (e) Seat E

3.3.2 Experiments with seats loaded with human occupants

Nine adult male subjects participated in experiments with human occupants. The participant did not have a previous history of back pain. Each participant was provided with detailed experiment protocol which was approved by the Human Research Ethics Committee of Concordia University. Each participant was further familiarized with the emergency stops. Owing to the strong dependence of the suspension behavior and manikins on the seated mass, the experiments were designed to consider three different total body masses around 55, 75 and 98 kg. The subjects were thus chosen to ensure their total body mass is in the vicinity of 55 kg, 75 kg and 98 kg. The mass ranges and age of the test subjects are summarized in Table 3.2.

Each subject was seated on the installed candidate seat. The seat was then adjusted to the mid-ride position for the particular seated subject. Furthermore, each subject was asked to assume one of the two upright postures; no back support (NB) and with back support (WB). Each subject was to assume a stable and upright sitting posture in accordance with ISO 7096, irrespective of the back support condition. The preliminarily experiments were also performed with hands placed in lap (HL) and on the steering wheel (SW) to study the effect of hands position. The results revealed insignificant effect of the hands position on the measured responses. The subsequent experiments were thus conducted for hands in lap and two back support conditions (NB and WB). The tests with human subjects were undertaken for all the seats except for seat E where the data on the subject were taken from an earlier study [55].

Table 3.2: Body mass and age of human subjects

Mass Group	N	Mass (kg)			Mean Age (years)
		Minimum	Mean	Maximum	
55 kg	3	53	57.5	60	35
75 kg	3	71	75	80	26
98 kg	3	93	93.6	94	29

Each subject was asked to attend two different test sessions, one involving the measurement of frequency response characteristics under random white noise excitations and the other involving vehicular vibration spectra. The experiments under white noise excitations involved 4 seats, 2 magnitudes of excitations, 2 postures and 3 repeats, which resulted in a total of 48 trials/subject. The duration of each trial was 90 seconds. The subject was asked to take rest for 2 to 4 minutes between successive trials. The experiments under vibration spectra of particular vehicles involved four different spectra for the four candidate seats (A, B, C and D), 2 postures and three repeats, which resulted in a total of 24 trials. Each trial lasted for a maximum of 180 seconds.

3.3.3 Experiments with manikins and inert masses

The experiments were also performed using the two manikins and equivalent inert mass. The equivalent inert mass in the study was taken as the static mass of the respective manikin corresponding to the three body mass configurations, as described in section (2.2). It should be noted that the manikins F and G represent different masses for 55, 75 and 98 kg configurations. The experiments with inert masses were thus conducted using the equivalent masses corresponding to each manikin, as summarized in Tables 2.1 and 2.2. The selected manikin was placed on a candidate suspension seat that was installed on

the WBVVS, as shown in Figure 3.2. Prior to the measurements, apart from the seat run-in period each manikin was also subjected to a run-in period of 15 minutes under a harmonic excitation in the vicinity of the

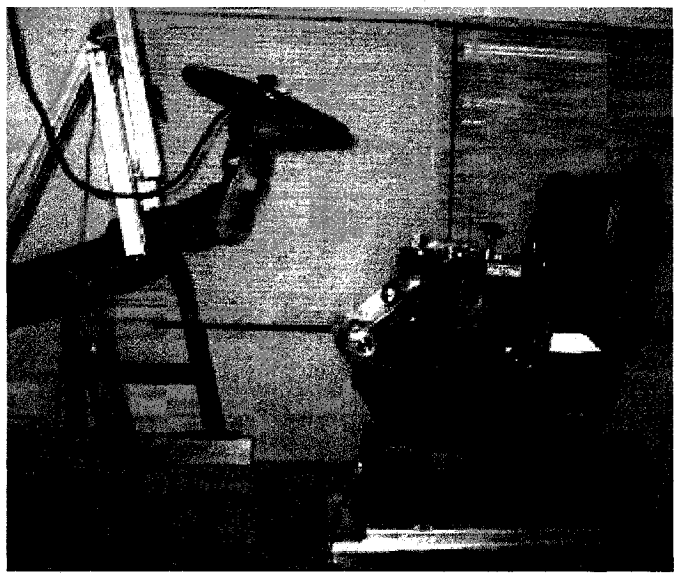

(a)

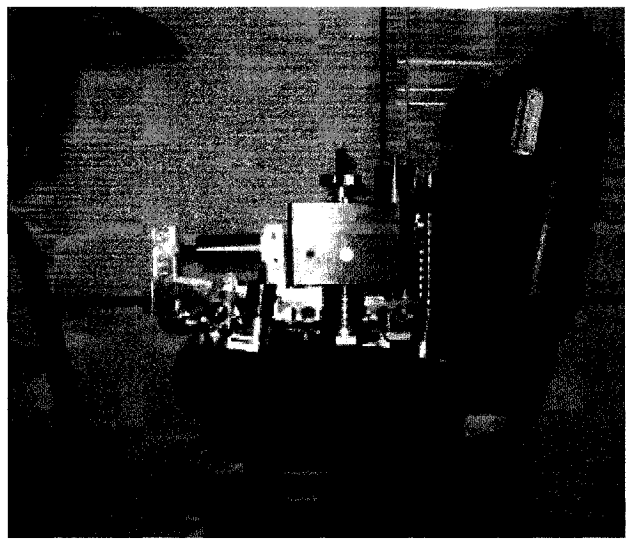

(b)

Figure 3.2: Pictorial views of manikins located on the seat: (a) manikin G; (b) manikin F

natural frequency of the seat. The equivalent inert masses for the test were realized by using different combinations of bags containing lead shots. The lead bags were secured in

a plastic bag and secured to the backrest of the seat. The vibration responses of each seat loaded with a manikin were measured under both types of excitations: random white-noise and vehicular spectra.

The experiments with each manikin involved 2 levels of white-noise excitation, 5 levels of vibration spectra for five different seats and 3 repeats, which resulted in a total of 30 trials per manikin. The experiments with inert masses involved 6 different masses (3 masses equivalent to each manikin), and same levels of excitations which resulted in a total of 40 trials.

3.3.4 Vibration Excitations

The relative vibration transmission properties of candidate seats loaded with human subject, manikin and equivalent inert masses, are evaluated under two different types of excitations. The frequency response characteristics of the seat-load combinations are initially evaluated under two different magnitudes of broad-band random excitations with constant acceleration power spectral density in the 0.5 to 20 Hz frequency range. Such excitations are chosen to identify the resonant frequencies, peak acceleration transmissibility and vibration isolation properties of the seats as functions of the load and excitation magnitude. The magnitudes of the selected broad-band excitations were chosen to yield total *rms* accelerations of 1.0 and 1.5 m/s^2. Higher excitation levels (*rms* values = 2.0 m/s^2 and 2.5 m/s^2), however, were synthesized for seat E to ensure sufficient displacement at the seat base in the vicinity of its resonant frequency.

The relative performance characteristics of the candidate seats with human subjects, manikins and inert mass are further assessed under excitations that are encountered in typical vehicles. The whole-body vertical vibration spectra of vehicles for

which the candidate seats are primarily intended for, are thus compiled and synthesized from the published studies and standards. The synthesis if the intended vehicular vibration spectra were available from earlier studies conducted by Concordia University and IRSST. The intended vehicles included the highway truck (Class II) for the pneumatic suspension seat A, agricultural tractor class II (AG2) for seat B, Class I industrial trucks (IT1) for seat D and a 2 ton Forklift truck vibration spectra (FL) for seat E. the chosen vehicular spectra are also summarized in Table 3.1. The vertical vibration spectra of the selected vehicles are described in the International Standards and earlier reported studies [8, 56, 80-82].

Figure 3.3 illustrates the acceleration PSD spectra of vertical vibration of selected vehicles. It is evident that Class II, AG2 and EM4 vibration spectra peak near 2.2 Hz, 2.3 Hz and 2.2 Hz, respectively, with peak PSD value near 1.0, 5.0 and 0.5 $(m/s^2)^2/Hz$, respectively. The IT1 and FL vibration spectra exhibit peak amplitudes of 0.6 and 0.7 $(m/s^2)^2/Hz$, respectively, which occur at relatively higher frequencies of 5.0 and 6.3 Hz. The acceleration PSD characteristics of vertical vibration of the selected vehicles were synthesized using low and high-pass filters in the following manners:

Highway trucks (Class II) [82] $$S_{\ddot{x}_1} = 1.13(HP_{24})^2(LP_{24})^2 \quad (3.2)$$

Agricultural tractor class II (AG2) [78] $$S_{\ddot{x}_1} = 7.22(HP_{48})^2(LP_{48})^2 \quad (3.3)$$

Earth moving vehicles-Grader (EM4) [56] $$S_{\ddot{x}_1} = 0.60(HP_{24})^2(LP_{24})^2 \quad (3.4)$$

Industrial truck-class 1 (IT1) [81] $$S_{\ddot{x}_1} = 1.66(HP_{24})^2(LP_{12})^2 \quad (3.5)$$

Forklift truck-2tons (FL) [8]

$$S_{\ddot{x}_1} = \left\{ k_m \frac{s\prod_{i=1}^{n}(s^2 + A_{mi}s + B_{mi})}{\prod_{k=1}^{p}(s^2 + C_{mk}s + D_{mk})} \right\}^2 \quad (3.6)$$

In the above formulations, the function LP_{12}, LP_{24} and LP_{48} are the Low-pass filter function of the Butterworth type of order 2, 4 and 8, respectively. HP_{24} and HP_{48} define high-pass filter functions of order 4 and 8, respectively. The subscripts refer to the roll-off rate of the filter in decibels per octave. These filter transfer functions are given by:

$$LP_{12} = \frac{1}{1+1.414s+s^2} \quad (3.7)$$

$$LP_{24} = \frac{1}{1+2.613s+3.414s^2+2.631s^3+s^4} \quad (3.8)$$

$$LP_{48} = \frac{1}{1+5.126s+13.137s^2+21.846s^3+25.888s^4+21.846s^5+13.137s^6+5.128s^7+s^8} \quad (3.9)$$

$$HP_{24} = \frac{s^4}{1+2.613s+3.414s^2+2.613s^3+s^4} \quad (3.10)$$

$$HP_{48} = \frac{s^8}{1+5.126s+13.137s^2 21.846s^3 25.588s^4+21.846s^5+13.137s^6+5.128s^7+s^8} \quad (3.11)$$

where, $s = \frac{jf}{f_c}$, f is the excitation frequency and f_c is the cut-off frequency. The Table 3.3 summarizes the cut-off frequencies for various high-pass and low-pass filters [56, 80-82]. Table 3.4 lists peak acceleration PSD, unweighted and frequency-weighted *rms* accelerations over a defined frequency band for each vehicular excitation. The overall *rms* acceleration a_1 due to different excitations have been computed from:

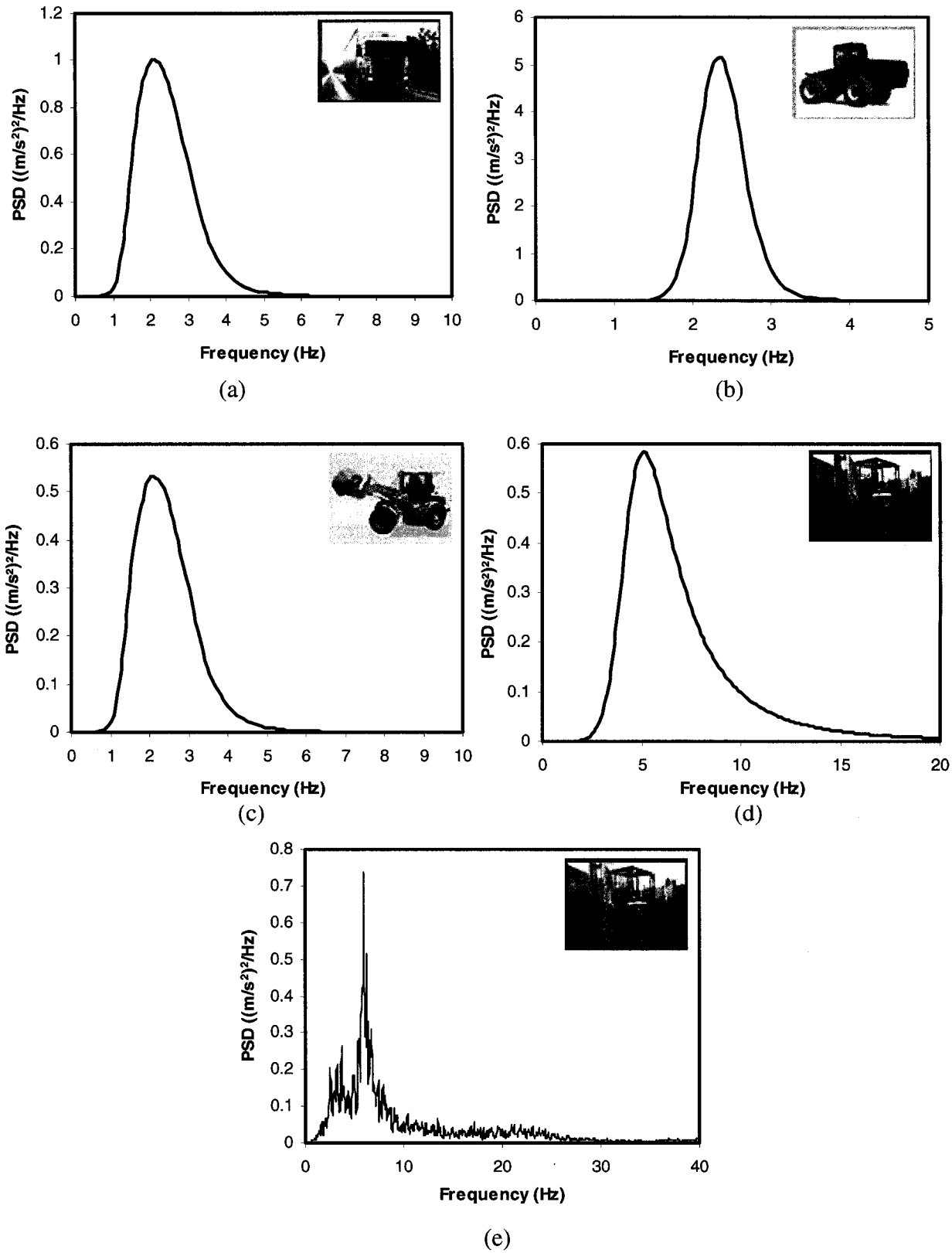

Figure 3.3: Acceleration PSD of selected classes of vehicles vibration spectra: (a) Class II trucks; (b) AG2, class 2 agricultral tractor; (c) EM4,earth moving vehicles; (d) IT1,industrial trucks; (e) FL, forklift

$$a_1 = \sqrt{\int_{f_1}^{f_2} S_{\ddot{x}_1}(f)df} \tag{3.12}$$

where a_1 is overall *rms* acceleration due to vibration at the seat base or that of the simulator platform, and f_1 and f_2 are the lower and upper limits of the frequency range of interest.

The overall frequency-weighted *rms* acceleration a_{1w} due to selected excitations are also computed using the weighting function defined in ISO-2631 [], such that

$$a_{1w} = \sqrt{\int_{f_1}^{f_2} \left[|H_w(f)|^2 S_{\ddot{x}_1}(f) \right] df} \tag{3.13}$$

where a_{1w} is the frequency-weighted *rms* acceleration due to platform vibration and $H_w(f)$ is the frequency-weighted function.

Table 3.3: Cut-off frequencies for various high and low pass filters

Input Spectral Class	LP_{12}	LP_{24}	LP_{48}	HP_{24}	HP_{48}
Class II	-	3 Hz	-	1.5 Hz	-
AG2	-	-	2.6 Hz	-	2.1 Hz
EM4	-	3 Hz	-	1.5 Hz	-
IT1	5 Hz	-	-	4.5 Hz	-

Table 3.4: Some specification of vibration spectra of selected vehicles

Input Spectral class	Seat	Vehicles	$G_{p(f)}$ $(m/s^2)^2/Hz$	f_1 and f_2 (Hz)	a_{rms} (m/s²)	a_{peak} (m/s²)
ClassII	A		0.87	f_1= 1 f_2= 4	1.23	0.95
AG2	B		5.17	2.35 Hz (central frequency)	1.94	1.5
EM4	C		0.53	f_1= 0.89 f_2= 11.22	0.96	0.75
IT1	D		0.58	f_1= 0.89 f_2= 17.78	1.58	1.59
FL Spectra	E		0.74	f_1= 0.63 f_2= 25.00	1.35	-

3.3.5 Data Analysis

The whole body vertical simulator was operated to produce the motion signals corresponding to a selected magnitude of vibrations. The resulting base acceleration and seat acceleration signals were acquired using 6 channel B&K (Type 3032A) data collector. The software PluseLab View™ version 8 was used for data acquisition and analysis. The analysis was performed using 800 spectral lines in the 50 Hz frequency band with a resolution of 0.0625 Hz and an overlap of 75%.

The measured data were analyzed to compute the vertical acceleration transmissibility characteristics of the seat-occupant, seat-manikin and seat-inert mass combinations under broad band excitations using EQ (3.1). The acceleration transmissibility for each combination was evaluated for the three different mass groups

and two levels of excitations. The mean transmissibility for the seat-occupant system, the acceleration transmissibility was determined by taking the mean of the 9 data sets acquired for each mass group (3 subjects × 3 trial) for each level of excitation and posture and seat of the seat-manikin and seat-inert mass combination was derived upon averaging the data sets corresponding to 3 trials for each mass group. Moving average based on 8 data points technique was employed for smoothening of the curves.

The responses of different seat-load combinations to random vehicular vibration were evaluated in te*rms rms* acceleration spectra and overall *rms* accelerations. The unweighted *rms* acceleration responses of candidate seats under the selected vehicular vibration spectrum and loaded with manikins, human subjects and inert masses were measured using the constant proportional band analyzer (CPB) of the Pulse software. The acceleration responses measured at the seat-load interface were thus derived at the centre frequencies of each one-third octave frequency band. The data acquired from three trials with the seats loaded with manikin and inert masses were evaluated to derive the mean and standard deviation of the *rms* acceleration corresponding to each mass group. For each seat-human subject combinations the mean and standard deviation of the *rms* acceleration response were computed from the nine data sets corresponding to each mass group.

The overall *rms* acceleration responses of different seat-load combinations were further computed to derive the seat effective amplitude transmissibility (SEAT), which is commonly employed for assessing the effectiveness of a suspension seat. The SEAT value of a seat is defined as the ratio of the frequency-overall weighted *rms* acceleration

of vibration transmitted to the seat to that of the vibration encountered at the seat base, and can be expressed as:

$$S.E.A.T._{weighted} = \sqrt{\frac{\int_{f_l}^{f_u} S_{\ddot{x}_2}(f)|W_k(f)|^2 df}{\int_{f_l}^{f_u} S_{\ddot{x}_1}(f)|W_k(f)|^2 df}} \tag{3.14}$$

where $W_k(f)$ is the frequency-weighting function defined in ISO-2631-1 [60]. f_l and f_u define the lower and upper frequency limits of the vibration signal. In the present analysis, the SEAT values are computed upon consideration of 0.5 to 20 Hz frequency range. The SEAT value can also be computed from the third-octave band *rms* acceleration values, such that

$$S.E.A.T._{weighted} = \sqrt{\frac{\sum_{j=1}^{N} a_{2w}^2(\bar{f}_j)}{\sum_{j=1}^{N} a_{1w}^2(\bar{f}_j)}} \tag{3.15}$$

where $a_{1w}(f_j)$ is the frequency-weighted *rms* acceleration due to platform vibration corresponding to the centre frequency $\bar{f}_j$ of the j^{th} frequency band and N is the number of third octave bands considered. $a_{2w}(f_j)$ is the frequency-weighted *rms* acceleration measured at the seat-load interface in the j^{th} frequency band. The frequency-weighted *rms* acceleration values are computed using EQ (3.13).

The S.E.A.T values are also computed on the basis of unweighted *rms* acceleration, such that:

$$S.E.A.T. = \sqrt{\frac{\sum a_2^2(\bar{f}_j)}{\sum a_1^2(\bar{f}_j)}} \tag{3.16}$$

where $a_1(\bar{f}_j)$ $a_2(\bar{f}_j)$ are the *rms* acceleration due to vibration at the seat base and the seat-load interface respectively, at the center frequency $\bar{f}_j$ of the j^{th} frequency band.

The validity of a seat-manikin combination for a particular seat and the vehicular vibration is assessed by comparing its SEAT values with these derived from the seat-mass and seat-human combination. The deviations of the measured values of the seat-manikin system with respect to those of the other measures are computed as:

$$\%D_{M\text{-}H} = \frac{(S.E.A.T.)_M - (S.E.A.T.)_H}{(S.E.A.T.)_H} \times 100 \tag{3.17}$$

$$\%D_{M\text{-}R} = \frac{(S.E.A.T.)_M - (S.E.A.T.)_R}{(S.E.A.T.)_H} \times 100 \tag{3.18}$$

where $D_{M\text{-}H}$ and $D_{M\text{-}R}$ describe the percent deviation of the S.E.A.T. values of a seat-manikin combination with respect to the seat-human and seat-inert mass combinations, respectively. $(S.E.A.T.)_M$, $(S.E.A.T.)_R$ and $(S.E.A.T.)_H$ are the SEAT values of a seat loaded with manikin, inert mass and human subject, respectively.

It has been suggested that the vibration attenuation preface of a seat-inert mass system is comparable to that of a seat-human system, when low-frequency suspension seats are concerned [55]. The deviations $D_{R\text{-}H}$ of $(S.E.A.T.)_R$ with respect to $(S.E.A.T.)_H$ are thus also computed for each seat:

$$\%D_{R\text{-}H} = \frac{(S.E.A.T.)_R - (S.E.A.T.)_H}{(S.E.A.T.)_H} \times 100 \tag{3.19}$$

3.4 Assessment of vibration transmission of seats with manikins

The vertical acceleration transmissibility characteristics of seat-occupant, seat-manikin and seat-mass combinations under broad-band excitations is calculated using EQ (3.1).The EQ (3.1) may be mathematically correct but it may misrepresent the physical

phenomenon it is intended to describe. The principal problem is the reliability of the transfer function, as often happens with real motions, there is little or no energy at some frequencies. The transfer function at such frequencies may thus lead to considerable errors. To assist the interpretation of transfer functions the coherence function may be determined which is given by:

$$\gamma^2_{x_2x_1} = \frac{\left|S_{\ddot{x}_2\ddot{x}_1}\right|^2}{S_{\ddot{x}_1} S_{\ddot{x}_2}} \tag{3.19}$$

where $\gamma^2_{x_2x_1}$ is the coherence of the response $(\ddot{x}_2)$ and $(\ddot{x}_1)$ acceleration signals, and $S_{\ddot{x}_2}$ is the auto spectral density of response acceleration. The coherence function lies in the 0 to 1 range, and a value of 1 suggests high coherence of the signals. During measurements, the coherence between the excitation and response signals was constantly monitored, which generally ranged from 0.85 to 1.0.

The dynamic response characteristics of a suspension seat are influenced by the nature of vibration spectrum and the mass supported by suspension, apart from the static and dynamic properties of its components hence the influence of excitation and manikin mass are studied for the four candidate suspension seats.

3.4.1 Influence of body mass

Figures 3.4 (a, b) illustrate the acceleration transmissibility of seat A coupled with manikin G, configured for three masses (55, 75 and 98 kg), under 1.0 and 1.5 m/s^2 random white noise excitations, respectively. Figures 3.4 (c, d, e) in a similar manner illustrate the acceleration transmissibility of the seat loaded with manikin F, configured for 55, 75 and 98 kg masses, and subject to 1.0, 1.5 and 2.0 m/s^2 excitations. The results generally show a slight decrease in the resonant frequency with increasing manikin mass,

while the corresponding peak transmissibility increases slightly. The seat A with 55 and 75 kg manikin G exhibits resonant frequency in the vicinity of 1.5 Hz under 1 m/s^2 excitation, which decreases to 1.38 Hz for the 98 kg manikin mass. The peak transmissibility increases from 1.23 to 1.29, when the manikin mass is increased from 75 kg to 98 kg. The peak transmissibility of 55 kg configuration, however, is very close to that of the 75 kg manikin, since the effective masses of both configurations are quite close. An increase in excitation magnitude to 1.5 m/s^2 also yields lower resonant frequency but slightly higher peak transmissibility, which is partly attributed to nonlinear property of the suspension system. The resonant frequencies of seat A with manikin G decrease to 1.38 Hz for the 55 kg and 75 kg configuration and to 1.25 Hz for the 98 kg manikin mass. The acceleration transmissibility of seat A loaded with manikin F also exhibit similar influence of body mass and excitation magnitude. While the resonant frequency decreases slightly with an increase in manikin mass, the peak transmissibility increases slightly. The relative change in the resonant frequency, however, tends to be extremely small under 2.0 m/s^2 excitation, which is most likely attributed to relatively smaller contribution of the manikin friction under higher excitation.

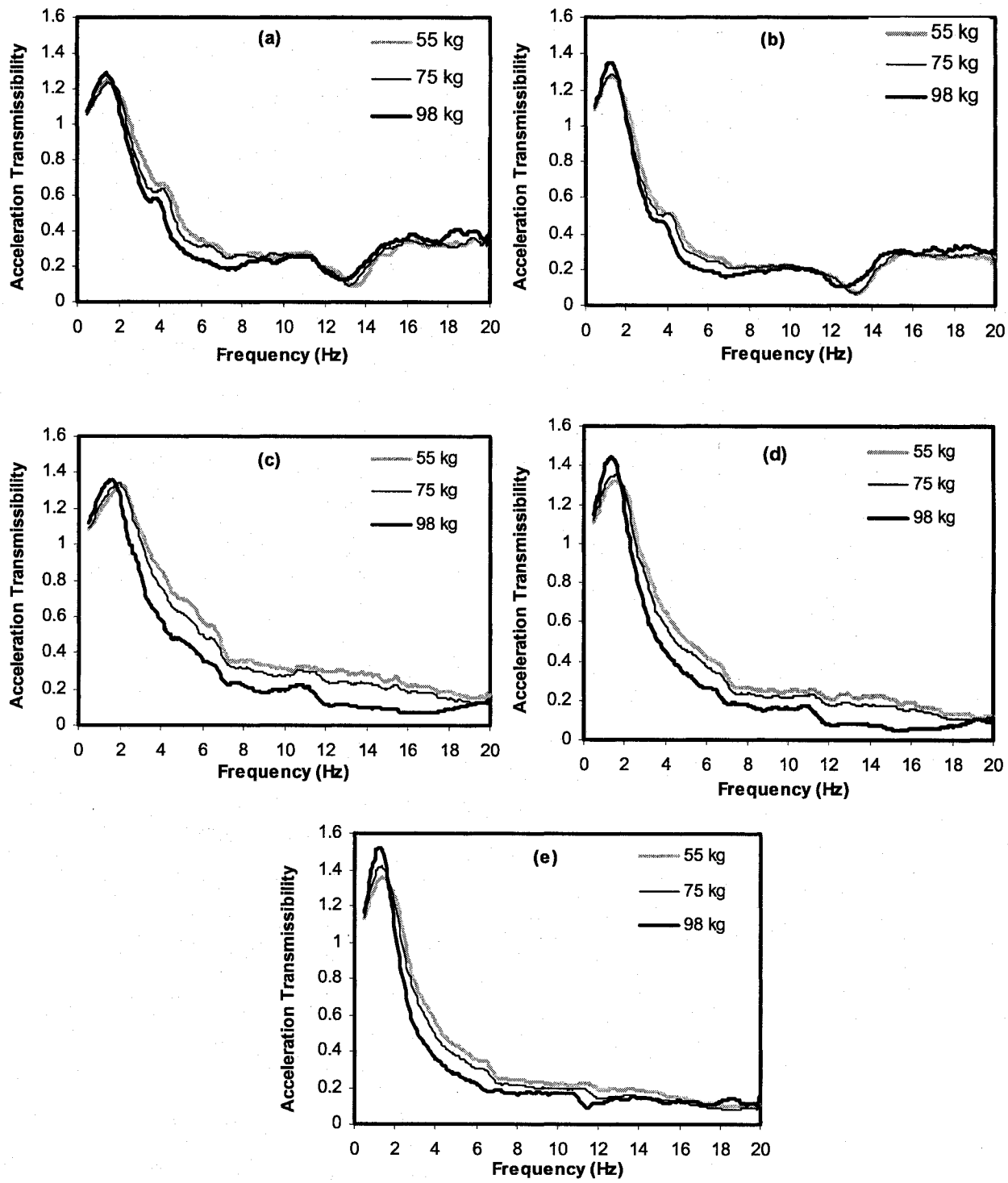

Figure 3.4: Influence of body mass and magnitude of broadband excitation on the acceleration transmissibility for seat A with manikins; (a) Manikin G: $a_1 = 1$ m/s^2; (b) Manikin G: $a_1 = 1.5$ m/s^2; (c) Manikin F: $a_1 = 1$ m/s^2; (d) Manikin F: $a_1 = 1.5$ m/s^2; (e) Manikin F: $a_1 = 2$ m/s^2

Figures 3.5 illustrate the acceleration transmissibility characteristics of seat B loaded with manikin G and manikin F, and subject to broadband excitations of different magnitudes. The response of seat B with manikin G exhibits negligible effect of the manikin mass on both the resonant frequency and the peak transmissibility for both excitation magnitudes (Figure 3.5-a, b). This is attributed to high friction of the mechanical suspension mechanisms. The resonant frequency of the seat lies around 2 Hz under 1 m/s^2 excitation and it decreases to nearly 1.5 Hz under 1.5 m/s^2 excitation. The peak acceleration transmissibility also increases from 1.09 to 1.16, when excitation magnitude is increased from 1.0 m/s^2 to 1.5 m/s^2 *rms*. The frequency response characteristics of the seat with manikin F exhibit slightly lower resonant frequency for higher mass and excitation magnitude as observed in the case of seat A. the important effect of the suspension friction on the response is also evident under 1 m/s^2 excitation. The peak transmissibility, however, decreases with increasing manikin mass and decreasing excitation magnitude. These trends are attributed to high friction due to suspension.

The behind-the-seat suspension design caused pitching motion of the seat at frequencies above 3 Hz. This pitching motion encouraged considerable pitch oscillations of the manikin F, which was not restrained to the seat back. The frequency response characteristics of the seat with manikin F thus show the presence of a secondary peak in the 3.5 to 5 Hz range. This secondary frequency decreased considerably with increase in body mass. It should be noted that this secondary peak is not evident for manikin G, where pitching motion was not clearly evident. This may be due to the restraints used to support manikin G against the backrest.

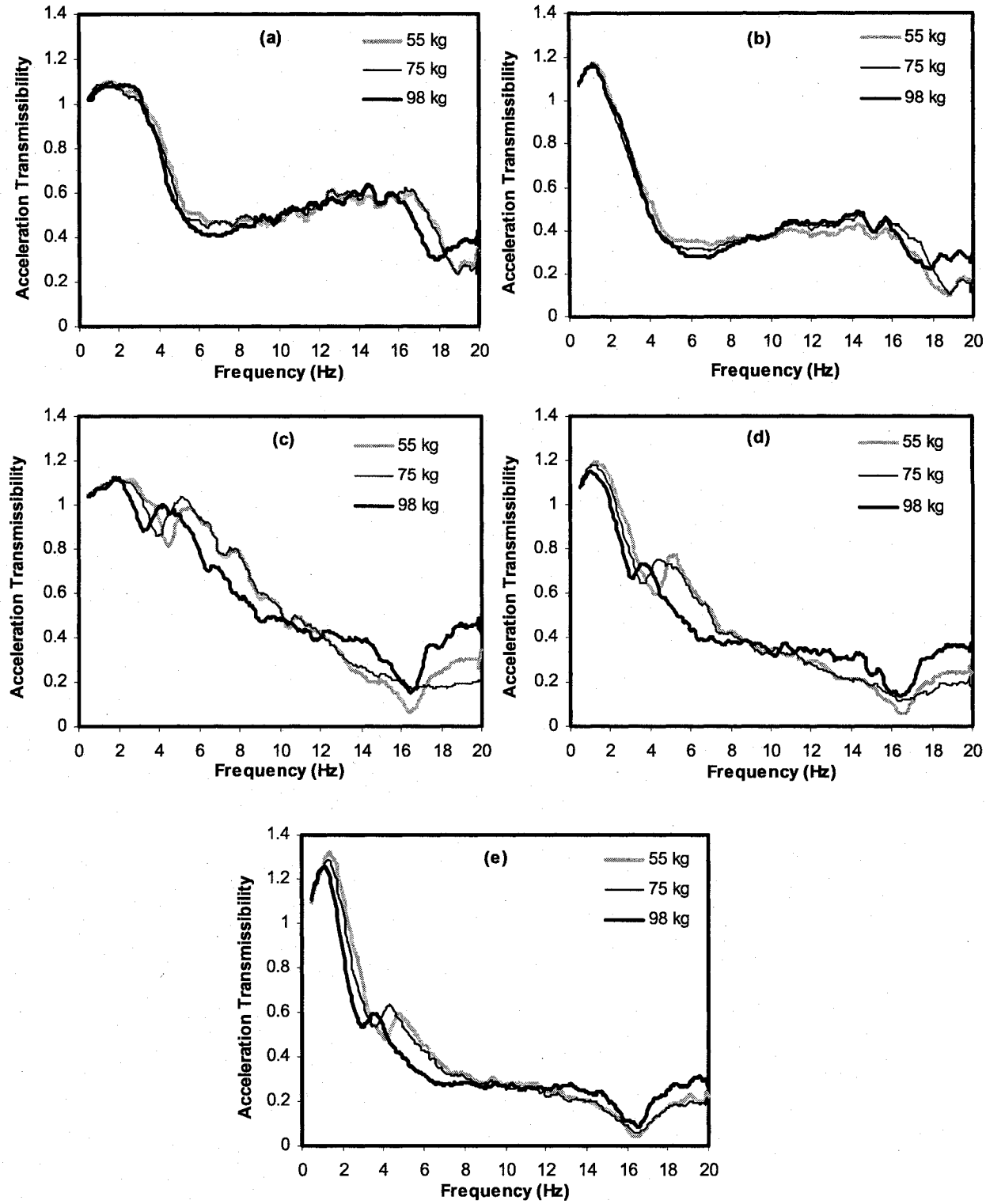

Figure 3.5: Influence of body mass and magnitude of broadband excitation on the acceleration transmissibility of seat B with manikins; (a) Manikin G: a_1 = 1 m/s^2; (b) Manikin G: a_1 = 1.5 m/s^2; (c) Manikin F: a_1 = 1 m/s^2; (d) Manikin F: a_1 = 1.5 m/s^2; (e) Manikin F: a_1 = 2 m/s^2

The manikin mass effect on the acceleration transmissibility of seat C with manikin G and manikin F is presented in Figures 3.6. The results in general show negligible effect of the manikin mass on both the peak transmissibility and the resonant frequency, for both manikins. This is due to the design of the suspension seat with automatic ride height adjustment and thus the weight compensations. The air springs yields higher stiffness under higher manikin mass, which tends to lower the effective damping ratio and causes only slightly higher peak acceleration transmissibility. The frequency response characteristics of seat C with manikin G also exhibit a secondary peak near 5 Hz, which is most likely the vibration mode associated with the manikin. This mode, however, is not evident for manikin F, most likely due to its high friction.

Figure 3.7 illustrate the acceleration transmissibility characteristics of seat D loaded with manikin G and manikin F and subject to broadband excitations of different magnitudes. The results in general show a slight decrease in the resonant frequency with increasing manikin mass and an increase in the peak transmissibility with increasing excitation magnitude, as observed for other seats. The frequency response characteristics of seat with manikin G, as illustrated in Figures 3.7 (a,b), reveal resonant frequency of the seat around 3 Hz under 1 m/s^2 excitation, which decreases to nearly 2 Hz under 1.5 m/s^2 excitation. This decrease in the resonant frequency is attributed to high friction due to suspension.

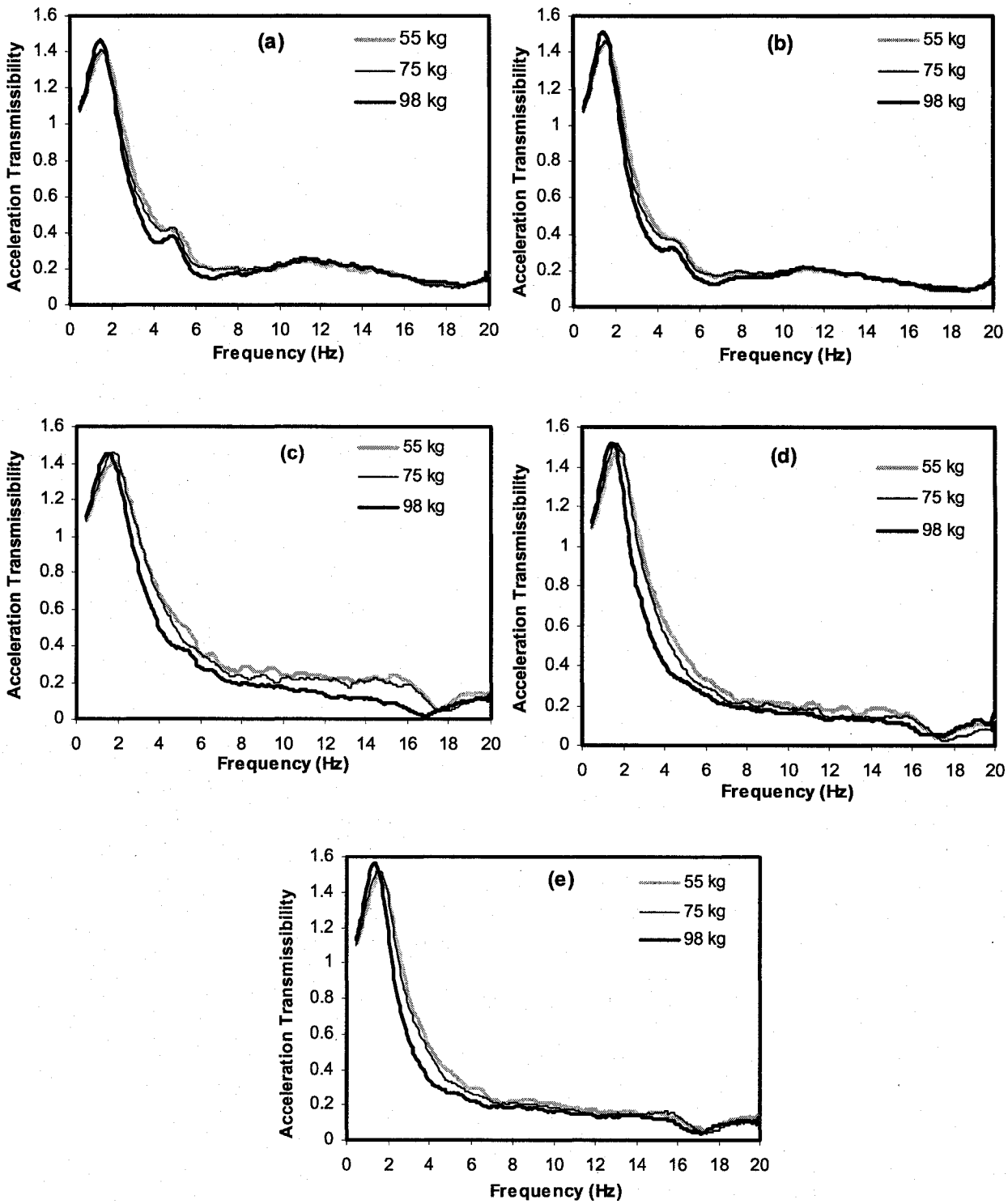

Figure 3.6: Influence of body mass and magnitude of broadband excitation on the acceleration transmissibility of seat C with manikins; (a) Manikin G: a_1 = 1 m/s^2; (b) Manikin G: a_1 = 1.5 m/s^2; (c) Manikin F: a_1 = 1 m/s^2; (d) Manikin F: a_1 = 1.5 m/s^2; (e) Manikin F: a_1 = 2 m/s^2

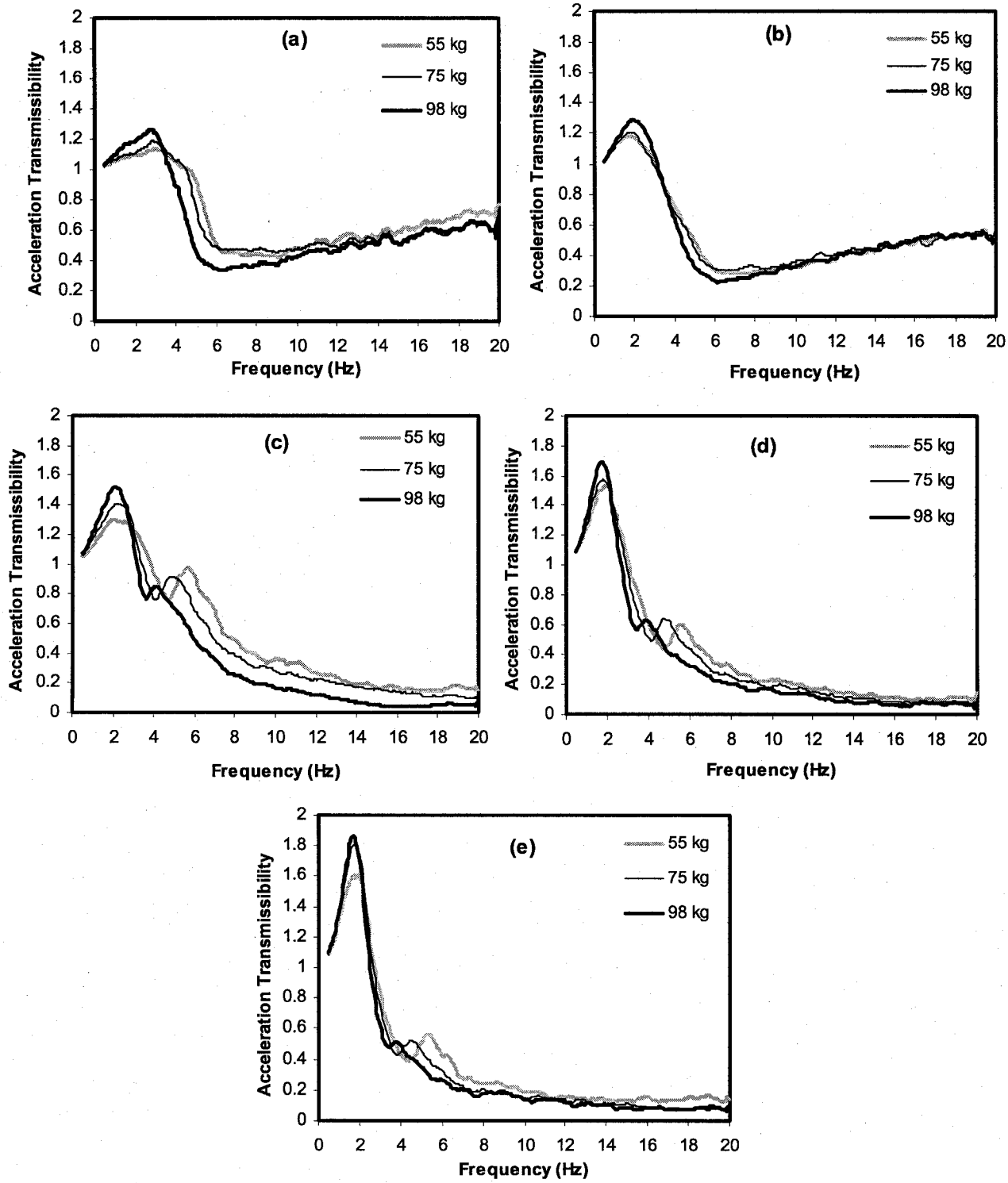

Figure 3.7: Influence of body mass and magnitude of broadband excitation on the acceleration transmissibility of seat D with manikins; (a) Manikin G: a_1 = 1 m/s^2; (b) Manikin G: a_1 = 1.5 m/s^2; (c) Manikin F: a_1 = 1 m/s^2; (d) Manikin F: a_1 = 1.5 m/s^2; (e) Manikin F: a_1 = 2 m/s^2

Figures 3.7 (c,d,e) illustrate the frequency response characteristics of seat with manikin F, which exhibit slightly lower resonant frequency for higher manikin mass and excitation magnitude. The acceleration transmissibility characteristics of he seat with manikin F show a second peak in the frequency range of 4 to 6 Hz, irrespective of the manikin mass and excitation magnitude. The frequency of the secondary peak decreased with an increase in the manikin mass, while its magnitude also decreased with increasing excitation magnitude. The presence of the secondary peak can be attributed to the pitching motion of the seat with behind-the-seat suspension design as in the case of seat B. This excited the pitch oscillations of manikin F, which was not restrained at the seat back. It should be noted that the secondary peak is not evident for manikin G, which may be due to the restraints used to support the manikin against the backrest.

3.4.2 Influence of Excitation

The frequency response characteristics of the candidate suspension seats with manikins G and F, illustrated in Figures 3.4 to 3.7, show varying influences of excitation magnitudes. The responses attained under different. Figures 3.8 and 3.9 illustrate the influence of vibration magnitude on the acceleration transmissibility of seat A loaded with manikin G and manikin F, respectively, for the three mass configurations. The results generally show a decrease in the resonant frequency and an increase in the peak magnitude as the vibration magnitude is increased, irrespective of the manikin mass. The peak acceleration transmissibility of the seat with manikin G tends to be lower than that with manikin F. This may be attributed to relatively higher peak value of the normalized APMS magnitude of the manikin F.

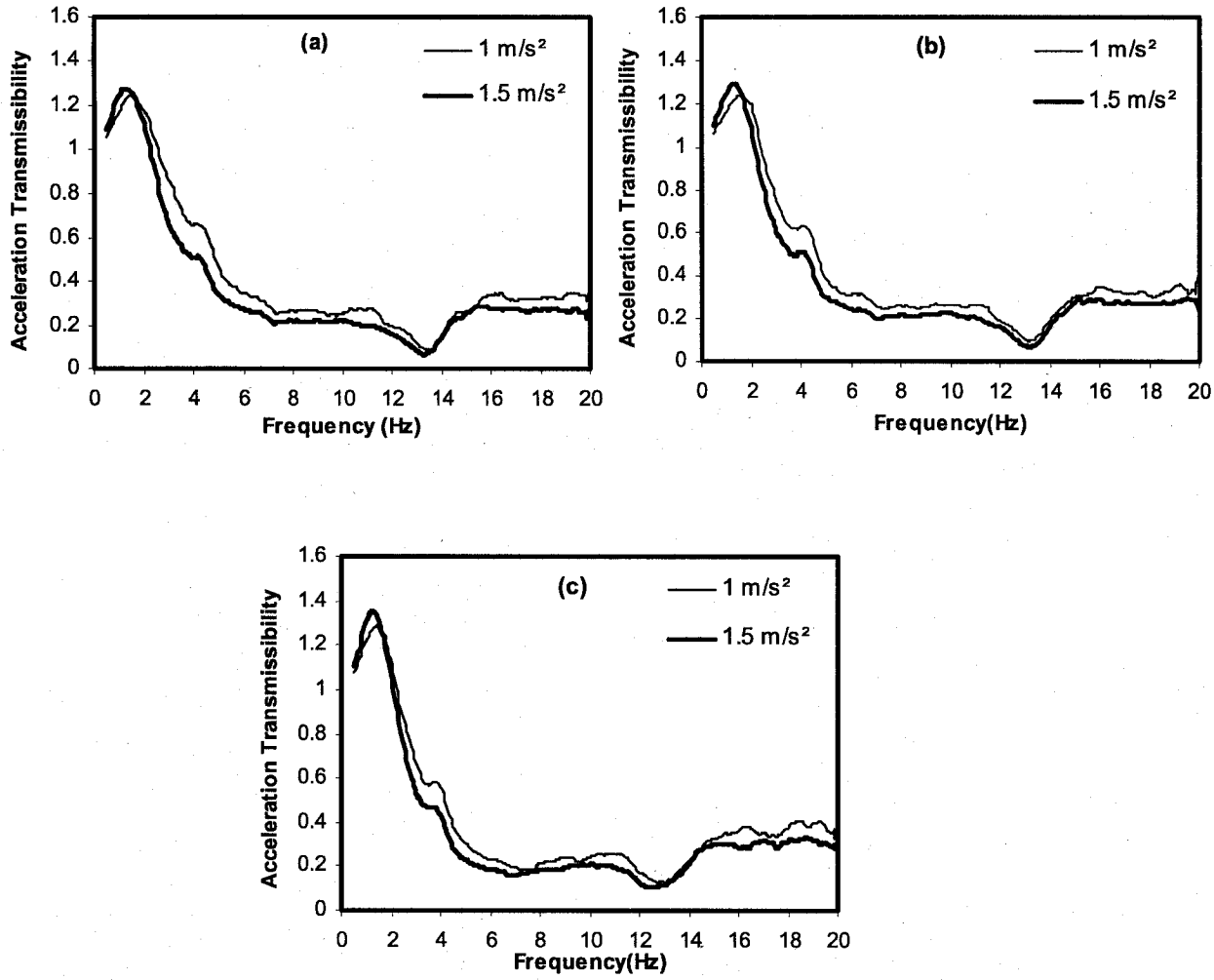

Figure 3.8 Influence of vibration magnitude on the acceleration transmissibility of seat A with manikin G :(a) 55 kg; (b) 75 kg; (c) 98 kg

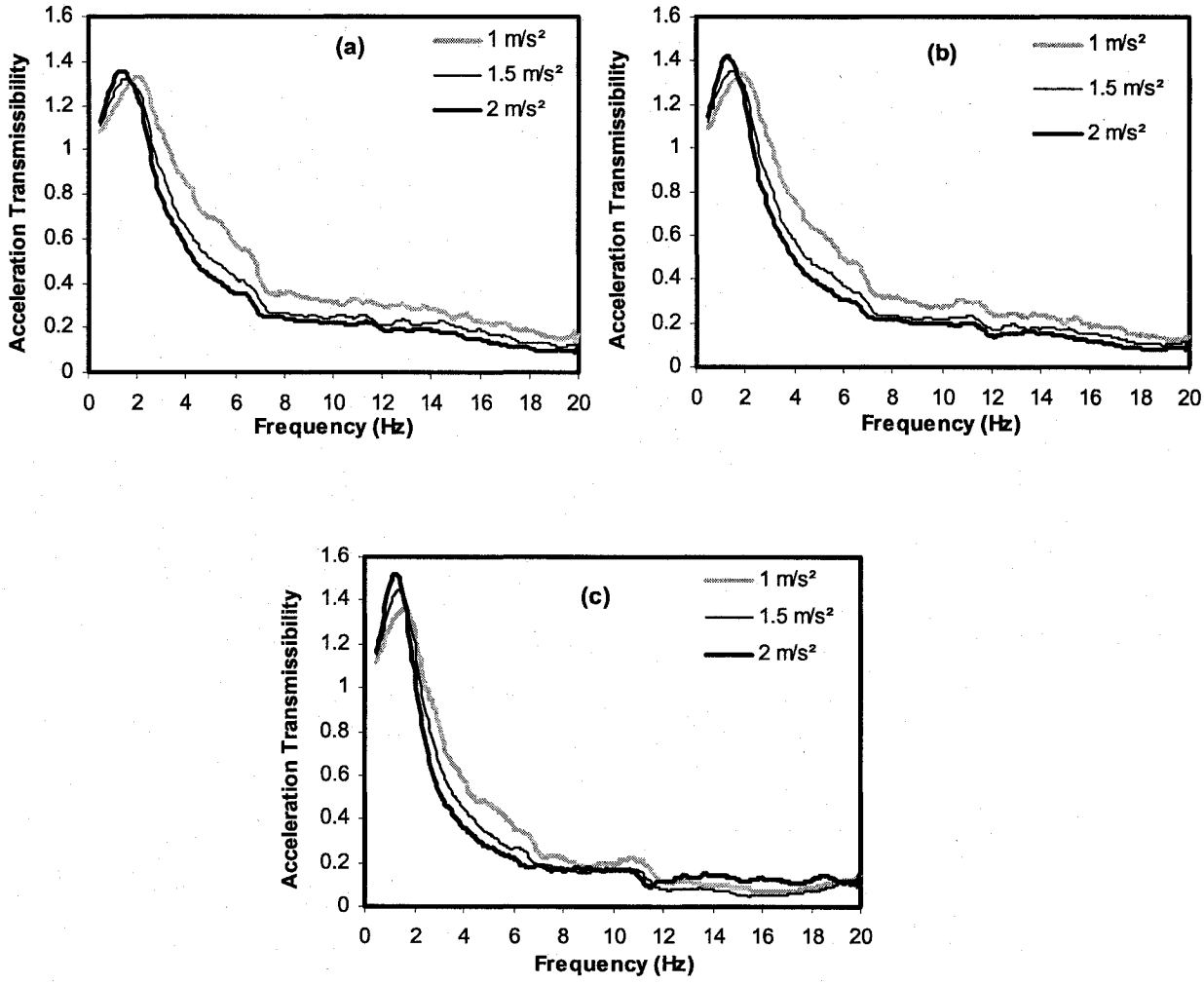

Figure 3.9 Influence of vibration magnitude on the acceleration transmissibility of seat A with manikin F: (a) 55 kg; (b) 75 kg; (c) 98 kg

The results also show the presence of a secondary peak near 4 Hz in the response with manikin G, irrespective of the manikin mass. This is most likely related to the deflection mode of the manikin, which is excited by relatively higher vibration at the seat cushion near 4 Hz (Transmissibility ≈ 0.5 to 0.7). This secondary peak is also evident for manikin F near 6 Hz, although the relative magnitude is very small. The lower magnitude of this peak is partly attributed to the lower levels of seat vibration near 6 Hz (Transmissibility ≈ 0.2 to 0.5), and partly due to coupled dynamics of the seat-manikin system.

Figure 3.10 and 3.11 illustrate the influence of vibration magnitude on the acceleration transmissibility of seat B loaded with manikin G and manikin F, respectively, for the three mass configurations. The results generally show a decrease in the resonant frequency and increase in the peak transmissibility as the excitation magnitude is increased. The frequency response of seat with manikin G showed a broader peak under 1 m/s^2 excitation level which can be attributed to the high friction present in the seat suspension. This effect of high friction is also seen with manikin F. The peak acceleration transmissibility of the seat with manikin G tends to be lower than the manikin F, irrespective of the manikin mass, as seen for the seat A. The results also show the presence of a second peak around 5 Hz in the response with manikin F, irrespective of the manikin mass. This is most likely related to the pitch motion of the seat and fundamental deflection mode of the unrestrained manikin. This secondary peak is not evident for manikin G.

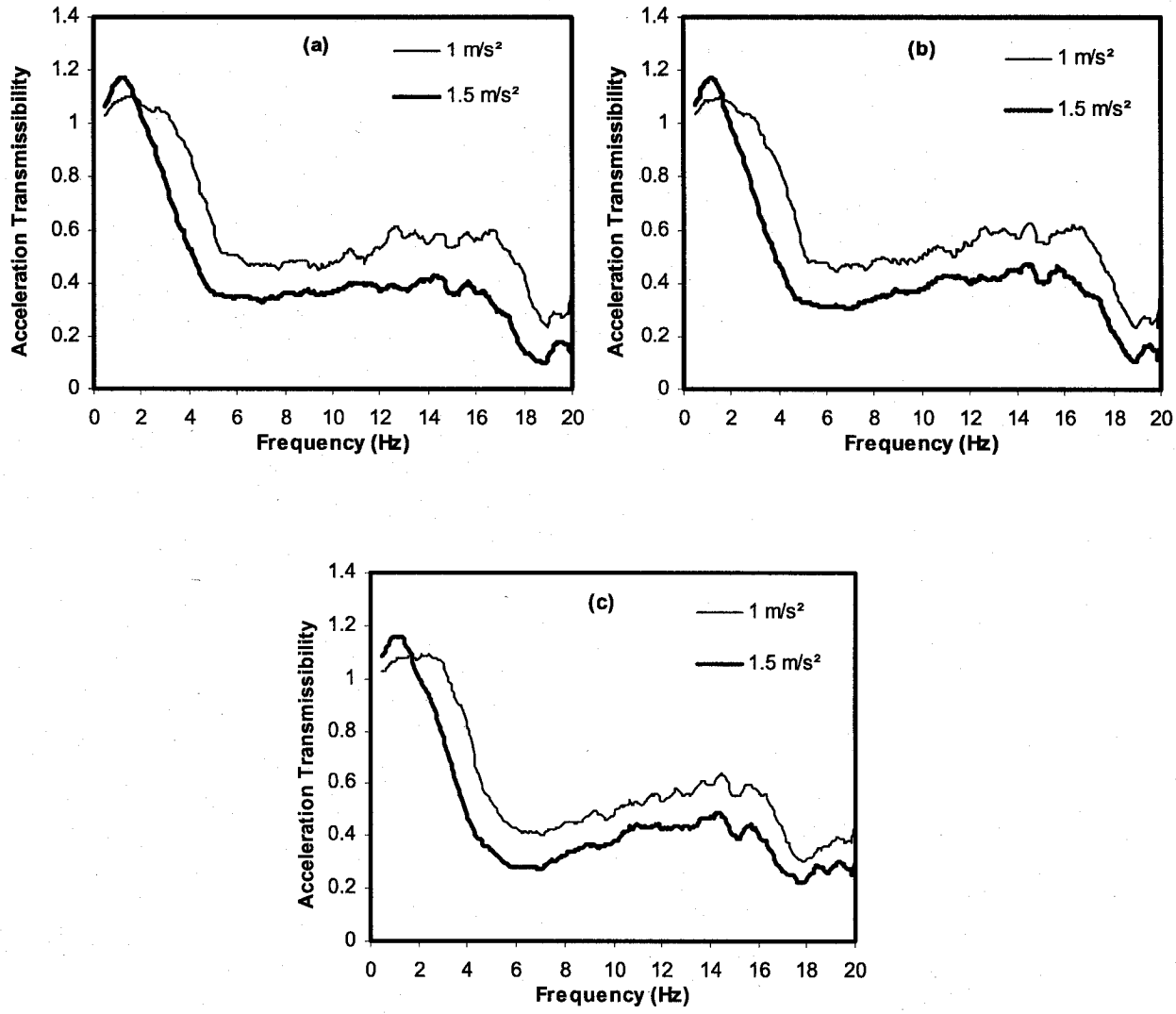

Figure 3.10: Influence of vibration magnitude on the acceleration transmissibility of seat B with manikin G: (a) 55 kg; (b) 75 kg; (c) 98 kg

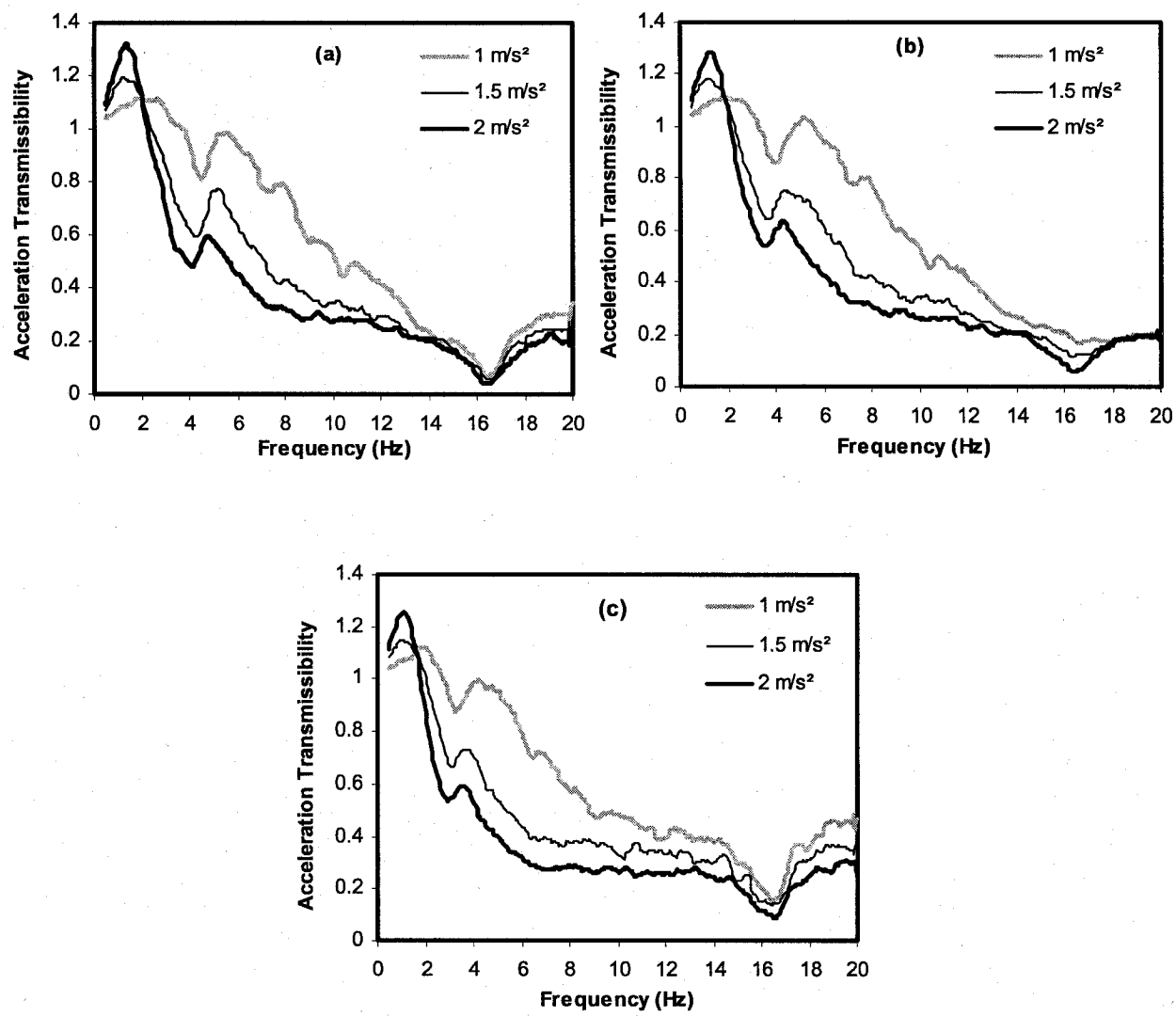

Figure 3.11 Influence of vibration magnitude on the acceleration transmissibility of seat B with manikin F: (a) 55 kg; (b) 75 kg; (c) 98 kg

Figures 3.12 and 3.13 illustrate the influence of vibration magnitude on the acceleration transmissibility of seat C loaded with manikin G and F, respectively. The results generally show slight decrease in the resonant frequency and slight increase in the peak magnitude as the excitation magnitude is increased. The peak acceleration transmissibility of seat with manikin G is similar to that with manikin F, unlike seat A and seat B, where the two manikins yield different magnitudes of transmissibility. The frequency response characteristics of the seat with manikin G show the presence of a secondary peak around 4 Hz, irrespective of the manikin mass. This secondary peak is also seen for manikin F, although it is not clearly evident. The presence of the secondary peak is again attributed to the vertical mode of the manikins and pitch motion of the seat.

Figures 3.14 and 3.15 illustrate the influence of vibration magnitude on the acceleration transmissibility of seat D loaded with manikins G and F, respectively. The results show trends similar to the observed for other seats. The peak acceleration transmissibility of seat with manikin G is lower than that of the seat with manikin F, which may be attributed to the higher normalized APMS of manikin F. The frequency response characteristics of the seat with manikin G show a wider peak at resonance due to its high friction, which is also evident for manikin F under lower excitation magnitude. The results also show the presence of a secondary peak with the unrestrained manikin F around 5 Hz, which is not evident for manikin G.

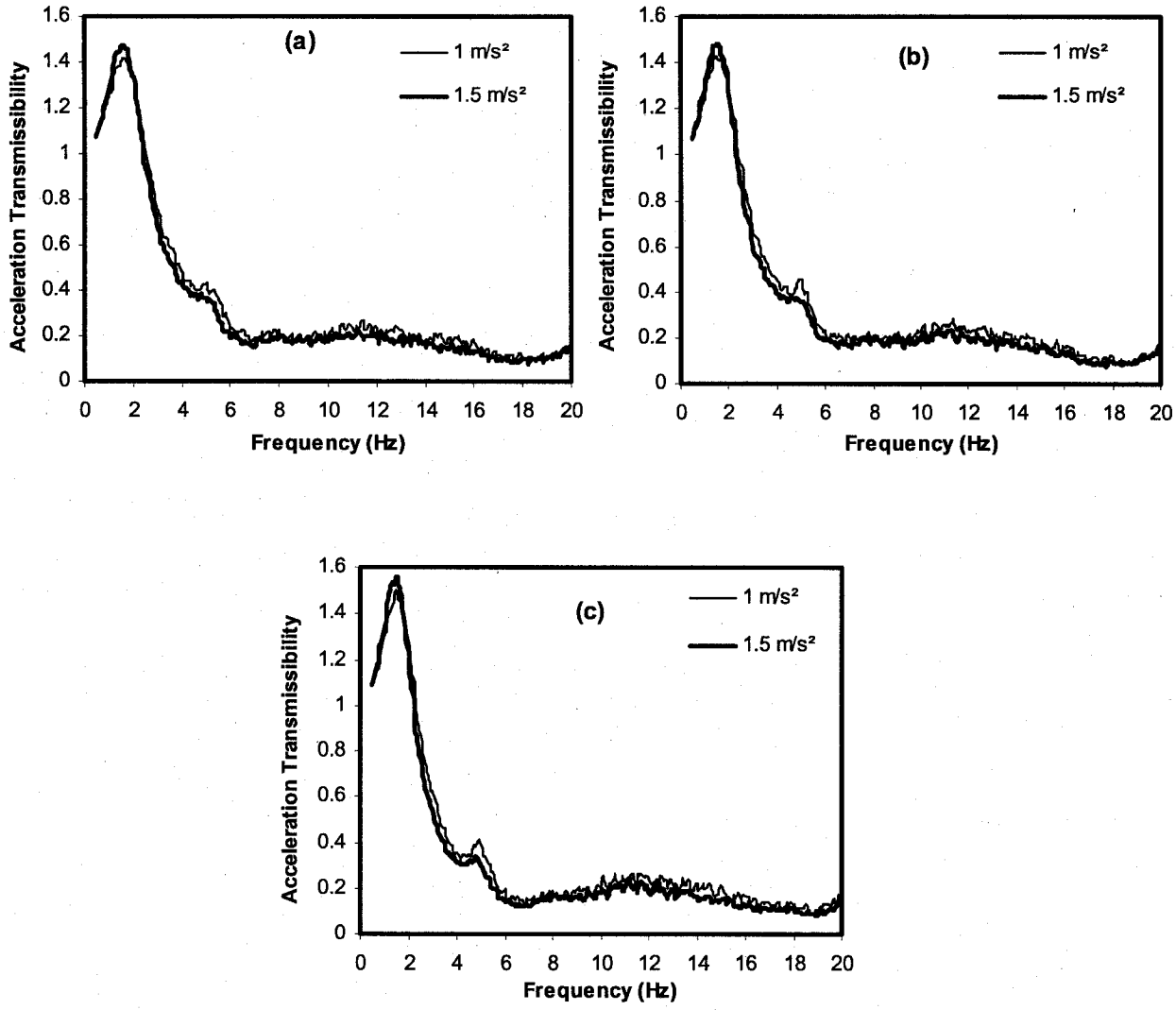

Figure 3.12: Influence of vibration magnitude on the acceleration transmissibility of seat C with manikin G: (a) 55 kg; (b) 75 kg; (c) 98 kg

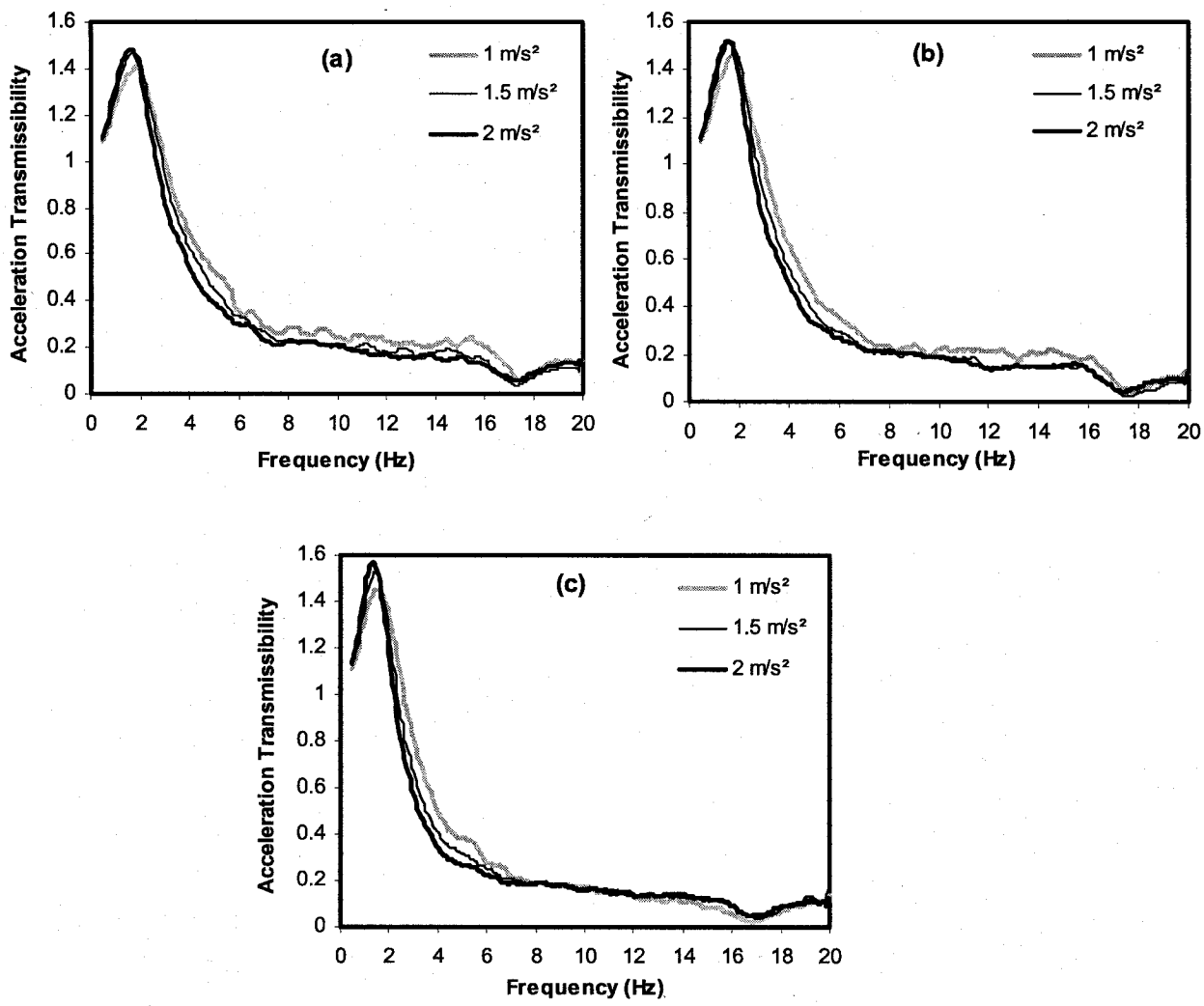

Figure 3.13: Influence of vibration magnitude on the acceleration transmissibility of seat C with manikin F: (a) 55 kg; (b) 75 kg; (c) 98 kg

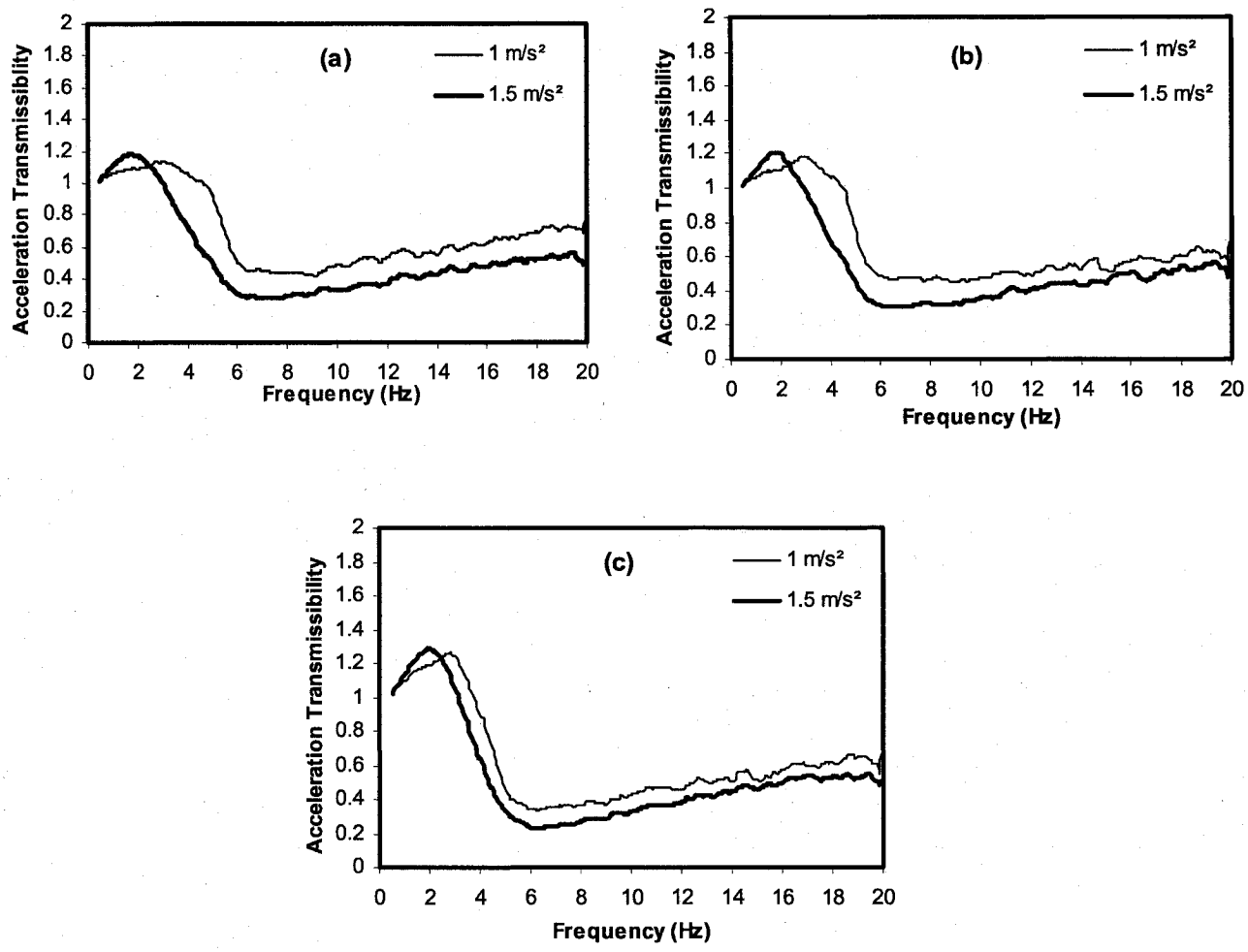

Figure 3.14: Influence of vibration magnitude on the acceleration transmissibility of seat D with manikin G: (a) 55 kg; (b) 75 kg; (c) 98 kg

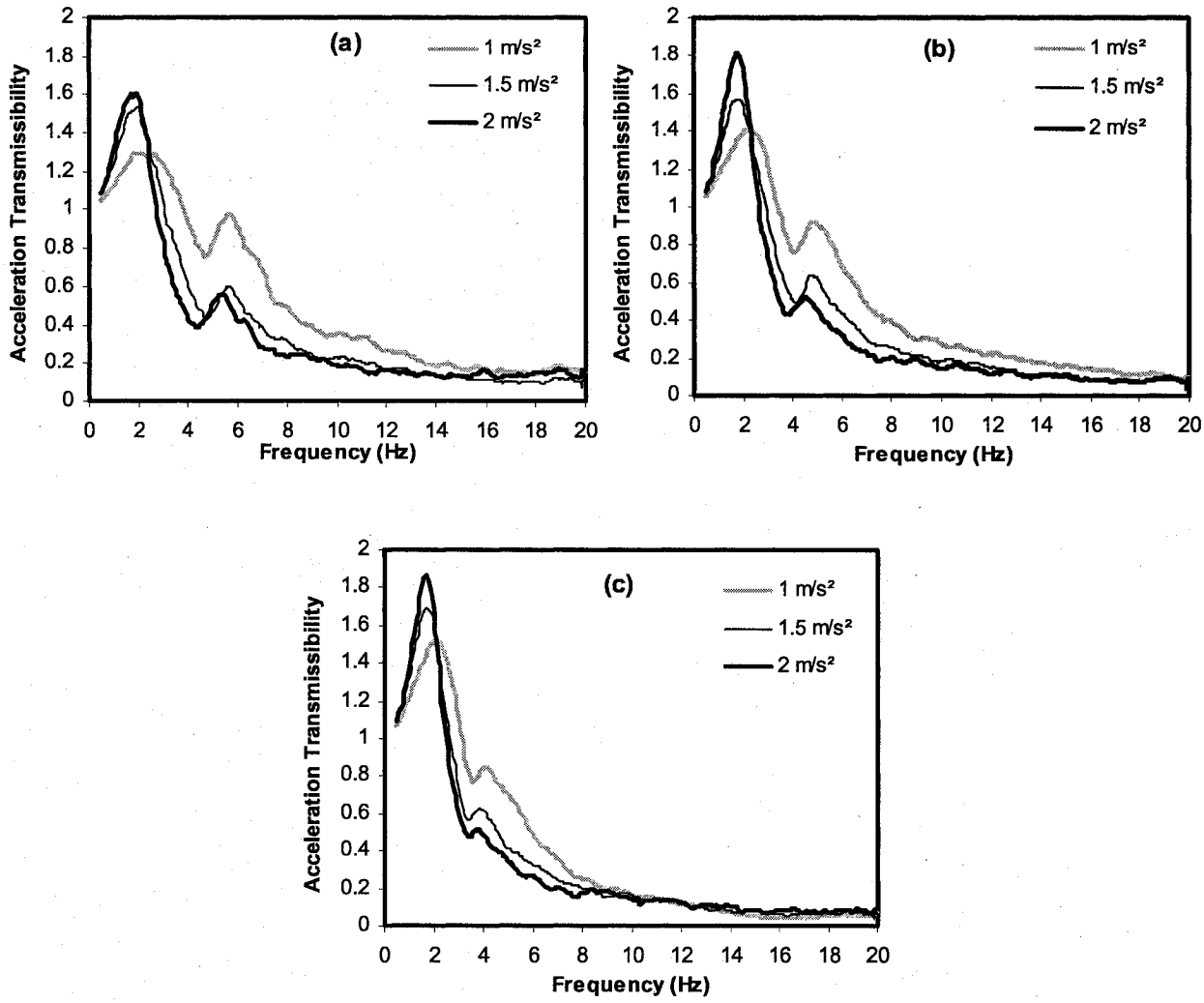

Figure 3.15: Influence of vibration magnitude on the acceleration transmissibility of seat D with manikin F: (a) 55 kg; (b) 75 kg; (c) 98 kg

3.5 Comparisons of Frequency Responses of Seat-Manikin and Seat-Human Systems

The validity of the manikins for seating dynamics applications is evaluated by comparing the frequency response characteristics of the seat-manikin system with that of the seat-human system under identical broad-band excitations and comparable masses. The frequency response characteristics of the selected seats with human subjects were thus evaluated under identical white noise excitations. The analysis were performed for a total of three human subjects with body mass within the selected mass configurations of the manikins, as summarized earlier in the Table 2.1 and Table 2.2. The frequency response characteristics of the seats with human subjects were evaluated for two different sitting postures: (i) back not supported-NB; and (ii) with back supported-WB. The data acquired for the three subjects with each mass group were analyzed to derive the mean and standard deviation of the mean responses. The results revealed comparable response of all three subjects with peak standard deviation in the order of 0.04, 0.02 and 0.09 for the 55, 75 and 98 kg groups, which occurred in the vicinity of the suspension resonance. The mean responses of the seat-human combinations are thus compared with those of the seat-manikin system to assess the validity of the manikins. The responses are also compared with those of the seat-rigid system of representative mass.

3.5.1 Seat A

Figures 3.16 and 3.17 illustrate comparison of mean acceleration transmissibility response of the seat A loaded with human subjects with those of the seat with equivalent rigid mass, and manikin G and F, respectively. It should be noted that the equivalent inert mass for the two manikins differ, as described earlier in Tables [2.1 and 2.2]. The figures show the results attained for three mass groups and two different levels of white-noise

random excitations (1.0 and 1.5 m/s^2 *rms*). The acceleration transmissibility characteristics of seat A loaded with inert mass and manikins (F and G) exhibit trends similar to those of seat-human system in the entire frequency range. The resonant frequencies and the transmissibility magnitudes however differ. The results show that the resonant frequency of the seat loaded with manikin G and equivalent inert mass are slightly lower than that of the seat-human system, irrespective of the mass and the excitation. Moreover, the peak transmissibility magnitude of the seat-mass and seat-manikin (G) system are consistently lower than that of the seat-human system for both sitting postures. It is further noted that the back support condition affects the responses only at frequencies above 2.5 Hz. The peak response of the seat-manikin system resembles closely to that of the seat-mass system. The response with human subject exhibit a secondary peak around 8 Hz, which has also been observed in the reported studies on the apparent mass characteristics of the seated human subjects exposed to vertical vibration [21]. Both the inert mass and the manikins do not exhibit this secondary peak.

The manikin F yields resonant frequencies that are closer to those of the seat-human system, irrespective of the mass and the excitation level, as shown in Figure 3.17. The resonant frequencies are also generally comparable with those of the seat-mass system, except for slight deviation for the 75 kg configuration. Unlike the response of the seat with manikin G, the peak magnitudes with manikin F are generally comparable with those of the seat-human system. The response of the 55 and 75 kg configurations under 1.5 m/s^2 excitation, however, form exception and yield slightly lower peak magnitudes.

The seat-mass system consistently reveals lower peak magnitudes, as observed in Figure 3.17.

The seat A with manikin G generally yields an underestimate of the acceleration transmissibility in the 3-14 Hz range, when compared to that of the seat with human subject, irrespective of the mass and excitation level. The deviation between the response of with the manikin and human however, tend to be small for the 98 kg configuration. The response of the seat with manikin F are comparable with those of the seat with human subjects in the mid to high frequency range, particularly under higher excitation of 1.5 m/s^2. Relatively poor agreements between the manikin F and human response at higher frequencies and lower magnitude excitation are most likely caused by high damper friction.

From the comparisons, it can be concluded that manikin F could provide reasonably good estimates of the vibration behavior of seat A loaded with human subjects of varying masses and exposed to white-noise random excitations. The manikin G, however yields an underestimate of both the resonant frequency and the peak magnitude, while considerable differences are also observed at higher frequencies for the 55 and 75 kg body masses. The responses of the seat with the inert mass are also somewhat comparable with that of the seat with manikin G, particularly around the resonant frequencies.

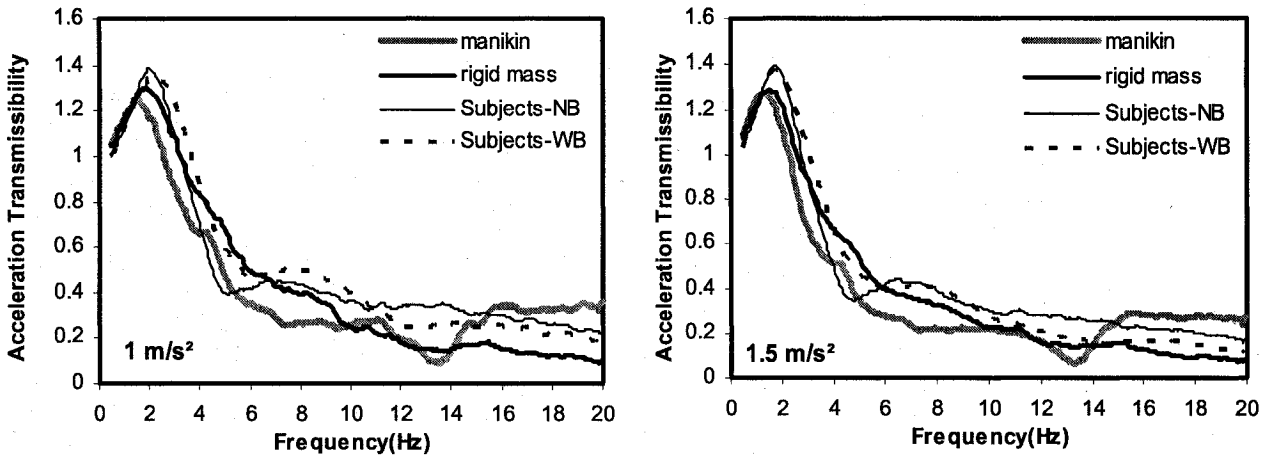

(a)

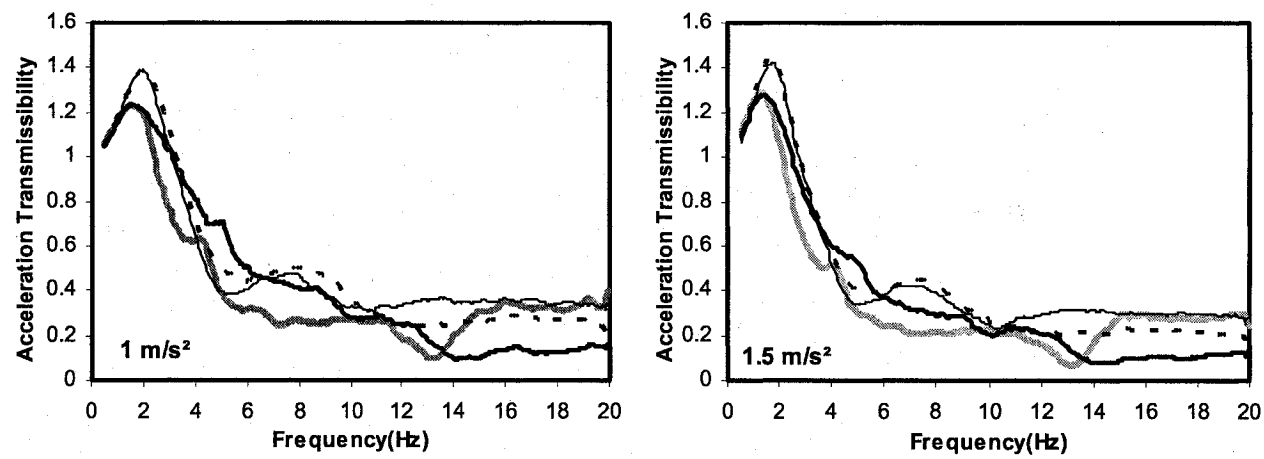

(b)

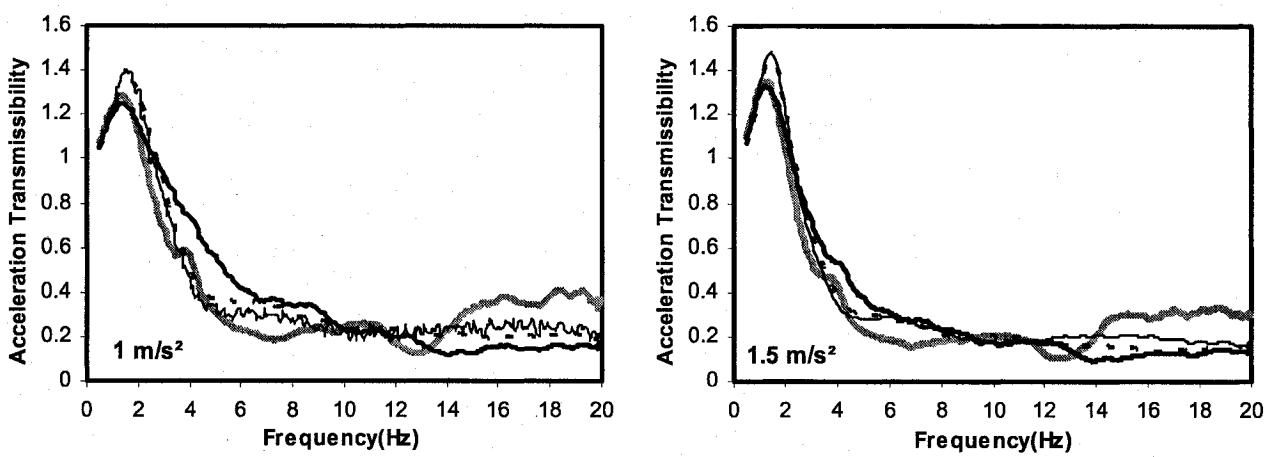

(c)

Figure 3.16: Comparisons of acceleration transmissibility responses of seat A loaded with inert mass, manikin G and human subjects under white noise excitations: (a) 55 kg; (b) 75 kg; (c) 98 kg

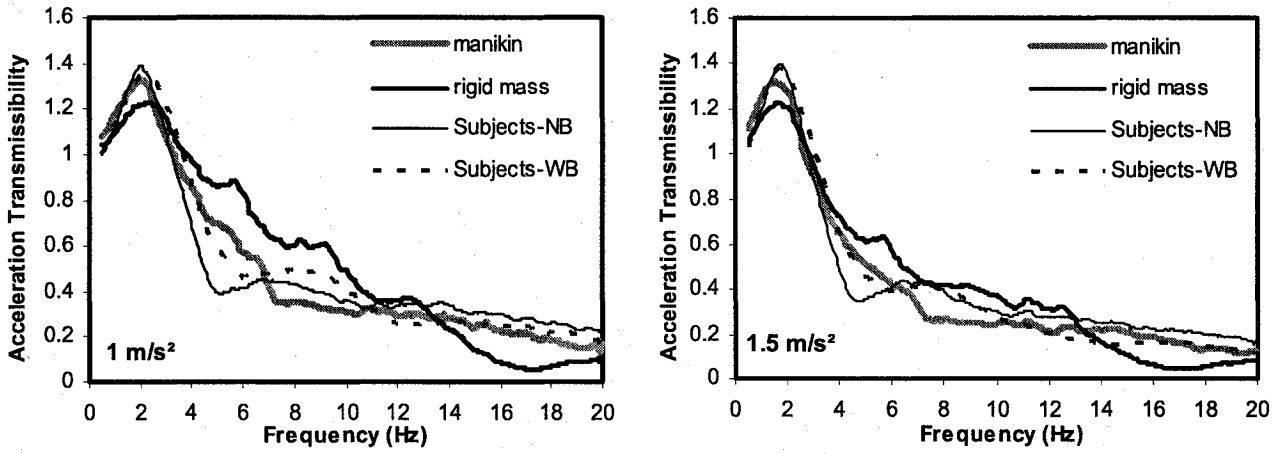

(a)

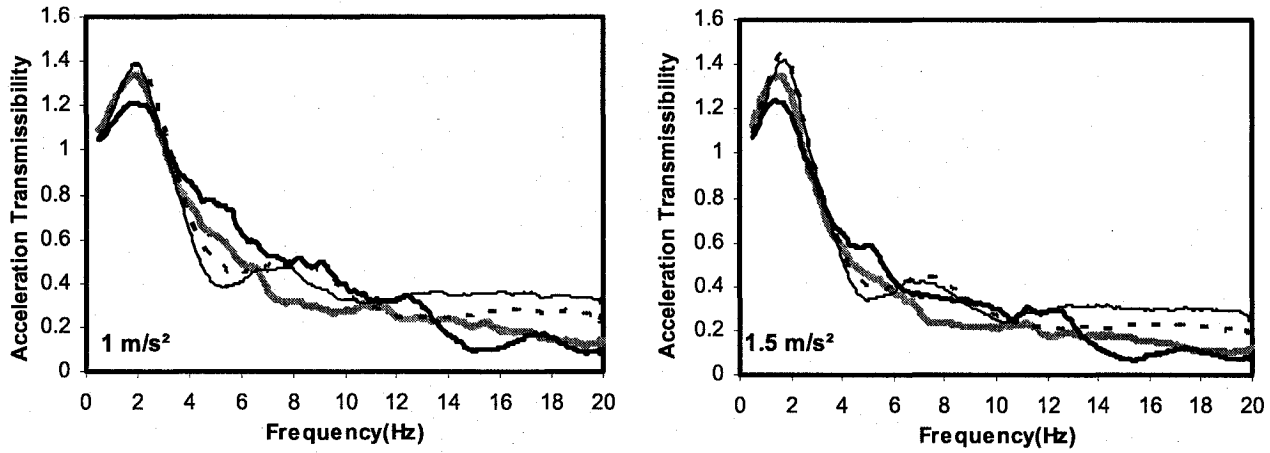

(b)

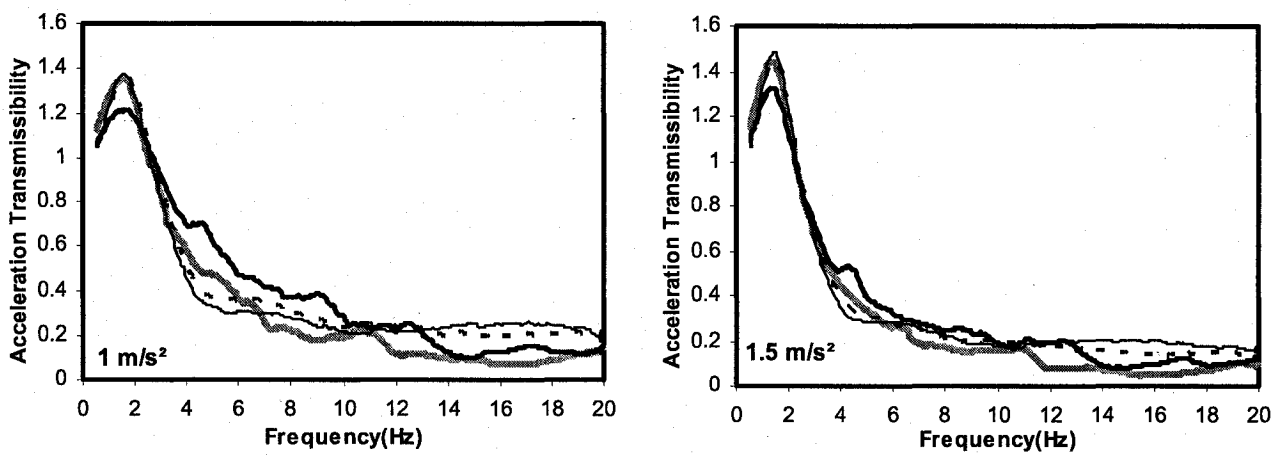

(c)

Figure 3.17: Comparisons of acceleration transmissibility responses of seat A loaded with inert mass, manikin F and human subjects under white noise excitations: (a) 55 kg; (b) 75 kg; (c) 98 kg

3.5.2 Seat B

Figures 3.18 and 3.19 illustrate comparisons of mean acceleration transmissibility responses of seat B loaded with human subjects with those of the seat with equivalent inert mass, and manikins G and F, respectively. The figures show the results attained for three mass groups and two different levels of white-noise excitations (1.0 and 1.5 m/s^2 *rms*). The results in general show that the resonant frequencies of the seat loaded with manikin G and equivalent inert mass are slightly lower than that of the seat-human system, as observed for seat A, irrespective of the mass and the excitation level. Moreover, the peak transmissibility magnitudes of the seat-mass and seat-manikin G systems are lower than those of the seat-human system for 55 and 98 kg, whereas for 75 kg the peak transmissibility magnitude of seat-mass system is higher than that of seat-human system for back-not supported posture.

The seat with manikin F yields resonant frequencies that are closer to those of the seat-human system, irrespective of the mass and excitation level, as shown in Figure 3.19. The resonant frequencies are also comparable with those of the seat-mass system under 1.5 m/s^2 excitation level, whereas the resonant frequency of the seat-mass system is observed to be slightly lower than that of seat-manikin system under 1 m/s^2 excitation level. The peak transmissibility magnitude of the seat-manikin and seat-human systems for back not supported posture are consistently the same, irrespective of the mass and excitation level. The acceleration transmissibility responses of seat with manikin F show a second peak in the 4-5.5 Hz range for all the mass groups and both levels of excitations, which is attributed to the resonance of the manikin.

The responses with the human subjects exhibit a secondary peak around 8 Hz for back not supported posture which was not evident for manikin G and corresponding inert mass. A secondary peak is also evident in the 4-5.5 Hz range with manikin F, while the responses with corresponding inert mass show a second peak around 7 Hz which could be caused by the movement of the unrestrained inert mass. It is further noted that the back support condition affects the responses at resonant frequency and also at frequencies above 6 Hz. The responses of 55 kg seat-human system, however, form an exception, wherein the effect of back support is not seen at resonant frequency but at frequencies above 6 Hz.

The seat B loaded with manikin G generally yields an overestimate of the acceleration transmissibility for frequencies above 10 Hz, irrespective of the mass and excitation level. The responses of the seat with manikin F are comparable with those of the seat-human system with back not supported posture in the low and high frequency ranges, particularly under 1.5 m/s^2 excitation level.

From the above comparisons, it can be concluded that manikin F provides reasonably good estimates of the vibration behavior of seat B loaded with human subjects in low and high frequency range. The manikin G, however, yields an overestimation of the acceleration transmissibility at higher frequencies and an under estimation of resonant frequency, irrespective of the mass and excitation level. The responses of the seat with inert mass are also comparable with that of the seat with manikin G, whereas the responses of seat-mass system are comparable with those of seat-manikin F system only for higher magnitude of excitation level.

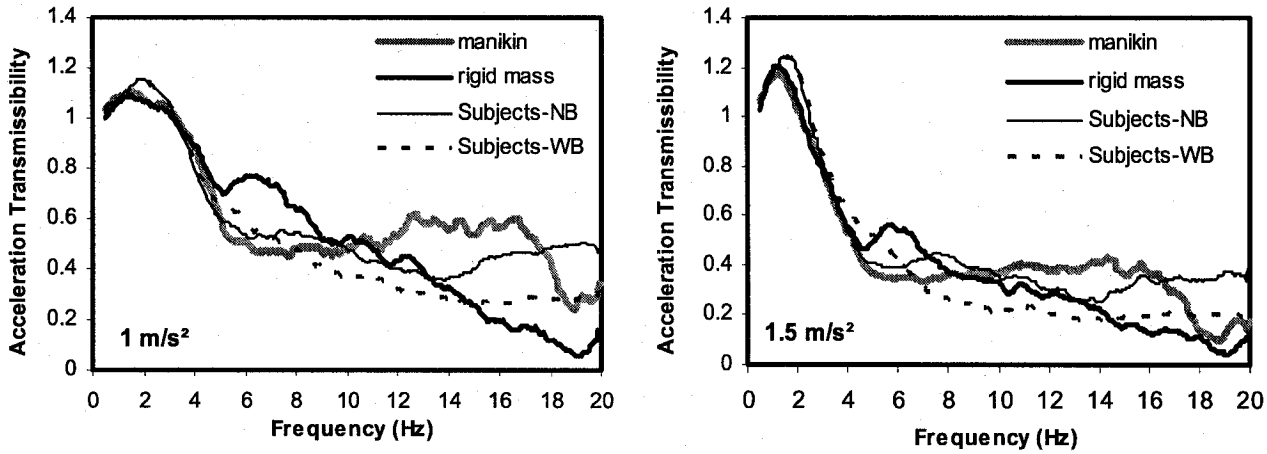

(a)

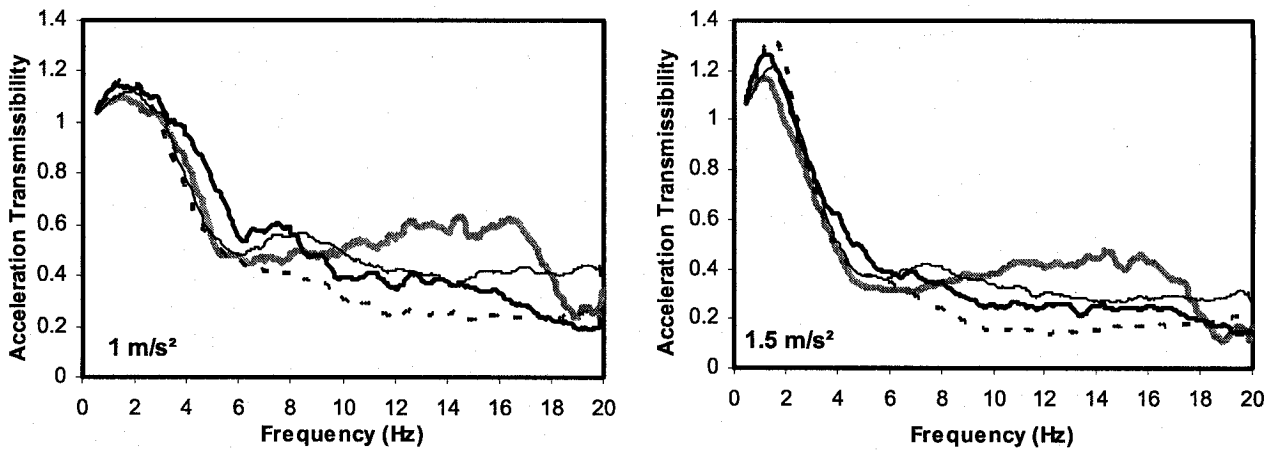

(b)

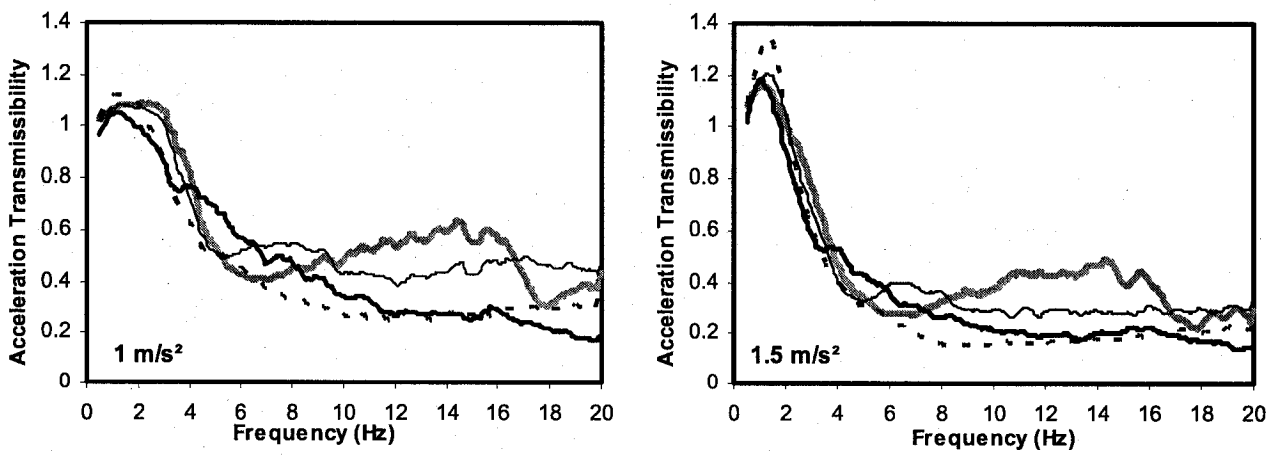

(c)

Figure 3.18: Comparisons of acceleration transmissibility responses of seat B loaded with inert mass, manikin G and human subjects under white noise excitations: (a) 55 kg; (b) 75 kg; (c) 98 kg

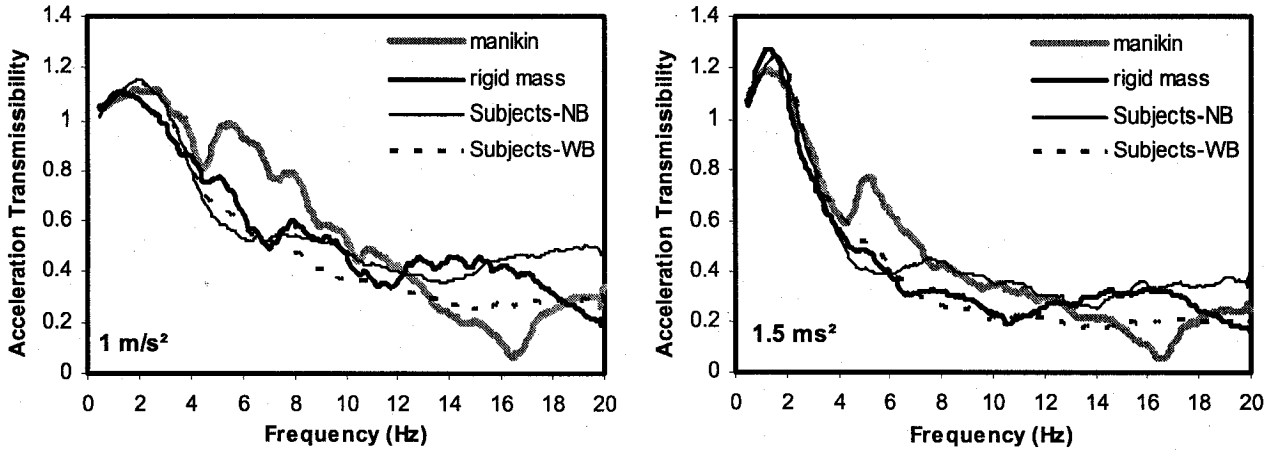

(a)

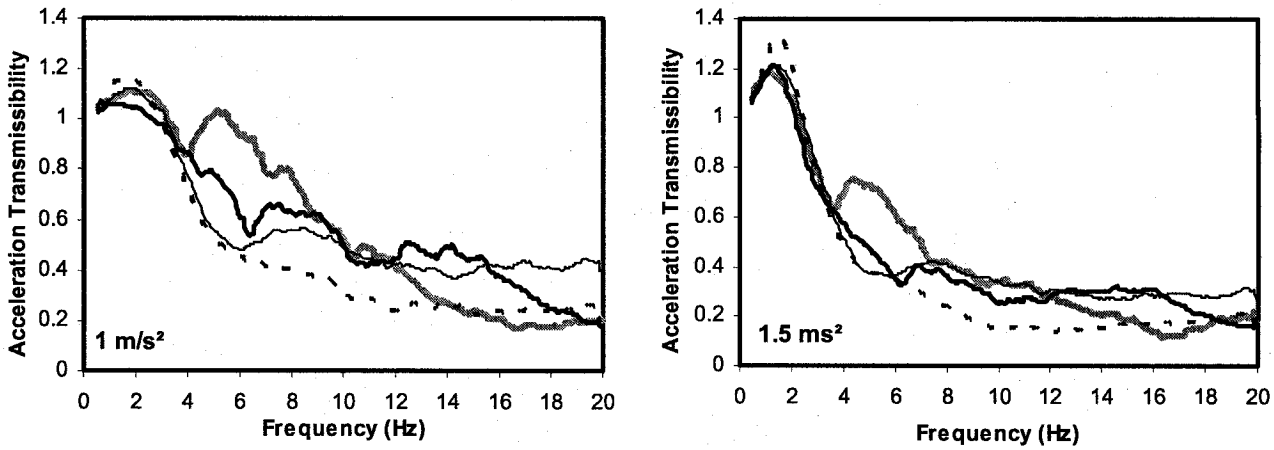

(b)

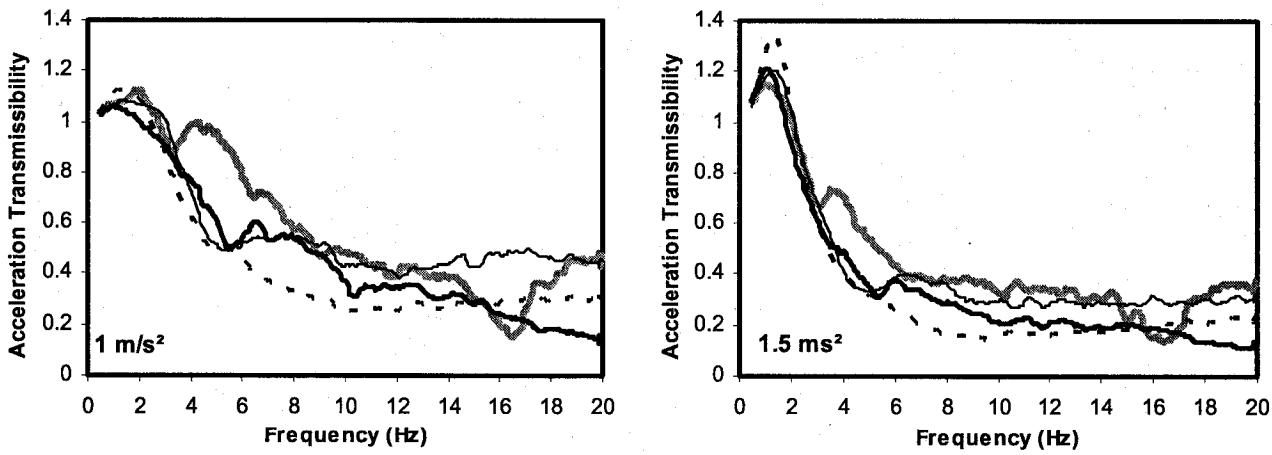

(c)

Figure 3.19: Comparisons of acceleration transmissibility responses of seat B loaded with inert mass, manikin F and human subjects under white noise excitations: (a) 55 kg; (b) 75 kg; (c) 98 kg

3.5.3 Seat C

Figures 3.20 and 3.21 illustrate comparisons of mean acceleration transmissibility responses of seat C loaded with human subjects with those of the seat loaded with manikins G and F and equivalent inert masses, respectively. The results in general show that the resonant frequencies of the seat loaded with manikin G are slightly lower than those of the seat-human systems, whereas the seat-mass system reproduced the same resonant frequency as the seat-human system, irrespective of the mass and the excitation level. Moreover, the peak transmissibility magnitudes of the seat-mass and seat-manikin G systems are consistently lower than those of the seat-human systems for both sitting postures. It is further noted that the peak transmissibility magnitude of the seat-mass system is consistently lower than that of the seat-manikin G system, although the difference tends to diminish for 98 kg configurations. The seat-mass system responses suggest the presence of a weak second peak around 6 Hz, while the seat-manikin G responses show a second peak around 5 Hz, irrespective of the mass and excitation level. These secondary peaks are most likely caused by the movements of the inert masses and manikin relative to the seat.

The responses with the human subject also suggest the presence of a weak secondary peak around 8 Hz, which was also observed for the other seats. It is further noted that the back support condition affects the responses only at the resonant frequency but the differences are very slight for 98 kg, particularly under1.5 m/s^2 excitation level, the effect of back support is not seen on the responses of the human subject.

The seat with manikin F yields resonant frequencies that are same to those of the seat-human system, irrespective of mass and excitation level, as shown in Figure 3.21. The

resonant frequencies are also the same with those of the seat-mass system. Unlike the responses of the seat with manikin G, the peak magnitudes with manikin F are generally comparable with those of the seat-human system for back not supported posture. The response of the seat-mass system is also comparable with that of the seat-manikin F system. The seat-manikin F and seat-mass system reproduces the acceleration transmissibility of seat-human system for 98 kg mass group under 1.5 m/s^2 excitation level. The seat C with manikins G and F generally yields comparable acceleration transmissibility in the frequency range of 0.5-20 Hz except at resonant frequency, irrespective of mass and excitation level.

From the comparison, it an be concluded that manikin F could provide reasonably better estimate of the vibration transmissibility behavior of seat C as compared to seat loaded with human subjects of varying masses and exposed to white-noise random excitations. The manikin G, however, yields an underestimate of both the resonant frequency and the peak magnitude.

3.5.4 Seat D

Figures 3.22 and 3.23 illustrate comparisons of mean acceleration transmissibility responses of seat D loaded with human subjects with those of the seat with equivalent inert mass, and manikins G and F, respectively. The results show that the resonant frequencies of the seat loaded with manikin G and equivalent inert mass are the same as those of the seat-human systems, irrespective of the mass and the excitation level. Moreover, the peak transmissibility magnitudes of the seat-mass systems are consistently comparable to those of the seat-human systems for both the postures, whereas the peak

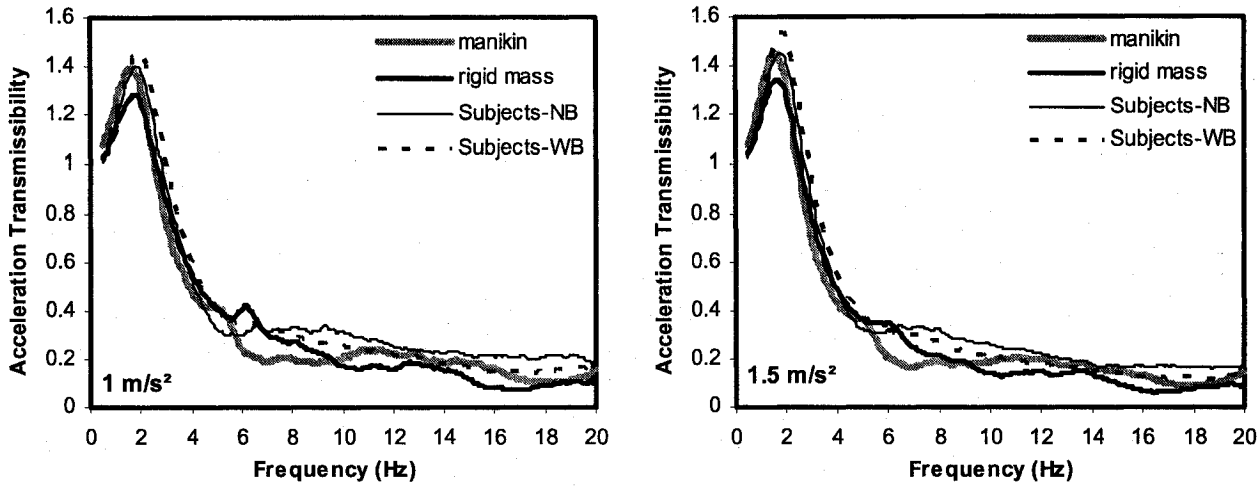

(a)

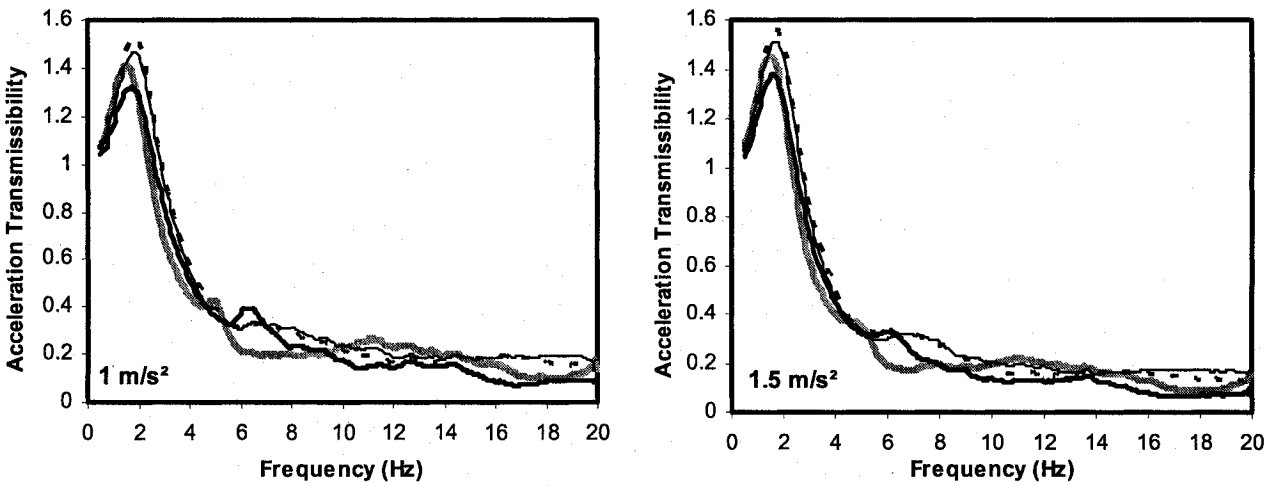

(b)

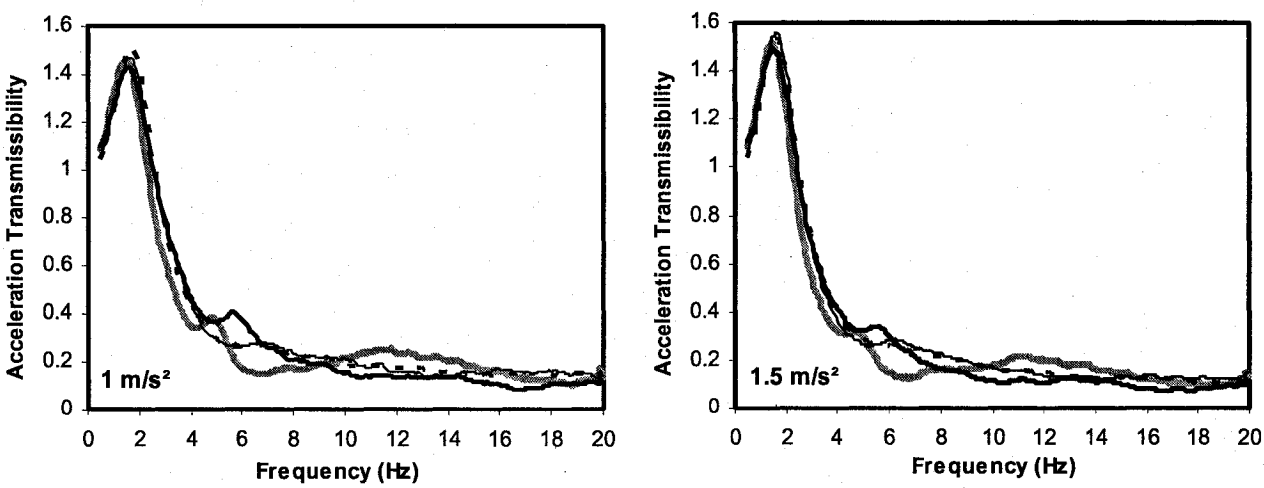

(c)

Figure 3.20: Comparisons of acceleration transmissibility responses of seat C loaded with inert mass, manikin G and human subjects under white noise excitations: (a) 55 kg; (b) 75 kg; (c) 98 kg

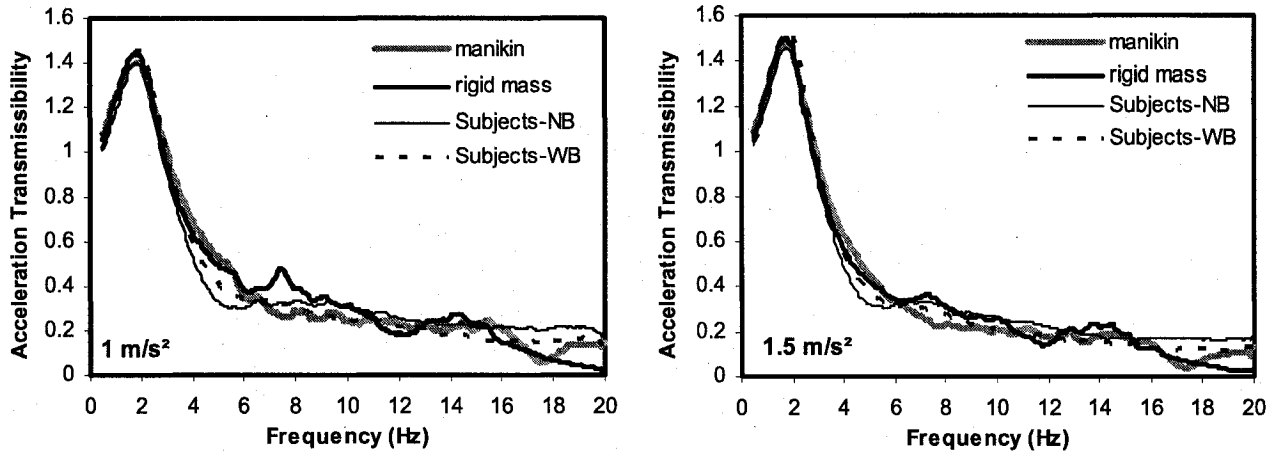

(a)

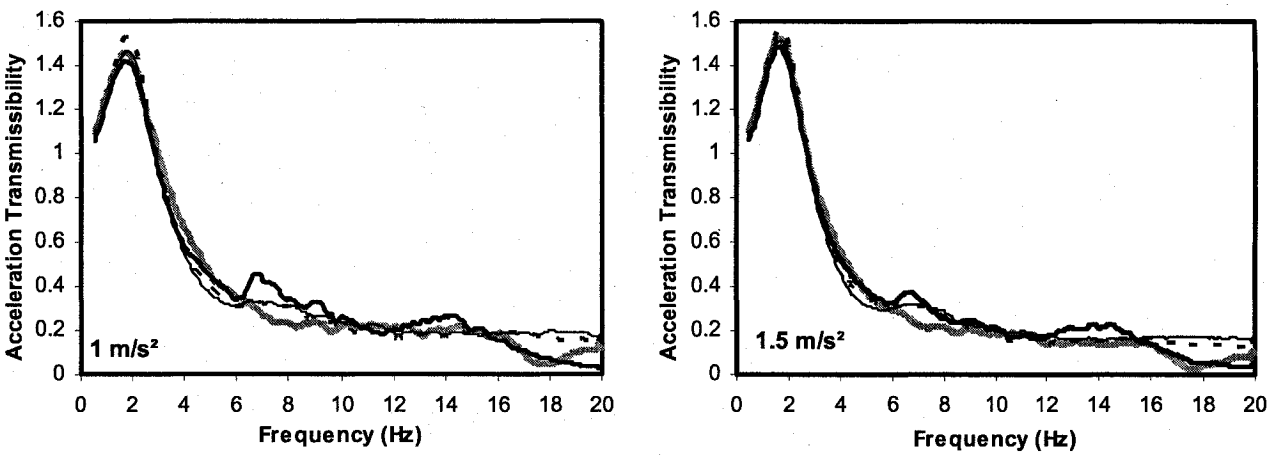

(b)

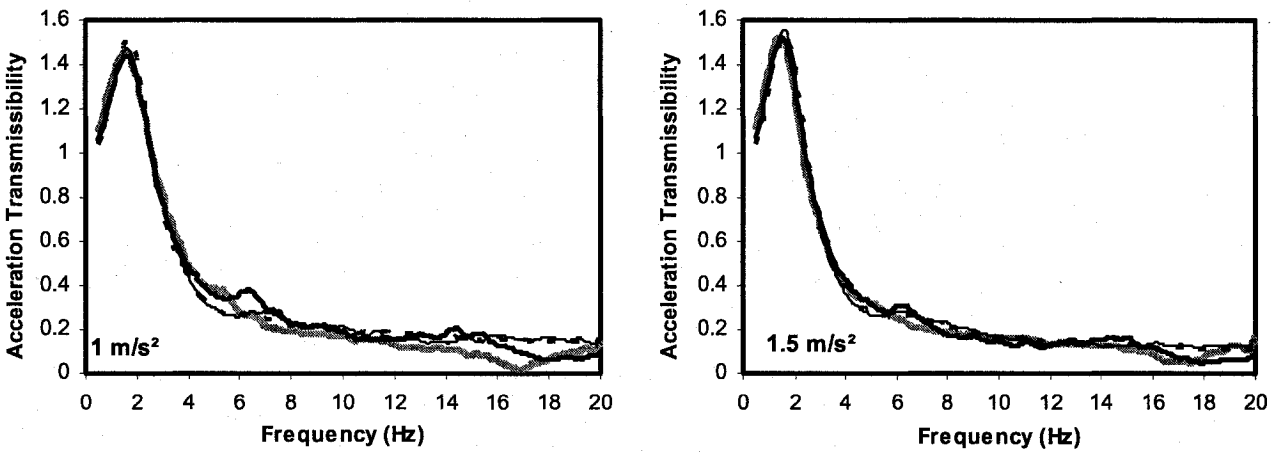

(c)

Figure 3.21: Comparisons of acceleration transmissibility responses of seat C loaded with inert mass, manikin F and human subjects under white noise excitations: (a) 55 kg; (b) 75 kg; (c) 98 kg

transmissibility of seat-manikin G system is consistently lower when compared to that of the seat-mass system It is further noted that the back supported condition affects the responses only at frequencies above 4 Hz. The responses with the inert mass exhibit a secondary peak in the 6-7 Hz range, which is due to the pitch motion of the seat. The responses with the human subjects also exhibit a secondary peak around 8 Hz, which is not evident with manikin G. The seat responses with manikin F show a second peak in the frequency range of 4-6 Hz.

The responses of seat-manikin F and seat-mass systems yield slightly lower resonant frequencies compared to those of the seat-human system for both the postures. The peak acceleration transmissibility magnitude of the seat-manikin F system is higher than that of seat-human system for both the postures, particularly for the 75 and 98 kg configurations. The peak acceleration transmissibility magnitude of the seat-mass system is closer to that of seat-manikin F system, irrespective of the mass and excitation level.

The seat D with manikin G generally yields an overestimation of the acceleration transmissibility at frequencies above 10 Hz, when compared to that of the seat with human subjects, irrespective of the mass and excitation level. The responses of the seat with manikin F yields an underestimation of the acceleration transmissibility for frequencies above 6 Hz.

From the comparisons, it can be concluded that the equivalent inert mass corresponding to manikin G could provide reasonably good estimates of the vibration transmissibility behavior of the seat D loaded with human subjects of varying masses and exposed to white-noise random excitation, with the exception of the secondary peak around 6 Hz. This secondary peak could most likely be suppressing by adequately

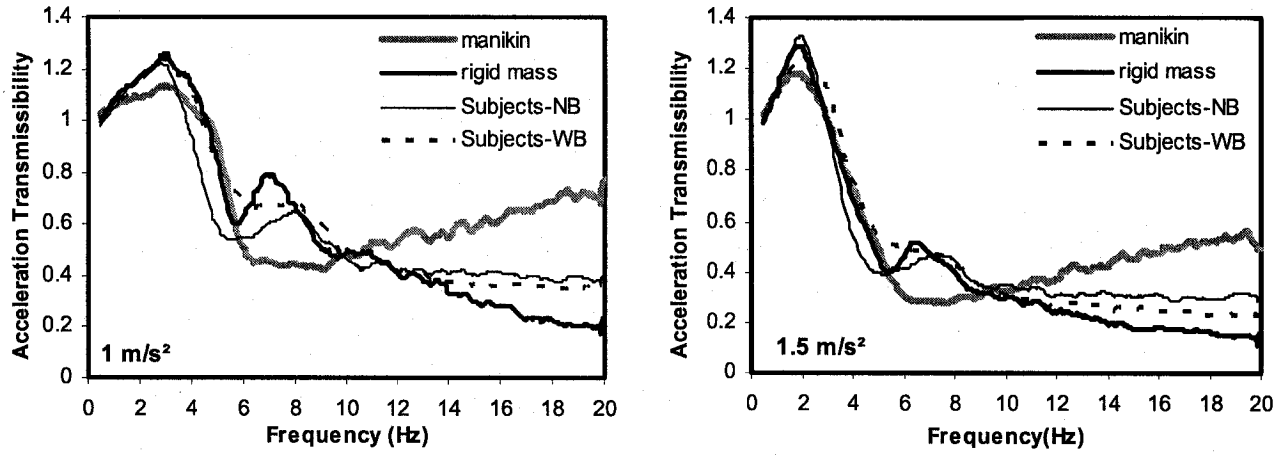

(a)

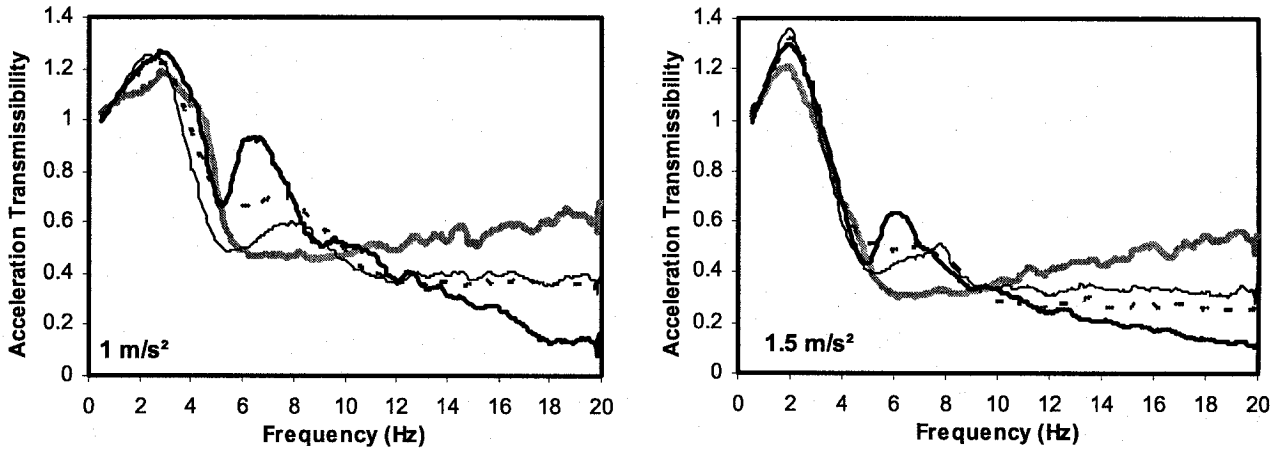

(b)

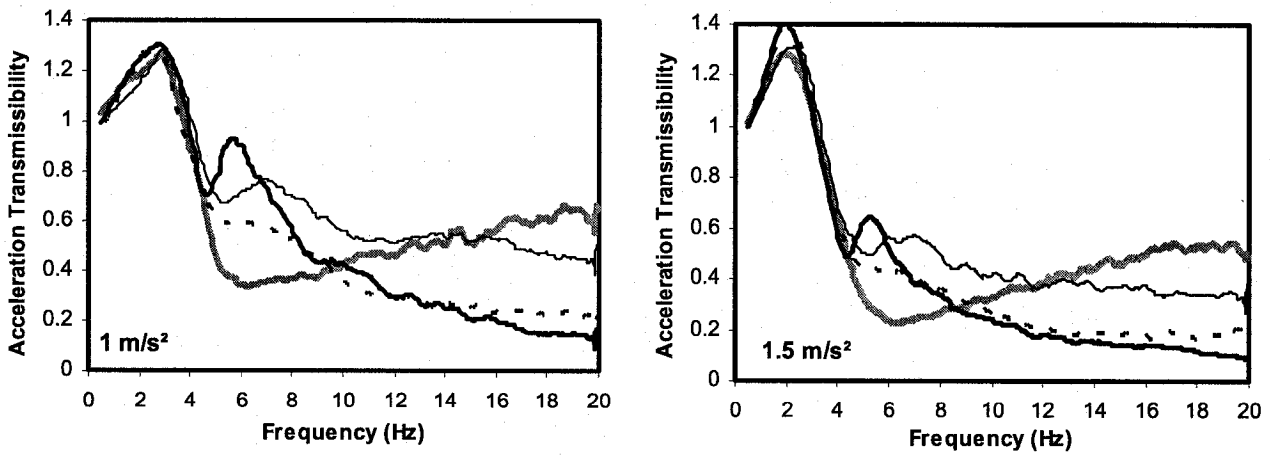

(c)

Figure 3.22: Comparisons of acceleration transmissibility responses of seat D loaded with inert mass, manikin G and human subjects under white noise excitations: (a) 55 kg; (b) 75 kg; (c) 98 kg

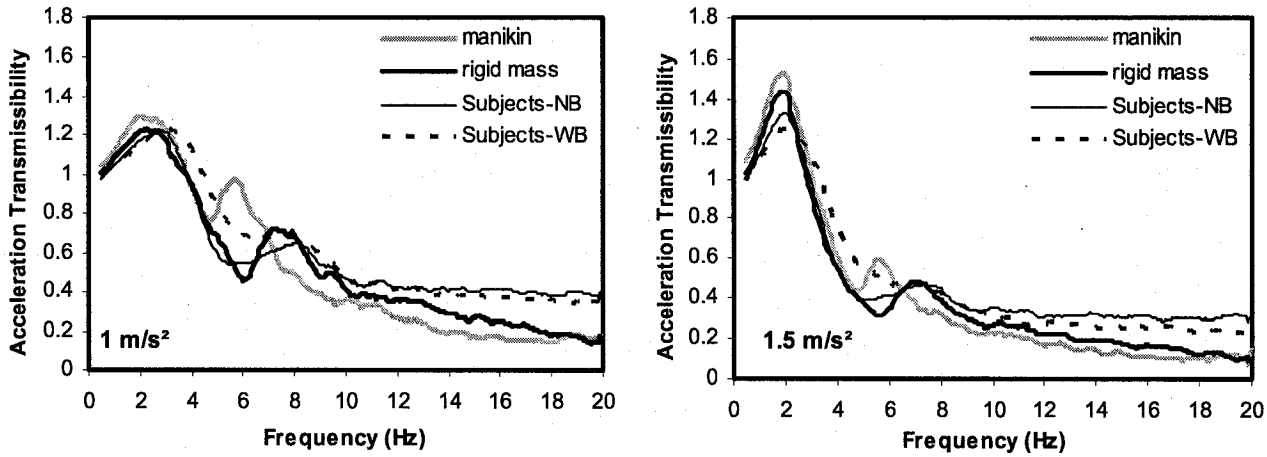

(a)

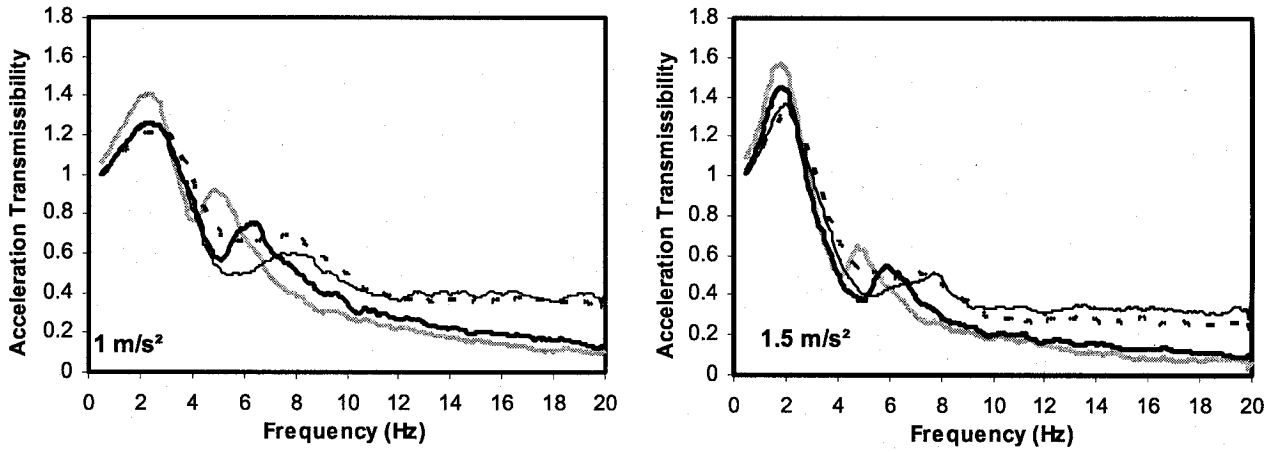

(b)

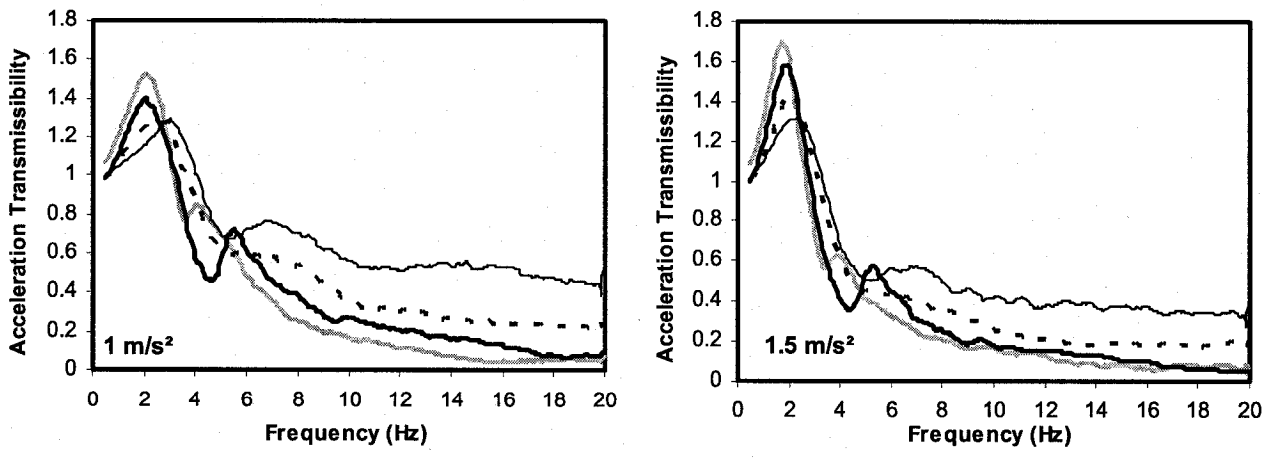

(c)

Figure 3.23: Comparisons of acceleration transmissibility responses of seat D loaded with inert mass, manikin F and human subjects under white noise excitations: (a) 55 kg; (b) 75 kg; (c) 98 kg

securing the mass to the seat. The manikin G, however, yields an underestimation of peak magnitude, while overestimates the acceleration transmissibility at higher frequencies. The manikin F yields slightly lower resonant frequency but considerably higher peak magnitude, and underestimates of the acceleration transmissibility at higher frequencies. The responses with the equivalent inert mass are also comparable to those of the seat-manikin F system.

3.5.5 Seat E

Figure 3.24 illustrate the comparison of mean acceleration transmissibility responses of the seat E loaded with human subjects to those of seat loaded with equivalent inert mass, manikins G and F, respectively. The figures show the results attained for 50^{th} percentile mass group (body mass = 75 kg) and two different levels of white-noise random excitations (2.0 and 2.5 m/s^2 *rms*). The results show that the resonant frequency of the seat loaded with manikin G is slightly lower than that of the seat-human system, irrespective of the mass and excitation level. Significantly higher resonant frequency, however, is observed for the seat-mass system. This trend for high natural frequency seats has also been reported in a few studies [55]. Moreover, the peak magnitudes of the seat-manikin G system responses are considerably lower than those of seat-human system, while those of the seat-mass system are considerably higher. It is further noted that the effect of back support on the seat-human system responses is evident only in the mid frequency range. The responses with the human subjects show a second peak around 8 Hz, which is not evident from the responses with inert mass and the manikins.

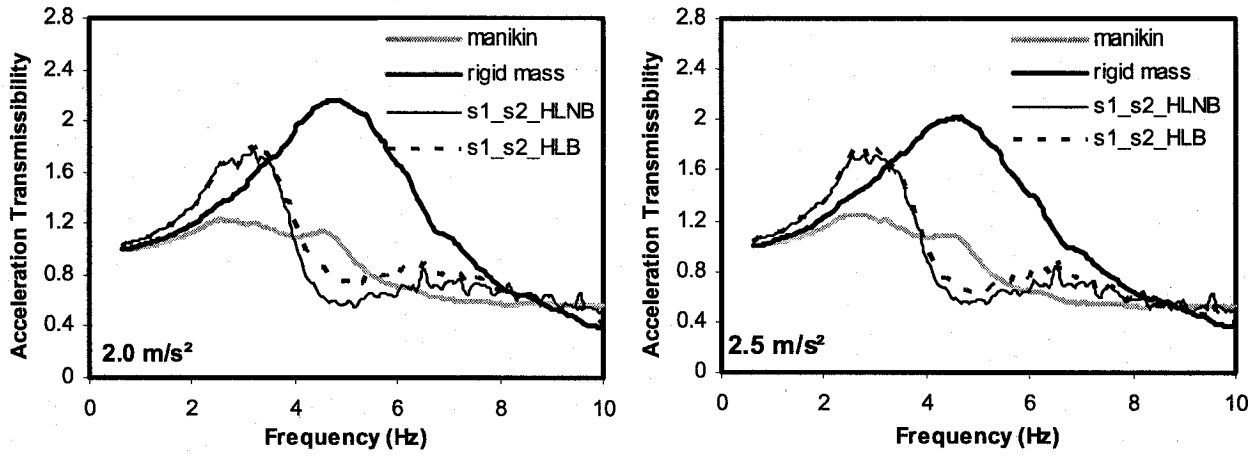

(a)

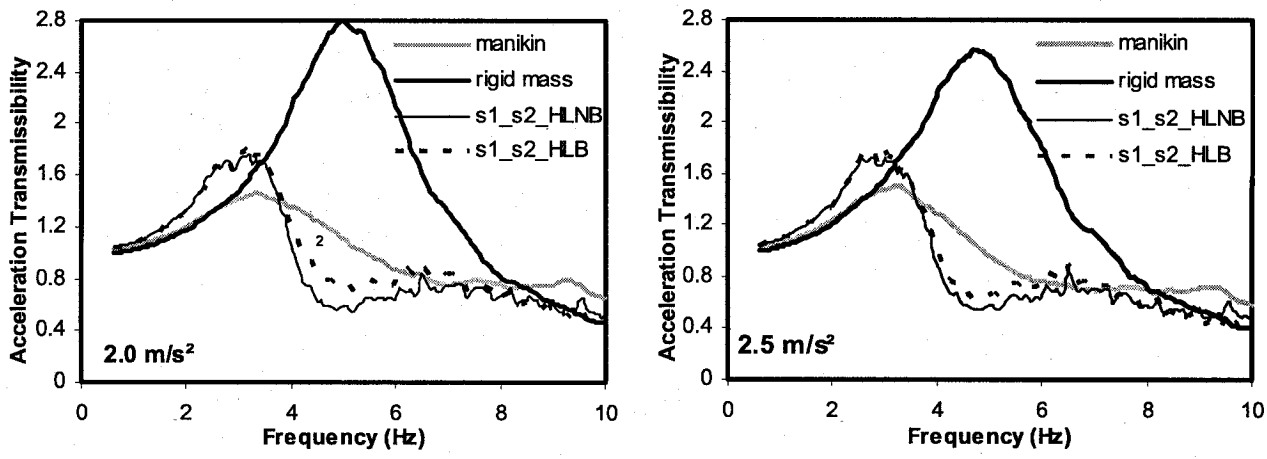

(b)

Figure 3.24: Comparisons of acceleration transmissibility responses of seat E for 75 kg under white noise excitations: (a) Manikin G; (b) Manikin F

The seat with manikin F yields slightly higher resonant frequency than those of the seat-human system, while the seat-mass system yields a considerably higher resonant frequency. Moreover, the peak transmissibility magnitudes of the seat-manikin F are comparable to those of the seat-human system, whereas a considerably higher peak transmissibility magnitude is observed for the seat-mass system.

From the comparisons, it can be concluded that the seat-mass systems yield considerably higher resonant frequencies and peak acceleration transmissibility magnitudes compared to those of the seat-human and seat-manikins systems. This can be attributed to the fact that broad-band excitations coupled with high natural frequency of the seat tend to excite the fundamental body mode. The contributions due to the seated human body dynamics are thus significant, which has also been suggested in an earlier study [55].

3.6 Relative response characteristics under vehicular excitations

As stated earlier, the overall vibration performances of a suspension seat depends upon the nature of excitation, primarily the predominant frequencies and magnitudes of excitation. Although the broad-band excitations tend to excite the seat as well as the seated manikin or the body modes, low natural frequency suspensions generally suppress the excitations corresponding to important body or manikin modes. Broad-band excitations, however, yield important properties of a suspension seat but do not characterize the vibration spectra of majority of vehicles, which may predominate in a narrow frequency band. The validity of the manikins for seating dynamics applications can be truly evaluated by comparing the seat acceleration response characteristics of the seat-manikin system with that of seat-human system under representative vibration

spectra of specific vehicles. In this study, the relative responses of the seat-human, seat-manikins and seat-mass systems are evaluated under vibration spectra of selected vehicles, as summarized in Table 3.4. The comparisons are performed in terms of seat acceleration responses in the 1/3-octave frequency bands, while the frequency bands for different excitations is limited to ranges where sufficient energy is ensured. The responses attained for the seat-human system are presented by their mean values, while the data for the NB posture alone is used.

3.6.1 Seat A

Figures 3.25 and 3.26 illustrate the comparisons of mean unweighted *rms* acceleration responses of seat A loaded with human subjects, with those of the seat loaded with manikins G and F, inert mass respectively. The spectrum used to excite seat A is that of a class II trucks, which yields predominant vertical motion in the vicinity of 2.2 Hz (a_{2w} = 0.95 m/s^2). The results show that the resonant frequencies of the seat loaded with manikin G and equivalent inert mass are similar to those of the seat loaded with human subjects. Moreover, the peak acceleration responses of the seat with manikin G and equivalent masses are consistently lower than those of the seat-human system. The peak acceleration response with the inert mass, however, is greater than that with manikin G, irrespective of the mass.

The seat with manikin F also yields resonant frequencies that are quite close to those of the seat-human system and seat-mass systems, irrespective of the mass. Unlike the manikin G, the peak acceleration responses of the seat-manikin F system are closer to those of the seat-human system, particularly for the 55 kg configurations. The seat-mass system yields lower peak acceleration, for the 55 and 75 kg configurations, and

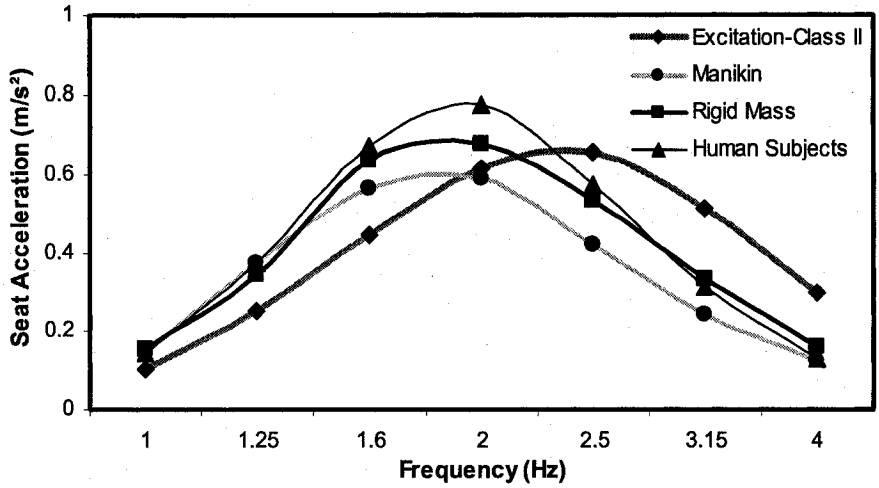

(a)

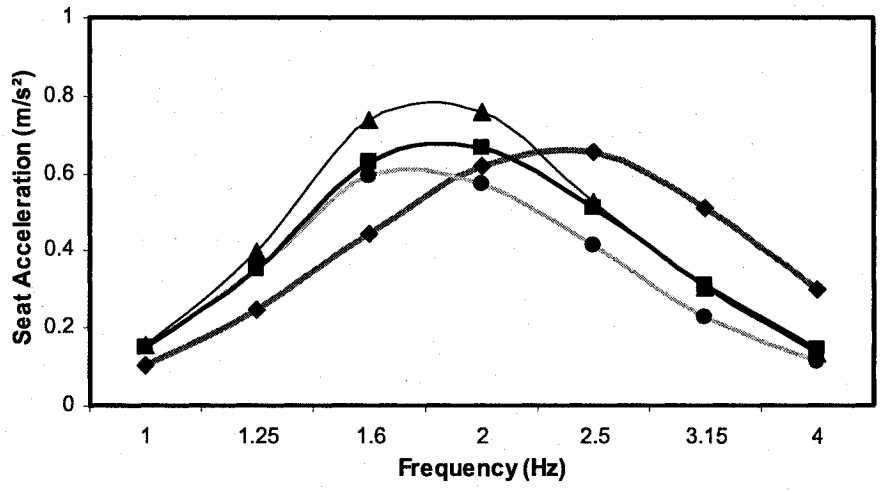

(b)

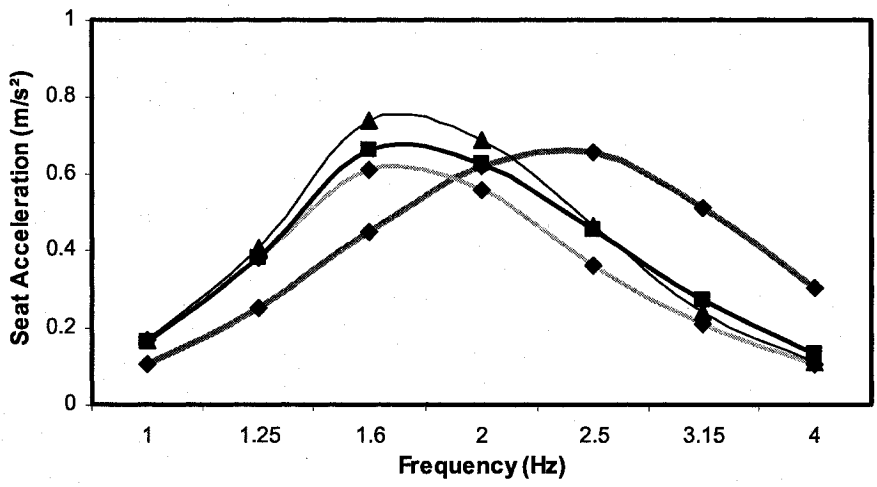

(c)

Figure 3.25: Comparisons of unweighted *rms* acceleration response of seat A loaded with manikin G and subject to Class II excitation: (a) 55 kg; (b) 75 kg; (c) 98 kg

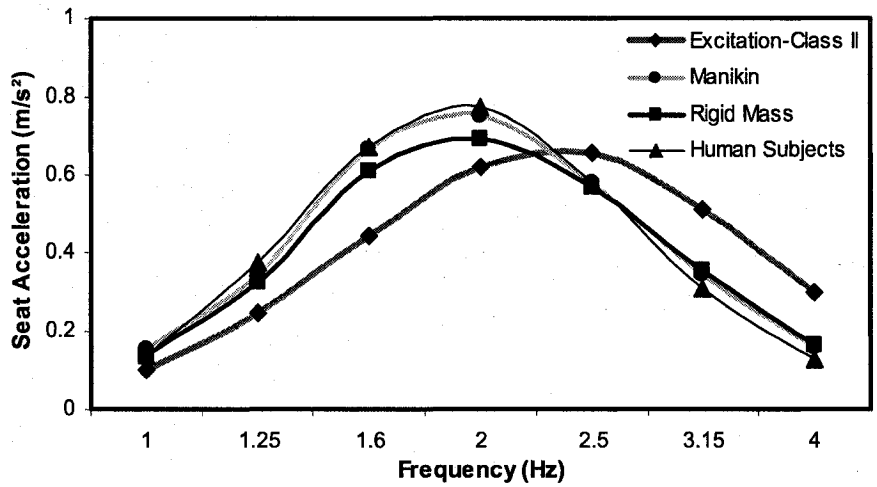

(a)

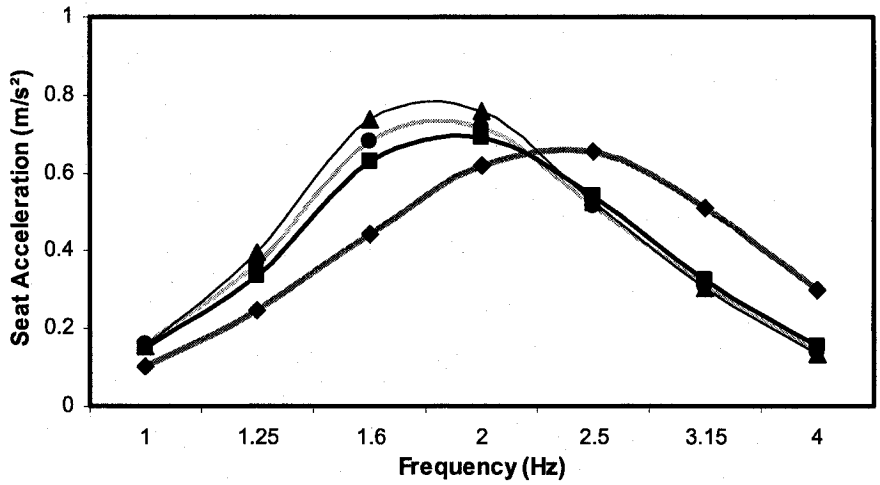

(b)

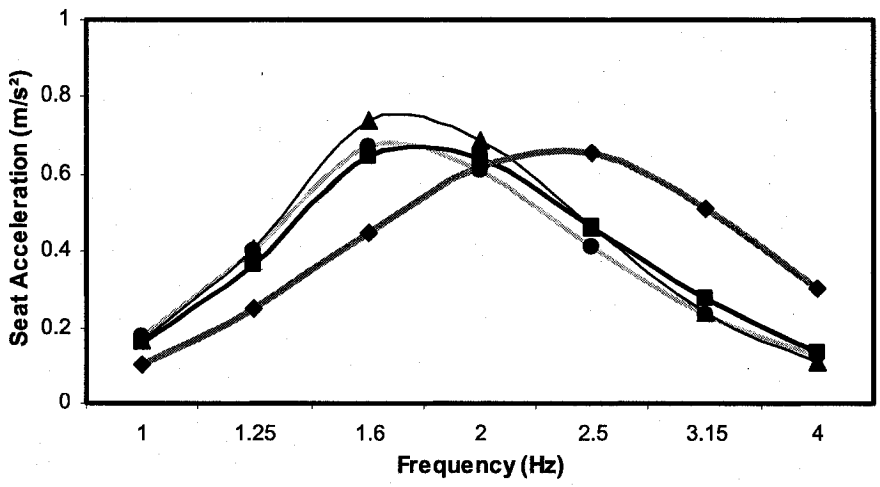

(c)

Figure 3.26: Comparisons of unweighted *rms* acceleration response of seat A loaded with manikin F and subject to Class II excitation: (a) 55 kg; (b) 75 kg; (c) 98 kg

magnitudes, yields magnitudes comparable to that of seat-manikin F system for the 98 kg configurations.

The results suggest that manikin F could provide reasonably good predictions of the seat-human system resonant frequency and acceleration responses for different body masses. The seat-mass system could also provide a reasonably good estimate of the seat-human system responses for seat A under class II excitations. The manikin G however consistently yields lower seat acceleration responses, irrespective of mass.

3.6.2 Seat B

Figures 3.27 and 3.28 illustrate the comparisons of mean unweighted *rms* acceleration responses of seat B loaded with manikins G and F and inert mass with those of seat loaded with human subjects. The responses were attained under excitation due to an agricultural tractor (AG2), which yields predominant vertical motion in the vicinity of 2.35 Hz (a_{2w} = 1.5 m/s^2). The results attained with manikin G tend to deviate considerably from those with the human subject, particularly for the 55 and 75 kg configurations. The magnitudes of deviations however depend upon the mass, as evident in Figure 3.27. The acceleration responses for all combinations peak in the 2 Hz band, which mostly corresponds with the predominant excitation frequency. The deviations in the responses of the seat with manikin, mass and subjects mostly occur in the frequency bands in the vicinity of the predominant excitation and seat resonant frequencies, namely 1.6, 2 and 2.5 Hz bands. The responses of the seat with manikin G are consistently lower than those of the seat-human and seat-mass systems for the 55 and 75 kg configurations. The seat-mass system responses are comparable with those of the seat-human system, except for 98 kg mass group where the manikin G also yields comparable responses. The

acceleration responses of the seat-mass system however are consistently comparable to those of the seat-human system, irrespective of the seated mass. For the 75 and 98 kg configurations, the responses with the human subjects tend to be higher than those with the manikin F and equivalent inert masses, in the frequency bands centered around the predominant excitation (1.25 to 2 Hz).

The seat with manikin F also yields considerably lower peak acceleration responses in the same frequency bands, when compared to those with human subjects and inert masses. Seat-mass system is again comparable to those of seat-human system, irrespective of the mass. The comparisons, suggest that both manikins yield a poor estimate of the seat B responses under AG2 excitations, while the equivalent inert mass can provide reasonably good estimates of the responses of the seat-human system. The relatively larger deviations between the seat-human and seat-manikin systems for this seat may be partly attributed to relatively higher magnitude of vibration excitation due to AG2 and slightly higher predominant frequency.

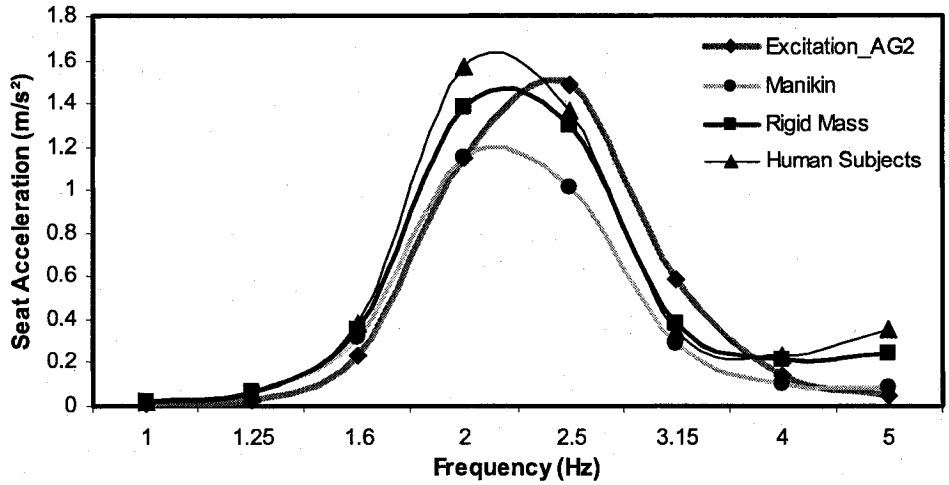

(a)

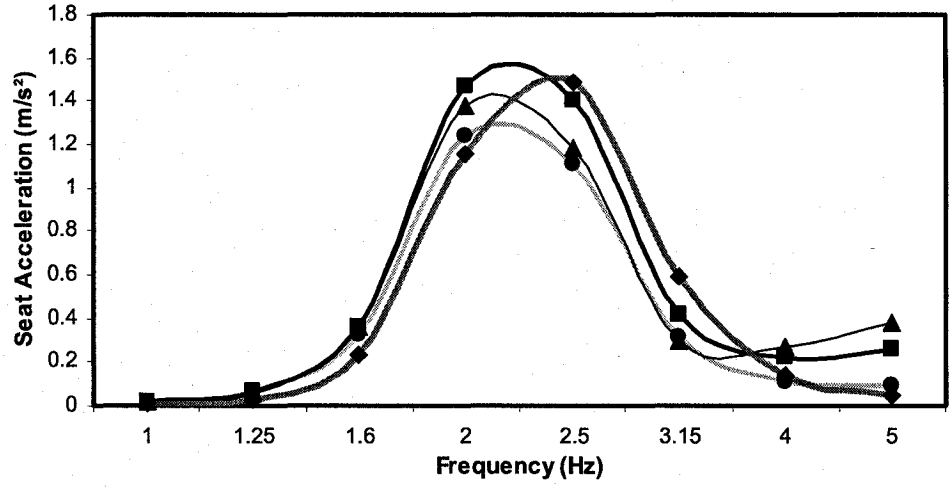

(b)

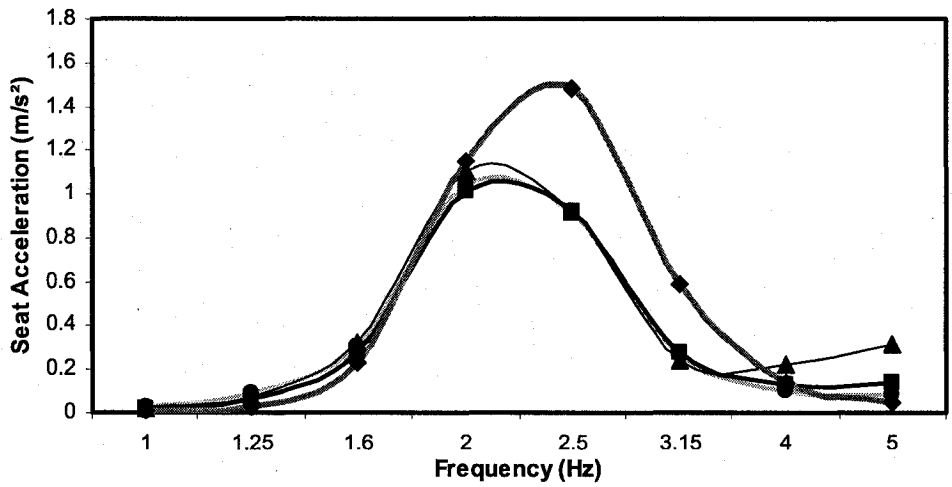

(c)

Figure 3.27: Comparisons of unweighted *rms* acceleration response of seat B loaded with manikin G and subject to AG2 excitation: (a) 55 kg; (b) 75 kg; (c) 98 kg

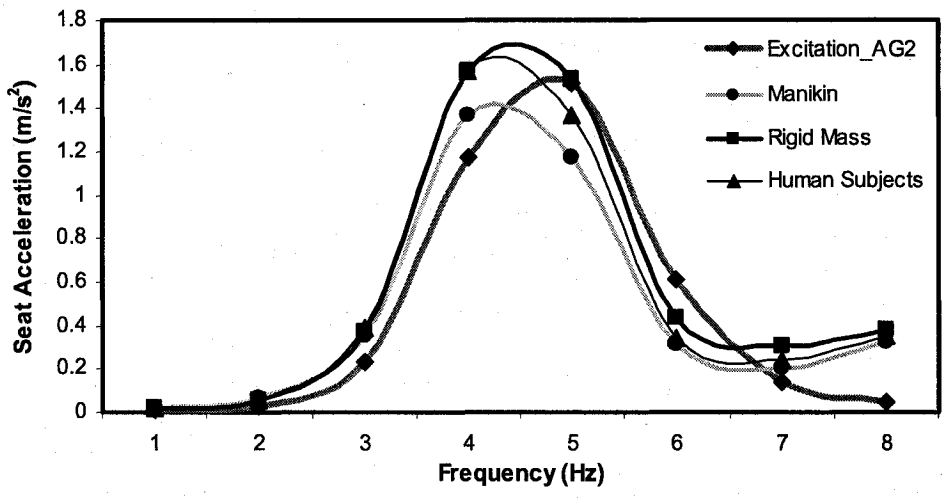

(a)

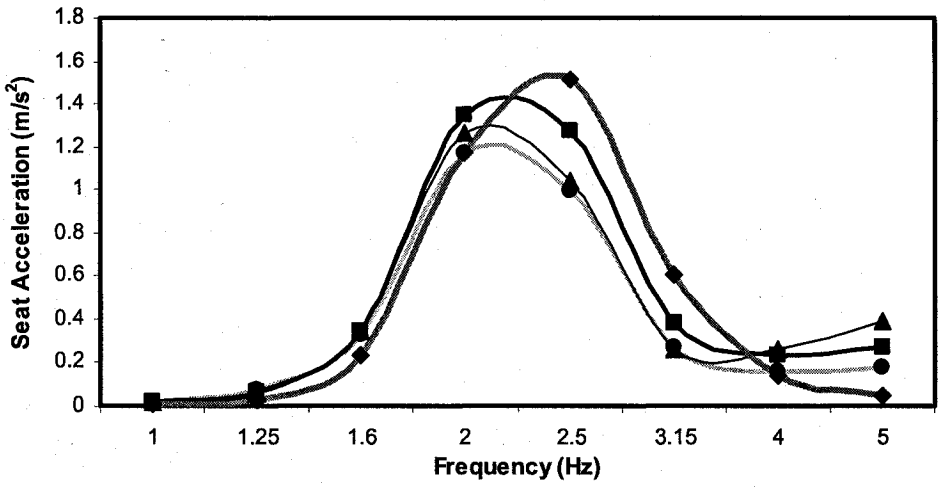

(b)

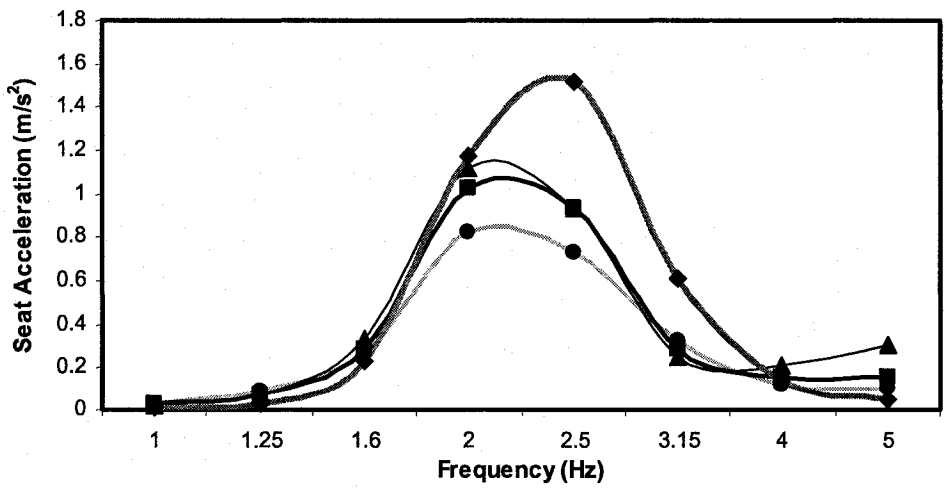

(c)

Figure 3.28: Comparisons of unweighted *rms* acceleration response of seat B loaded with manikin F and subject to AG2 excitation: (a) 55 kg; (b) 75 kg; (c) 98 kg

3.6.3 Seat C

Figures 3.29 and 3.30 illustrate comparisons of the mean unweighted *rms* acceleration responses of seat C loaded with human subjects with those of the seat loaded with manikins G and F, and equivalent inert masses respectively. The vehicular spectrum used to excite seat C is that of class 4 construction vehicle (EM4), which yields predominant vertical motion in the vicinity of 2.2 Hz (a_{2w} = 0.75 m/s^2). This excitation is somewhat comparable to that used for seat A (class II trucks). The result show that the peak acceleration responses of the seat with manikin G and are consistently lower than those of the seat-human system, as observed in case of seat A. Unlike the responses of seat A with inert mass, the seat C with inert mass yields responses comparable to those with the manikin. The seat with manikin F, however, yields responses comparable to those of the seat-human system, except for the 98 kg configuration, where it tends to be lower. The seat-mass systems responses are quite close to those of the seat-human systems, irrespective of the seated mass. The results suggest that manikin F could provide a reasonably good estimate of the seat-human system response to EM4 excitation, particularly for the 55 and 75 kg configurations. The seat-human system response under this excitation could also be predicted using equivalent inert mass.

3.6.4 Seat D

Figures 3.31 and 3.32 illustrate the comparisons of mean unweighted *rms* acceleration responses of seat D loaded with human subjects with those of the seat loaded with manikins G and F, and equivalent inert masses respectively. The results are attained under excitation spectrum for class I industrial trucks (IT1), which yields predominant vertical motion in the vicinity of 5 Hz (a_{2w} = 1.59 m/s^2).

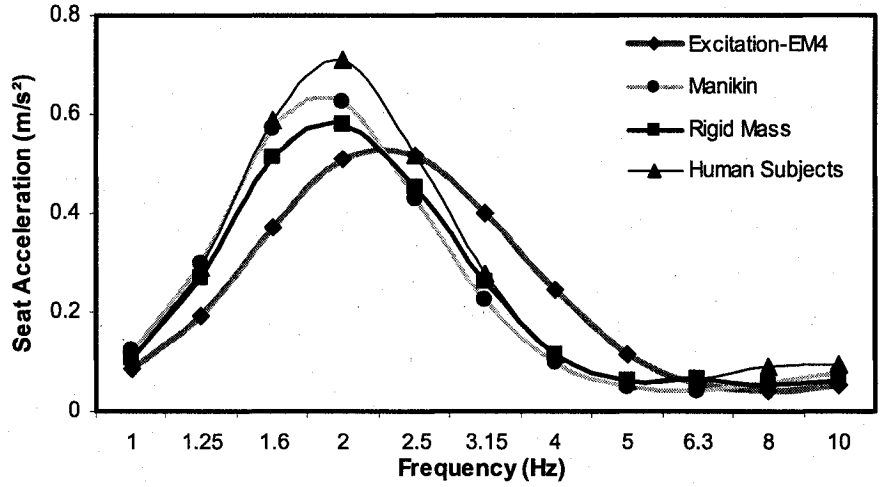

(a)

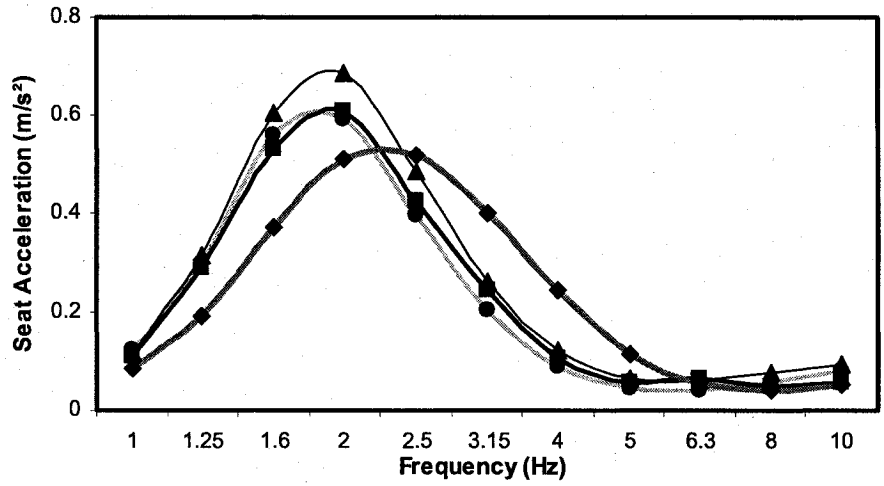

(b)

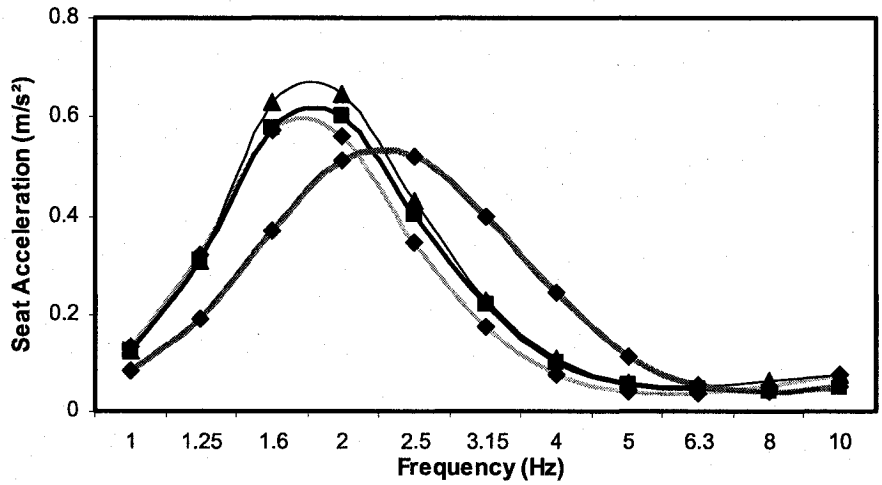

(c)

Figure 3.29: Comparisons of unweighted *rms* acceleration response of seat C loaded with manikin G and subject to EM4 excitation: (a) 55 kg; (b) 75 kg; (c) 98 kg

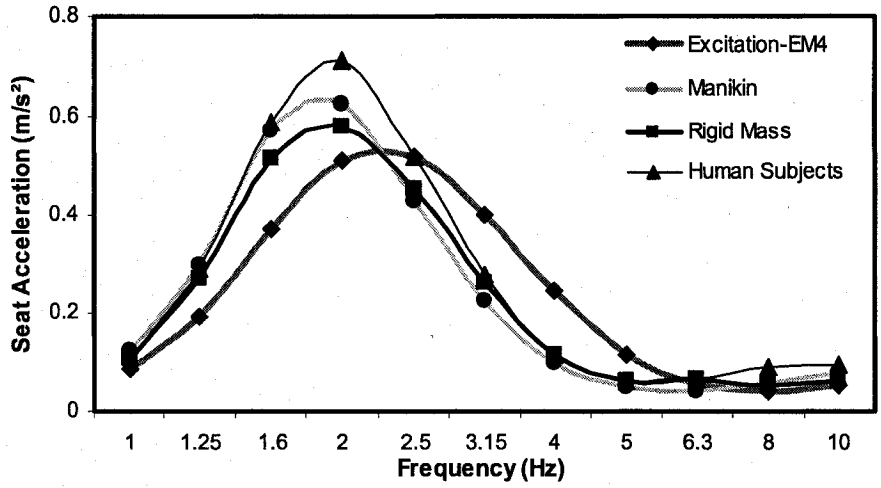

(a)

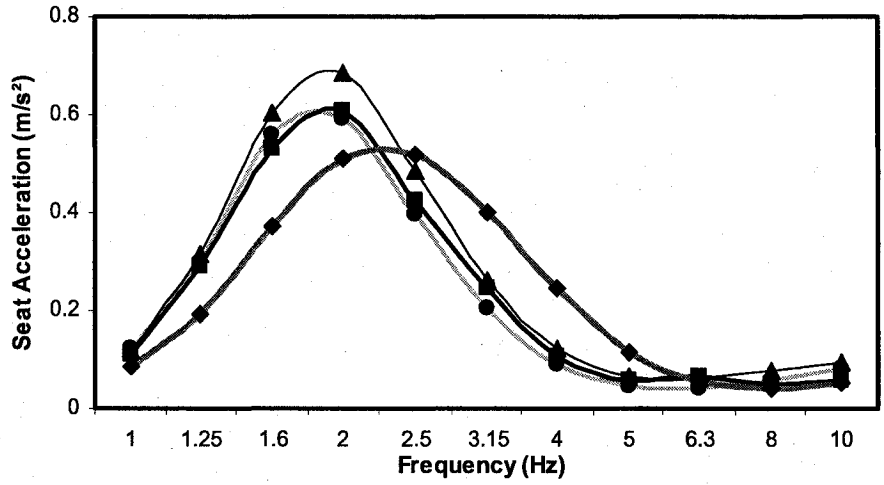

(b)

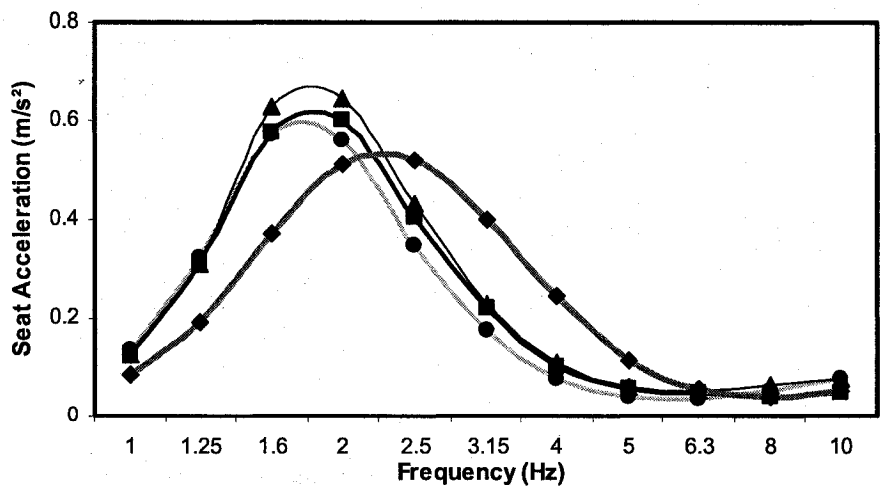

(c)

Figure 3.30: Comparisons of unweighted *rms* acceleration response of seat C loaded with manikin F and subject to EM4 excitation: (a) 55 kg; (b) 75 kg; (c) 98 kg

It should be noted that this spectrum could excite the fundamental body mode as well as the vertical mode of the manikins, while considerably attenuation of vibration is expected around 5 Hz by the seat suspension D with natural frequency near 2 Hz. Moreover, the seat resonance mode will may not be evident since very little vibration is present around 2 Hz. The acceleration responses of the seat with all three loads are somewhat comparable only up to 4 Hz band. The peak acceleration responses with inert mass tend to be higher than those with the human subject, while those with manikin G tend to be lower. Unlike the responses of seats A, B and C under relatively low frequency vibration, the responses of seat D with inert mass deviate considerably from those with the human subjects. Such deviations are mostly attributed to higher frequency of the predominant excitation due to class 4 earthmoving machinery (EM4), which tends to excite the seated body modes.

The rms acceleration response spectra of the seats with manikin F consistently show peak response in the 5 Hz band, although a second peak tends to emerge at frequencies well above the 16 Hz band. The manikin F yields higher peak response for 55 and 75 kg configuration, when compared to those of the seat with human subjects in the frequency bands centered up to 6.3 Hz, and tend to be lower at higher frequencies. The results in general suggest that both the manikins yield poor estimate of the seat responses with human subjects.

The rms acceleration spectra of the seat loaded with human subjects, manikin G and equivalent inert mass, exhibit presence of two peaks. These peaks occur in the 4 and 6.3 Hz bands for the seats with human subject and inert mass.

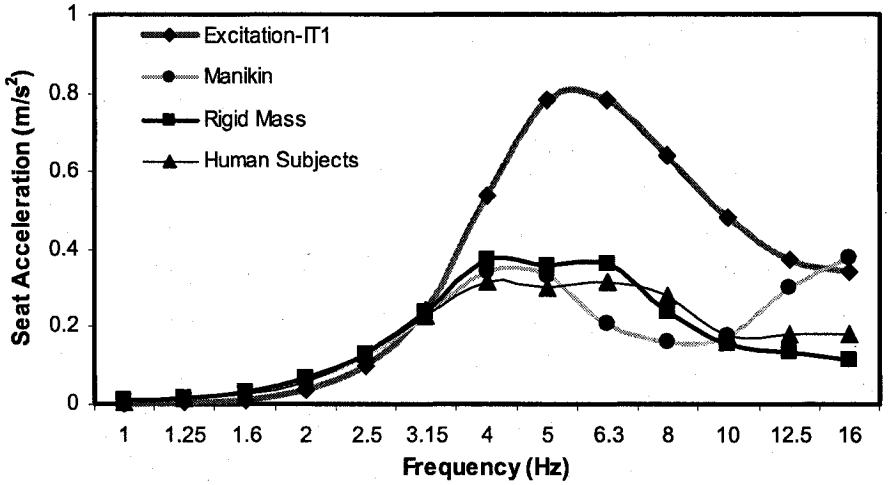

(a)

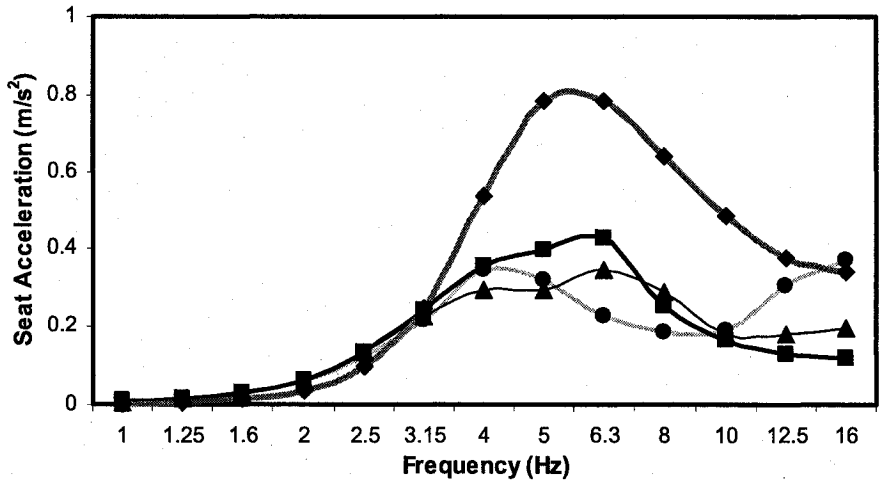

(b)

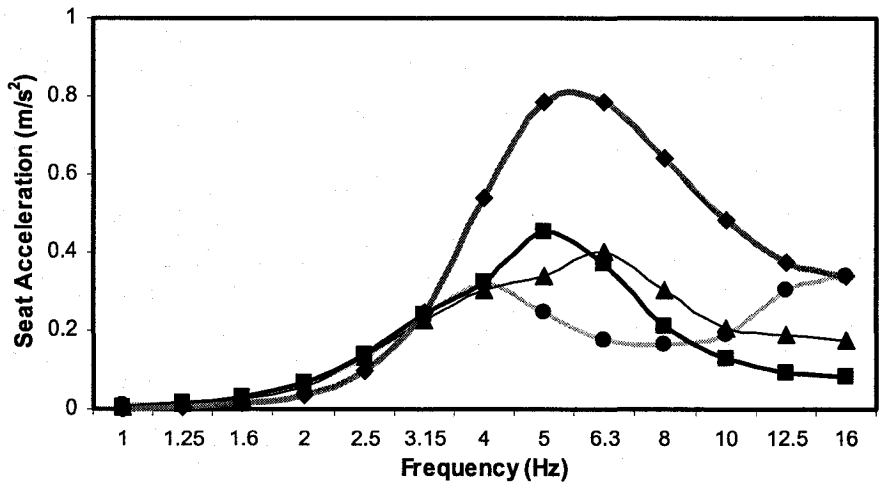

(c)

Figure 3.31: Comparisons of unweighted *rms* acceleration response of seat D loaded with manikin G and subject to IT1 excitation: (a) 55 kg; (b) 75 kg; (c) 98 kg

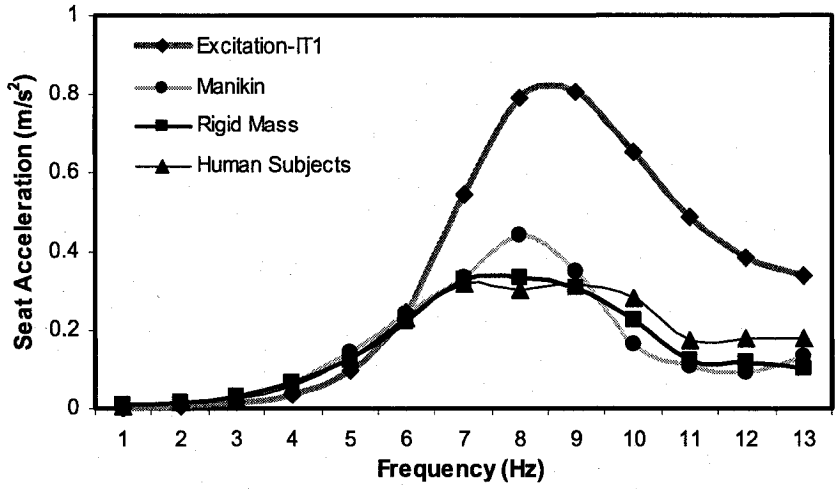

(a)

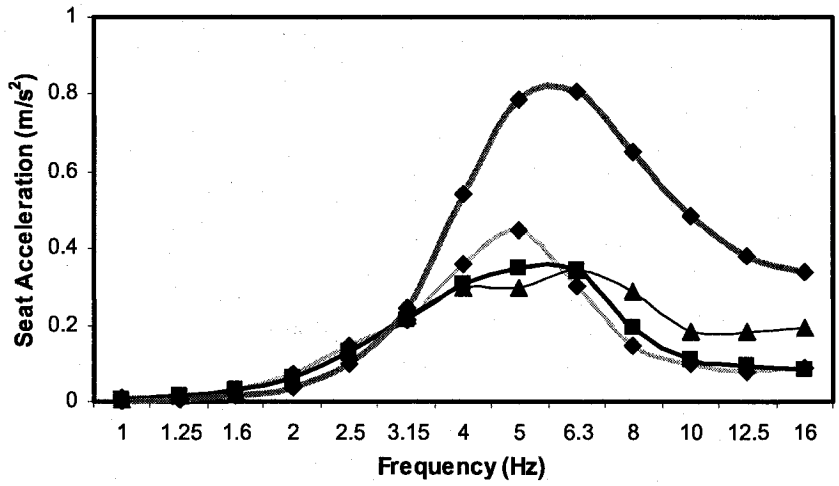

(b)

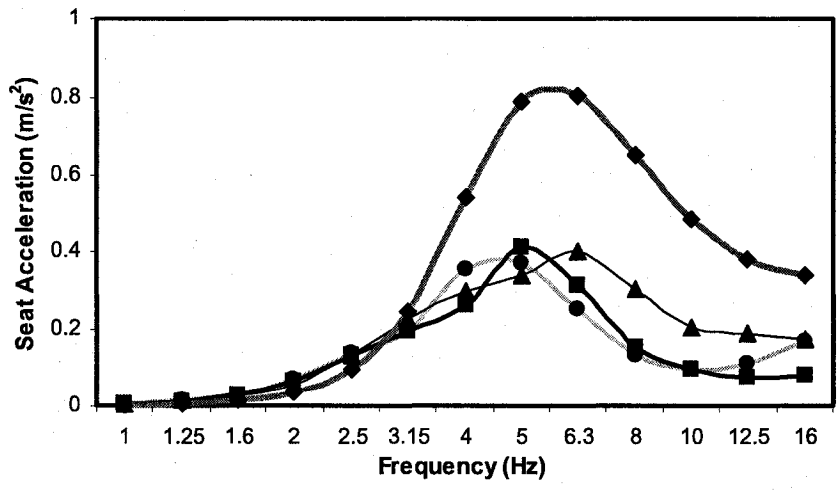

(c)

Figure 3.32: Comparisons of unweighted *rms* acceleration response of seat D loaded with manikin F and subject to IT1 excitation: (a) 55 kg; (b) 75 kg; (c) 98 kg

The second peak in response with inert mass, however, forms an exception and occurs in the 5 Hz band. The seat with manikin G also exhibits first response peak in the 4 Hz band, while the second peak occurs at frequencies near or above 16 Hz, which is attributed to the dynamic behavior of manikin G, as observed earlier in Figure(2.6). The seat responses with the manikin and inert mass differ considerably from those with the human subject at frequencies above 3 Hz.

3.6.5 Seat E

Figure 3.33 illustrate the comparisons of mean unweighted *rms* acceleration responses of seat E loaded with human subject with those of the seat loaded with manikins G and F, and equivalent inert mass. The responses are attained under excitations of a forklift truck (FL), which yields predominant vertical motion in the vicinity of 6.3 Hz (a_{2w} = 1.21 m/s^2), while the seated mass is representative of 75 kg body mass. The rms acceleration response spectra exhibit two peaks in the 3.15 and 6.3 Hz bands, which are attributed to the suspension resonance and frequency of predominant excitation, respectively. Both the manikins and the equivalent inert masses also yield peak responses in the same frequency bands. The response trends of the seat with manikin G are comparable to those obtained for the seat with human subjects. The manikin, however, under estimates the response in the 3.15 Hz band, as shown in Figure 3.33 (a). Moreover, the responses of the seat with manikin exhibits additional peak in the 20 Hz band, which is also evident with inert mass. The inert mass exhibits considerably larger peak response in the 6.3 Hz band, when compared to those of the seat with manikin G and human subjects. The response in the 3.15 Hz band tends to be considerably lower.

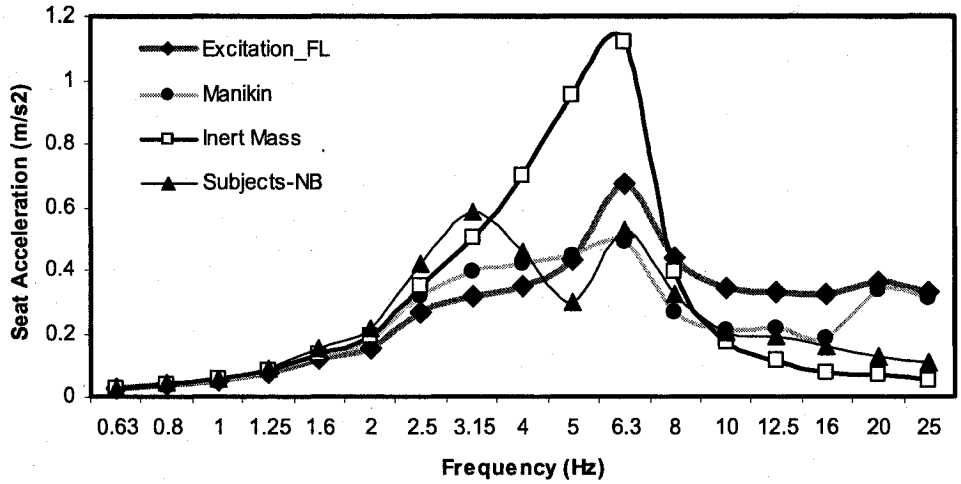

(a)

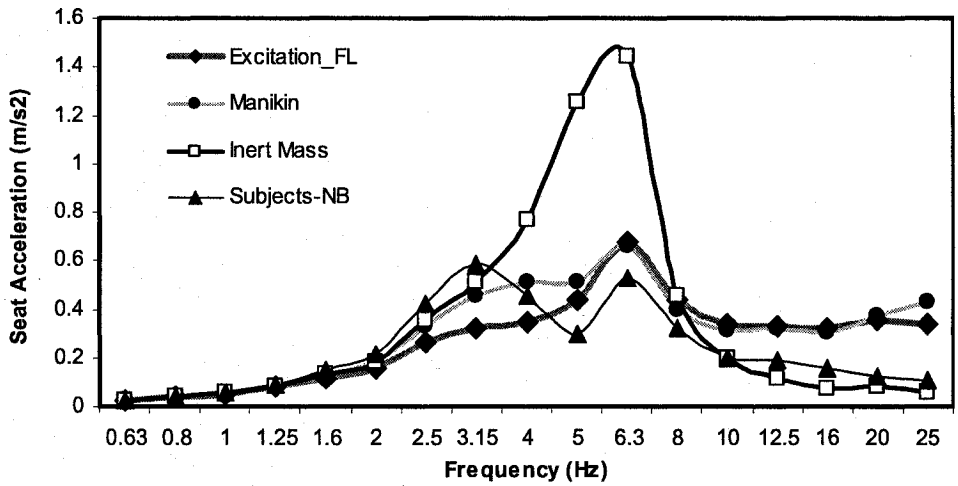

(b)

Figure 3.33 Comparisons of unweighted *rms* acceleration response of seat E subject to FL excitation: (a) Manikin G; (b) Manikin F

The peak seat-mass system response, however, is very close to that with manikin F in the 6.3 Hz band. Both the peak responses are considerably larger than that of the seat with human subjects.

The results suggest that both the manikins provide a better estimate of the seat-human system than the rigid mass, which high frequency excitations are encountered with a high natural frequency seat. The responses with both manikins, however, differ considerably from those attained with the human subjects.

3.7 Relative responses in terms of *S.E.A.T* values

The vibration attenuation performance of a suspension seat is widely assessed in terms of a convenient single index referred to as the seat effective amplitude transmissibility (SEAT) [1, 5, 14, 18]. The SEAT value inherently derives from three important response measures related to seat dynamic performance, vibration excitation spectrum of a particular vehicle, frequency response characteristics of the suspension seat, and human response frequency weighting. The applicability of the manikins for seating applications is thus further assessed in terms of SEAT values which are computed using EQS (3.15) and (3.16). The SEAT values for the seat-mass and seat-manikin systems are compared with those attained for the seat-human system assuming both back postures, NB and WB. The relative performance of the seat-load combinations are also assessed in terms of percent deviations in SEAT values, using EQS (3.17) to (3.19). The results attained for the candidate seats and selected excitations are discussed below.

3.7.1 Seat A

Figure 3.34 illustrates the comparisons of the SEAT values of seat A loaded with manikin G and F, human subjects and equivalent inert masses subject to class II

excitation. The results generally show that the suspension system yields better vibration isolation with higher seated mass. This is attributed to lower resonant frequency with higher body mass in relation to the frequency of predominant excitation of 2.2 Hz. The effect of back support is relatively small and can only be observed for 55 kg and 75 kg mass groups, as it was observed under broad-band excitations. The results show that the manikin G underestimates the suspension seat response with human subjects, while the inert mass responses are closer to the human subjects, irrespective of the mass. The responses with manikin F are very close to those with the inert mass, while both are slightly lower than those attained with human subjects. Table 3.5 further summarizes the mean and standard deviations of SEAT values of seat A loaded with manikins G and F, and human subjects with back support posture. The results attained with human subject show only marginal inter-subject variability, while the manikins produced lesser variability as compared to the human subjects. Table 3.6 illustrates the comparisons of deviations of SEAT values of seat A measured with manikin G and F, inert mass and human subjects. The deviations in SEAT values of seat with manikins and inert mass with respect to the human subjects are computed using data acquired with back support posture. The results generally show that the equivalent inert mass yields SEAT values that are comparable to those of the seat-human system, with peak deviation being in the order of 10 %. The seat with rigid mass, however, underestimates the response of the seat-human system. The manikin G yields far more underestimation in the order of 22 % for 55 and 75 kg and 16 % for 98 kg subjects. The deviations with manikin F are comparable to those with rigid mass.

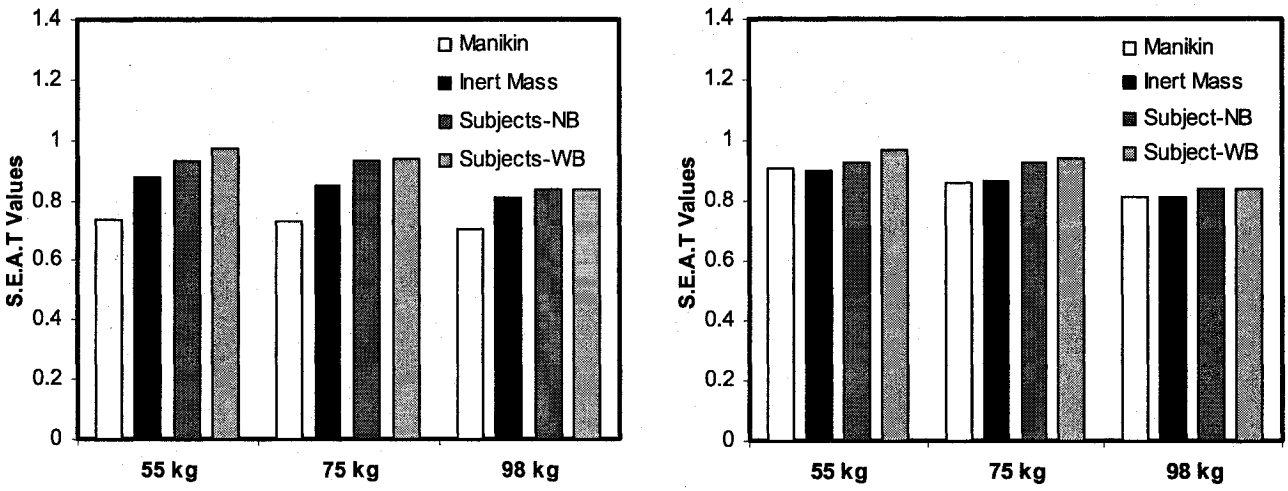

(a) (b)

Figure 3.34: Comparison of S.E.A.T values for seat A subject to class II excitation: (a) Manikin G; (b) Manikin F

Table 3.5: Minimum, maximum, mean and standard deviation of SEAT values of seat A with Manikins and Human subjects

Seat A	Human Subjects (WB)			Manikin G			Manikin F		
Mass Group	55 kg	75 kg	98 kg	55 kg	75 kg	98 kg	55 kg	75 kg	98 kg
min	0.92	0.90	0.79	0.73	0.72	0.69	0.89	0.85	0.80
mean	**0.97**	**0.94**	**0.84**	**0.74**	**0.73**	**0.70**	**0.91**	**0.86**	**0.81**
max	1.03	0.98	0.88	0.75	0.74	0.72	0.92	0.87	0.82
std. devn	0.04	0.03	0.03	0.01	0.01	0.02	0.02	0.01	0.01

Table 3.6: Comparisons of mean SEAT values and percent deviations of seat A measured with human subject, inert mass and manikins (Excitations: Class II trucks)

	Subjects		Manikin G		% Deviations†			Manikin F		% Deviations†		
Mass Group	NB	WB	Manikin	Mass	D_{M-H}	D_{R-H}	D_{M-R}	Manikin	Mass	D_{M-H}	D_{R-H}	D_{M-R}
55 kg	0.93	0.97	0.74	0.88	-23.7	-9.3	-15.9	0.91	0.90	-6.2	-7.2	1.1
75 kg	0.93	0.94	0.73	0.85	-22.3	-9.6	-14.1	0.86	0.87	-11.3	-10.3	-1.1
98 kg	0.84	0.84	0.70	0.81	-16.7	-3.6	-13.6	0.81	0.81	-3.6	-3.6	0.0

'†' deviations with respect to human subject data with back support

3.7.2 Seat B

Figure 3.35 illustrates comparisons of SEAT values of seat B loaded with manikin G and F, human subjects and equivalent inert mass under AG2 excitation. An increase in seated mass generally yields better vibration isolation by the suspension seat, as observed for seat A. The use of back support suggests only minimal effect on the SEAT values, irrespective of the mass, as it was observed under broad-band excitations. The seat with both manikins yields an underestimate of the SEAT response of the seat with human subject with peak deviation in the order of 24 %. The manikin G with 98 kg configurations, however, forms an exception and yields very good agreement with the SEAT response with human subjects. The inert mass generally yields SEAT values that lie between those of the seat-manikin and seat-human systems. The peak deviations between the SEAT values for the seat-mass and seat-human system lie below 11.5 %. Table 3.7 summarizes the minimum, maximum, mean and standard deviation of the measured SEAT values for seat B loaded with manikin G and F and human subjects with back support posture. The inter-subject variability in data acquired with human subjects

is relatively small, as it was observed for seat A. Moreover, the variability with manikins was much lesser when compared to that with human subjects. Table 3.8 illustrates comparisons of percent deviations in the SEAT values for seat B measured with manikins G and F, inert mass and human subjects. The results show the deviations in SEAT values of the seat-manikin and seat-mass systems with respect to those of the seat-human system, and the deviations between the SEAT values attained with manikins with respect to the inert mass. The results generally show that the seat-mass and seat manikin systems underestimate the response of the seat-human system. The deviations in the SEAT values of the seat-manikin systems, however, are considerably large when compared to those of the seat-mass system.

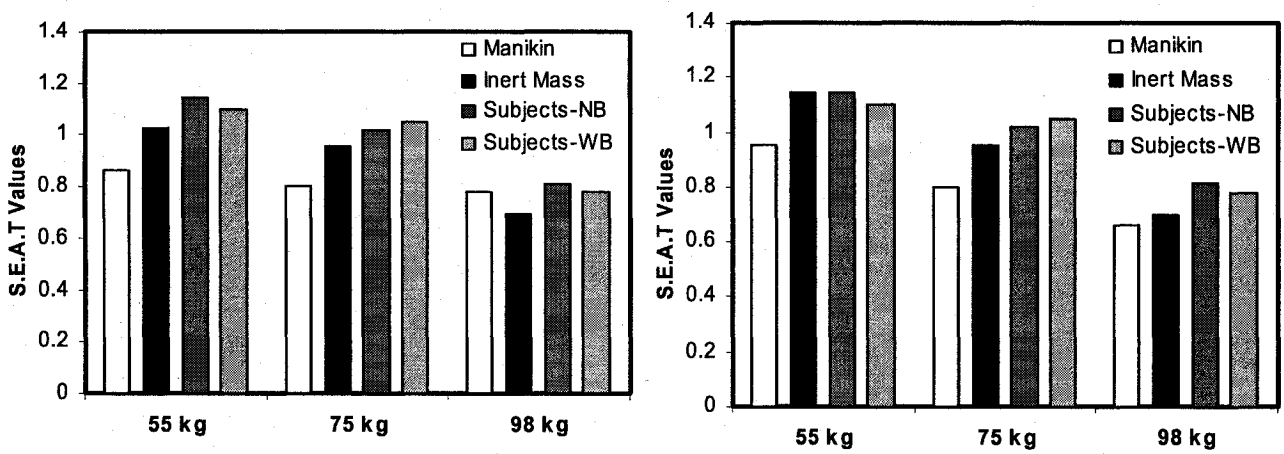

Figure 3.35: Comparison of S.E.A.T values for seat B subject to AG2 excitation: (a) Manikin G; (b) Manikin F

Table 3.7: Minimum, maximum, mean and standard deviation of SEAT values of seat B with Manikins and Human subjects

Seat B	Human Subjects (WB)			Manikin G			Manikin F		
Mass Group	55 kg	75 kg	98 kg	55 kg	75 kg	98 kg	55 kg	75 kg	98 kg
min	1.01	0.91	0.74	0.85	0.79	0.77	0.95	0.79	0.63
mean	**1.10**	**1.05**	**0.78**	**0.86**	**0.80**	**0.78**	**0.95**	**0.80**	**0.66**
max	1.18	1.15	0.83	0.87	0.81	0.79	0.95	0.80	0.69
std. devn	0.07	0.09	0.03	0.01	0.01	0.01	0	0.01	0.03

Table 3.8: Comparisons of mean SEAT values and percent deviations of seat B measured with human subject, inert mass and manikins (Excitations: AG2)

	Subjects		Manikin G		% Deviations†			Manikin F		% Deviations†		
Mass Group	NB	WB	Manikin	Mass	D_{M-H}	D_{R-H}	D_{M-R}	Manikin	Mass	D_{M-H}	D_{R-H}	D_{M-R}
55 kg	1.14	1.10	0.86	1.03	-21.8	-6.4	-16.5	0.95	1.14	-13.6	3.6	-16.7
75 kg	1.02	1.05	0.80	0.96	-23.8	-8.6	-16.7	0.80	0.95	-23.8	-9.5	-15.8
98 kg	0.81	0.78	0.78	0.69	0.0	-11.5	13.0	0.66	0.70	-15.4	-10.3	-5.7

'†' deviation with respect to human subject data with back support

3.7.3 Seat C

Figure 3.36 illustrates comparisons of SEAT value of seat C loaded with manikin G and F, human subjects and equivalent inert mass, while subject excitations due to a class of earthmoving machine (EM4).The effect of the back support condition on the SEAT values is very small, while a higher seated mass yields lower SEAT values, as observed for seat A and B. The SEAT responses with manikin G are consistently lower than those with human subject, while those with manikin F are quite comparable. Table 3.9 summarizes minimum, maximum, mean and standard deviation of SEAT values for

seat C loaded with manikins G and F, and human subjects. The results show only minimal inter-subject variability in the data acquired with human subjects. Table 3.10 illustrates comparison of percent deviations in SEAT values of seat C measured with manikins G and F, inert mass and human subjects. The deviations between the seat-manikin G and the seat-human systems are relatively small when compared to those observed for seats A and B, and range from 8.8 to 15.4 %. Such deviations for manikin F are extremely small and range from 1.1 to 1.9 %. The SEAT values with rigid mass are also quite close to those with manikins. The mass like behavior of manikin F is most likely caused by its high damper friction.

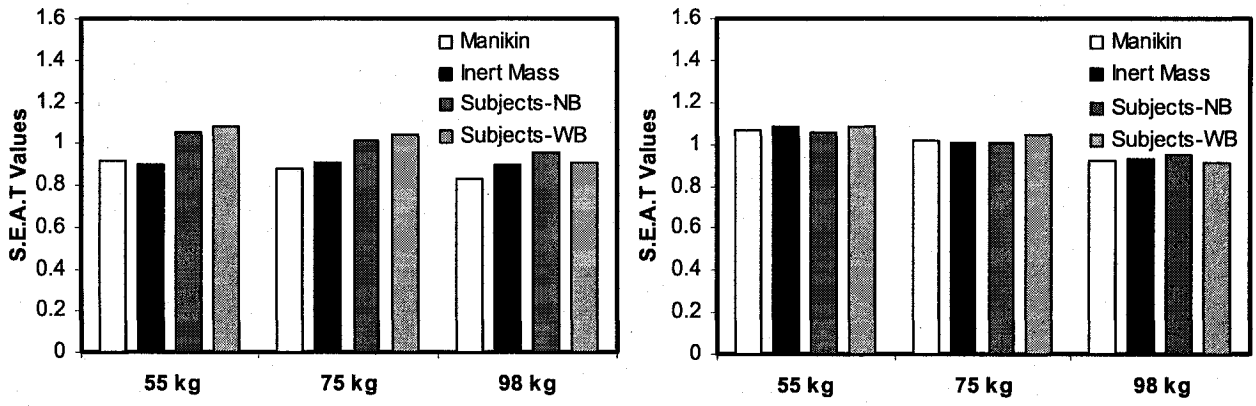

(a) (b)

Figure 3.36: Comparison of S.E.A.T values for seat C subject to EM4 excitation: (a) Manikin G; (b) Manikin F

Table 3.9: Minimum, maximum, mean and standard deviation of SEAT values of seat C with Manikins and Human subjects

Seat C	Human Subjects (WB)			Manikin G			Manikin F		
Mass Group	55 kg	75 kg	98 kg	55 kg	75 kg	98 kg	55 kg	75 kg	98 kg
min	0.99	0.98	0.86	0.90	0.87	0.83	1.04	1.00	0.91
mean	**1.08**	**1.04**	**0.91**	**0.92**	**0.88**	**0.84**	**1.06**	**1.02**	**0.92**
max	1.17	1.09	0.97	0.93	0.89	0.84	1.07	1.03	0.93
std. devn	0.07	0.04	0.04	0.02	0.01	0.01	0.02	0.02	0.01

Table 3.10: Comparisons of mean SEAT values and percent deviations of seat C measured with human subject, inert mass and manikins (Excitations: EM4)

	Subjects		Manikin G		% Deviations†			Manikin F		% Deviations†		
Mass Group	NB	WB	Manikin	Mass	$D_{M\text{-}H}$	$D_{R\text{-}H}$	$D_{M\text{-}R}$	Manikin	Mass	$D_{M\text{-}H}$	$D_{R\text{-}H}$	$D_{M\text{-}R}$
55 kg	1.05	1.08	0.92	0.90	-14.8	-16.7	2.2	1.06	1.08	-1.9	0.0	-1.9
75 kg	1.01	1.04	0.88	0.91	-15.4	-12.5	-3.3	1.02	1.01	-1.9	-2.9	1.0
98 kg	0.95	0.91	0.84	0.90	-8.8	-1.1	-7.8	0.92	0.93	1.1	2.2	-1.1

'†' deviation with respect to human subject data with back support

3.7.4 Seat D

Figure 3.37 illustrates the comparisons of SEAT value of seat D loaded with manikin G and F, human subjects and equivalent inert mass, while subject to IT1 excitation. Unlike the seats A, B, and C, the SEAT responses of this seat show considerable influence of the back support, which is most likely caused by higher frequency components of the IT1 excitation. The back support posture yields relatively higher SEAT values for the 55 and 75 kg configurations. An opposite trend, however, can

be observed for the 98 kg configuration, which is most likely caused by lower vibration transmitted near the predominant excitation frequency of 5 Hz. The seat with manikins F and G yield SEAT values that are lower than those of the seat-human system, while the manikin G deviates more from the responses with human subjects. Table 3.11 summarizes the minimum, maximum, mean and standard deviation of SEAT values for seat D loaded with manikins G and F, and human subjects. The results show only minimal inter-subject variability of the data acquired with human subject. Table 3.12 illustrates comparisons percent deviations of the SEAT values for seat D measured with manikins G and F, and inert mass with respect to those measured with human subjects, and also the deviations between the manikins with respect to the inert mass. The results generally show greater deviation of seat-manikin G system with respect to the seat-human system with an exception of 98 kg configurations, where the SEAT value for seat-manikin system is identical to that of the seat-human system. The seat-mass system also yields comparable SEAT values as compared to the seat-human system, except for the 98

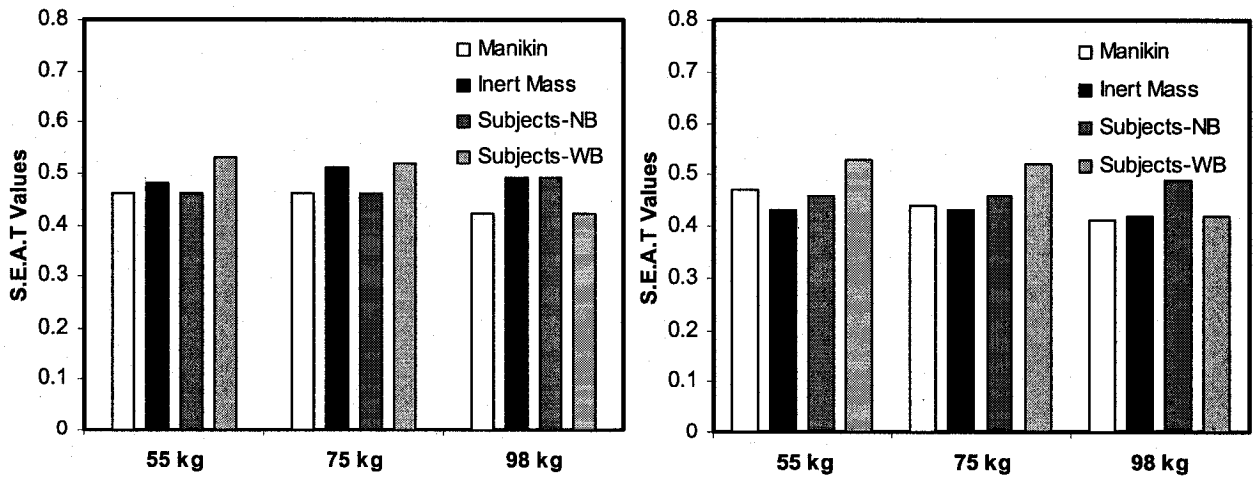

Figure 3.37: Comparison of S.E.A.T values for seat D subject to IT1 excitation: (a) Manikin G; (b) Manikin F

kg configuration. The seat-manikin F system also yields consistently larger deviations from the seat-human system, while the seat-mass system yields even larger deviations 98 kg mass group.

Table 3.11: Minimum, maximum, mean and standard deviation of SEAT values of seat D with Manikins and Human subjects

Seat D	Human Subjects (WB)			Manikin G			Manikin F		
Mass Group	55 kg	75 kg	98 kg	55 kg	75 kg	98 kg	55 kg	75 kg	98 kg
min	0.49	0.46	0.39	0.46	0.46	0.41	0.47	0.43	0.41
mean	**0.53**	**0.52**	**0.42**	**0.46**	**0.46**	**0.42**	**0.47**	**0.44**	**0.41**
max	0.57	0.56	0.45	0.46	0.47	0.43	0.48	0.44	0.41
std. devn	0.02	0.03	0.02	0	0.01	0.01	0.01	0.01	0

Table 3.12: Comparisons of mean SEAT values and percent deviations of seat D measured with human subject, inert mass and manikins (Excitations: IT1)

	Subjects		Manikin G		% Deviations†			Manikin F		% Deviations†		
Mass Group	NB	WB	Manikin	Mass	$D_{M\text{-}H}$	$D_{R\text{-}H}$	$D_{M\text{-}R}$	Manikin	Mass	$D_{M\text{-}H}$	$D_{R\text{-}H}$	$D_{M\text{-}R}$
55 kg	0.46	0.53	0.46	0.48	-13.2	-9.4	-4.2	0.47	0.43	-11.3	-18.9	9.3
75 kg	0.46	0.52	0.46	0.51	-11.5	-1.9	-9.8	0.44	0.43	-15.3	-17.3	2.3
98 kg	0.49	0.42	0.49	0.41	0.0	16.7	-14.3	0.41	0.42	-2.4	0.0	-2.4

'†' deviation with respect to human subject data with back support

3.7.5 Seat E

Figure 3.38 illustrates comparisons of the SEAT values of manikins G and F, inert mass and human subjects within 50th percentile mass group, while subject to FL excitation. The back support effect is seen although it is marginal. The inert mass yields significantly higher values of SEAT when compared to those for the seat-human systems.

The manikin F also overestimates the SEAT value, while manikin G provides a reasonably good estimate of the SEAT of the seat-human system. Table 3.13 illustrates comparisons of the percent deviations in the SEAT values of seat E measured with manikins G and F, inert mass and human subjects. The results show that the seat-manikin G system yields comparable SEAT values with those of seat-human system. It is further noted that the seat-mass system overestimates the SEAT value compared with seat-human system, with deviations in the order of 62 %. The seat-manikin F system yields slightly higher SEAT value as compared to those of seat-human system, while the corresponding mass yields a deviation exceeding 100 %.

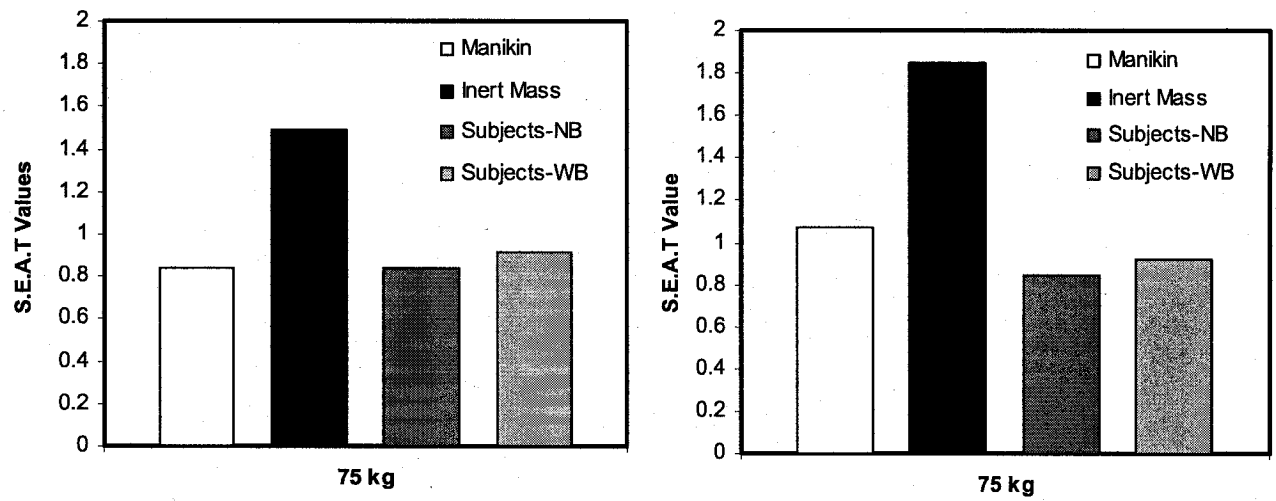

(a) (b)

Figure 3.38: Comparison of S.E.A.T values for seat E subject to FL excitation: (a) Manikin G; (b) Manikin F

Table 3.13: Comparisons of mean SEAT values and percent deviations of seat E measured with human subject, inert mass and manikins (Excitations: FL)

	Subjects		Manikin G		% Deviations†			Manikin F		% Deviations†		
Mass Group	NB	WB	Manikin	Mass	$D_{M\text{-}H}$	$D_{R\text{-}H}$	$D_{M\text{-}R}$	Manikin	Mass	$D_{M\text{-}H}$	$D_{R\text{-}H}$	$D_{M\text{-}R}$
75 kg	0.84	0.92	0.84	1.49	8.4	-62.5	-43.6	1.07	1.85	-16.7	-101.7	-62.5

'†' deviation with respect to human subject data with back support

3.8 Summary

The applicability of manikins for dynamic testing of seats is investigated by comparing the responses of candidate seats loaded with inert mass, human subjects and manikins under broad-band as well as vehicular excitations. The vibration transmissibility characteristics of the suspension seats are determined using the manikins and the effect of body mass and vibration magnitude is discussed. The transmissibility of seats with the manikins is compared with equivalent inert mass and human subjects assuming two different back postures (NB, WB). The *rms* acceleration responses of the seats with manikins are also compared with the inert mass and human subjects response. The relative performances of the seats with manikins are further evaluated through analysis of deviation in the SEAT values attained with manikins, inert mass and human subjects.

The results in general suggest that equivalent inert mass could provide reasonably good predictions of seat-occupant responses, when the excitations predominate in the low frequency range. The manikins generally yield poor estimate of the seat-human system response under such excitations. Under high frequency excitations, the inert mass yields a poor estimate of the seat-human system performance, while the manikins provide better estimations. Further tuning of the manikins, however, is needed to obtain comparable responses of the seat-manikin and seat-human systems.

CHAPTER 4

DEVELOPMENT AND DESIGN REFINEMENTS OF A MANIKIN MODEL

4.1 Introduction

The transmission of vibration through a seat depends on the dynamic properties of the seat and the dynamic response of the body supported by the seat. The dynamic response of the human body is complex, and differs from that of an equivalent rigid mass. The current standards thus recommend the use of human subjects to measure and assess the seat vibration transmissibility. The use of human subjects, however, raises many ethical concerns as it may expose subjects to risk. Moreover, the variability in the dynamic responses of the subjects leads to high uncertainty in the measured seat vibration transmission.

Alternatively, anthropodynamic manikins have been proposed to replace human subjects for assessments of vertical seat vibration transmissibility [11-20]. The common features of practical seat-test manikins include an indenter, simulating the contact conditions between a human occupant and the seat cushion, a rigid frame providing supports and guides for one or more moving masses, and mechanical components for simulating the biodynamic response of the seated body. Springs and dampers are used to support the moving masses on the rigid frame and to reproduce the idealized values of biodynamic response of the seated body. Mechanical models that can be used to define the parameters of mechanical manikins with up to three moving masses have been described by Fairley and Griffin [21], Wei and Griffin [83], International Organization for Standardization [35], Boileau et al. [22], Deutches Institut for Normung [36], Wu et al. [43] and Rakheja et al. [47].

Prototype anthropodynamic manikins for seat testing using passive components have been described by Huston et al. [16], Richter and Wertin [84], Suggs et al. [12] and Tomlinson and Kyle [13]. The validity of such manikins have been explored by comparing the results attained for the manikins and on automotive seat with those attained with human subjects using through experimentation laboratory simulator and in automobiles [11-20, 84]. Two such passive prototype anthropodynamic manikins have been recently developed by INRS (France) and BaUA (Germany), which characterize the biodynamic characteristics of seated occupants of three different body masses in the vicinity of 5^{th}, 50^{th} and 95^{th} percentile male population. The two prototypes anthropodynamic manikins showed considerable differences in the APMS response when compared to with those recommended in DIN 45676 [36] and ISO 5982 [35], as evident from the results presented in chapter 2.

The applicability of the manikins could be enhanced by improving their APMS response prediction ability through design modifications. This chapter describes the development of mathematical model of one of the manikins on the basis of the component properties, and the design of linkages. A constrained optimization based parameter identification method was applied for identifying the desired components properties such that the manikin could accurately reproduce the idealized APMS responses of the seated human occupants for the three body masses.

4.2 Design of Manikin F

The manikin F, as shown in Figure 4.1(a), comprises of a wooden seat base, an aluminum base frame attached to the wooden seat base, springs, masses and two hydraulic dampers. An aluminum back support is also provided to position the manikin

against the backrest of the seats. The manikin is placed on the seat, the base frame and the principal mass M1 are oriented along the horizontal axis by using the adjustable articulation provided with the base frame. The base frame supports three different masses namely, M1, M2, and M3, as shown in Figure 4.1(a). The mass M1 serves as the principal mass and is supported on the base frame through three pairs of springs, denoted as K1, K12 and K13. A particular pair of springs is used for a selected body mass configuration.

Apart from the adjustable principal mass, the manikin comprises of two fixed but independent masses M2 and M3, as shown in Figure 4.1(a). The mass M2 (5 kg) is guided along a vertical column and is supported by two coil springs (K2) and a viscous damper. The mass M3 (2 kg) slides on a vertical shaft and is supported on a single coil spring (K3). Four cylindrical masses with total mass of 4 kg are also attached to the wooden base, which add to the base mass.

The manikin F is designed with two hydraulic dampers. One of the hydraulic dampers is introduced between the mass M2 and the base and the other damper is supported between the principal mass M1 and the base frame through a linkage mechanism. This second damper serves as the principal damping element of the manikin, which is oriented along the horizontal axis. An L-shaped linkage with a pivot fastens the horizontal damper to the mass M1, as shown in Figure 4.1 (a). The position of the principal damper 'C1' is varied for different body mass configurations, by shifting the attachment points of the damper on the L-shaped link, which provides three different settings for three body moss configurations. These positions are marked with color codes on the damper support.

4.3 Development of Manikin Model

The proposed manikin model shown in Figure 4.1(b) comprises four masses including the mass m_0 fixed to the base. The remaining three masses are coupled to the fixed mass by linear elastic and damping elements. The mass m_0 corresponds to mass due to wooden base, aluminum frame and the four cylindrical masses attached to the wooden base. The masses m_1, m_2, m_3 represent the principal mass M1, M2, and M3 of the manikin. The masses m_2 and m_3 form uncoupled single-DOF systems, as evident from the design and shown in Figure 4.1 (b). The principal mass M1 coupled to the fixed mass m_0 through the linear spring K1 (stiffness k_1) and the horizontal damper C1 can also be represented by an uncoupled single-DOF system upon consideration of the equivalent viscous damping coefficient (c_{eq}) as shown in Figure 4.1 (c). The value of c_{eq} however varies with the chosen setting of the damper mount. The principal damper thus yields different values of c_{eq} for the three masses. The equivalent damping coefficient due to the principal damper C1 can be derived from the linkage geometry. The angular displacement 'θ' of the L-shaped link is related to the vertical displacement of the principal mass M1, such that

$$\theta = \frac{x_1 - x_0}{l} \tag{4.1}$$

Where l is the link length, x_1 is the displacement of mass m_1 with respect to its static equilibrium and x_0 is that of the fixed mass, m_0. The above relation is derived upon assuming small motions and horizontal orientation of the link corresponding to static equilibrium.

Figures 4.1 (b) and (d) also show the three damper mount settings corresponding to 55, 75, and 98 kg configurations respectively. The heights of the mounts with respect

to the link's oscillation centre are designated by h_{55}, h_{75}, and h_{98}, respectively. The relative velocity across the principal damper is thus expressed as a function of the displacement x_1 of m_1:

$$v_i = \frac{h_i}{l}(\dot{x}_1 - \dot{x}_0) \tag{4.2}$$

where i = 55, 75, and 98 kg

Assuming viscous damping, the damping force F_{v_i} developed by the damper along horizontal axis is derived from:

$$F_{v_i} = c_1 v_i \tag{4.3}$$

where c_1 is the damping coefficient due to the principal damper. The equivalent damper force acting on the mass can then be derived from:

$$F_d = c_1(\frac{h_i}{l})^2(\dot{x}_1 - \dot{x}_0) \tag{4.4}$$

The equivalent damping coefficient c_{eq} is thus expressed as a function of the damper mount height as:

$$c_{eq} = c_1(\frac{h_i}{l})^2 \tag{4.5}$$

where i = 55, 75 and 98 kg

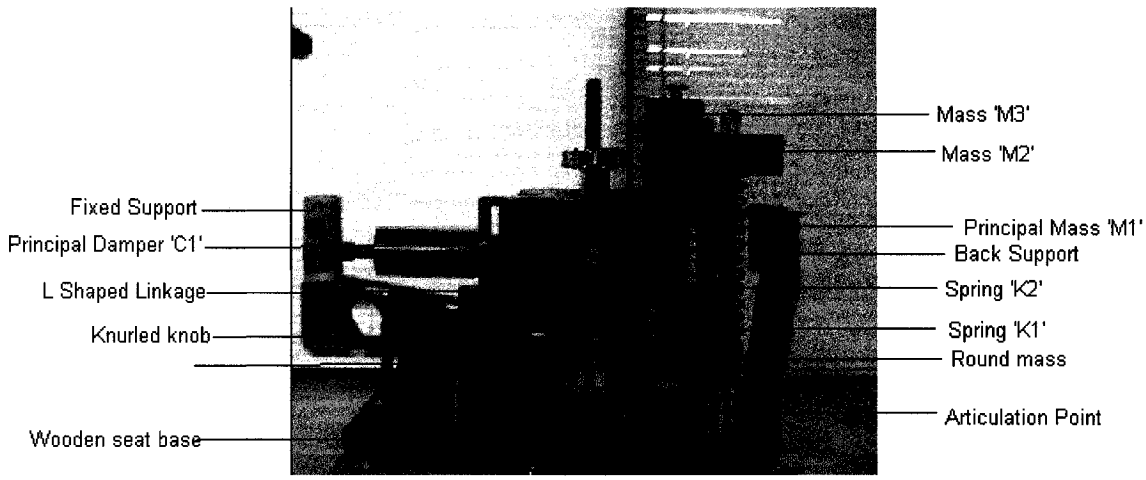

(a)

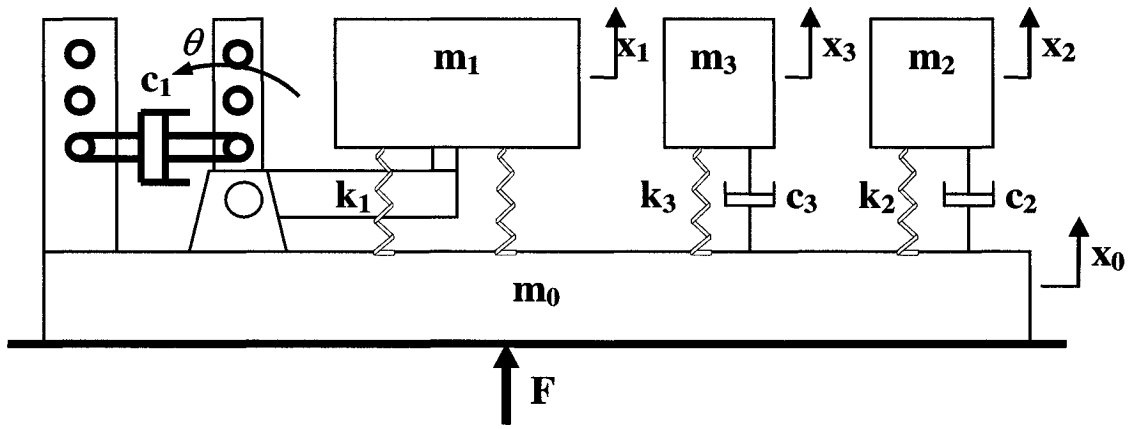

(b)

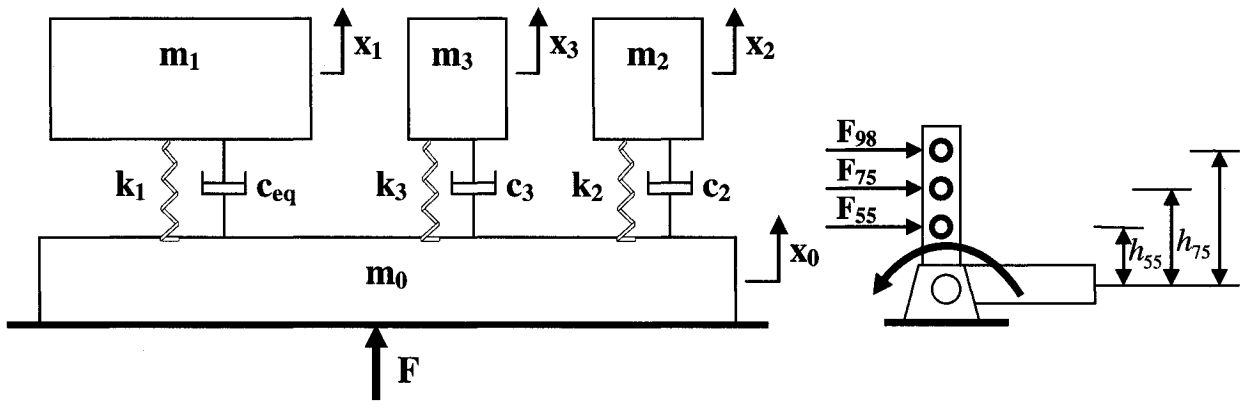

(c) (d)

Figure 4.1: (a) Pictorial view of manikin F; (b) schematic of the analytical model of the manikin F; (c) analytical model with equivalent damping; and (d) damper mount settings.

The equations of motion of the model shown in Figure 4.1(c) are formulated as follows:

$$m_1\ddot{x}_1 + c_{eq}(\dot{x}_1 - \dot{x}_0) + k_1(x_1 - x_0) = 0 \tag{4.6}$$

$$m_2\ddot{x}_2 + c_2(\dot{x}_2 - \dot{x}_0) + k_2(x_2 - x_0) = 0 \tag{4.7}$$

$$m_3\ddot{x}_3 + c_3(\dot{x}_3 - \dot{x}_0) + k_3(x_3 - x_0) = 0 \tag{4.8}$$

where k_1, k_2, and k_3 are the spring rates due to springs supporting masses m_1, m_2, and m_3, respectively. c_2 and c_3 are viscous damping coefficients representing the damping coefficients due to damper and friction due to guiding rods for masses m_2 and m_3, respectively. Laplace transform of Equations (4.6), (4.7), (4.8) yields the following expressions for the transfer functions, where each function relates to the ratio of a mass response to the base motion:

$$\frac{X_1(s)}{X_0(s)} = \frac{(k_1 + c_{eq}s)}{m_1s^2 + c_{eq}s + k_1} \tag{4.9}$$

$$\frac{X_2(s)}{X_0(s)} = \frac{(k_2 + c_2s)}{m_2s^2 + c_2s + k_2} \tag{4.10}$$

$$\frac{X_3(s)}{X_0(s)} = \frac{(k_3 + c_3s)}{m_3s^2 + c_3s + k_3} \tag{4.11}$$

The APMS response is derived from the resultant force acting at mass m_0 and the driving-point acceleration $\ddot{x}_0$. The resultant force F at the lower mass can be computed from the equation of motion for mass m_0:

$$F = m_0\ddot{x}_0 + c_{eq}(\dot{x}_0 - \dot{x}_1) + k_1(x_0 - x_1) + c_2(\dot{x}_0 - \dot{x}_2) + k_2(x_0 - x_2) + c_3(\dot{x}_0 - \dot{x}_3) + k_3(x_0 - x_3) \tag{4.12}$$

Equations (4.6), (4.7), 4.8) and (4.12) yields:

$$F = m_0\ddot{x}_0 + m_1\ddot{x}_1 + m_2\ddot{x}_2 + m_3\ddot{x}_3 \tag{4.13}$$

The APMS response of the model can then be derived as follows:

$$M(s) = \frac{F(s)}{s^2 X_0(s)} = m_0 + m_1 \frac{X_1(s)}{X_0(s)} + m_2 \frac{X_2(s)}{X_0(s)} + m_3 \frac{X_3(s)}{X_0(s)} \tag{4.14}$$

4.4 Model Validation

Equation (4.14) is initially solved to determine the APMS response of the model using the parameters reported by INRS, which are summarized in Tables 4.1, 4.2 and 4.3. The validity of the analytical model of the manikin is then examined by comparing the computed results with the measured data reported in chapter 2. Figures 4.2, 4.3 and 4.4 illustrates the comparison of the computed and measured results of the model and the manikin for the 55, 75 and 98 kg body mass configurations. The comparison reveals poor agreement in terms of the resonant frequency and the peak APMS magnitude. The discrepancies in the resonant frequency and the peak APMS magnitude response, irrespective of the body mass configurations, are mostly attributed to the significantly high seal friction of the principal damper used in the prototype manikin. It should be noted that new seals were used, which were significantly stiffer than those used in the original design of INRS. Moreover, for 98 kg body mass configuration the difference in the resonant frequency and the acceleration transmissibility is also attributed to the fact that the reported study considered 90 kg body mass configuration for higher body mass. A parametric sensitivity analysis of the model is undertaken to identify the parameters that can influence the APMS response, particularly the c_{eq} due to the principal damper.

4.4.1 Parameter Sensitivity

The apparent mass response characteristics of the manikin are known to be influenced by the manikin design and parameters, such as the spring rates, damping coefficients and individual masses. A study of the influence of variations in such

Table 4.1: Reported parameters for the 55 kg body mass configuration

Model Parameter	Reported
m_0 (kg)	7.5
m_1 (kg)	24
m_2 (kg)	5
m_3 (kg)	2
k_1 (N/m)	17140
k_2 (N/m)	12650
k_3 (N/m)	9000
c_{eq} (Ns/m)	500
c_2 (Ns/m)	125
c_3 (Ns/m)	67
h_{55} (m)	0.060
l (m)	0.105

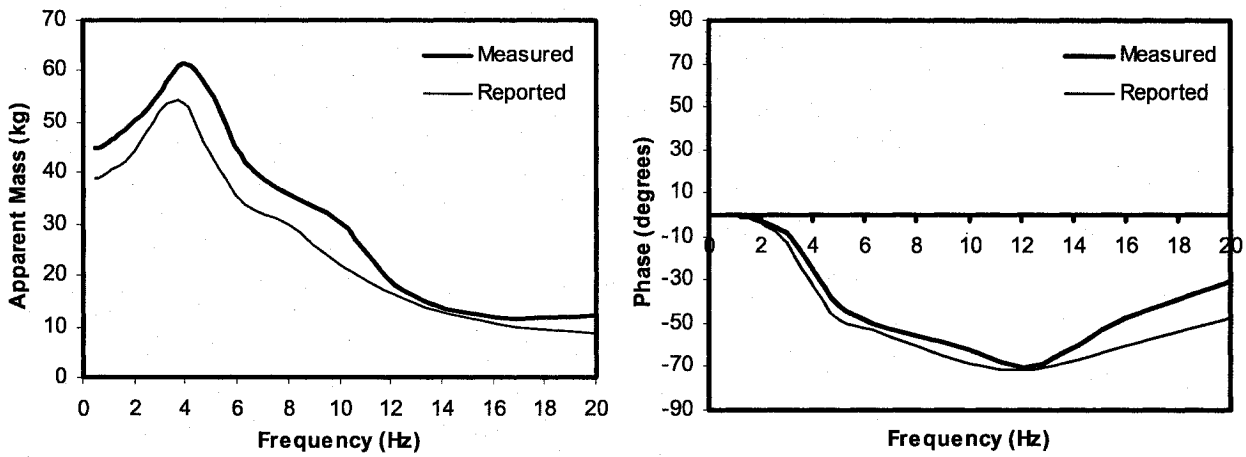

Figure 4.2: Comparisons of APMS responses of the analytical model with the reported parameters, and the measured data (55 kg mass configuration)

Table 4.2: Reported parameters for the 75 kg body mass configuration

Model Parameter	Reported
m_0 (kg)	7.5
m_1 (kg)	33.5
m_2 (kg)	5
m_3 (kg)	2
k_1 (N/m)	30870
k_2 (N/m)	12650
k_3 (N/m)	9000
c_{eq} (Ns/m)	715
c_2 (Ns/m)	125
c_3 (Ns/m)	67
h_{75} (m)	0.080
l (m)	0.105

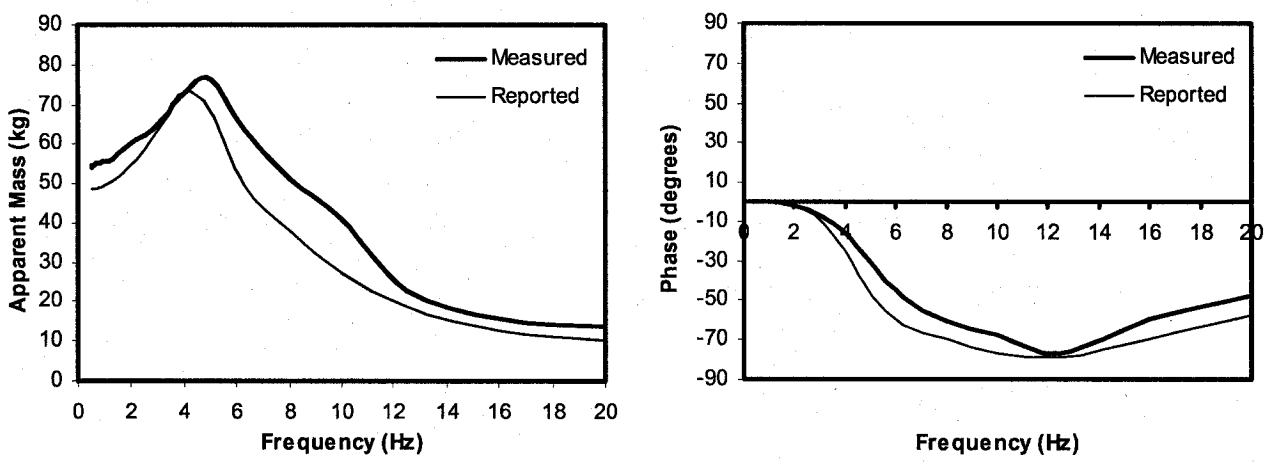

Figure 4.3: Comparison of APMS responses of the analytical model with the reported parameters, and the measured data (75 kg mass configuration)

Table 4.3: Comparison of reported and identified parameters for the 98 kg body mass configuration

Model Parameter	Reported
m_0 (kg)	3.5
m_1 (kg)	58
m_2 (kg)	5
m_3 (kg)	2
k_1 (N/m)	44270
k_2 (N/m)	12650
k_3 (N/m)	-
c_{eq} (Ns/m)	1150
c_2 (Ns/m)	125
c_3 (Ns/m)	-
h_{98} (m)	0.1
l (m)	0.105

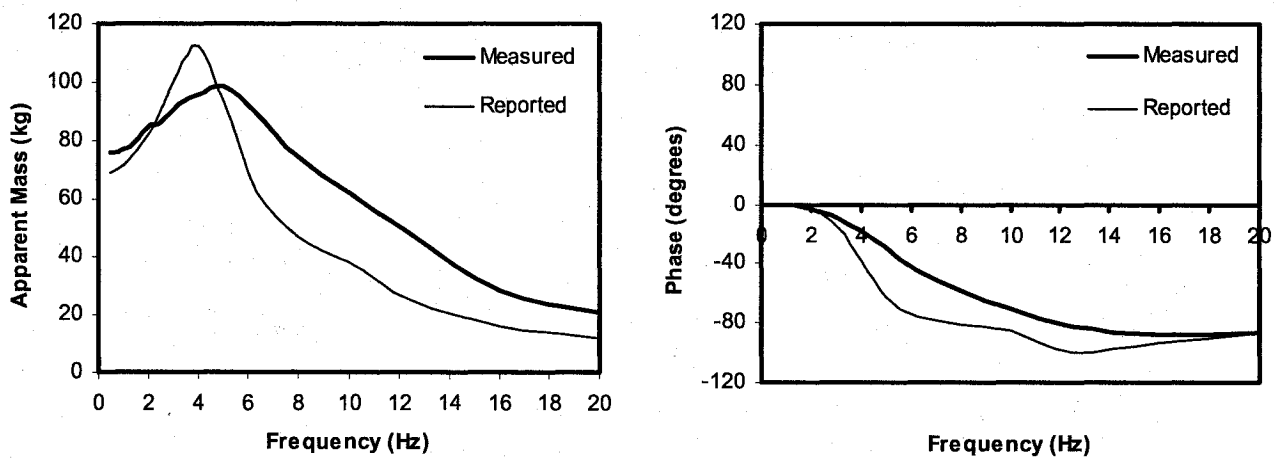

Figure 4.4: Comparison of APMS responses of the analytical model with the reported parameters and the measured data (98 kg mass configuration)

parameters on the APMS response could yield significant insight into the most desirable parameters for the manikin. In this section, the influence of variations in a single parameter at one time on the APMS magnitude response is investigated for the 75 kg body mass configuration. The parameters studied are the spring rates (*k1, k2, k3*) and the damping (c_{eq}, c_2 and c_3). Each parameter is varied by ± 20% about its nominal value to study the effect on the APMS magnitude response.

Figure 4.5 illustrates the influence of variations in k_1, k_2 and k_3 on the APMS responses of the manikin configured to 75 kg mass. The results show that an increase in the spring rate of the principal spring 'K1' yields increases in both the resonant frequency and the peak APMS magnitude response. The variations in k_2 and k_3, however yield negligible changes in the resonant frequency and the peak APMS magnitude response, with the exception of the response in the frequency range of 6-12 Hz. An increase in k_2 causes higher APMS response and formation of a secondary peak around 10 Hz.

Figure 4.6 illustrates the influence of variations in the damping coefficients, c_{eq}, c_2 and c_3 on the APMS response of the manikin. The variations in c_{eq} are expressed in terms of those in c_1 using the relation in Equation (4.4). The results show that an increase in the principal damping co-efficient c_1 strongly influences the peak APMS magnitude response. The peak magnitude decreases with increasing value of c_1, while the resonant frequency remains nearly the same. The results also show that variations in the damping co-efficient c_2 and c_3 affect the response only slightly in the frequency range of 6-12 Hz. The results thus suggest that a higher value of c_1, arising from higher seal friction, could help achieve better agreements between the model and measured responses.

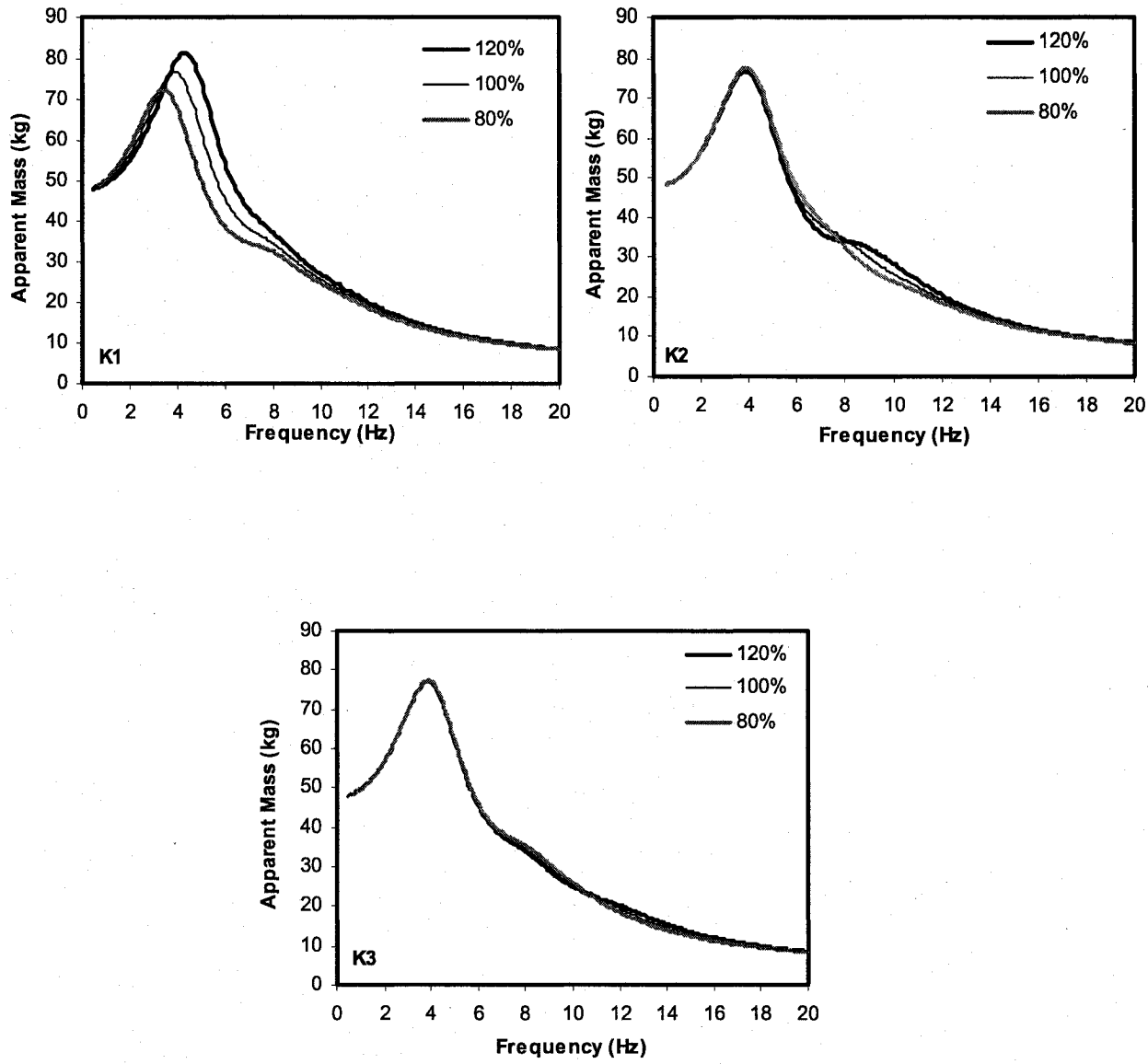

Figure 4.5: Influence of variations in the spring rates on the APMS response of the manikin: (a) k_1; (b) k_2; and (c) k_3.

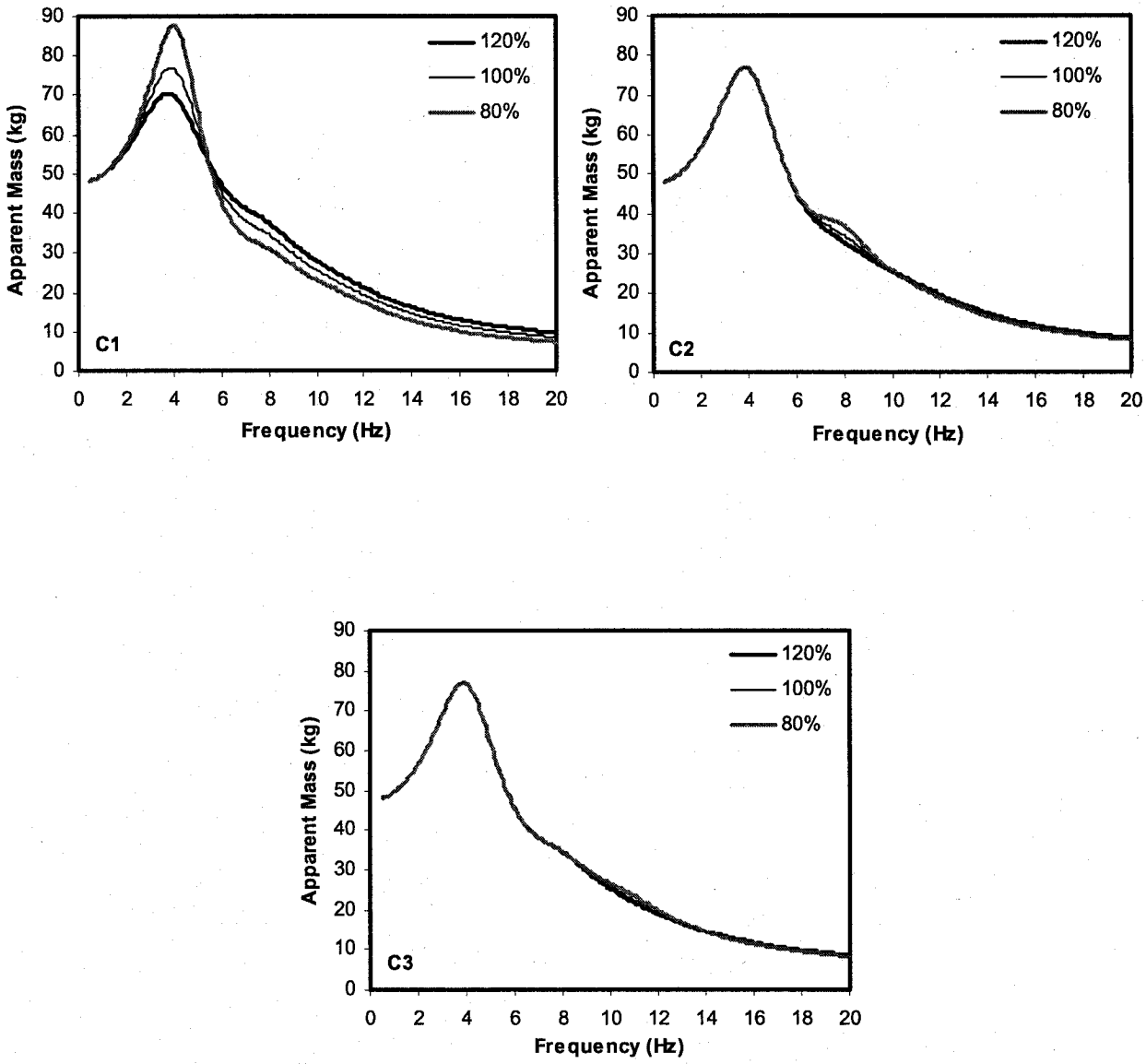

Figure 4.6: Influence of variations in damping coefficients on the APMS response of the manikin: (a) c_1; (b) c_2; and (c) c_3.

4.4.2 Estimation of Model Parameters:

A parametric optimization technique was further used to determine the model parameters. An objective function was defined to minimize the error between the computed and the measured values of the biodynamic response function over a specific frequency range. The objective function is defined as the weighted sum of the squared magnitude and phase errors associated with APMS function and expressed as:

$$U(\chi) = \lambda \sum_{i=1}^{N} \left\{ \left| M_c(\omega_i) \right| - \left| M_t(\omega_i) \right| \right\}^2 + \sum_{i=1}^{N} \left\{ \left| \phi_c(\omega_i) \right| - \left| \phi_t(\omega_i) \right| \right\}^2 \qquad (4.15)$$

where $M_c(\omega_i)$ and $\phi_c(\omega_i)$ are the APMS magnitude and phase responses of the model corresponding to excitation frequency ω_i. $M_t(\omega_i)$ and $\phi_t(\omega_i)$ are the corresponding measured values. N is the number of discrete frequencies selected in the 0.5 to 20 Hz frequency range, and χ is the vector of model parameters to be identified:

$$\chi = \left\{ m_1, k_1, c_{eq}, c_2, c_3 \right\}^T \qquad (4.16)$$

where 'T' designates the transpose.

λ is the weighting factor used with the APMS magnitude error to ensure somewhat comparable contributions of the magnitude and phase errors in the objective function. Since the range of APMS magnitude and phase over the frequency range of interest are in the same order, the weighting factor λ is selected as 1.

The minimization problem expressed in Equation 4.10, is solved subject to constraints applied on the total model mass. Since the static weight of the manikin estimated from the experiments for 75 kg body mass configuration is 53 kg, supported by the seat, a limit constraint is defined to allow the total mass to vary within a narrow band (± 4 kg), such that;

$$49 \leq \sum_{i=0}^{3} m_i \leq 57kg \tag{4.17}$$

The optimization function is further subject to the following parameter constraints:

$$\begin{gathered} m_0 = 7.5 \text{ kg};\ m_2 = 5 \text{ kg};\ m_3 = 2 \text{ kg};\ m_1 > 35 \text{ kg} \\ 30000 < k_1 < 50000;\ k_2 = 12650 \text{ N/m};\ k_3 = 9000 \text{ N/m} \\ 700 < c_{eq} < 1300;\ 100 < c_2 < 150;\ c_3 > 0 \end{gathered} \tag{4.18}$$

Different constraints were applied for the 55 and 98 kg body mass configurations, in accordance with the design. Moreover, for the 55 and 98 kg configurations, the damping parameter c_1 was replaced by the heights h_{55} and h_{98}, respectively. This approach permits for the use of same damper C1 for all three mass configurations, while the damping coefficient c_1 is identified only for the 75 kg mass configuration.

4.4.3 Model Parameters Values

The constrained optimization problem defined in Equations (4.15) through (4.18) is solved using MATLAB optimization toolbox [85]. Tables 4.1, 4.2 and 4.3 presents comparisons of the identified parameter values with the reported parameters for the 55, 75 and 98 kg body mass configurations, respectively. The higher value of the principal mass m_1, irrespective of the body mass configuration, is due to the differences in the experimental and reported static weights, supported by the seat. It should be noted that the three configurations employ identical parameters, with exception of m_1, k_1 and damper mount height (h_{55}, h_{75} and h_{98}). Moreover, the identified parameters k_2, k_3, c_2 and c_3 are quite comparable with the nominal reported values.

4.4.4 Model Validation

The response characteristics of the models with identified parameters are compared with the measured responses to demonstrate the validity of the model and its

structure in Figures 4.7, 4.8, 4.9 for the 55, 75 and 98 kg configurations respectively. The figures also show the reported responses. The results, in general, show reasonably good agreements between the measured and computed response characteristics, with the exception of deviations in the phase responses in the higher frequency range. While APMS magnitudes, computed from the models, correlate very well with the measured data in the 0-20 Hz frequency range, irrespective of the body mass configuration, the phase responses correlate well upto 10 Hz for 75 and 98 kg, and upto 6 Hz for 55 kg body mass configurations.

The validity of the analytical model is further examined by comparing the computed acceleration transmissibilities of individual masses with the corresponding measured data. Figures 4.10, 4.11 and 4.12 illustrate the comparison of the acceleration transmissibilities of the three vibrating masses for the 55, 75 and 98 kg body mass configuration. The figure also presents the results attained from the baseline model parameters reported by INRS. The results show reasonably good agreements in terms of resonant frequency of the computed acceleration transmissibilities with the measured data, while the results attained from the reported model deviate significantly, particularly for the acceleration transmissibility of masses m_2 and m_3, irrespective of the body mass configuration. However, for 98 kg body mass configuration, the result show a poor agreement in terms of the acceleration transmissibility for mass m_1 which may be attributed to some error in the measurement of the acceleration transmissibility of the mass m_1.

Table 4.4: Comparison of reported and identified parameters for the 55 kg body mass configuration

Model Parameter	Reported	Identified
m_0 (kg)	7.5	7.5
m_1 (kg)	24	29
m_2 (kg)	5	5
m_3 (kg)	2	2
k_1 (N/m)	17140	24684
k_2 (N/m)	12650	12650
k_3 (N/m)	9000	9000
c_1 (Ns/m)		1943.85
c_{eq} (Ns/m)	500	713.10
c_2 (Ns/m)	125	150
c_3 (Ns/m)	67	30
h_{55} (m)	0.060	0.064

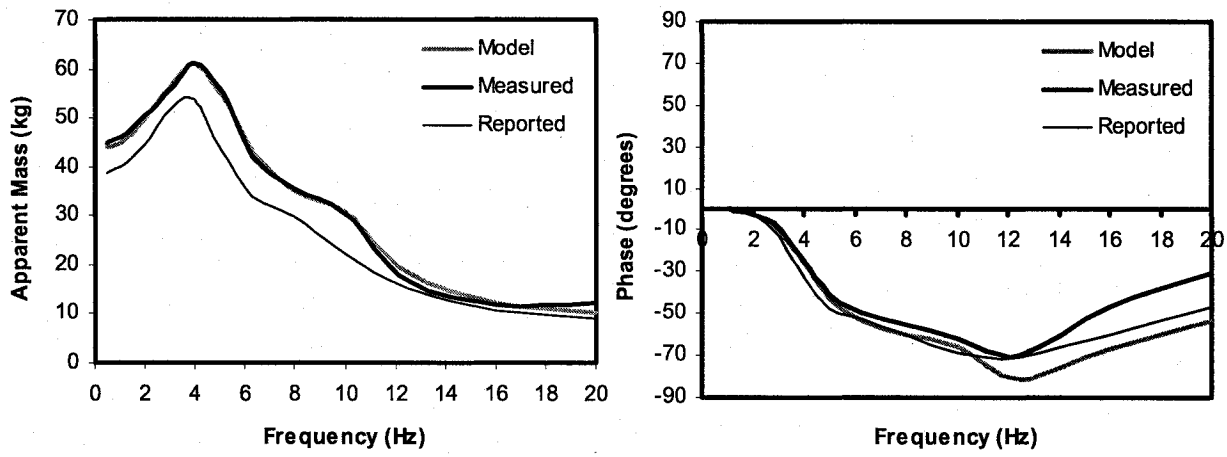

Figure 4.7: Comparisons of APMS responses of the analytical model with the identified and reported parameters, and the measured data (55 kg mass configuration)

Table 4.5: Comparison of reported and identified parameters for the 75 kg body mass configuration

Model Parameter	Reported	Identified
m_0 (kg)	7.5	7.5
m_1 (kg)	33.5	38.5
m_2 (kg)	5	5
m_3 (kg)	2	2
k_1 (N/m)	30870	44290
k_2 (N/m)	12650	12650
k_3 (N/m)	9000	9000
c_1 (Ns/m)		1943.85
c_{eq} (Ns/m)	715	1128.40
c_2 (Ns/m)	125	150
c_3 (Ns/m)	67	30
h_{75} (m)	0.080	0.080

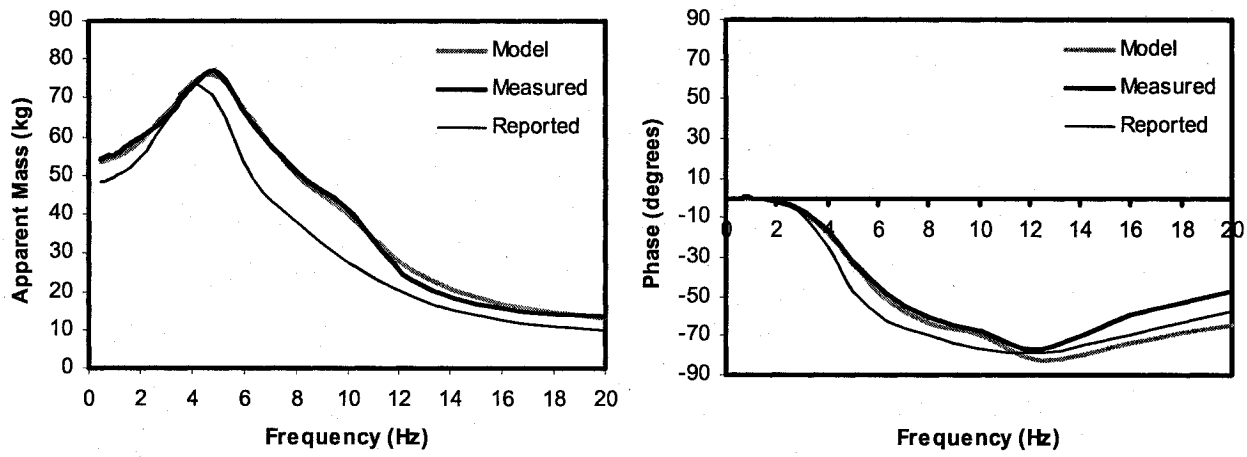

Figure 4.8: Comparison of APMS responses of the analytical model with the identified and reported parameters, and the measured data (75 kg mass configuration)

Table 4.6: Comparison of reported and identified parameters for the 98 kg body mass configuration

Model Parameter	Reported	Identified
m_0 (kg)	3.5	3.5
m_1 (kg)	58	63
m_2 (kg)	5	5
m_3 (kg)	2	2
k_1 (N/m)	44270	74470
k_2 (N/m)	12650	12650
k_3 (N/m)	-	9000
c_1 (Ns/m)		1943.85
c_{eq} (Ns/m)	1150	2499
c_2 (Ns/m)	125	150
c_3 (Ns/m)	-	30
h_{98} (m)	0.1	0.119

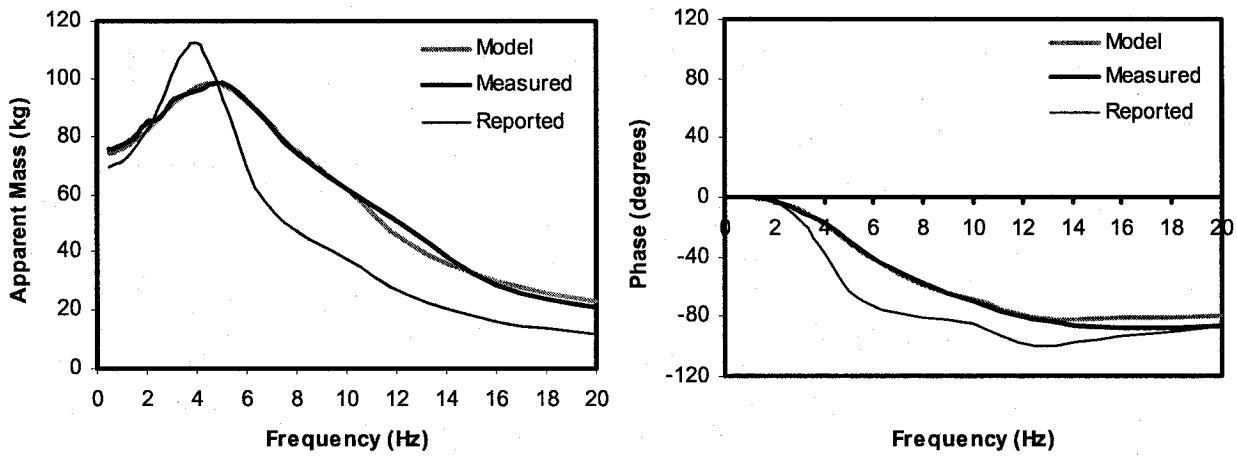

Figure 4.9: Comparison of APMS responses of the analytical model with the identified and reported parameters, and the measured data (98 kg mass configuration)

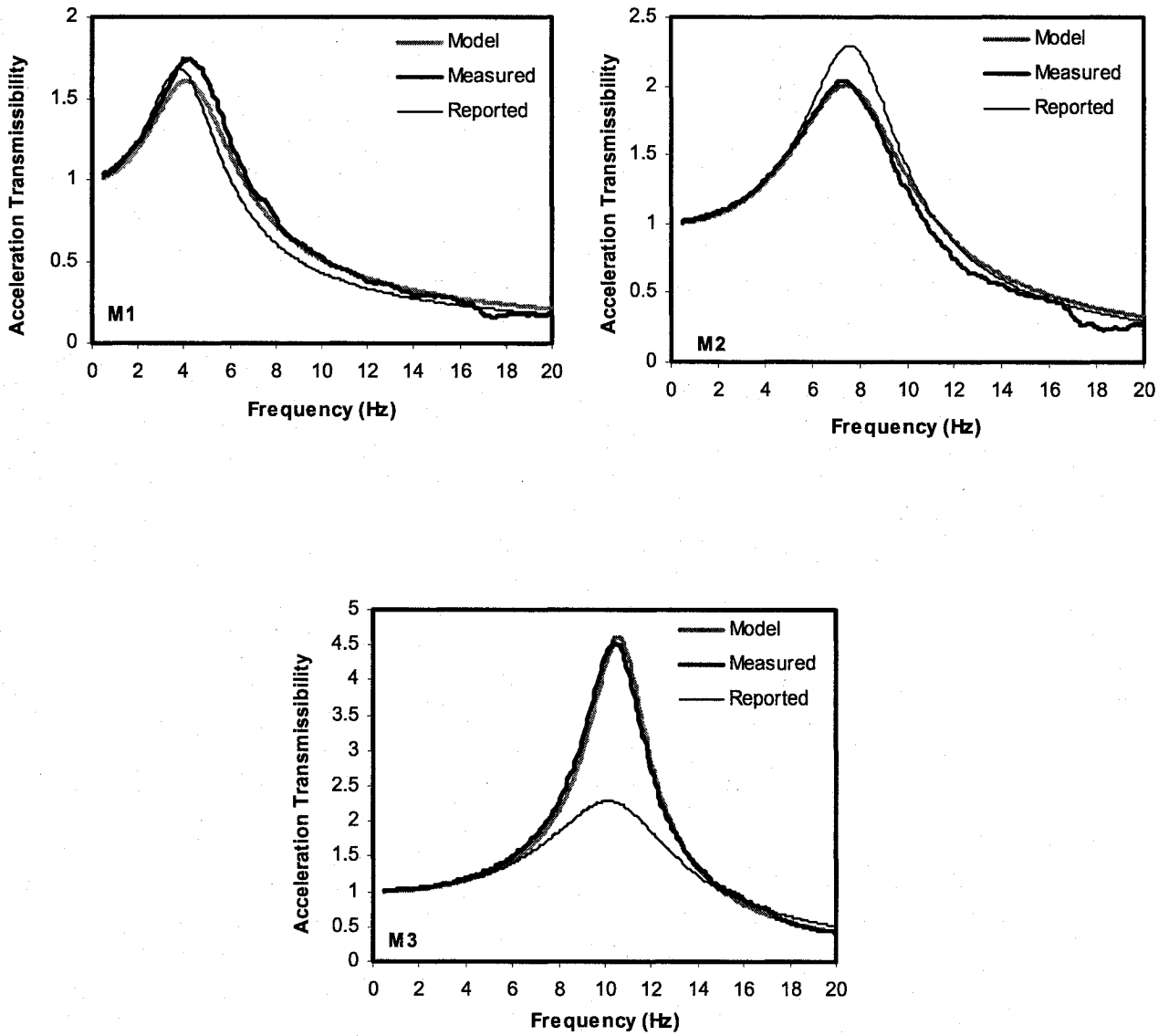

Figure 4.10: Comparisons of acceleration transmissibility characteristics of the identified model with the measured data and the responses of the reported baseline model (55 kg mass configuration)

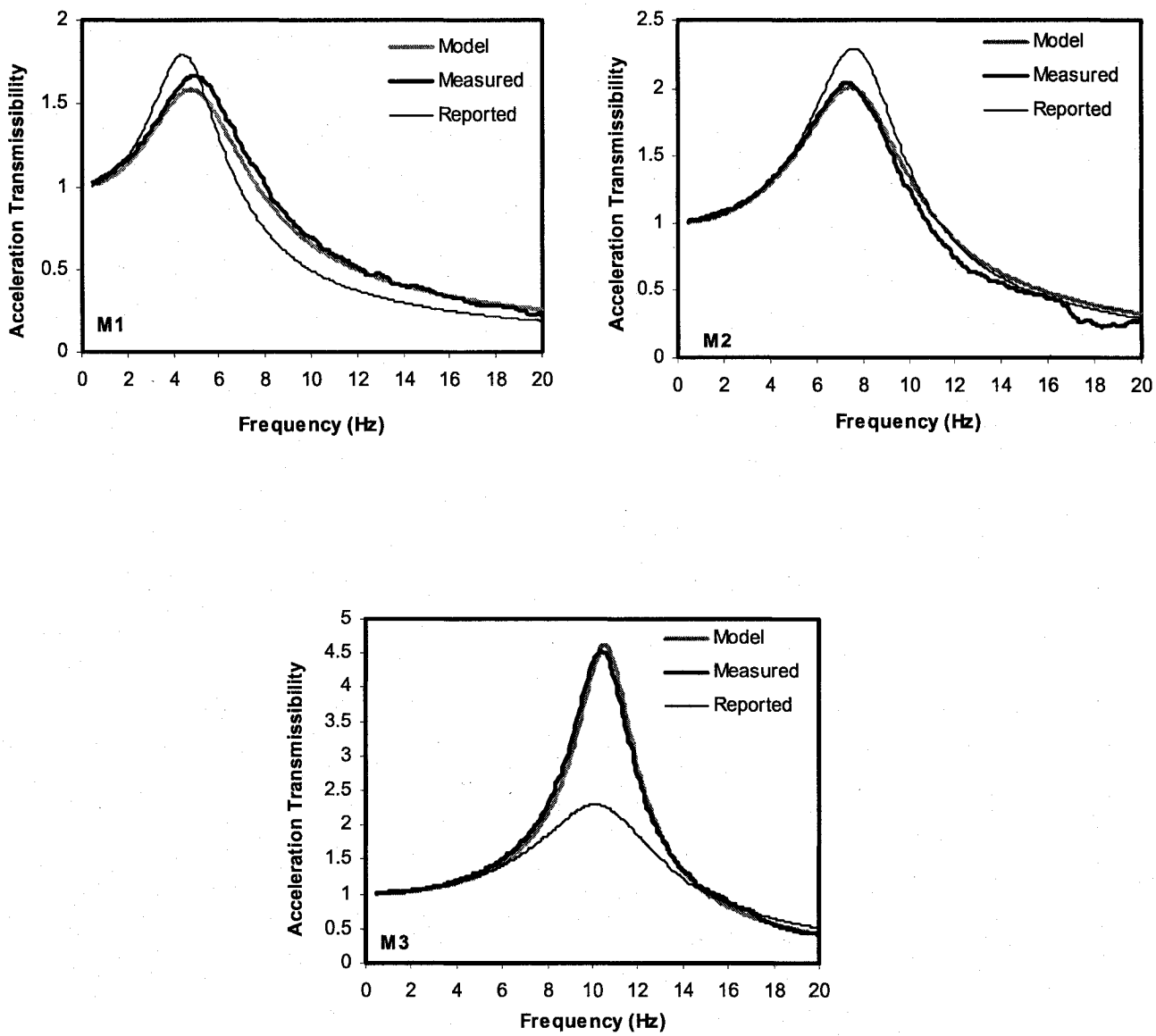

Figure 4.11: Comparisons of acceleration transmissibility characteristics of the identified model with the measured data and the responses of the reported baseline model (75 kg mass configuration)

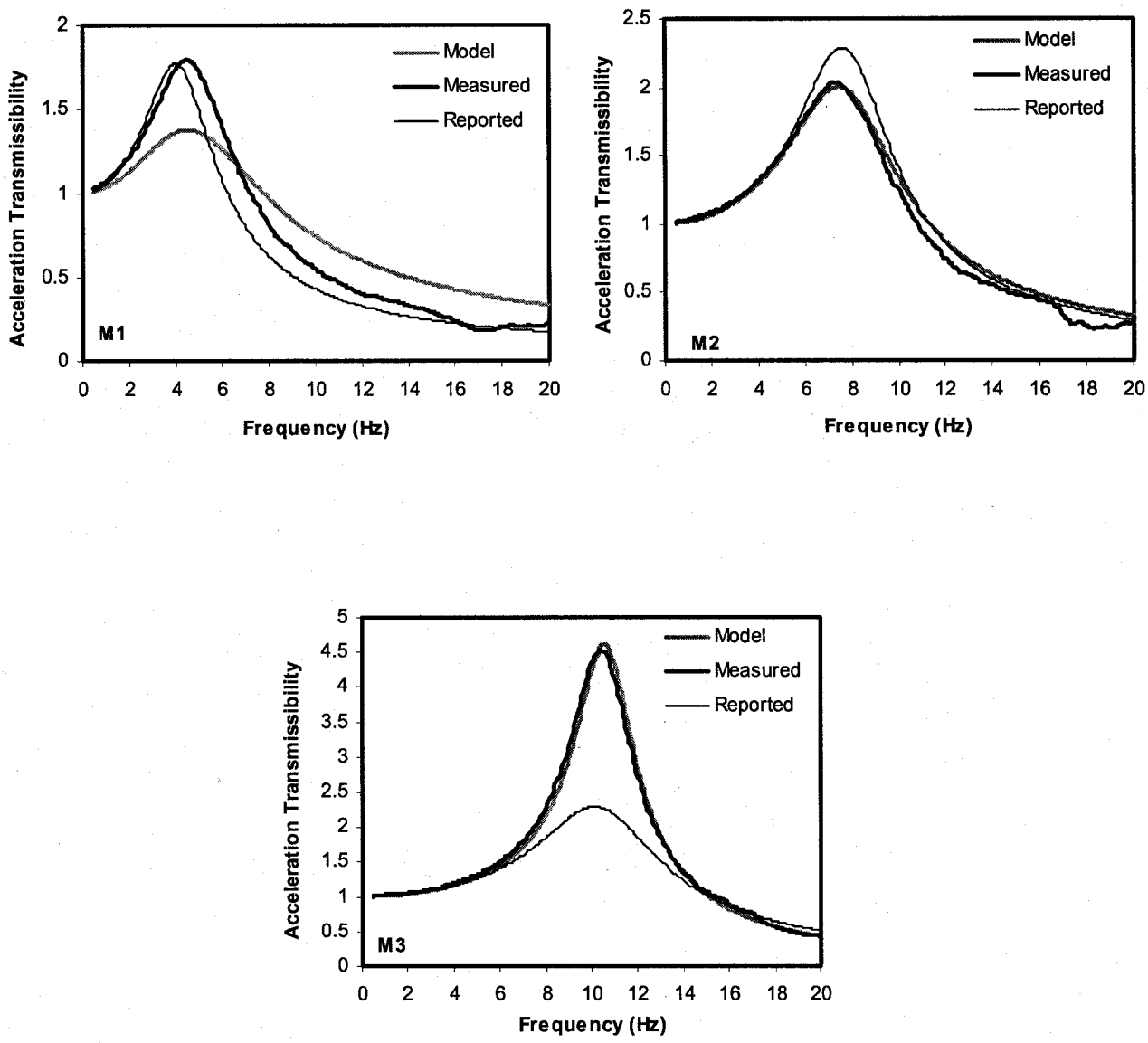

Figure 4.12: Comparisons of acceleration transmissibility characteristics of the identified model with the measured data and the responses of the reported baseline model (98 kg mass configuration)

4.5 Refinement of Manikin Parameters

Although the responses of the model identified in the previous section agree very well with the measured data, both the model and measured responses differ from the standardized target responses reported in ISO 5982 [35], as discussed in chapter 2, irrespective of the body mass configurations. The results presented in the previous section, however, clearly demonstrate the validity of the model and the modeling methodology. The validated model and the identification methodology thus be applied to identify model modifications to achieve the target responses reported in ISO 5982. The model parameters are thus defined by minimizing the error between the model and target responses using error minimization technique. It should be noted that the ISO 5982 reports the mean responses for body masses of 55, 75 and 90 kg, while manikin has been configured for 55, 75 and 98 kg body masses. The mechanical model, reported in ISO 5982, was thus slightly modified on the basis of mass parameters defined in the standards to derive a target response set for the 98 kg body mass configuration.

4.5.1 Estimation of refined model parameters

The refined model parameters are identified using the parametric optimization technique described in section 4.4.2. An objective function is defined to minimize the error between the model response and the target values, either defined in or derived from the standard. The objective function is defined as the weighted sum of the squared magnitude and phase errors associated with APMS function and expressed as:

$$U(\chi) = \lambda \sum_{i=1}^{N} \left\{ \left| |M_c(\omega_i)| - |M_t(\omega_i)| \right| \right\}^2 + \sum_{i=1}^{N} \left\{ \left| |\phi_c(\omega_i)| - |\phi_t(\omega_i)| \right| \right\}^2 \qquad (4.19)$$

where $M_t(\omega_i)$ and $\phi_t(\omega_i)$ are the APMS magnitude and phase target values respectively, and N is the number of discrete frequencies selected in the 0.5 to 20 Hz frequency range.

Owing to the relatively small influences of the parameters k_2, k_3, c_2 and c_3, the error function is minimized using a limited parameter vector, such that:

$$\chi = \left\{m_1, k_1, c_{eq}\right\}^T \tag{4.20}$$

where 'T' designates the transpose.

The minimization problem expressed in Equation 4.19 is solved subject to parameter constraints applied on the total model mass, while the values of the masses m_0, m_2 and m_3 are limited by the equality constraints. For 75 kg body mass configuration, the static mass supported by the seat is in the order of 55 kg, as defined in ISO 5982. the total model mass is thus constrained by a limit constraint that permits the mass variation within ± 4 kg:

$$51 \leq \sum_{i=0}^{3} m_i \leq 59kg \tag{4.21}$$

The remaining model masses are limited to those identified earlier, namely, m_0 = 7.5 kg, m_2 = 5 kg, m_3 = 2 kg. On the basis of the results presented in Tables 4.2 to 4.4, following equality and inequality constraints are imposed on the stiffness and damping parameters:

$$\begin{gathered} m_0 = 7.5 \text{ kg};\ m_2 = 5 \text{ kg};\ m_3 = 2 \text{ kg};\ m_1 > 35 \text{ kg} \\ k_1 > 25000 \text{ N/m};\ k_2 = 12650 \text{ N/m};\ k_3 = 9000 \text{ N/m} \\ c_{eq} > 700 \text{ Ns/m};\ c_2 = 150 \text{ Ns/m};\ c_3 = 30 \text{Ns/m} \end{gathered} \tag{4.22}$$

For the 55 kg and 98 kg body mass configurations, the parameter constraints were varied in accordance with the prototype design, as described earlier.

4.5.2 Refined Parameter values

The constrained optimization problem defined in Equations (4.19) through (4.22) is solved using MATLAB optimization toolbox [85] to identify the model parameters. Tables 4.7, 4.8, and 4.9 illustrate comparisons of the identified parameters for the 55, 75 and 98 kg body mass configurations, respectively, with the baseline model parameters. The higher value of the principal mass m_1, irrespective of the body mass configuration, is due to the differences in the reported and standardized static weights, supported by the seat. Figures 4.13, 4.14, 4.15 illustrate comparisons of the refined and baseline model responses with the target results defined from ISO 5982, for 55, 75 and 98 kg configuration, respectively. The results, in general show reasonably good agreements between the refined model and target response characteristics, which suggests that the manikin with refined parameters can accurately predict the idealized APMS response for all the three body mass configurations. APMS magnitude responses correlate well with the target APMS magnitude response both in terms of resonant frequency and peak APMS magnitude, irrespective of the body mass configurations. The phase response correlates well upto 10 Hz for 55 and 75 kg body mass configurations whereas upto 6 Hz for 98 kg body mass configuration. The figures also show that the baseline prototype responses differ from the target responses, particularly for the 55 and 75 kg configurations.

Table 4.7: Comparison of baseline and optimized parameters for 55 kg body mass configuration

Parameter	Baseline	Optimized
m_0 (kg)	7.5	7.5
m_1 (kg)	24	26
m_2 (kg)	5	5
m_3 (kg)	2	2
k_1 (N/m)	17140	26373
k_2 (N/m)	12650	12650
k_3 (N/m)	9000	9000
c_1 (Ns/m)		1874.08
c_{eq} (Ns/m)	500	984.30
c_2 (Ns/m)	125	150
c_3 (Ns/m)	67	30
h_{55} (m)	0.060	0.076

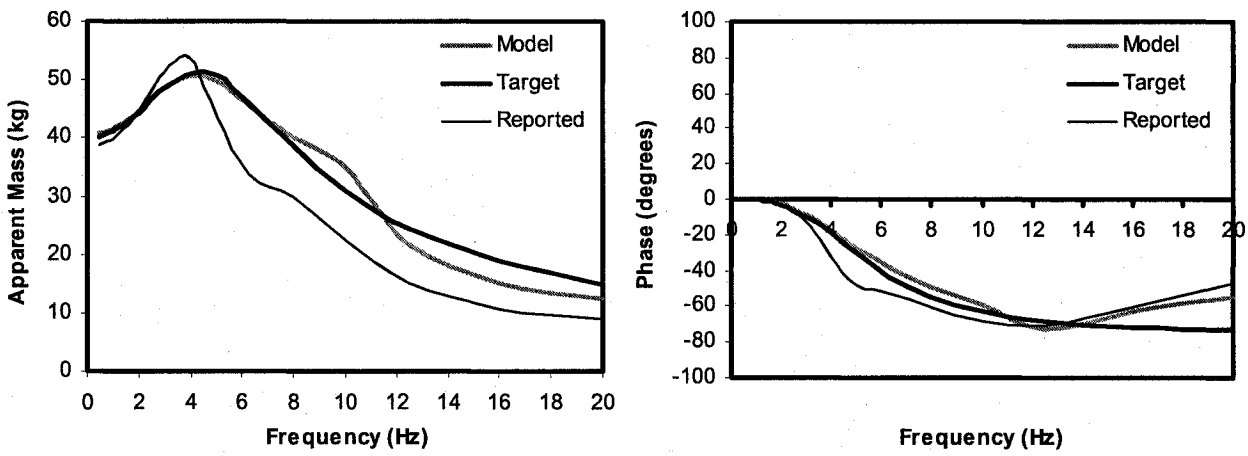

Figure 4.13: Comparisons of APMS response of the refined model with the target and reported baseline model responses (55 kg configuration)

Table 4.8: Comparison of baseline and optimized parameters for 75 kg body mass configuration

Parameter	Baseline	Optimized
m_0 (kg)	7.5	7.5
m_1 (kg)	33.5	41
m_2 (kg)	5	5
m_3 (kg)	2	2
k_1 (N/m)	30870	32868
k_2 (N/m)	12650	12650
k_3 (N/m)	9000	9000
c_1 (Ns/m)		1874.08
c_{eq} (Ns/m)	715	1087.9
c_2 (Ns/m)	125	150
c_3 (Ns/m)	67	30
h_{75} (m)	0.080	0.080

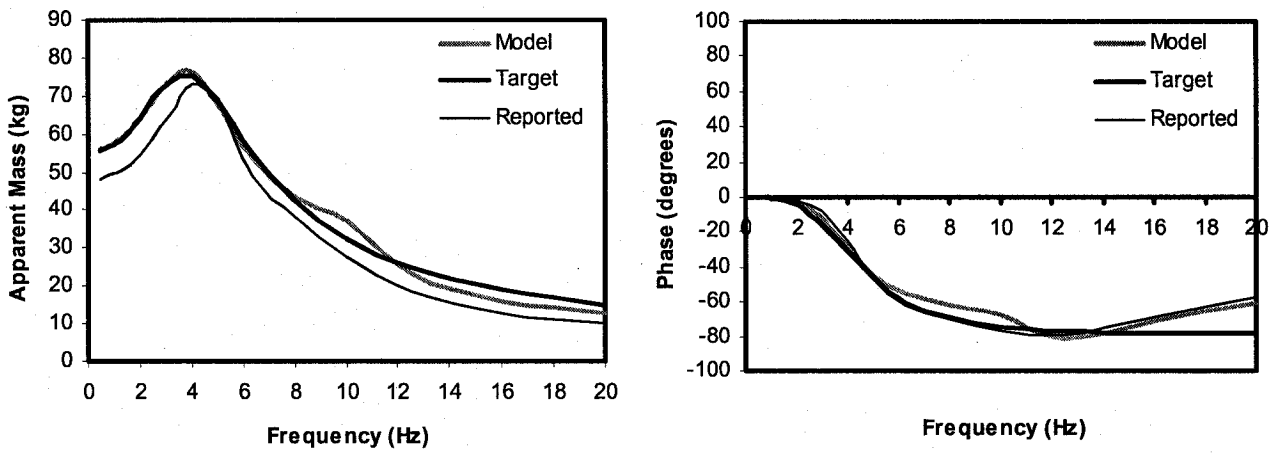

Figure 4.14: Comparisons of APMS response of the refined model with the target and reported baseline model responses (75 kg configuration)

Table 4.9: Comparison of baseline and optimized parameters for 98 kg body mass configuration

Parameter	Baseline	Optimized
m_0 (kg)	3.5	3.5
m_1 (kg)	58	63
m_2 (kg)	5	5
m_3 (kg)	2	2
k_1 (N/m)	44270	36453
k_2 (N/m)	12650	12650
k_3 (N/m)	-	9000
c_1 (Ns/m)		1874.08
c_{eq} (Ns/m)	1150	1354
c_2 (Ns/m)	125	150
c_3 (Ns/m)	-	30
h_{98} (m)	0.1	0.089

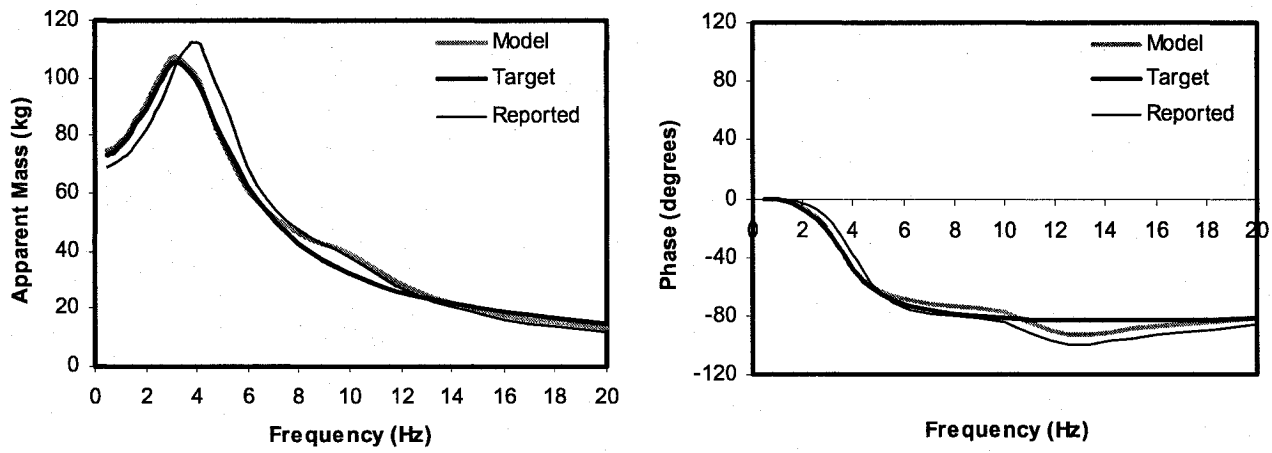

Figure 4.15: Comparisons of APMS response of the refined model with the target and reported baseline model responses (98 kg configuration)

4.6 Assessment of APMS response of the human subjects

In the previous section, the design parameters for enhancement of manikin's APMS prediction abilities are identified in accordance with the standardized values specified in ISO 5982 [35]. However, it is to be noted that the lower and upper limits of the idealized range are not indicative of the biodynamic responses of the three body mass groups. Moreover, the dynamic response of the manikin showed considerable deviations from those of the standardized APMS responses reported in DIN 45676 [36] for all the three mass groups. Therefore, the design of an effective anthropodynamic manikin requires identification of reliable biodynamic responses of subjects of particular body masses seated in a vertical whole body vibration environment.

For this purpose the biodynamic responses of seated subjects within three different mass groups were measured in the laboratory. The standardized seat test method, defined in ISO-7096, requires the use of three different human subjects with body mass in the vicinity of 55, 75 and 98 kg. Laboratory measurements were thus undertaken to establish the apparent mass characteristics of seated vibration-exposed human subjects within the three mass groups. For this purpose, a total of 27 adult male subjects with body mass in the vicinity of the defined masses (9 subjects for each mass group) were used in the study. The means and standard deviations of subjects masses within the groups are shown in Table 4.10, together with the lower and upper limits. The participants did not have a previous history of low back pain. Each subject was seated on a rigid seat without a backrest and advised to maintain an erect upright seated posture with hands in lap. The APMS response characteristics of each subject were measured under three different levels of white-noise random excitations in the 0.5 to 20 Hz range

with overall *rms* acceleration values of 0.5, 1 and 2 m/s^2. Each measurement was repeated three times.

Table 4.10: Body Mass of human subjects with standard deviations

Mass Group	N	Mass (kg)			
		Minimum	Mean	Maximum	Standard Deviation
55 kg	9	50.00	55.73	60.00	3.3
75 kg	9	70.12	75.23	81.88	3.9
98 kg	9	93.00	97.63	107	5.5

The vertical dynamic force and acceleration signals were acquired into a multi-channel signal analyzer and analyzed to derive the APMS magnitude and phase responses. The measurement and data analysis methods, including the inertial correction, were derived as described in section 2.3.3. Figures 4.16 to 4.18 illustrate the APMS responses of individual subjects along with the mean values for the three mass groups and under 0.5 m/s^2, 1 m/s^2 and 2 m/s^2 excitation levels, respectively. It is to be noted that the measurements with subjects S4, S5 and S6 within the 55 kg and S1 within the 98 kg group were not acquired for the 0.5 m/s^2 excitation level. A total of 6 data sets were thus available for 55 kg mass group, and 8 data sets for 98 kg mass group under 0.5 m/s^2 excitation level. The data under higher excitations, however, were acquired for all nine subjects. The results clearly demonstrate the influence of the body mass on the APMS response of the subjects, irrespective of the excitation level, which has also been reported in many studies [21, 75].

Apart from the body mass, the biodynamic responses are also influenced by the magnitude of excitation. Figure 4.19 illustrates the effect of vibration magnitude on the APMS response of the subjects. The results clearly suggest softening of the body with increasing vibration intensity, which has also been reported in a few previous studies [75-76]. These results indicate non-linear nature of the biodynamic response, and thus would require reference values to be defined as a function of the excitation magnitude.

4.6.1 Analysis of the measured data

The measured data are further examined for any outliers. A data set exceeding one standard deviation about the mean value was considered as an outlier, and removed from the further analysis for defining the reference values for a given mass and excitation. Figure 4.20, as an example, illustrates a comparison of the datasets with the bounds formed by ± standard deviation for the 55 kg mass group under the three levels of excitation. The results suggest that the data for subjects S2 and S3 within the 55 kg mass group may be considered outliers under a 0.5 m/s^2 excitation. Similarly the data for subject S3 under 1 m/s^2, and subject S3 and S4 under 2 m/s^2 excitations are considered outliers. The reference value for a particular excitation level and within a mass group is derived by taking the mean of the subject APMS response after removal of the outliers. Similar methodology is applied for the other mass group for the determination of the reference values. The final synthesis involved 4, 8 and 7 datasets within the 55 kg mass group under 0.5 and 1.0 and 2 m/s^2 excitations. For the 75 kg mass group, a total of 8 datasets were within the defined bound for all three excitations. For the 98 kg group, a total of 7, 8 and 8 datasets were considered under the three excitations, respectively.

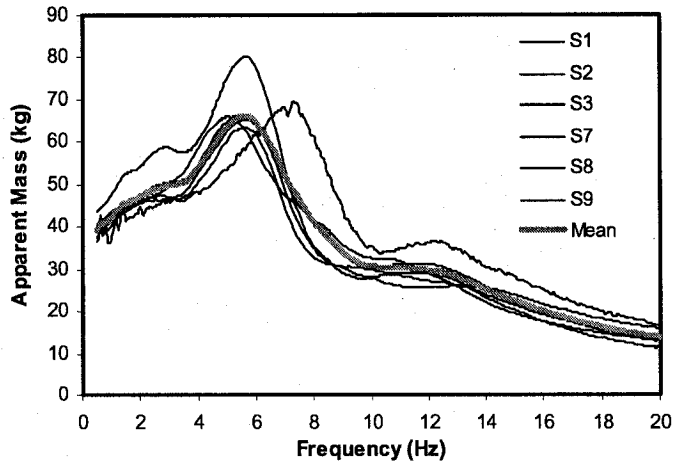

(a)

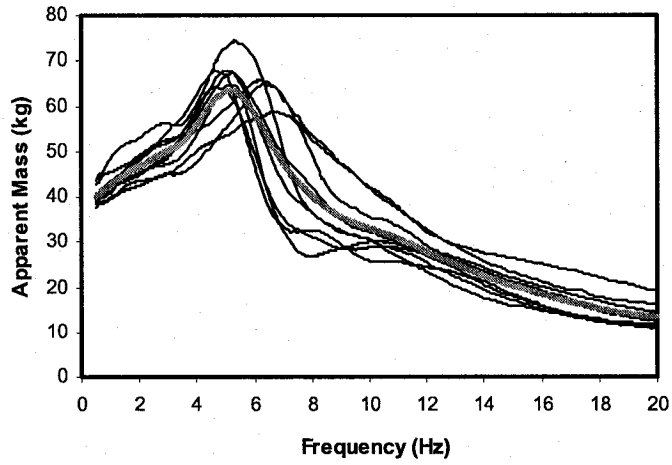

(b)

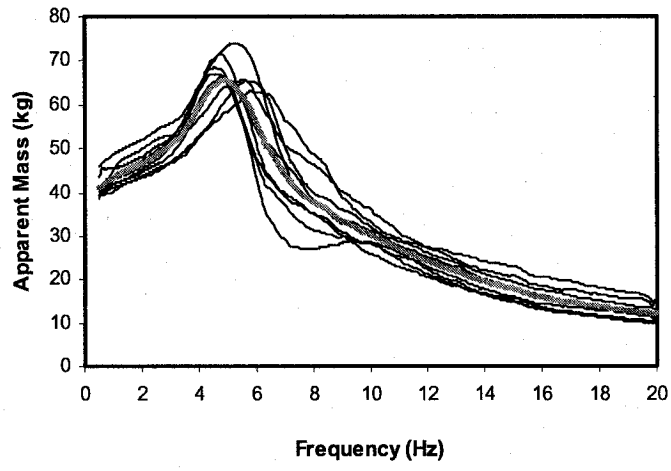

(c)

Figure 4.16: Comparisons of APMS magnitude responses of seated subjects within the 55 kg mass group, and the mean response under excitation: (a) 0.5 m/s^2; (b) 1 m/s^2; and (c) 2 m/s^2

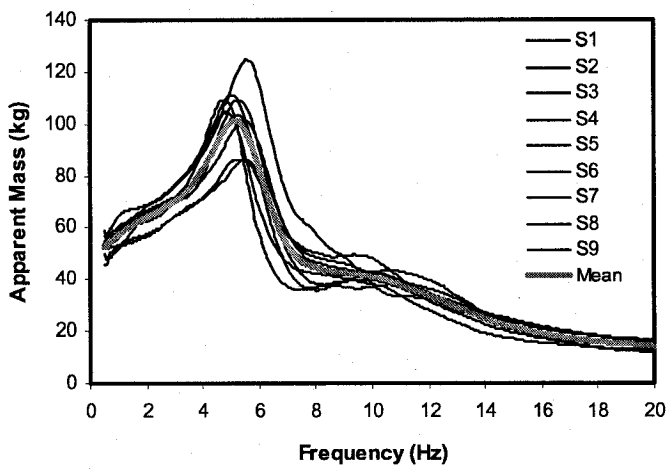

(a)

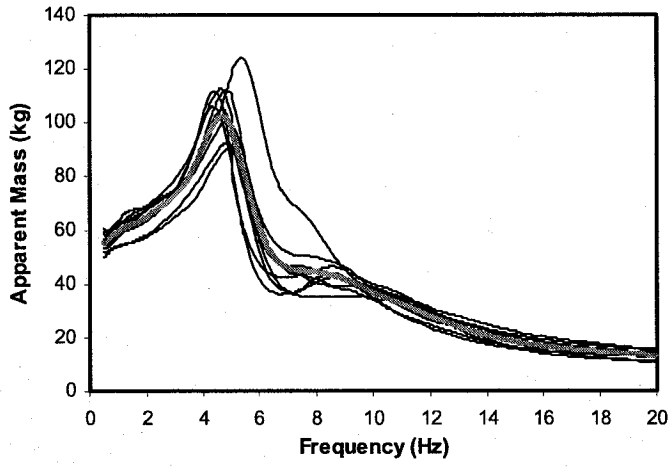

(b)

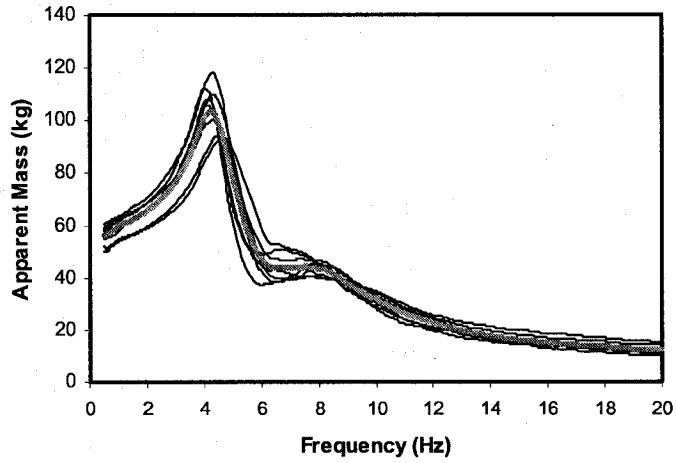

(c)

Figure 4.17: Comparisons of APMS magnitude responses of seated subjects within the 75 kg mass group, and the mean response under excitation: (a) 0.5 m/s^2; (b) 1 m/s^2; and (c) 2 m/s^2

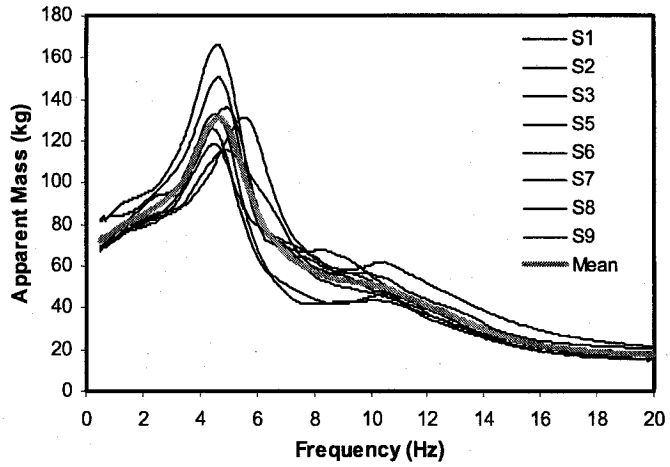

(a)

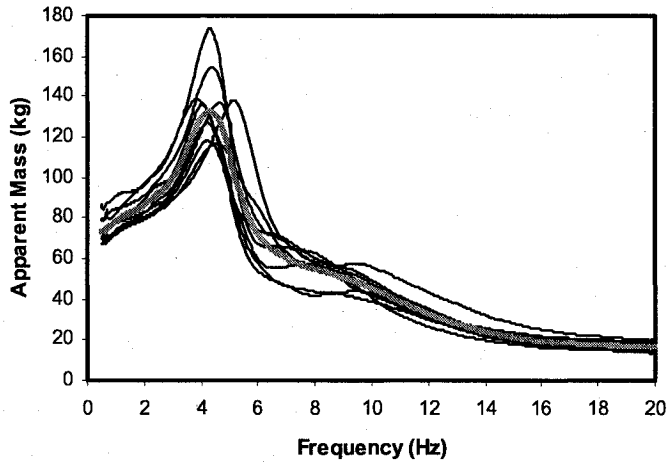

(b)

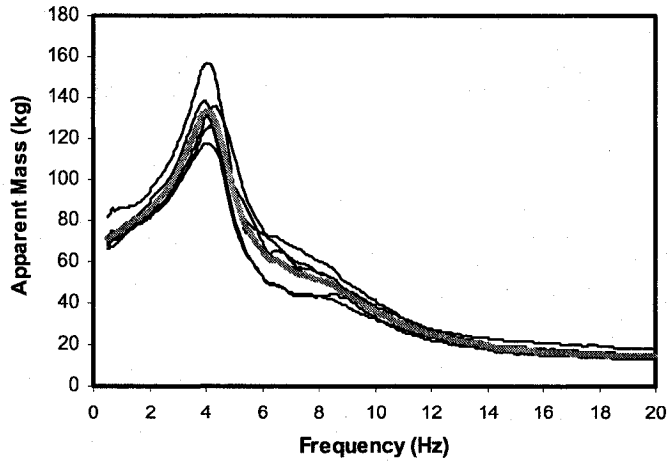

(c)

Figure 4.18: Comparisons of APMS magnitude responses of seated subjects within the 98 kg mass group, and the mean response under excitation: (a) 0.5 m/s^2; (b) 1 m/s^2; and (c) 2 m/s^2

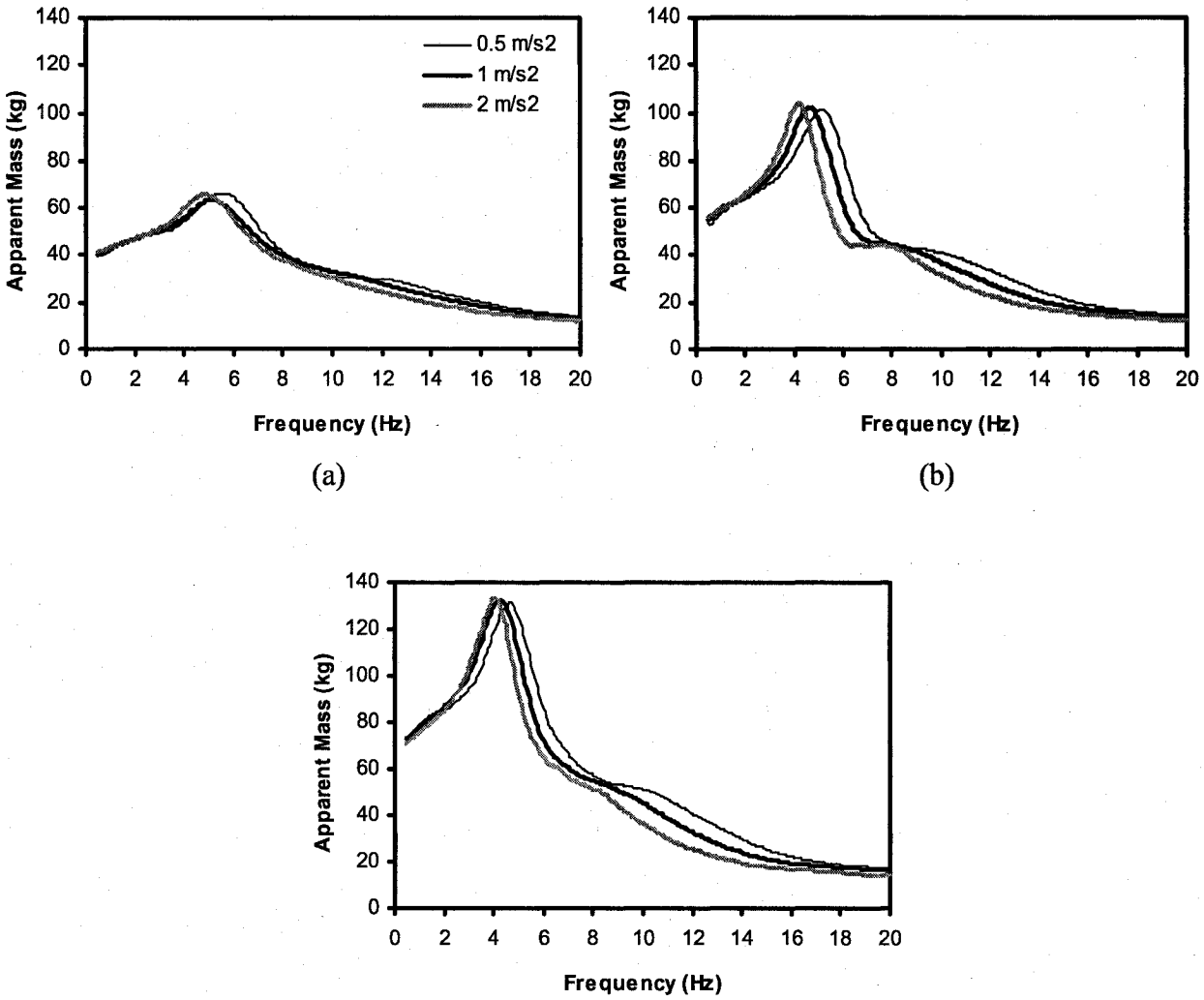

Figure 4.19: Influence of vibration magnitude on the APMS response of the human subjects for mass of: (a) 55 kg; (b) 75 kg and (c) 98 kg

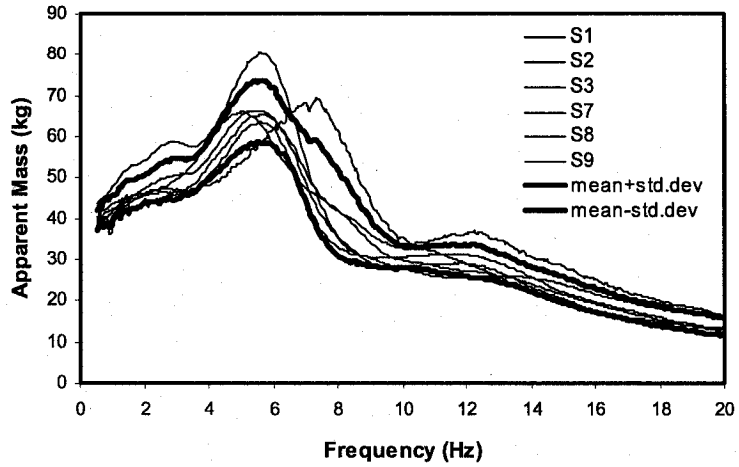

(a)

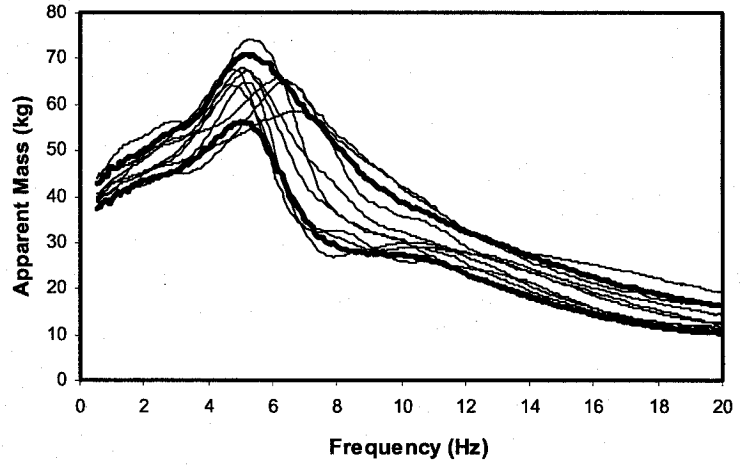

(b)

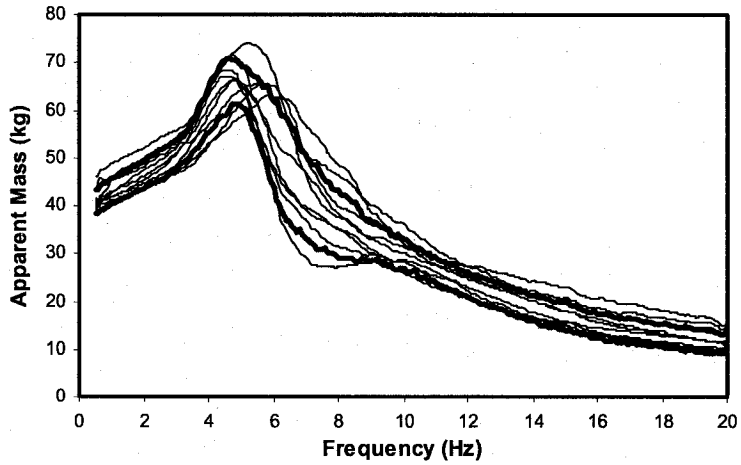

(c)

Figure 4.20: Identification of outliers in the dataset for 55 kg mass group under white noise excitations of: (a) 0.5 m/s^2; (b) 1 m/s^2 and (c) 2 m/s^2 overall *rms* acceleration.

4.7 Comparison of the Reference values with ISO 5982 and DIN 45676

The measured APMS magnitude responses of subjects under 2 m/s^2 excitation level are compared with those defined in ISO 5982 and DIN 45676 for different body mass group, as shown in Figure 4.21. The results clearly show significant deviations between the measured and the standardized values. The comparison for the 55 kg subjects data is illustrated with the lower limit of the range defined in ISO 5982. the results show significant differences from the lower ISO limit and that defined in DIN 45676 for the same mass group in both the resonant frequency and the peak magnitude. The low frequency magnitude for the 55 kg body mass, considered to represent the body mass supported by the seat, is higher for the DIN response when compared to the subject response, whereas it is somewhat comparable with the ISO lower limit. Even larger deviations are observed in the measured responses of the 75 kg subjects with respect to the mean ISO and DIN data for the 75 kg subjects. The also applies, when the measured data is compared to the upper limit of the ISO range and the DIN data for the 98 kg subject response. It should be noted that the data synthesis in realizing the idealized range in ISO 5982 involved data subjects of maximum mass of 93 kg.

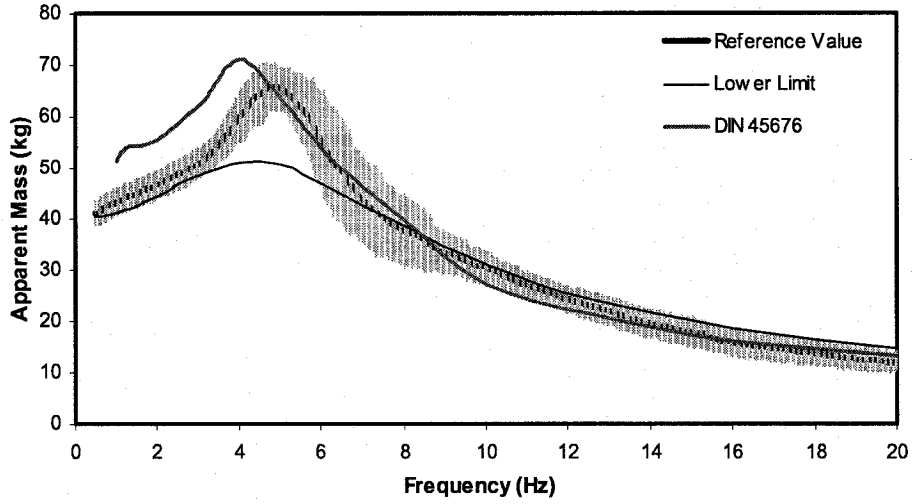

(a)

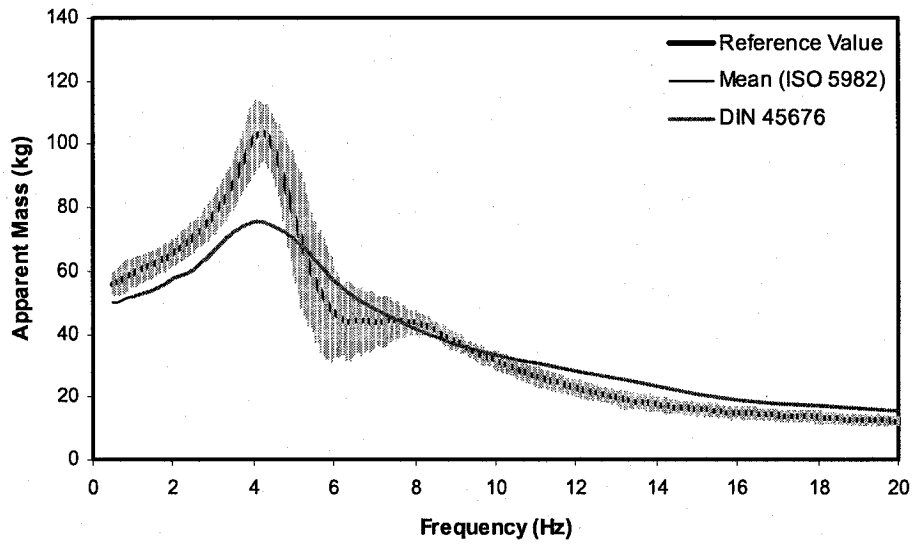

(b)

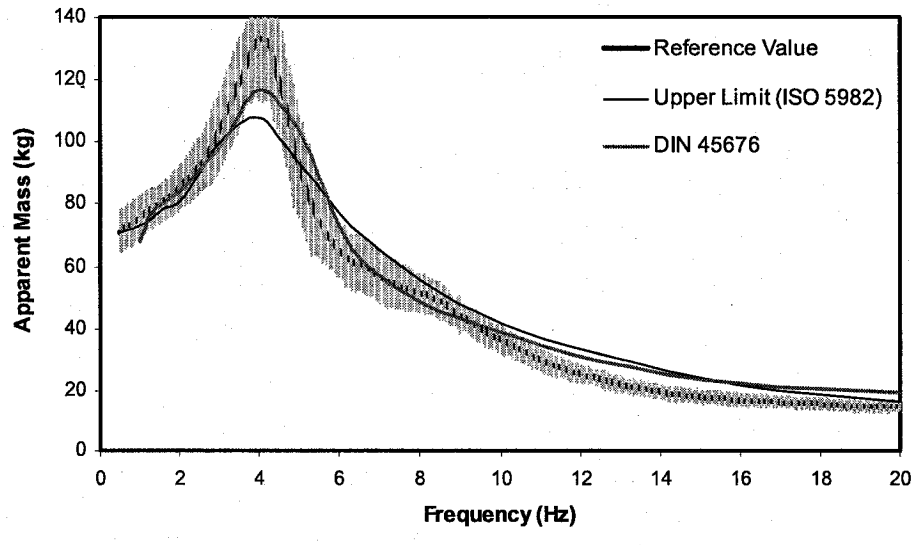

(c)

Figure 4.21: Comparison of the measured human subject APMS magnitude response with those of the standardized response of ISO 5982 and DIN 45676 within the mass group of: (a) 55 kg; (b) 75 kg; and (c) 98 kg

4.8 Reference Values

The reference values are estimated as discussed in section 4.6.1. Figures 4.22-4.24 illustrates the reference values for different mass groups as a function of the excitation magnitude. These reference values can be used for the design synthesis of effective anthropodynamic manikins. The reference values presented are the mean biodynamic responses of magnitude of seated subject within a mass group along with the standard deviations, when exposed to a broadband whole-body vertical vibration of a particular magnitude.

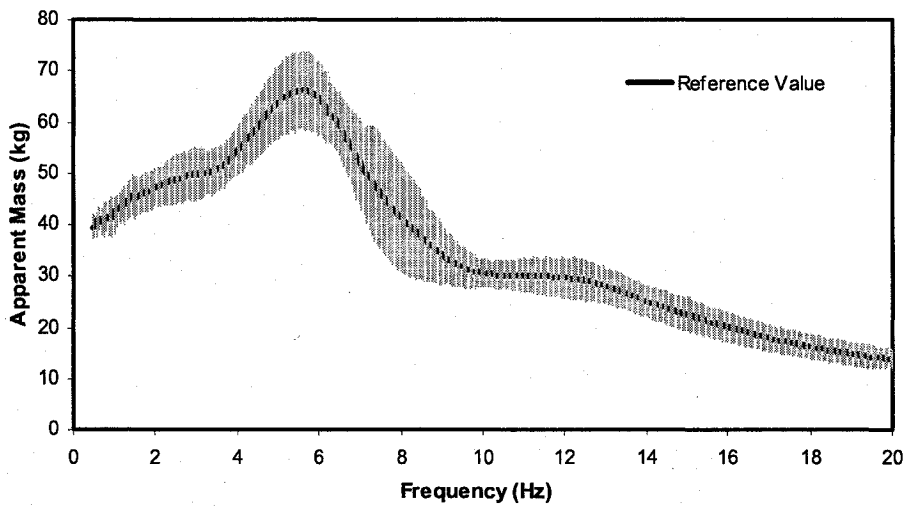

(a)

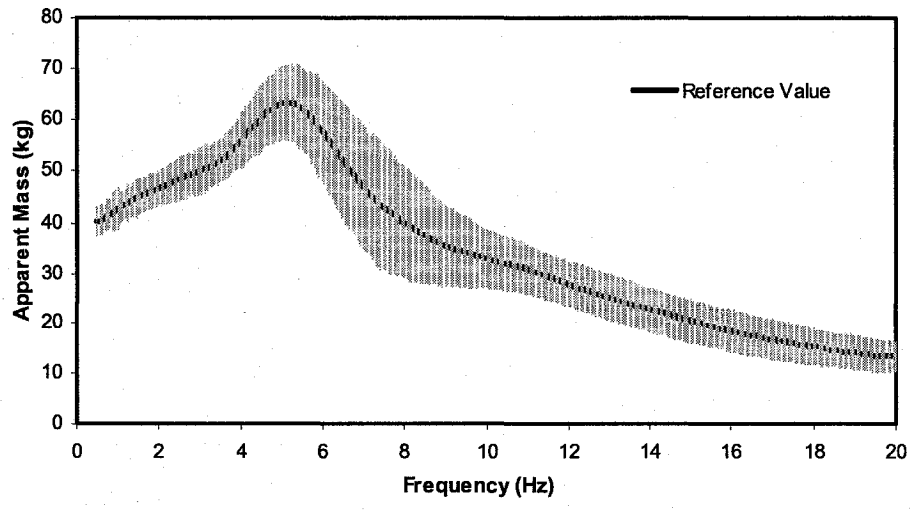

(b)

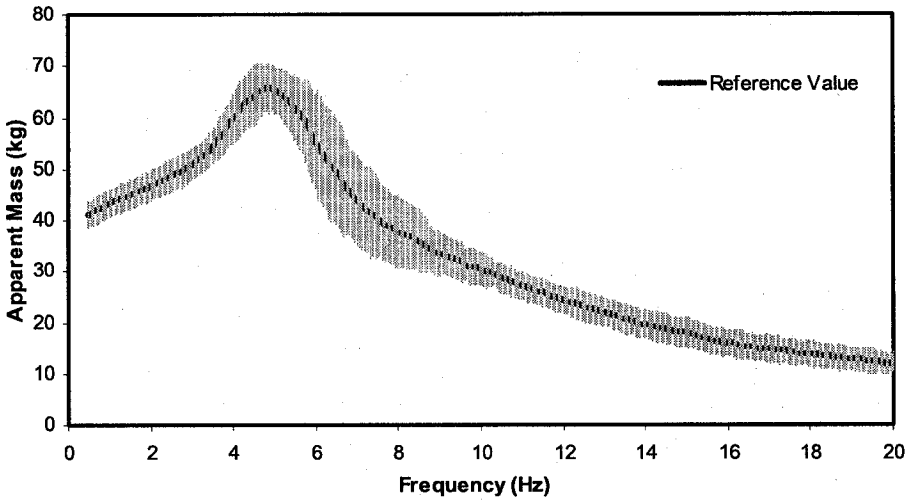

(c)

Figure 4.22: Reference values for the APMS response for the 55 kg mass group under white noise excitation of: (a) 0.5 m/s^2; (b) 1 m/s^2; (b) 2 m/s^2

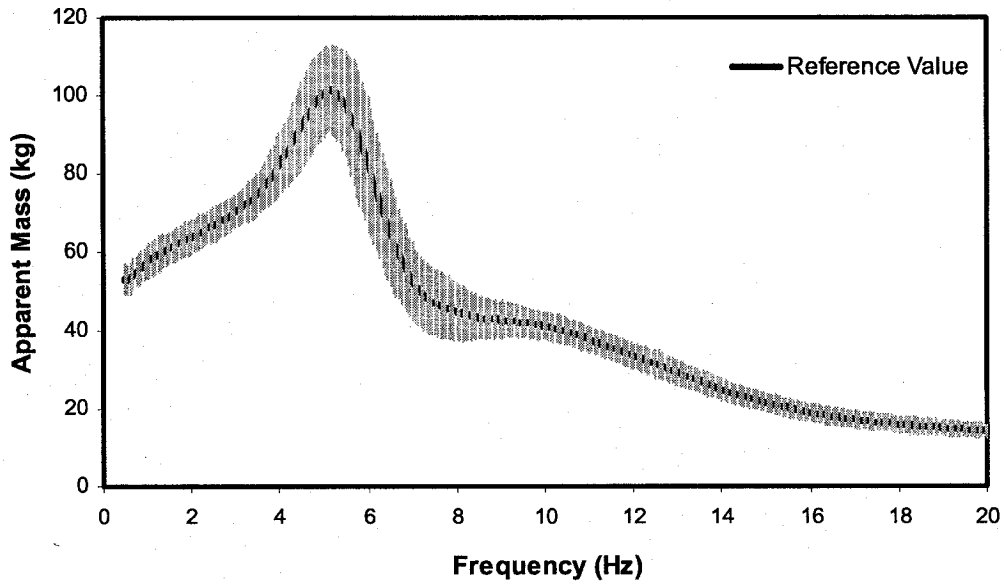

(a)

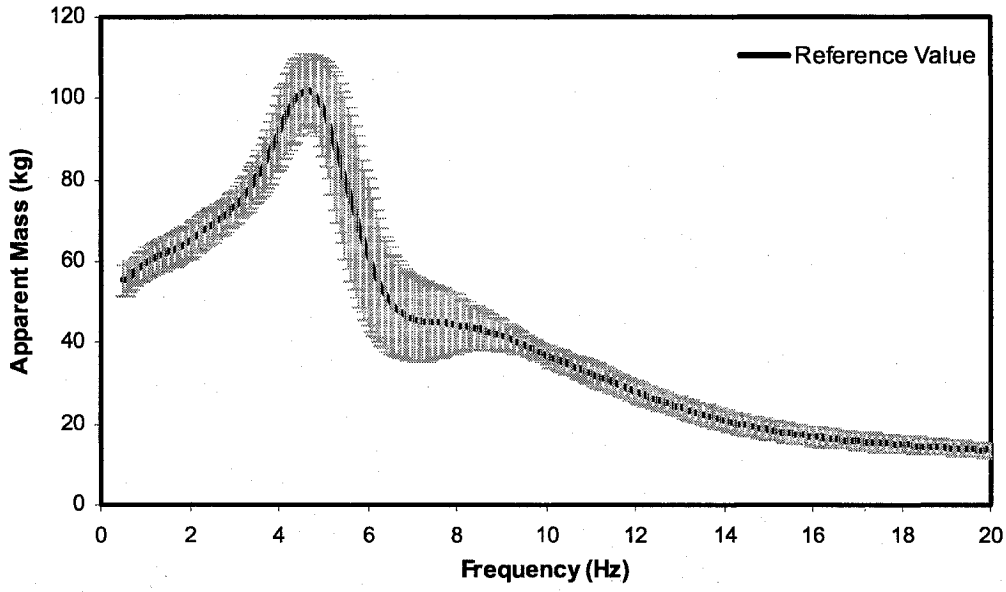

(b)

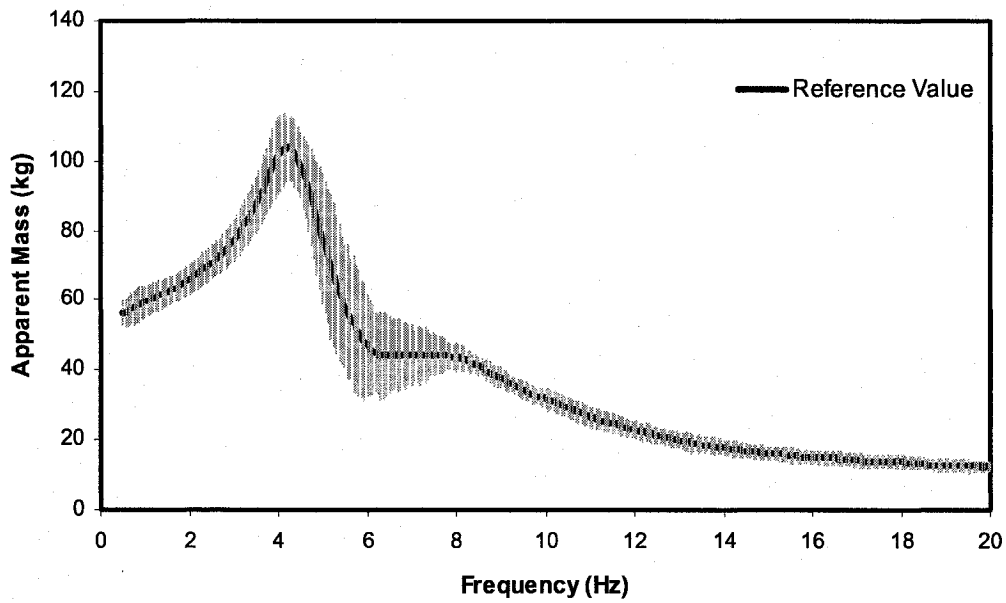

(c)

Figure 4.23: Reference values for the APMS response for the 75 kg mass group under white noise excitation of: (a) 0.5 m/s^2; (b) 1 m/s^2; (b) 2 m/s^2

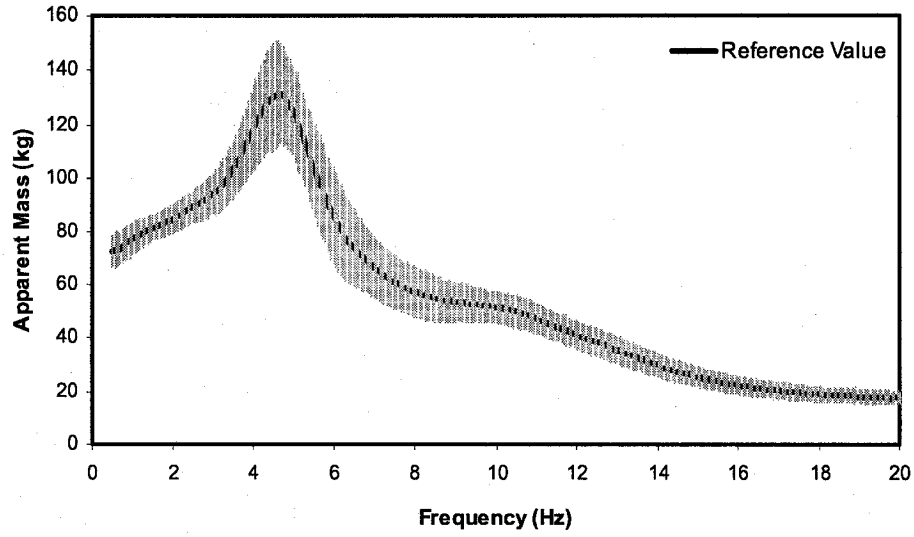

(a)

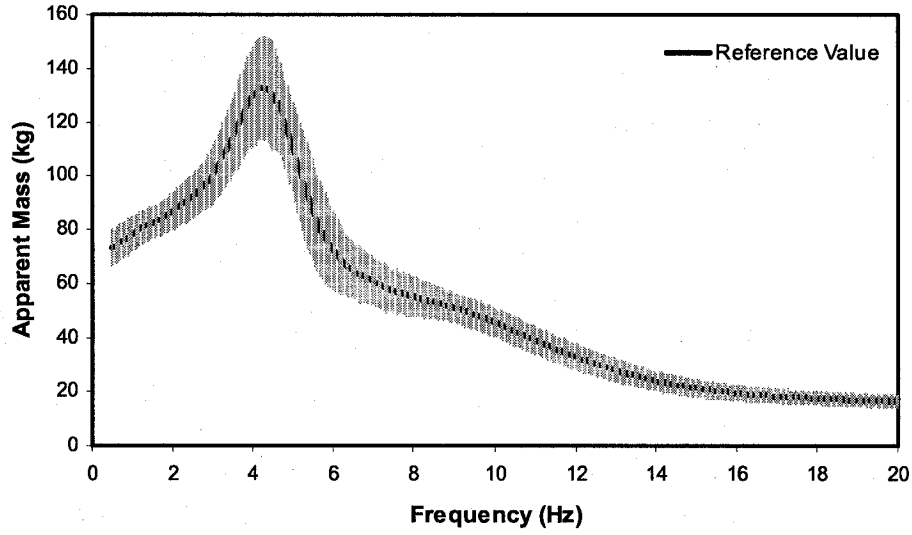

(b)

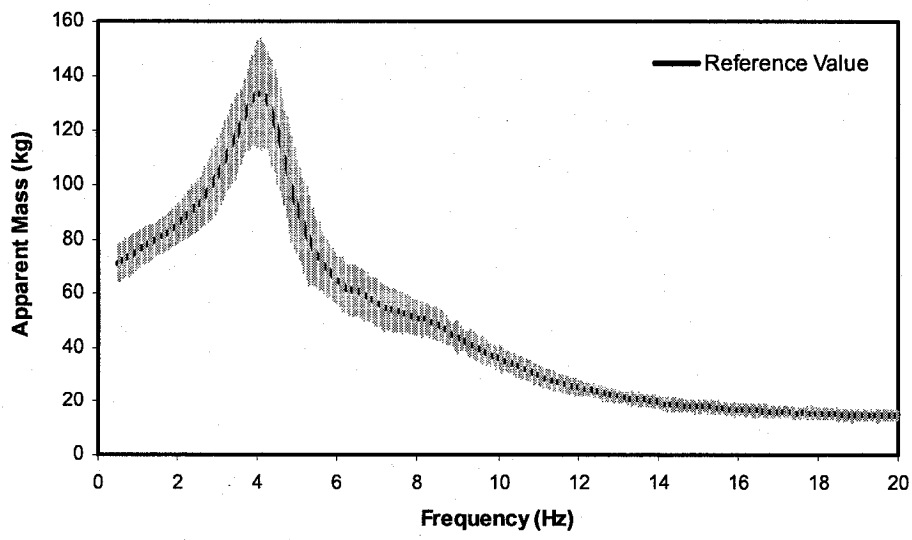

(c)

Figure 4.24: Reference values for the APMS response for the 98 kg mass group under white noise excitation of: (a) 0.5 m/s^2; (b) 1 m/s^2; (b) 2 m/s^2

4.9 Summary

An analytical model of one of the prototype manikins was derived upon identifying the system components. The validity of the model was examined by comparing the model responses with the measured data. Owing to the significant differences in model and measured responses, model parameters were identified through solution of a constrained minimization function. The validity of the identified model and methodology is demonstrated by comparing the model responses with the measured data. An alternate error minimization problem is solved to minimize the error in the model response and the target values defined in ISO 5982. The model refinements are thus proposed to enhance the biodynamic response prediction ability of the anthropodynamic manikin. APMS response when the baseline parameters are used which is mainly due to the difference in the target curves chosen.

Owing to the lack of reliable target values for the three mass groups, the biodynamic responses of a total of 27 human subjects were measured in the laboratory to define the reference values which can be used to design an effective anthropodynamic manikin. The comparison of the established reference values with the standardized limits as reported in ISO 5982 and DIN 45676 revealed significant deviations in both the resonant frequency and the peak APMS magnitude. The reference values are suggested for the three mass groups as a function of the vibration magnitude

CHAPTER 5

CONCLUSIONS AND RECOMMENDATION FOR THE FUTURE WORK

5.1 Highlights of the Investigation

The thesis research was formulated to effectively characterize the apparent mass characteristics of two different prototype anthropodynamic manikins for applications in performance assessment of different suspension seats under representative vibration excitations. The design refinement of one of the prototype manikin to enhance its apparent mass prediction ability also formed the secondary goal of this dissertation research. The major highlights of the thesis include:

- Characterization of the apparent mass response of the prototype anthropodynamic manikins under different excitation and evaluation of their APMS prediction abilities for various body masses.

- Investigation of influence of vibration magnitude and body mass effect on the APMS response characteristics of the manikins and comparison with those reported in the literature for human subjects.

- Evaluation of the vibration isolation performances of the seat-occupant, seat-manikins and seat-inert mass systems using five different suspension seats subject to vertical vibration excitations of the corresponding target vehicles.

- Response analysis of the seat-manikins, seat-human, and seat-inert mass in terms of SEAT values to assess the suitability of the manikins for application to different seats, vehicular excitations and body mass configurations.

- Determination of vibration transmissibility characteristics of seats with manikins.

- Comparisons of the seat-occupant, seat-manikins, and seat-inert mass response in terms of deviations in the SEAT values.

- Development of a linear analytical model of one of the prototype anthropodynamic manikin incorporating the linkage mechanism attached to the primary mass.

- Evaluation of the APMS response of the analytical model and validation of analytically derived APMS response characteristics against the experimental results for the three body mass configurations.

- Parametric sensitivity analysis of the analytical model and identification of the design parameters of the manikin to enhance its APMS response prediction ability.

- Development of reliable reference APMS responses of human subjects for the three mass groups.

5.2 Conclusions

The following conclusions are drawn from the experiment and analytical studies conducted in this investigation.

- The resonant frequencies of both the manikins lie in the frequency range of 4-6 Hz, irrespective of the body mass configurations and vibration excitation magnitude, which correspond to those reported for the seated human body.

- The static property of the manikin G tends to be considerably higher than the reported percent body mass supported by the seat, particularly for 55 kg configurations. However, for manikin F the percent of the body mass supported by the seat is closer to that of the reported range, near 75 %.

- The influence of excitation magnitude on the APMS magnitude response of manikin G is not significant whereas a significant influence was observed for manikin F, irrespective of the body mass configurations. The reported APMS studies on the APMS responses of the vibration exposed to seated subjects generally show insignificant effect of vibration magnitude. The strong influence of excitation magnitude on the APMS response of manikin F was attributed to the presence of high seal friction in the principal damper.

- The influence of body weight on the APMS response of manikin G was observed to be significant, whereas a definite trend was not observed for manikin F, irrespective of the excitation magnitude.

- The measured APMS responses of manikin G, showed better agreements with the data reported in DIN 45676, whereas a considerable difference was observed for 55 kg and 98 kg body mass configurations with the idealized range of apparent mass reported in ISO 5982.

- The measured responses of manikin F agreed more with the standardized values reported in DIN 45676 for 55 kg and 98 kg body mass configurations.

- Influence of manikin mass on the seat vibration transmissibility was observed for low frequency pneumatic seat A and the high frequency mechanical suspension seat D, irrespective of the manikins, whereas no such effect was observed for low frequency pneumatic seat C. Moreover, for seat B, the manikin F showed an influence of manikin mass on the seat vibration transmissibility, which was not apparent with manikin G.

- Influence of excitation magnitude on the seat vibration transmissibility with the manikins was generally observed for the candidate seats. The results generally showed a decrease in the resonant frequency and an increase in the peak magnitude as the vibration magnitude increased, irrespective of the manikin mass.

- The results from the comparative analysis of the seat acceleration transmissibilities and percent deviation of SEAT values, of seat-human, seat-manikin, and seat-inert mass systems revealed that equivalent inert mass could provide reasonably good prediction of the seat performance, when the excitations dominated in the low frequency range. This would be generally applicable for a large class of heavy-road and wheeled off-road vehicles, where the vertical vibration predominates in the 1.5 – 2.5 Hz range. The manikins generally provided a poor estimate of the seat-human system performance, under higher frequency excitations and for higher natural frequency seats.

- The parametric studies conducted on the linear analytical model illustrate that principal stiffness 'K1' and principal damper 'C1' were the two significant design parameters for enhancement of the manikin's prediction abilities of the idealized values of APMS response. Moreover, the stiffness 'K2' and 'C2' showed only minimal effect on the APMS response in the frequency range of 6-10 Hz.

- The static and dynamic APMS response prediction ability of the prototype manikin F can be easily enhanced by selecting the proposed values of the principal mass (m_1), stiffness (k_1) and damping (c_1) parameters. The use of such parameters is expected to improve the applicability of the manikins for assessment of suspension seats.

- The comparison of the APMS responses of human subjects with those reported in standardized data reported in ISO 5982 and DIN 45676 revealed considerable deviations with respect to the resonant frequency and the peak APMS magnitude, irrespective of the mass group.

- The established mean values could serve as more reliable target responses for design of effective anthropodynamic manikins.

5.3 Recommendations for Further Investigation

The experimental and analytical studies performed in this investigation focus on the assessment of the prototype anthropodynamic manikins for their applicability in laboratory assessments of suspension seats. However, the occupant of the off-road vehicle is continuously subjected to shocks due to frequent discontinuities in the terrain. Therefore, studies incorporating shock excitations and multiple axes vibration are recommended.

Further studies in development of human-like base for the manikins in place of wooden base are recommended so as to improve the coupling of the seat-manikin system. Attachments in the manikin also need to be incorporated so as to increase the stability of the manikins under high magnitude of vibration. It is also suggested that further efforts be made to realize actively controlled manikins to achieve better correlations with the biodynamic responses of human subjects of different body mass.

References

1. Griffin, M. J., 1990 *Handbook of Human Vibration.* Academic Press, London.

2. Magnusson, M. L., Pope, H., Hulshof, C. T. J., Bovenzi, M., 1998 *Journal of sound and vibration 215(4), 643-651.* Development of a Protocol for Epidemiological studies of Whole-Body Vibration and Musculoskeletal Disorders of the Lower Back.

3. Schwarze, S., Notbohm, G., 1998 *Journal of sound and vibration 215(4), 613-628.* Dose-Response Relationships between Whole-Body Vibration and Lumbar Disk Disease-A Field Study on 328 Drivers of Different Vehicles.

4. Bovenzi, M., Pinto, I., Stacchini, N., 2002 *Journal of sound and vibration 253(1), 3-20.* Low Back Pain in Port Machinery Operators.

5. Mansfield, N. J., 2005 *Human Resposne to Vibration.* CRC Press Boca Raton. ISBN 0-415-28239-X.

6. Varterasian, J. H. 1982 *Society of Automotive Engineers, SAE Technical Paper No. 820309* On Measuring Automobile Seat Ride Comfort.

7. Rakheja. S., Ahmed, A. K. W., 1991 *American Society of Agricultural Engineers, ASAE Paper No 917569, 26pp.* Ride Performance Characteristics of Seat-Suspension Systems and Influence of the Seated Driver.

8. Boileau, P. E., Rakheja, S., 2000 *Rapport IRSST* Caractérisation de l'environnement vibratoire dans différentes catégories de véhicules : industriels, utilitaires et de transport urbain.

9. Tchernychouk, V., 1999 *Ph.D. Thesis in the Department of Mechanical Engineering (Concordia University).* Objective Assessment of Static and Dynamic Seats Under Vehicular Vibrations.

10. Boileau, P. E., 1995 *Ph.D. Thesis in the Department of Mechanical Engineering (Concordia University).* A Study of Secondary Suspension and Human Driver Response to Whole Body Vehicular Vibration and Shock.

11. Matthews, J., 1967 *Engineering symposium of the Institute of Agricultural Engineers Agricultural Engineering College Silsoe* Progress in the Application of Ergonomics to Agricultural Engineering.

12. Suggs, C. W., Stikeleather, L.F., Harrison, J.Y., Young, R.E., 1969 *American Society of Agricultural Engineers, Purdue University 69-172* Application of a Dynamic Simulator in Seat Testing.

13. Tomlinson, R. W., Kyle, D. J., 1970 *Departmental Note National Institute of Agricultural Engineering Silsoe DN/TE/037/1445* The development of a dynamic model of the seated human operator.

14. Mansfield, N. J., Griffin, M. J., 1996 *Inter-noise'96 Proceeding of 25th Anniversary Congress 4 1725-1730* Vehicle Seat Dynamics Measured with an anthropodynamic dummy and human subjects.

15. Gu, Y., 1999 *SAE Technical Paper 01-0629 1999* A new dummy for vibration transmissibility measurement in improving ride comfort.

16. Huston, D. R., Johnson, C. C., Zhao, X. D., 1998 *Journal of Sound and Vibration 214 (1) 195-200* A human analog for testing vibration attenuation seating.

17. Lewis, C. H., 1998 *33rd UK Group Meeting on Human Response to Vibration* The implementation of an improved anthropodynamic dummy for testing the vibration isolation of vehicle seats.

18. Toward, M. G. R., 2000 *35th UK Group Meeting on Human Response to Vibration* Use of an Anthropodynamic Dummy to measure Seat Dynamics.

19. Cullmann, A., Wölfel, H. P., 2001 *Clinical Biomechanics 16 S64-S72* Design of an active vibration dummy of sitting man.

20. Lewis, C. H., 2005 *40th UK Group Meeting on Human Response to Vibration* Variability in measurements of seat transmissibility with an active anthropodynamic dummy and with human subjects.

21. Fairley, T. E., Griffin, M. J., 1989 *Journal of Biomechanics 22(2), 81-94* The Apparent Mass of the Seated Human Body: Vertical Vibration.

22. Suggs, C. W., Abrams, C. F., Stikeleather, L. F. 1969 *Ergonomics 12, 79-90* Application of a damped spring-mass human vibration simulator in vibration testing of vehicle seat.

23. Coermann, R. R., 1962 *Human Factors, 227-253*, The mechanical impedance of the Human Body in Sitting and Standing position at low frequencies.

24. Vogt, H. L., Coermann, R. R., Fogt, H. D., 1968 *Aerospace Medicine, 39, 675-679* Mechanical Impedance of Sitting Human under Sustained Acceleration.

25. Miwa, T., 1975 *Industrial Health, 13, 1-22.*, Mechanical Impedance of Human Body in Various Postures.

26. Donati, P.M., Bonthoux, C., 1983 *Journal of Sound and Vibration 90 423-442*

Biodynamic response of the human body in the sitting position when subjected to vertical vibration.

27. Boileau, P. E., Rakheja, S., Wu, X., 2002 *Journal of Sound and Vibration 253 (1), 243-264* A body mass dependent mechanical impedance model for applications in vibration seat testing.

28. Kitazaki, S., Griffin, M. J., 1998 *Journal of Biomechanics 31, 143-149* Resonance behavior of the seated human body and effect of posture.

29. Wang, W., Rakheja, S., Boileau, P. E., 2004 *International Journal of Industrial Ergonomics 289-306* Effects of sitting postures on biodynamic response of seated occupants under vertical vibration.

30. Wang, W., Rakheja, S., Boileau, P. E., 2006 *Journal of Industrial Ergonomics 36 171-184*. The role of seat geometry and posture on the mechanical energy absorption characteristics of seated occupants under vertical vibration.

31. Wu. X., Rakheja. S, Boileau, P. E., 1999 *Journal of Sound and Vibration 226 (3), 595-606* Analysis of the relationship between biodynamic response functions.

32. Paddan, G. S., Griffin, M. J., 1998 *Journal of Sound and Vibration 253(4), 863-882*. A review of the transmission of translational seat vibration to the head.

33. Rakheja, S., Boileau, P. E., Stiharu, I., 2002 *Journal of Sound and Vibration 253 (1), 57-75*, Seated occupant apparent mass characteristics under automotive postures and vertical vibration.

34. Boileau, P. E., Wu, X., Rakheja, S., 1998 *Journal of Sound and Vibration 215 (4), 841-862* Definition of a range of idealized values to characterize seated body biodynamic response under vertical vibration.

35. International Standard 5982 2001 Mechanical vibration and shock-range of idealized values to characterize seated-body biodynamic response under vertical vibration.

36. International Standard DIN 45676 1992 Mechanical Impedances at the driving point and transfer functions of the human body.

37. Payne, P. R., 1978 *Aviation, Space, and Environmental Medicine, 262-269*, Method to Quantify Ride Comfort and Allowable Accelerations.

38. Suggs, C. W., Stikeleather, L. F., 1970, *Transactions of ASAE 13, 378-381*, Application of a Dynamic Simulator in Seat Testing.

39. Allen, G.,1978, *A25-5-A25-15, Paper A25, AGARD Conference Proceeding No. 253 Models and Analogues for the Evaluation of Human Biodynamic Response, Performance and Protection*, A Critical Look at Biodynamic Modeling in Relation to specifications for Human Tolerance of Vibration and Shock.

40. Mertens, H., 1978 *Aviation, Space, and Environmental Medicine 287-298* Nonlinear Behavior of Sitting Humans under Increasing Gravity.

41. Mertens, H., Vogt, L., 1978 *A26-1-A26-16, Paper A26, AGARD Conference Proceeding No. 253 Models and Analogues for the Evaluation of Human Biodynamic Response, Performance and Protection*, The Response of a Realistic Computer Model for Sitting Humans to Different Types Shocks.

42. ISO Committee Draft CD 5982, Mechanical Driving Point Impedance and Transmissibility of the Human body.

43. Wu, X., 1998 *Ph.D. Thesis in the Department of Mechanical Engineering (Concordia University)* Study of Driver-Seat interactions and enhancement of vehicular ride vibration environment.

44. Boileau, P. E., Rakheja, S., Yang, X., Stiharu, I., 1997 *Noise and Vibration Worldwide, 28(9)* Comparison of Biodynamic Response Characteristics of various Human body Models as Applied to Seated Vehicle Drivers.

45. Amirouche, F. M. L., Ider, S. K., 1998 *Journal of Sound and Vibration 128 281-292* Simulation and analysis of a biodynamic human model subjected to low accelerations-A correlation study.

46. Patil, M. K., Palanichamy, M. S., 1998 *Applied Mathematical Modeling 12 63-71* A mathematical model of tractor-occupant system with a new seat suspension for minimization of vibration response.

47. Rakheja, S., Stiharu, I., Zhang, H., Boileau, P. E 2006 *Journal of Sound and Vibration*, Seated occupant interactions with seat backrest and pan, and biodynamic responses under vertical vibration.

48. Rakheja, S., 1983 *Ph.D. Thesis in the Department of Mechanical Engineering (Concordia University)* Computer Aided Dynamic Analysis and Optimal Design of Suspension Systems for Off-Road Tractors.

49. Burdoff, A., Swuste, P., 1993 *Annals of Occupational Hygiene 37 (1) 45-55* The effect of seat suspension on exposure to whole-body vibration of professional drivers.

50. Rebelle, Jerome., 2000 *Proceedings of the 35th UK conference on Human*

Responses to Vibration, University of Southampton 221-238 Development of a numerical model of seat suspension to optimize the end-stop buffers.

51. Gunston, Thomas. P., 2002 *Proceedings of the 37^h UK conference on Human Responses to Vibration Loughborough University* Two methods of simulating a suspension seat cushion.

52. Stikeleather, L. F., Suggs, C. W., 1970 *Transactions of ASAE 13 (1) 99* An Active Suspension System for Off-Road Vehicles.

53. Young, R. E., Suggs, C. W., 1973 *Transactions of ASAE 16 (5) 876* Seat-Suspension System for Isolation of Roll and Pitch in Off-Road Vehicles.

54. Wu. X., Rakheja. S, Boileau, P. E., Dynamic Performance of Suspension Seats under Vehicular Vibration and Shock Excitations.

55. Politis, H., Rakheja, S., Boileau, P. E., Juras, D., Boutin, J., 2003 *Society of Automotive Engineers, SAE Paper No 2003-01-0953* Limits of application of human body dynamics in assessing vibration comfort of seats.

56. International Organization for Standardization ISO 7096 2000 Earth-moving machinery-Laboratory Evaluation of Operator Seat Vibration.

57. Janeway, R. N., 1968 *Society of Automotive Engineers Journal 77 (1) 346-370* Passenger Vibration Limits.

58. Janeway, R. N., 1975 *Society of Automotive Engineers SAE Paper 751066* Human Vibration Tolerance Criteria and Application to Ride Vibration.

59. Van Deusen, B. D., 1968 *Transactions of SAE 77 (1) 328-345* Human Response to Vehicle Vibration.

60. International Organization for Standardization ISO-2631/1 1994 33 Mechanical Vibrations and Shock-Evaluation of Human Exposure to Whole-Body Vibration Part 1: General Requirements.

61. International Organization for Standardization ISO 2631 1974 Guide for the Evaluation of Human Exposure to Whole-Body Vibration.

62. Lee, R. A., Pradko, F. 1968 *Society of Automotive Engineers, SAE Paper No. 680091.* Analytical Analysis of Human Vibration.

63. Fukuda, T., Takeuchi, D., Shimizu, H., 2001 *Japan Group Meeting in Human Response to Vibration* Study on the Evaluation of Vibration Exposure During Vehicle Operation-Comparison of Results Calculate by Respective Standards.

64. Xie, X., 2001 *M.A.Sc. Thesis in the Department of Mechanical Engineering (Concordia University)* Absorbed Power as a Measure of Whole Body Vehicular Vibration Exposure.

65. Mansfield, N. J., Griffin, M. J., 1998 *Journal of Sound and Vibration 215 (4) 813-825* Effect of Magnitude of Vertical Whole-Body Vibration on Absorbed Power for the Seated Human Body.

66. Mansfield, N.J., Holmlund, P., Lundstorm, R., 2000 *Journal of Sound and Vibration 230 (3) 477-491* Comparison of Subjective Responses to Vibration and Shock with Standard Analysis Methods and Absorbed Power.

67. Mansfield, N.J., Holmlund, P., Lundstorm, R., 2001 *Journal of Sound and Vibration 248 (3) 427-440* Apparent Mass and Absorbed Power During Exposure to Whole-Body Vibration and Repeated Shocks.

68. Ograwa, S., 1991 *Japanese Railway Engineering 21 (1) 16-22* Study of Riding Quality with New Concept.

69. Oborne, D. J., 1978 *Applied Ergonomics 9 (1) 211-225* Techniques Available for the Assessment of Passenger Comfort.

70 Society of Automotive Engineers 1980 *SAE J1013* Measurement of Whole-Body Vibration of the Seated Operator of Off-Highway Work Machines.

71 International Organization for Standardization ISO-2631/1 1985 17 Mechanical Vibrations and Shock-Evaluation of Human Exposure to Whole-Body Vibration Part 1: General Requirements.

72 International Organization for Standardization ISO 10326-1 1992 Mechanical Vibration-Laboratory Method for Evaluating Seat Vibration-Part-I: Basic Requirements.

73 British Standards Institution BS 6841 1987 Measurement and evaluation of human exposure to whole0body mechanical vibration and repeated shock.

74 Hinz, B., Menzel, G., Blüthner, R., Seidel, H., 1998 *Journal of Sound and Vibration 215 (4) 977-988* Laboratory testing of operator seat vibration with 37 subjects-Critical Comment on ISO/DIS 7096.

75 Mansfield, N. J., Griffin, M. J., 2000 *Journal of Biomechanics 33 933-941* Non-linearities in apparent mass and transmissibility during exposure to whole-body vertical

76 Holmlund, P., Lundstorm, R., Lindberg, L., 2000 *Applied Ergonomics 31, 415-422* Mechanical impedance of the human body in vertical direction.

77 Rakheja, S., Boileau, P.E. Wang, Z., Politis, H., 2003 *journal of Low Frequency Noise, Vibration And Active Control 22(4)* Performance Analysis of Suspension Seats Under High Magnitude Vibration Excitations: Part 1:Model Development and Validation

78 Rakheja, S., Boileau, P.E. Wang, Z., Politis, H., 2003 *journal of Low Frequency Noise, Vibration And Active Control 23(1)* Performance Analysis of Suspension Seats Under High Magnitude Vibration Excitations: II. Design Parameter Study

79 Boileau, P. E., Rakheja, S., Liu, P. J., 1997 *Heavy Vehicle Systems, International Journal of Vehicle Design Vol 4 Nos 2-4* A combined suspension seat-vehicle driver model for estimating the exposure to whole-body vehicular vibration and shock

80 International Organization for Standardization 1990 ISO 5007 Agricultural wheeled tractors-Operators Seat-Laboratory measurement of transmitted vibration

81 European Standard 2001 prEN 13490 Mechanical Vibration-Industrial Trucks-Laboratory evaluation and specification of operator seat vibration

82 French Standard Association 1990 NF R18-401 ed Road vehicles. Vibrations transmitted by the seats of commercial vehicle of laden weight greater than 12 tons. Test methods.

83 Wei, L., Griffin, M. J., 1998 *Journal of Sound and Vibration 212(5) 855-874* Mathematical model for the mechanical impedance of the seated human body exposed to vertical vibration.

84 Richter, B., Werdin, S., 1998 *Federal Institute of occupational safety and health, summary of research project F1687* Design review and realization of a mechanical vibration model representing the sitting human.

85 "MATLAB", *The Language of Technical Computing*, Version 6.5.1. 199709 Release 13, Copyright 1984-2003, The MathWorks, Inc.